

# Engineering Economic Policy Assessment of Concentrated Solar Thermal Power Technologies for India

Capital Cost/MW (₹-Lakh)

LCOE (₹/kWh)

Capacity (MW)

50 MW;  $t_s=0$ ; SM=1;

Frequency

# Engineering Economic Policy Assessment of Concentrated Solar Thermal Power Technologies for India

*Project Investigator*

M A Ramaswamy

*Co-Investigator*

V S Chandrasekaran

*Advisor*

R Krishnan

*Team Members*

N C Thirumalai

N S Suresh

Badri S Rao

Smita Kumari Dolly

V Chaitanya Kanth

V Arun Kumar

December 2012

**Center for Study of Science, Technology and Policy  
Bangalore**

Center for Study of Science, Technology and Policy (CSTEP) is a private, not-for-profit (Section 25) Research Corporation registered in 2005. CSTEP's vision is to enrich the nation with science and technology-enabled policy options for equitable growth. CSTEP's studies do not necessarily reflect the opinions of its sponsors.

#### Disclaimer

While every effort has been made for the correctness of data/information used in this report, neither the authors nor CSTEP accept any legal liability for the accuracy or inferences for the material contained in this report and for any consequences arising from the use of this material.

© 2012 Center for Study of Science, Technology and Policy

No part of this report may be disseminated or reproduced in any form (electronic or mechanical) without permission from CSTEP.

December, 2012

CSTEP/E/7, 2012

Center for Study of Science, Technology and Policy  
Dr. Raja Ramanna Complex, Raj Bhavan Circle,  
High Grounds, Bangalore – 560 001  
Tel.: +91 (80) 4249-0000  
Fax: +91 (80) 2237-2619

*Email:* [admin@cstep.in](mailto:admin@cstep.in)

*Website:* [www.cstep.in](http://www.cstep.in)

# THE SUN ALSO RISES

Ecclesiastes (1:5) is not the only version that describes the eternal presence of the sun, its rises and sets drenching the entire earth with its radiation. The radiation is so huge and bountiful that an hour of sunshine is enough to meet the global needs of energy for a year! But there are a few disclaimers. While the total radiative energy is large, the flux (energy per square meter) is modest and to derive useful power, the radiation has to be concentrated into a sizeable level. The sunshine is also intermittent with no energy during night or when shielded by cloud. These two deficiencies have to be overcome if we have to draw useful power from sun.

This study addresses these issues of aligning a large number of mirrors to concentrate and focus the radiation on suitable absorbers, which carry the heat transfer fluid. All these make this option expensive and vulnerable until we become familiar with this technology and its limits. The cost of this Concentrating Solar Power (CSP) route is expensive when compared to solar photovoltaic. But the advantages of energy storage and hybridization, where various sources of energy systems are combined, make CSP an option that also has to be pursued.

This report covers the techno-economic options for various CSP technologies and discusses their relative advantages and limits. In addition, this report focuses on which would be more appropriate to our country taking into account the resident expertise and materials availability. The report also develops a computational user interactive model, which can be used to evaluate the techno – economic viability of CSP technologies. Any reader of this report will appreciate the complexities inherent in introducing new innovations that are yet to mature. We should not have to wait until this technology matures. We shall then be a mere imitator with indigenous innovative assets locked out.

This work was made possible by the support of Ministry of New and Renewable Energy. I am grateful to Prof. M. A. Ramaswamy for leading this group and to all the other members for their unstinting commitment and contributions to the project. Shri N.C Thirumalai worked as an able colleague to Prof. Ramaswamy in executing this project. To all my thanks are due.

*V.S. Arunachalam*  
Chairman, CSTEP

## **Acknowledgements**

We express our gratitude to Dr. V S Arunachalam, Chairman CSTEP for his support and encouragement. We are grateful to Dr. Anshu Bharadwaj, Executive Director, CSTEP for his constant encouragement, advice and for critical review of the report. We thank Dr. K C Bellarmine, Chief Financial Officer, CSTEP for his contributions in the economic assessment methodology. We thank Mr. H S Ramakrishna, Advisor, CSTEP for discussions on grid connectivity related issues. We thank Mr. S V Narasimhan and Mr. Murali Krishna Ganji for their contributions in this study. Thanks are also due to Dr. Shuba Raghavan, former Principal Investigator for initiating this project.

We thank Dr. Ashvini Kumar, Director, Solar Energy Corporation of India, Government of India for his keen interest in this study. We gratefully acknowledge the financial support provided by Ministry of New and Renewable Energy, Government of India. This report is the outcome of the project “Engineering Economic Policy Assessment of Concentrating Solar Thermal Power Technologies in India” sanctioned by the Ministry of New & Renewable Energy (vide letter No. 15/26/2010-11/ST dated 19<sup>th</sup> November 2010).

We also thank the Communications and Policy Engagement team as well as the administrative staff of CSTEP for their support.

# Contents

Nomenclature.....	vi
List of Figures.....	ix
List of Tables.....	xiv
Executive Summary.....	xvii
1 Introduction.....	1
2 Global Experience.....	2
2.1 Introduction.....	2
2.2 Parabolic Trough.....	2
2.2.1 Description.....	2
2.2.2 Deployment of PT.....	4
2.2.3 New Developments.....	7
2.2.4 Merits and Demerits of PT.....	8
2.3 Solar Tower.....	9
2.3.1 Description.....	9
2.3.2 Deployment of ST.....	18
2.3.3 Merits and Demerits of ST.....	24
2.4 Linear Fresnel.....	25
2.4.1 Description.....	25
2.4.2 Deployment of Linear Fresnel.....	28
2.4.3 New Developments.....	29
2.4.4 Merits & Demerits of LFR.....	30
2.5 Parabolic Dish.....	30
2.5.1 Parabolic Dish with Stirling Engine.....	30
2.5.2 Merits and Demerits of Dish System with Stirling Engines.....	36
2.5.3 Dish Technology with Steam Rankine Cycle.....	36
2.6 Relative Assessment of CSP Technologies.....	38
2.6.1 Technology Utilization/Maturity.....	38
2.6.2 Mirror Area/Land Area Requirements.....	38
2.6.3 Cost Comparison.....	39
2.7 Salient Observations.....	40
3 Model for Techno Economic Analysis of Parabolic Trough Technology.....	41
3.1 Introduction.....	41
3.2 Model for Engineering Analysis.....	42
3.2.1 An Overview.....	42

3.2.2	Inputs for Technical Assessment of CSP .....	46
3.2.3	Details of Engineering Model.....	52
3.3	Model for Economic Analysis of PT Technology .....	59
3.3.1	Inputs Required from Technical Model for Economic Analysis.....	59
3.3.2	Estimation of Capital Costs.....	59
3.3.3	Methodology for Estimation of O&M Expenses .....	62
3.3.4	Financial Parameters for Computing LCOE.....	63
3.3.5	Cost Estimates of Components.....	65
3.3.6	Estimation of O&M expenses.....	68
3.3.7	Values of the Financial Parameters.....	69
3.3.8	Methodology for Computing LCOE & IRR.....	70
3.4	Technical Assessment – Case Study at Jodhpur.....	72
3.4.1	No Thermal Storage and No Hybridization.....	72
3.4.2	Thermal Storage without Hybridization.....	77
3.4.3	Hybridization without Thermal Storage.....	83
3.4.4	With Thermal Storage and Hybridization .....	86
3.5	Economic Assessment – Case Study at Jodhpur .....	87
3.5.1	Determination of Optimum SM based on LCOE.....	87
3.5.2	Economic Parameters of PT plants .....	94
3.6	Salient Observations .....	103
4	Interactive Desktop Tool .....	105
4.1	Introduction .....	105
4.2	Overview of the Tool.....	105
4.3	Start of the Application.....	106
4.4	Input Tabs .....	107
4.4.1	Location Details.....	107
4.4.2	Plant Details.....	109
4.4.3	Capital Costs .....	112
4.4.4	O&M Expenses .....	113
4.4.5	Financial Parameters .....	114
4.4.6	Simulation and Results.....	115
4.5	Output Tabs .....	115
4.5.1	Summary .....	116
4.5.2	Technical Outputs.....	116
4.5.3	Equipment Cost Outputs.....	117
4.5.4	Overall Costs.....	118

4.5.5	Monthly Profile Graphs .....	119
4.5.6	Time Series Graph .....	119
4.5.7	Parametric Variation Graphs .....	120
5	Sensitivity Analysis of PT Plant Parameters.....	122
5.1	Introduction .....	122
5.2	Sensitivity to Power Block Efficiency.....	122
5.3	Sensitivity to Capital Cost .....	124
5.4	Sensitivity to Loan Rate .....	125
5.5	Sensitivity to Assumed Tariff .....	126
5.6	Deviation from Optimum SM.....	127
6	Techno Economic Viability of Solar Tower Technology in India .....	129
6.1	Introduction .....	129
6.2	Choice of Type of ST Technology in India .....	129
6.2.1	Direct Steam Generation with Rankine cycle.....	129
6.2.2	Air as HTF Coupled with Brayton Cycle .....	129
6.2.3	Molten Salt as HTF with Rankine Cycle.....	129
6.3	Techno-Economic Assessment of ST Technology using Molten Salt as HTF .....	130
6.3.1	Procedure to Determine Solar Field Area and Stored Thermal Energy .....	131
6.3.2	Inputs and Assumptions in Economic Assessment .....	132
6.4	Assessment of 50 MW ST Plant with 3 Hours of Thermal Storage .....	133
6.4.1	Determination of Various Technical Parameters .....	133
6.4.2	DCC, ICC & O&M Expenses .....	135
6.4.3	LCOE & IRR.....	136
6.4.4	Comparison of ST with PT of 50 MW with 3 Hours Storage .....	136
6.5	Sensitivity Analysis for ST Plant Parameters .....	137
6.5.1	Sensitivity to Capital Cost.....	137
6.5.2	Sensitivity to Tariff.....	138
6.5.3	Sensitivity to Annual Solar to Electric Efficiency .....	139
6.5.4	Sensitivity to Solar Field Cost.....	140
7	Techno Economic Viability of Linear Fresnel Technology in India.....	142
7.1	Introduction .....	142
7.2	Viability of Using Synthetic Oil as HTF in LFR Systems.....	142
7.3	Techno-Economic Assessment of a LFR using Synthetic Oil as HTF.....	143
7.3.1	Determination of Solar Field Area and Stored Thermal Energy .....	143
7.3.2	Inputs and Assumptions in Economic Assessment .....	144
7.4	Assessment of 50 MW LFR Plant with 3 Hours Storage.....	146
7.4.1	Determination of Various Technical Parameters .....	147

7.4.2	DCC, ICC and O&M Expenses.....	148
7.4.3	LCOE and IRR .....	149
7.4.4	Comparison of MLFR with PT of 50 MW with 3 Hours Storage .....	149
7.5	Sensitivity Analysis for MLFR Parameters .....	149
7.5.1	Sensitivity to Capital Cost.....	150
7.5.2	Sensitivity to Tariff.....	151
7.5.3	Sensitivity to Annual Solar to Electric Efficiency .....	152
7.5.4	Sensitivity to Solar Field Cost.....	153
7.6	Salient Observations .....	155
8	Techno Economic Viability of Dish Technology in India .....	156
8.1	Introduction .....	156
8.2	Dish with Stirling Engine .....	157
8.2.1	Limited Techno-Economic Data .....	157
8.3	Commercial Ventures.....	160
8.4	Plant Cost.....	160
8.5	Discussion .....	161
9	Air Condensing for CSP Plants.....	162
9.1	Introduction .....	162
9.2	Gross Efficiency of the Power Block.....	162
9.2.1	Impact of Higher Turbine Outlet Temperature on Gross Efficiency .....	164
9.3	Wet Cooling Condenser System .....	165
9.4	Air Cooled Condensing System.....	166
9.5	Auxiliary Loads in Wet Cooling .....	167
9.5.1	Power Required for Circulating Water Pump.....	167
9.5.2	Power Required for Fan in Cooling Tower .....	168
9.5.3	Make-up Water Requirements.....	169
9.6	Efficiency and Auxiliary Loads in Air Cooling .....	169
9.7	Techno-Economic Analysis of Air Condensing.....	169
9.7.1	Technical Impact of Air Cooling Option .....	170
9.7.2	Economic Impact of Air Condensing Option.....	170
10	Cost of Grid Connectivity .....	172
10.1	Introduction .....	172
10.2	Cost of Substation.....	172
10.3	Cost of Transmission .....	173
11	Present Status of CSP Technologies in India.....	174
11.1	Introduction .....	174
11.2	JNNSM and CERC Baseline.....	174

11.3	CSP Projects under JNNSM .....	175
11.3.1	Projects Bid .....	175
11.3.2	Migration Scheme.....	177
11.4	Projects outside JNNSM .....	178
11.5	Progress of CSP in India.....	179
12	Indigenization Prospects of CSP .....	181
12.1	Introduction .....	181
12.2	Current Global Cost Structure for CSP.....	181
12.3	Indigenization Prospects.....	182
12.3.1	Possible Cost Reductions.....	183
13	Manpower Requirements for CSP Plants .....	185
13.1	Introduction .....	185
13.2	Manpower for PT & ST Plants .....	185
14	Policy Options for CSP in India.....	187
14.1	Storage and Hybridization.....	187
14.2	Land Zones.....	188
14.3	Small Capacity CSP.....	188
14.4	Indigenization.....	188
14.5	Heating Applications.....	189
14.6	Financing .....	189
	References .....	190

# Nomenclature

$A_a$	Actual mirror aperture area
$A_r$	Reference mirror aperture area
$C$	Chord of the mirror
$DNI_{annual}$	Annual solar resource
$E_{tea}$	Thermal energy available from storage
$E_{tes,max}$	Maximum amount of thermal energy that can be stored
$L_f$	Loss factor
$P_g$	Actual gross power generated
$P_{g,d}$	Rated gross power
$P_s$	Solar power impinging on the absorber tube per unit length
$P_{s,d}$	Solar power impinging on the absorber tube per unit length at design conditions
$P_{abs}$	Thermal power impinging on the absorber tube
$P_{abs,d}$	Thermal power impinging on the absorber tube at design conditions
$P_{hb}$	Maximum thermal power input to HTF from hybridization
$P_{htf}$	Thermal power input from HTF to heat exchanger
$P_{htf,d}$	Thermal power input from HTF to heat exchanger at design conditions
$P_{htf,s}$	Thermal power input from solar field to HTF
$P_{th,d}$	Thermal power of working fluid at design conditions
$P_{th,s,d}$	Solar power input to mirrors at design conditions
SM	Solar Multiple
$V_a$	Volume of Natural Gas required annually
$V_{st}$	Storage volume of NG as buffer
$e_g$	Gross electrical energy that would be generated without considering energy needed for start-up
$e_{g,a}$	Gross electrical energy generated accounting for start-up
$e_{g,t}$	$\sum e_{g,a}$

$e_{grid}$	Electrical energy supplied to grid
$e_{grid,t}$	$\sum e_{grid}$
$e_{hb}$	Electrical energy apportioned to hybridization
$e_{hb,t}$	$\sum e_{hb}$
$e_s$	Electrical energy apportioned to solar input
$e_{s,t}$	$\sum e_s$
$e_{start}$	Equivalent electrical energy required for start-up accounting for thermal losses during shut down period
$f_{hb}$	Maximum fraction of hybridization power permitted
$f_{hb,t}$	$\sum f_{hb,used}$
$f_{hb,used}$	Actual hybridization fraction used
$f_{th}$	Fraction of thermal power delivered to power block
$f_{th,max}$	Maximum fraction of thermal power permitted
$f_{th,min}$	Minimum fraction of thermal power required for power generation
$f_p$	Fraction of the gross electrical power generated ignoring thermal losses during shutdown
$f_{pa}$	Fraction of gross electrical power generated taking into account thermal losses during shutdown
$f_{th,s}$	Solar thermal power as a fraction of the design thermal power
$f_{th,st}$	Fraction of thermal power used from storage
$f_{th,sta}$	Fraction of thermal power available from storage
$t_s$	Number of hours of thermal storage
$\Delta t$	Time step
$\beta$	Angle of tilt of parabolic trough
$\gamma$	Intercept factor
$\delta$	Declination of the day
$\eta_{abs}$	Absorber efficiency
$\eta_{abs,d}$	Efficiency of absorber tube at design conditions
$\eta_c$	Efficiency of solar collection
$\eta_{he}$	Efficiency of power block heat exchanger

$\eta_m$	Optical efficiency of the mirror system
$\eta_{p,d}$	Power block efficiency at design conditions
$\eta_{pl}$	Part load efficiency of power block
$\eta_r$	Relative efficiency = $\eta_{pl}/\eta_{p,d}$
$\eta_{s-e}$	Annual solar to electric conversion efficiency
$\eta_{st}$	Efficiency of storage heat exchanger
$\theta$	Angle between the normal to the mirror aperture and sun's rays
$\rho$	Specular reflectivity of the mirror
$\phi$	Latitude of the location
$\omega$	Solar hour angle

## List of Figures

Figure 2.1: Parabolic trough collectors .....	2
Figure 2.2: PT plant with two tank thermal storage system .....	3
Figure 2.3: Solar Two – demonstration ST plant.....	9
Figure 2.4: External cylindrical receiver used in Solar Two.....	12
Figure 2.5: Cavity receiver used in PS-10.....	13
Figure 2.6: Schematic of open volumetric receiver .....	13
Figure 2.7: Schematic of the pressurized volumetric receiver .....	14
Figure 2.8: Heliostat field at Gemasolar, Spain.....	21
Figure 2.9: Heliostat field for PS 10 and PS 20, Spain.....	21
Figure 2.10: Heliostat field at Sierra Sun Tower, USA.....	22
Figure 2.11: Heliostat field of Jülich plant, Germany .....	22
Figure 2.12: Tower height variation with equivalent capacity for various plants .....	24
Figure 2.13: Linear Fresnel Reflector system.....	25
Figure 2.14: Schematic diagram of LFR and CLFR.....	26
Figure 2.15: Fresnel receiver types: (a) Novatech’s design (b) Ausra's design.....	27
Figure 2.16: Schematic of Ruths tank storage system.....	27
Figure 2.17: Maricopa dish system .....	31
Figure 2.18: Working principle of a simple Stirling engine .....	32
Figure 2.19: Sectional view of Infinia’s Stirling engine.....	33
Figure 2.20: Seasonal variation in tilt and profile needed for a Scheffler dish .....	36
Figure 2.21: Cast iron core cavity receiver and Scheffler dish .....	37
Figure 2.22: The SG4 dish in testing for the direct steam generation .....	37
Figure 3.1: Schematic of a CSP plant - PT .....	42
Figure 3.2: Absorber efficiency as a function of input power .....	49
Figure 3.3: Power block efficiency at design conditions .....	50
Figure 3.4: Efficiency of power block at part load .....	50
Figure 3.5: Electrical power generated at part load conditions.....	51
Figure 3.6: Variation of power block cost with capacity.....	66
Figure 3.7: Variation of reference mirror aperture area per MW with capacity.....	73

Figure 3.8: Variation of annual electrical energy generated per MW with SM.....	74
Figure 3.9: Variation of capacity factor with SM for all capacities.....	74
Figure 3.10: Frequency distribution graph.....	75
Figure 3.11: Variation of annual efficiency with SM for various capacities .....	76
Figure 3.12: Variation of the fractional solar thermal power and fractional electrical power generated during a typical day .....	77
Figure 3.13: Variation of annual electrical energy/MW with SM for $t_s= 0, 3$ and 6 hours .....	78
Figure 3.14: Variation of capacity factor with SM, for $t_s = 0, 3$ and 6 hours .....	79
Figure 3.15: Variation of capacity factor with thermal energy storage for various SMs and no hybridization.....	79
Figure 3.16: Variation of annual efficiency with SM for various capacities for $t_s= 3$ hours and no hybridization.....	80
Figure 3.17: Variation of annual efficiency with SM for various capacities for $t_s = 6$ hours and no hybridization.....	80
Figure 3.18: Variation of maximum annual efficiency with plant capacity.....	81
Figure 3.19: Optimum SM for maximum annual efficiency with thermal storage .....	81
Figure 3.20: Variations in $f_{th,s}$ and $f_{pa}$ during a typical day for $t_s= 3$ hours .....	82
Figure 3.21: Variations in $f_{th,s}$ and $f_{pa}$ during a typical day for $t_s= 6$ hours .....	82
Figure 3.22: Effect of hybridization on the electrical power generated during a typical day for SM=1 .....	83
Figure 3.23: Fraction of hybridization used during a typical day for SM=1.....	83
Figure 3.24: Effect of hybridization on the electrical power generated during a typical day for SM=1.5.....	84
Figure 3.25: Fraction of hybridization used during a typical day for SM=1.5.....	84
Figure 3.26: Variation of annual energy per MW with hybridization.....	85
Figure 3.27: Variation of annual efficiency with SM for $f_{hb}=0, 0.1$ and $0.2$ .....	85
Figure 3.28: Variation of capacity factor with SM for $t_s=0$ hours .....	86
Figure 3.29: Variation of capacity factor with SM for $t_s=3$ hours .....	86
Figure 3.30: Variation of capacity factor with SM for $t_s=6$ hours .....	87
Figure 3.31: Variation of LCOE with SM for different thermal storage hours with $f_{hb}=0$ .....	88
Figure 3.32: Variation of LCOE with SM for different thermal storage hours with $f_{hb}=0.1$ .....	89
Figure 3.33: Variation of LCOE with SM for different thermal storage hours with $f_{hb}=0.2$ .....	90

Figure 3.34: Variation of IRR with SM for different thermal storage hours with $f_{hb}=0$ .....	91
Figure 3.35: Variation of IRR with SM for different thermal storage hours with $f_{hb}=0.1$ .....	92
Figure 3.36: Variation of IRR with SM for different thermal storage hours with $f_{hb}=0.2$ .....	93
Figure 3.37: Variation of capital cost for various thermal storage conditions .....	98
Figure 3.38: Variation of mirror area per MW under different thermal storage conditions .....	98
Figure 3.39: Variation of LCOE for various thermal storage conditions.....	99
Figure 3.40: Variation of IRR for various thermal storage conditions .....	100
Figure 3.41: Variation of capacity factor for various thermal storage conditions.....	100
Figure 3.42: Effect of thermal storage on capital cost and capacity factor .....	101
Figure 3.43: Hybridization benefit for LCOE when $f_{hb}=0.1$ .....	103
Figure 3.44: Hybridization benefit for LCOE when $f_{hb}=0.2$ .....	103
Figure 4.1: Input tabs.....	106
Figure 4.2: Output tabs.....	106
Figure 4.3: Start page of the tool .....	107
Figure 4.4: Menu options in the tool.....	107
Figure 4.5: Location details tab.....	108
Figure 4.6: Steps for adding new location of user choice.....	109
Figure 4.7: Plant details tab.....	109
Figure 4.8: Enabling parametric simulation.....	111
Figure 4.9: Entering SM values for parametric simulation .....	111
Figure 4.10: Procedure to remove the parametric simulation.....	112
Figure 4.11: Capital costs tab.....	113
Figure 4.12: O&M expenses tab .....	114
Figure 4.13: Financial parameters tab.....	114
Figure 4.14: Simulation and results tab .....	115
Figure 4.15: Summary tab.....	116
Figure 4.16: Technical outputs tab.....	117
Figure 4.17: Equipment cost tab .....	117
Figure 4.18: Overall costs tab .....	118
Figure 4.19: Other costs tab .....	118

Figure 4.20: Monthly profile graphs tab .....	119
Figure 4.21: Time series graph tab.....	120
Figure 4.22: Zoomed in step graph .....	120
Figure 4.23: Parametric variation graphs tab.....	121
Figure 5.1: Effect of efficiency of power block on capital cost.....	123
Figure 5.2: Effect of efficiency of power block on LCOE.....	123
Figure 5.3: Effect of efficiency of power block on IRR.....	123
Figure 5.4: Variation of LCOE with capital costs.....	124
Figure 5.5: Variation of IRR with capital costs .....	125
Figure 5.6: Variation of LCOE & IRR with loan rate.....	126
Figure 5.7: Variation of IRR with assumed tariff .....	127
Figure 5.8: Variation of capital cost for deviation with optimum SM.....	128
Figure 5.9: Variation of capacity factor with deviation from optimum SM.....	128
Figure 6.1: Schematic of ST system.....	130
Figure 6.2: Capital cost for receiver and tower corresponding to receiver capacity .....	132
Figure 6.3: Capacity factor with thermal energy storage for the ST system.....	134
Figure 6.4: Variation of LCOE with capital costs.....	137
Figure 6.5: Variation of IRR with capital costs .....	138
Figure 6.6: Variation of IRR with tariff .....	138
Figure 6.7: Variation of capital cost with annual solar to electric efficiency .....	139
Figure 6.8: Variation of LCOE and IRR with annual solar to electric efficiency.....	140
Figure 6.9: Variation of LCOE with solar field cost.....	140
Figure 7.1: Variation of capacity factor with storage for PT.....	147
Figure 7.2: Variation of LCOE with capital costs.....	150
Figure 7.3: Variation of IRR due to variation of DCC .....	151
Figure 7.4: Variation of IRR with assumed tariff .....	152
Figure 7.5: Variation of capital cost with solar to electric efficiency .....	153
Figure 7.6: Variation of LCOE and IRR with conversion efficiencies.....	153
Figure 7.7: Variation of capital cost with solar field cost.....	154
Figure 7.8: Variation of LCOE and IRR with solar field cost .....	154

Figure 8.1: Conversion efficiencies of various solar technologies .....	156
Figure 8.2: Dish with gas turbine .....	157
Figure 8.3: Infinia dish performance .....	160
Figure 9.1: Relative efficiency of turbines against a 100 MWe baseline .....	163
Figure 9.2: Variation of $\eta_{gross-max}$ with turbine inlet temperature .....	164
Figure 9.3: Decrease in $\eta_{gross-max}$ for a 20°C increase in turbine outlet temperature .....	164
Figure 9.4: Relative change in $\eta_{gross-max}$ for a 20°C difference in turbine outlet temperature .....	165
Figure 9.5: Schematic of wet-cooling system.....	166
Figure 9.6: Schematic of air cooled condensing system .....	167
Figure 12.1: Cost range for CSP plants (PT & ST).....	182

## List of Tables

Table 2.1: Country-wise distribution of PT plants.....	5
Table 2.2: Data on operational PT plants .....	6
Table 2.3: PT plants under construction.....	7
Table 2.4: ST plants in operation & under construction .....	10
Table 2.5: ST plants under planning.....	11
Table 2.6: Merits & Demerits of HTF used in ST plants .....	15
Table 2.7: Information on receiver, HTF & power cycle (operational plants) .....	16
Table 2.8: Information on receiver, HTF & power cycle (under construction) .....	17
Table 2.9 :Parameters of the plants (operational and under construction) .....	19
Table 2.10: Mirror area based on equivalent capacity.....	20
Table 2.11: Land area based on equivalent capacity .....	20
Table 2.12: Tower height and distance of the farthest heliostat from tower .....	23
Table 2.13: Fresnel based power plants in operation, under construction & being planned.....	28
Table 2.14: Details of the Fresnel based solar thermal power plants .....	29
Table 2.15: Dish plants in operation & under construction.....	34
Table 2.16: Dish plants under planning .....	34
Table 2.17: Characteristics of various parabolic dishes .....	35
Table 2.18: Comparison of the capacities of the four types of CSP plants .....	38
Table 2.19: Cost of PT plants (in operation & under construction) .....	39
Table 2.20: Cost of ST plants (in operation).....	39
Table 2.21: Cost of LFR plants (in operation).....	40
Table 3.1: Cost break up of components used in economic assessment .....	67
Table 3.2: Number of staff required for various capacities.....	68
Table 3.3: Staff salaries .....	68
Table 3.4: Equipment maintenance costs.....	69
Table 3.5: Financial metrics used in economic analysis.....	70
Table 3.6: Parameters considered.....	72
Table 3.7: Variation in power block efficiency & reference aperture area with capacity .....	73
Table 3.8: Annual electrical energy generation with SM for various capacities .....	74

Table 3.9: Variation of annual electrical energy per MW with SM, for $t_s= 0, 3 \& 6$ .....	78
Table 3.10: Variation of capacity factor with SM for $t_s= 0, 3$ and 6 hours.....	78
Table 3.11: Variation of maximum annual efficiency and corresponding SM with plant capacity for $t_s= 0, 3$ and 6 .....	81
Table 3.12: Optimized SMs under different conditions .....	94
Table 3.13: Data corresponding to optimum SM for $f_{hb}=0$ .....	95
Table 3.14: Data corresponding to optimum SM for $f_{hb}=0.1$ .....	96
Table 3.15: Data corresponding to optimum SM for $f_{hb}=0.2$ .....	97
Table 3.16: Mirror area and land area details for various thermal storage conditions .....	99
Table 3.17: Hybridization benefit for case of $f_{hb}=0.2$ and $t_s=0$ .....	102
Table 3.18: Effect of storage on benefit of hybridization.....	102
Table 5.1: Sensitivity of capital costs, LCOE and IRR to efficiency of power block.....	122
Table 5.2: Sensitivity of LCOE and IRR to capital cost.....	124
Table 5.3: Sensitivity of LCOE and IRR to loan rate.....	125
Table 5.4: Sensitivity of IRR to assumed tariff .....	126
Table 5.5: Sensitivity of parameters to deviation of SM from optimum.....	127
Table 6.1: Comparison of 50 MW ST system and PT analysis.....	136
Table 6.2: Sensitivity of LCOE & IRR to capital cost.....	137
Table 6.3: Variation of capital cost with annual solar to electric efficiency.....	139
Table 6.4: Variation of LCOE & IRR with annual solar to electric efficiency.....	139
Table 6.5: Sensitivity of LCOE and IRR to solar field cost.....	140
Table 7.1: Novatec Solar’s LFR module configuration .....	144
Table 7.2: Cost of the PT components.....	145
Table 7.3: Cost of components for LFR.....	146
Table 7.4: Techno-economic comparison of a 50 MW capacity MLFR and PT plants.....	149
Table 7.5: Sensitivity of LCOE & IRR to capital cost.....	150
Table 7.6: Sensitivity of IRR to assumed tariff .....	151
Table 7.7: Sensitivity of capital costs, LCOE and IRR to solar to electric efficiency.....	152
Table 7.8: Sensitivity of capital costs, LCOE and IRR to solar field cost.....	154
Table 8.1: Earlier dish systems .....	158

Table 8.2: Summary of dish systems .....	159
Table 8.3: Cost break-up of dish Stirling plant.....	161
Table 9.1: Variation of $\eta_{gross-max}$ for different turbine inlet and outlet temperatures.....	163
Table 9.2: Technical parameters of wet cooling & air cooling options .....	170
Table 9.3: Economic impact of dry cooling option .....	171
Table 10.1: Voltage vs. capacity of generators .....	172
Table 10.2: Transmission costs vs. voltage.....	173
Table 11.1: Projects in bid category .....	175
Table 12.1: Cost breakup of a 50 MW plant with 6 hours of storage .....	184
Table 13.1: Data on manpower for PT plants .....	185
Table 13.2: Data on manpower for ST plants.....	186

## Executive Summary

The Government of India launched the Jawaharlal Nehru National Solar Mission (JNNSM) in January 2010 which targeted 20000 MW of grid connected solar power by 2022. When the mission was announced there was considerable familiarity with solar PV technologies because of their widespread deployment. However there was limited experience with solar thermal technologies. It was also felt that solar thermal technologies would be more cost effective as compared to PV and thus have good potential in India.

The Ministry of New and Renewable Energy (MNRE), Government of India, sanctioned a project titled “Engineering Economic Policy Assessment of Concentrating Solar Thermal Power Technologies in India” to Center for Study of Science, Technology and Policy to study the engineering economic and policy aspects for deployment of Concentrated Solar Power (CSP) in India. This report is an outcome of this project.

Chapter 2 covers the review of global experience of the four main CSP technologies viz. Parabolic Trough (PT), Solar Tower (ST), Linear Fresnel Reflector (LFR) and Parabolic Dish (PD). The total global operating capacity of CSP is 1267 MW, of which 700 MW is in Spain and 468 MW in the US. Further plants of 3653 MW capacity are under construction with 1155 MW in Spain and 1897 MW in the US. The PT is the most matured and commonly used CSP technology at present (1168 MW operating plants and 1377 MW under construction). However, recent trends indicate that ST is also being preferred because of the higher temperatures achievable leading to higher efficiencies (2011 MW under construction). LFR is a relatively simpler technology amenable for indigenization and cost reduction. The global experience has been limited to direct steam generation with this technology (with only 36 MW of operating plants). The Dish Stirling engine despite its high efficiency has had limited success (1.5 MW operating plants) so far because of reliability and costs.

Since PT is the most matured technology, we developed an engineering economic model for analysis of PT under Indian conditions (Chapter 3). This model calculates the reference mirror aperture area based on the hourly Directly Normal Insolation (DNI) data of the location of the plant and the chosen capacity. In this connection, a method was developed to obtain the DNI data for 22 stations in India for which ground based hourly global and diffuse radiation data was available. For the specified thermal storage & hybridization and chosen cost parameters, the model evaluates the Levelised Cost of Electricity (LCOE) and Internal Rate of Return (IRR) for different Solar Multiples (SM). Then the design is based on that SM for which LCOE is a minimum. The results indicate that the estimated capital cost for a 50 MW plant with no thermal storage is around ₹ 15.6 Cr/MW with an LCOE of 14.65 ₹/kWh and a capacity factor of 27%. If six hours of thermal storage is provided, then the capital cost increases to ₹ 26.11 Cr/MW with LCOE of 14.11 ₹/kWh and a capacity factor of 47.3%. The results also indicate that since the efficiency of steam cycle is low for plants of small capacity, they are not economically viable. However it was difficult to obtain precise cost estimates of various components and therefore the above results are subject to uncertainties.

We developed a Graphic User Interface (GUI) tool for the application of the model. This is an interactive tool for a user to input various technical and economic parameters and examine the

impact on the plant performance. The broad features of this tool are described in Chapter 4. This tool is available for public dissemination on MNRE and CSTEP websites.

Chapter 5 discusses the sensitivity of capital cost, LCOE and IRR to uncertainties in power block efficiency, loan rate, SM and tariff. For instance, the results indicate that a 5% increase in power block efficiency reduces LCOE by about 4% and increases IRR by 5%. A reduction in the loan rate from 14% to 8% reduces LCOE from ₹14.18 to ₹11.93 per kWh.

The techno-economic viability of the CSP plants in India using ST, LFR and Dish Stirling technologies are covered in chapters 6, 7 and 8 respectively. The study indicates that ST has several advantages over the PT and therefore it is recommended that this technology be pursued in India. LFR technology, as used presently, viz. Direct Steam Generation (DSG) for power generation permits only buffer storage. Hence, it may not be a viable option. Use of synthetic oil as HTF and molten salt for thermal storage could be considered as an option. Regarding the Dish Stirling engine, the study indicates that commercial viability of such a system has not yet been established so far.

Most CSP plants tend to be located in dry arid regions where water availability will be scarce. Therefore the impact of air condensing option on techno-economic aspects of CSP technologies is discussed in Chapter 9. The primary effect of air-condensing option is that it reduces the efficiency of the power block due to higher turbine outlet temperature. The results for a 50 MW plant indicate that air cooling instead of wet cooling increases LCOE by about 8%.

Chapter 10 gives the basic cost parameters of substation and transmission required to evacuate power generated by the plant.

The present status of CSP plants initiated under Phase I of JNNSM is covered in Chapter 11. Though the projects are scheduled to be completed by May 2013, the information available on the present status of these plants is limited. There is a need for open dissemination and exchange of technical information among all the participants employing CSP technologies.

Chapter 12 deals with the indigenization prospects of CSP technologies in India. The global cost structure of the various components of CSP is considered, from which one can identify the components amenable for indigenization with a possible reduction in cost.

Chapter 13 discusses the man power requirements during the construction and O&M phases. Final chapter enumerates the policy options for large scale deployment of CSP technologies in India.

# 1 Introduction

The Government of India announced a National Action Plan for Climate Change (NAPCC) in 2008. The overall objective was to ensure inclusive economic growth using options that lead to ecological sustainability and reduction in Green House Gas (GHG) emissions. Eight national missions were announced as part of the NAPCC. The Jawaharlal Nehru National Solar Mission (JNNSM) is one of the eight missions, and was launched in January 2010 to provide the much needed impetus to development of solar power in India. It set a target of 20 GW of grid connected solar power by 2022. Photo Voltaic (PV) and Concentrated Solar Power (CSP) are expected to contribute equally to meet this target.

When the mission was announced, the general expectation was that solar thermal would cost lower than that of solar PV. Further, it was expected that solar thermal would be an important contributor because of several reasons. First, unlike PV, solar thermal doesn't require major breakthroughs in fundamental science. It is an engineering challenge and provides an opportunity to achieve lower costs with indigenization and economies of scale. Second, solar thermal power is amenable for hybridization and energy storage, enabling dispatchable power round the clock. This study was undertaken with the objective of assessing the engineering economic viability of CSP technologies in India with focus on the following aspects:

- Global review of the four CSP technologies (Parabolic Trough, Solar Tower, Linear Fresnel Reflector and Parabolic Dish) to provide a bench mark for studies under Indian conditions
- Model for techno-economic analysis for PT with energy storage and hybridization
- A GUI for application of the model for PT
- Sensitivity analysis on cost
- Techno-economic viability of other CSP technologies
- Air condensing option
- Grid connectivity
- Man power requirement
- Present status and policy options

This study indicates that CSP combined with storage and hybridization has a good potential in India.

## 2 Global Experience

### 2.1 Introduction

In order to carry out an engineering economic policy assessment of the CSP technologies in India, it is necessary to carry out a global review of these technologies to get a reference base and guidance. The review is to bring out the present status of the four CSP technologies in terms of their deployment, maturity levels, relative merits and their viability under Indian conditions.

### 2.2 Parabolic Trough

#### 2.2.1 Description

Parabolic Trough (PT) technology is commercially the most proven system for solar power generation. The long term reliability of PT is well proven (Black & Veatch, 2008). A brief description of this technology is given below. Figure 2.1 (Source: <http://whatwow.org/parabolic-trough/a-broad-view-of-parabolic-trough-solar-collectors-at-kramer-junction-in-the-mojave-desert-in-california/> Last accessed: July 2012) shows a view of PT collectors.



**Figure 2.1: Parabolic trough collectors**

Figure 2.2 shows a schematic of a typical CSP plant using two tank storage system. The plant consists of a solar field, where solar energy is converted to thermal energy of the HTF, the power block, where the thermal energy of the HTF is used to operate a conventional steam turbine/generator to produce electricity and an optimal thermal storage system, which permits operation of the power block during cloud cover and when there is no sun-light.

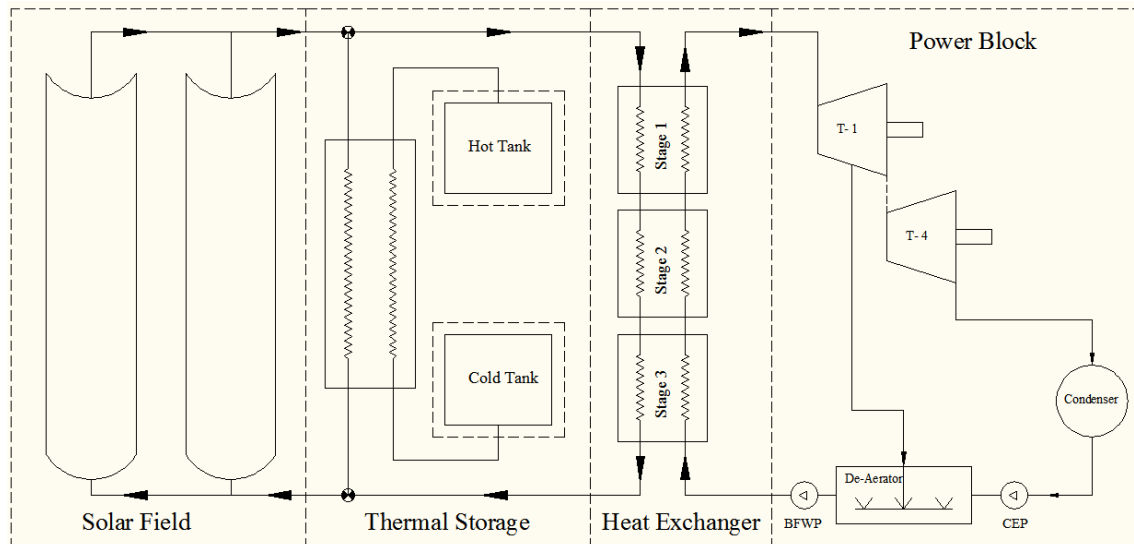


**Figure 2.2: PT plant with two tank thermal storage system**

### **i. Solar Field**

The solar field consists of rows of highly reflective parabolic mirrors mounted on support structures, which can be tilted about an axis (normally aligned in the North – South direction) to track the sun as it moves from East to West. At the focal line of the parabolic mirrors, a specially coated stainless steel tube called the receiver is mounted.

The receiver is encapsulated in a glass tube and the annular space between the glass tube and receiver is evacuated. The receiver tube is given a special coating which along with the evacuated glass cover leads to better absorption and transfer of heat to the HTF flowing inside the receiver. In most of the CSP plants, the aperture width of the parabolic mirrors (composed of 4 segments) is 5.75 m. The outer and inner diameters of the stainless steel receiver are 70 mm and 66 mm respectively and that of the glass cover are 115 mm and 109 mm respectively. The glass cover has an anti-reflecting coating to improve absorption characteristics. As of now, only two companies in the world, SCHOTT and Siemens manufacture and supply these receiver tubes.

The HTF flows in and out from the receiver tubes through header pipes. Since the axis of rotation of the trough assembly is far from the focal line, the receiver tube which is at the focal line moves considerably while the trough is tracking the sun. Therefore, flexible couplings between the header pipes and the receiver tubes are needed. The most commonly used HTF is synthetic oil whose maximum operating temperature is limited to 400°C. Therefore, the maximum outlet temperature of the HTF is limited to 390°C. It may also be noted that the freezing point of HTF is 13°C and hence care must be taken to prevent it from freezing. Since there is a possibility of the synthetic oil catching fire when exposed to atmosphere, the flexible couplings must be leak proof. However, such couplings have been developed and several plants have been operating successfully over many years. During plant operation, the inlet temperature of HTF is normally 290°C, which is dictated by the saturation temperature of steam inlet to the steam cycle.

### **ii. Power Block**

In the power block, the thermal energy acquired by the HTF is transferred to the feed water through heat exchangers to produce superheated steam, which drives the steam turbine coupled to a generator. The steam exiting from the turbine is condensed using wet or dry cooling and the

condensed water goes to the feed water pump which pumps it to the heat exchangers. The heat exchanger is equivalent to the boiler in a conventional power plant. Wet cooling option needs considerable amount of water (approximately 3-4 m<sup>3</sup>/MWh). Therefore availability of water becomes an issue since abundant solar energy is usually associated with arid regions. If air cooling is to be employed due to non-availability of water, cycle efficiency will decrease and the cost of power generation increases.

### iii. Thermal Storage System

Thermal storage is necessary as a buffer to take care of cloud cover, operation of the plant beyond sunset and to meet peak demand. In such a case, the size of the solar field should be more than that required to generate the rated electrical power. The excess solar thermal energy available would be utilized to heat a higher mass flow rate of HTF in the receiver tubes. The designed quantity of HTF would continue to go to the power block heat exchanger while the excess is fed into the storage heat exchanger (Figure 2.2). In this storage heat exchanger, the thermal storage medium from cold tank acquires the excess thermal energy of HTF and the heated storage medium is stored in the hot tank. In a majority of plants, the storage medium is molten salt (a mixture of 60% NaNO<sub>3</sub> and 40% KNO<sub>3</sub> by weight). The maximum amount of thermal storage is dependent on the capacity of the hot and cold tanks and the thermal properties of the storage medium.

During complete cloud cover or after sunset, the inlet and outlet valves of HTF in the solar field would be closed and the HTF returning from the power block heat exchanger would be sent to the storage heat exchanger in the reverse direction and hot storage medium from the hot tank would be sent to the cold tank through the storage heat exchanger. In the process, the HTF gets heated up and feeds the power block heat exchanger in the usual way to enable generation of power. Also, when the DNI values are low and when stored thermal energy is available, it can be used to augment power generation.

## 2.2.2 Deployment of PT

Table 2.1 gives the number of PT plants in operation, under construction and being planned in various countries (CSPToday, 2012). This list excludes plants less than 5 MW capacities. The present global capacity of operating plants is 1168 MW, mostly in Spain and USA. Further, 1377 MW of CSP plants are under construction. It may be noted that Spain followed by USA have the largest installed capacity and also plants under construction. In other countries, only one or two plants are under construction. However, several plants are reportedly planned in various countries. In particular, the USA has plans for 43 plants with a total capacity of about 20 GW. However, it is not clear how many of these planned projects are actually being implemented given the bankability challenge.

### i. Operational Plants

Table 2.1 gives information of the presently operating PT power plants. Out of the 28 operating plants, 14 each are in Spain and in USA.

Some of these plants have thermal storage capacity while others do not have. The total mirror aperture area of the solar field increases depending on the number of hours of storage employed. It is not appropriate to compare the mirror aperture per MW of installed capacity of plants with and without storage. Thus an “equivalent capacity” is computed as follows and the plants are compared based on this.

$$\text{Equivalent capacity} = \text{Rated capacity} \times \left( \frac{\text{Hours of storage} + \text{Nominal operational hours per day}}{\text{Nominal operational hours per day}} \right)$$

**Table 2.1: Country-wise distribution of PT plants**

Country	Operational		Under Construction		Planning	
	No. of Plants	Total Capacity (MW)	No. of Plants	Total Capacity (MW)	No. of Plants	Total Capacity (MW)
Algeria			1	25	3	215
Australia					2	350
China					5	281
Egypt			1	40	2	100
India			1	10	11	590
Iran					1	67
Israel					2	440
Italy			1	5		
Mexico			1	12		
Morocco			1	30	3	275
Spain	14	700	16	800	16	772
Tunisia					2	200
UAE			1	100		
USA	14	468	2	355	43	20377
<b>Total</b>	<b>28</b>	<b>1168</b>	<b>25</b>	<b>1377</b>	<b>90</b>	<b>23667</b>

Table 2.2 gives the basic data (NREL, 2012; CSPToday, 2012) along with derived data viz. equivalent capacity for plants with storage, mirror area/MW of equivalent capacity, ratio of land area to mirror area and overall efficiency of energy conversion. These derived data indicate the operational characteristics of the plants using PT technology. Nine hours of nominal operation has been considered. This brings the mirror area per equivalent capacity for plants with and without storage roughly to the same order of magnitude.

The mirror area varies from 5500 to 7500 m<sup>2</sup>/MW, the average being 6000 m<sup>2</sup>/MW. The land area to mirror area ratio varies from 3.4 to 5.2, the average being 3.8.

The overall conversion efficiency from solar to electric is determined by the following expression:

$$\eta_{s-e} = \left( \frac{\text{Electricity generation expected}}{\text{Incident solar energy} \times \text{Solar field aperture area}} \right) \times 100$$

The overall efficiency is found to vary from 13.5 to 20%. In this above definition, the expected electrical energy generation is assumed to be entirely due to solar. However as seen from Table 2.2 certain fraction of hybridization is allowed in some plants and energy generated due to this has not been separately accounted for. Thus the efficiency figures may not be truly representative of solar to electric conversion.

**Table 2.2: Data on operational PT plants**

Sl. No.	Plant Name	Country	Capacity (MW)	Incident Solar Energy (kWh/m <sup>2</sup> /yr)	Land Area (acres)	Electricity generation expected (MWh/yr)	Solar Field Aperture Area (m <sup>2</sup> )	Hours of Thermal Storage (h)	Hybridization	Equivalent Capacity (MW) (9 hrs day operation)	Mirror Area per MW of Eq. Capacity	Land Area/Mirror Area	Overall Efficiency (%)
1	Andasol-1	Spain	50	2136	494	158000	510120	7.5	12%	91.7	5565	3.92	14.5
2	Andasol-2	Spain	50	2136	494	158000	510120	7.5	12%	91.7	5565	3.92	14.5
3	La Dehesa*	Spain	50		494	175000	552750	7.5	12%	91.7	6030	3.62	
4	La Florida	Spain	50		494	175000	552750	7.5	12%	91.7	6030	3.62	
5	Extresol-1	Spain	50	2168	494	158000	510120	7.5	12%	91.7	5565	3.92	14.2
6	Extresol-2	Spain	50	2168	494	158000	510120	7.5	12%	91.7	5565	3.92	14.2
7	Alvarado I	Spain	50	2174	334	105200				50			
8	Manchasol-1	Spain	50	2208	494	158000	510120	7.5	12%	91.7	5565	3.92	14.0
9	Palma del Río II	Spain	50	2291		114500				50			
10	Puertollano	Spain	50	2061	371	103000	287760			50	5755	5.22	17.3
11	Solnova 1	Spain	50	2012		113520	300000			50	6000		18.8
12	Solnova 3	Spain	50	2012		113520	300000			50	6000		18.8
13	Solnova 4	Spain	50	2012		113520	300000			50	6000		18.8
14	Nevada Solar 1	USA	64	2606	400	134000	357200	0.5		67.6	5288	4.53	14.4
15	SEGS I	USA	13.8	2725	72	30100	82960	3	25%	18.4	4509	3.5	13.3
16	SEGS II	USA	30	2725	166	80500	190338		25%	30	6345	3.52	15.5
17	SEGS III	USA	30	2725	198	92780	230300		25%	30	7677	3.47	14.7
18	SEGS IV	USA	30	2725	198	92780	230300		25%	30	7677	3.47	14.7
19	SEGS V	USA	30	2725	215	91820	250500		25%	30	8350	3.47	13.4
20	SEGS VI	USA	30	2725	163	90850	188000		25%	30	6267	3.51	17.7
21	SEGS VII	USA	30	2725	168	92646	194280		25%	30	6476	3.5	17.5
22	SEGS VIII	USA	89	2725	400	252750	464340		25%	89	5217	3.49	19.9
23	SEGS IX	USA	89	2725	418	256125	483960		25%	89	5438	3.49	19.4

## ii. Plants under Construction

Table 2.3 gives a list of PT plants under construction (CSPToday, 2012). It is to be noted that, out of the 25 plants under construction, 16 are in Spain.

**Table 2.3: PT plants under construction**

Sl. No.	Plant	Country	Capacity (MW)
1	Agua Prieta II Project	Mexico	12
2	Ain-Ben-Mathar ISCC	Morocco	30
3	Andasol 3	Spain	50
4	Archimedes Prototype Project	Italy	5
5	Arcosol 50 (Valle 1)	Spain	50
6	C.SolarTermoelectrica "ASTE-1A"	Spain	50
7	C.SolarTermoelectrica "ASTE-1B"	Spain	50
8	C.SolarTermoelectrica "Astexol-2"	Spain	50
9	Hassi-R'mel ISCC	Algeria	25
10	HelioEnergy 1	Spain	50
11	HelioEnergy 2	Spain	50
12	Helios 1	Spain	50
13	Helios 2	Spain	50
14	Kuraymat ISCC	Egypt	40
15	Lebrija 1	Spain	50
16	MNGSEC	USA	75
17	PL. Termoelectrtica de Palma del Rio I	Spain	50
18	Rajasthan Solar One	India	10
19	Shams 1	UAE	100
20	Solaben II	Spain	50
21	Solaben III	Spain	50
22	Solana	USA	280
23	Solarcor 1	Spain	50
24	Solarcor 2	Spain	50
25	Termesol 50 (Valle 2)	Spain	50

### 2.2.3 New Developments

Even though PT is considered a mature technology, there are further attempts to improve its efficiency and reduce cost. Some examples of such attempts which have been demonstrated on prototypes are discussed below.

#### i. Direct Steam Generation (DSG)

All the operating PT plants use synthetic oil as HTF. At Plataforma Solar de Almería (PSA), Almería, Spain, a test facility has been set up which is capable of generating steam at 400°C at 100 bar. Details of this facility are given in <http://www.sollab.eu/psa.html>. The main advantage with DSG is steam at temperatures higher than 380°C (limit with synthetic oil as HTF) can be obtained. However, there are challenges in dealing with problems viz., control of solar field during solar

radiation transients, two-phase flow inside the receiver tubes and temperature gradients in the receiver tubes. DSG in PT is yet to be commercially proven.

## **ii. Archimede Solar Receiver Tubes**

Archimede Solar Energy, a company in Italy has designed and developed a receiver tube for operating temperatures up to 580°C and 20 bar pressure, to use molten salts as HTF (<http://www.archimedesolarenergy.it/>). The receiver has stainless steel pipe of outer and inner diameters 70 mm and 64 mm respectively. It is enclosed in an evacuated glass tube of 125 mm outer diameter and 119 mm inner diameter. Archimede, a 5 MW plant located in Priolo Gargallo (Sicily), Italy was unveiled in July 2010. This is the first CSP plant in the world to use molten salt as HTF and for storage. This plant is integrated with an existing combined cycle gas power plant. One of the problems in using molten salt as HTF in a PT is prevention of its freezing (freezing point 220°C) in the receiver tubes. This problem seems to have been resolved in this facility. Further details are not available.

## **iii. Flabeg's Ultimate Trough**

Flabeg is one of the leading mirror manufacturers for CSP industry (<http://www.flabeg.com/>). It has developed a solar collector, 'The Ultimate Trough' which has an aperture width of 7.5 m. Therefore, for the same total mirror aperture area, the number of loops and controls reduces. The Ultimate Trough is claiming a 25% cost benefit compared to the current Euro Trough (FLABEG, 2012). A prototype is being tested at SEGS VIII plant for validation of performance improvements.

## **iv. Gossamer Solar Trough Frame**

Gossamer has promoted aluminium space frames as support structures for PT solar collectors. Such frames have been used in Nevada Solar One (<http://www.gossamersf.com>). Jointly with 3M, they have come with a prototype Minitruss™ reflective panel of 7 m aperture width which uses a 3M solar mirror films, glued to a backup honeycomb structure. The advantages claimed for the Minitruss™ are lower cost, greater durability and an open-back design that does not trap water.

R&D on the various other components of the PT is reviewed by Kearney (Kearney, 2010).

## **2.2.4 Merits and Demerits of PT**

### **Merits**

- It is a proven technology with more than 1000 MW of operating plants.
- Supply chain for the components is reasonably well established.
- Thermal storage is proven.
- It permits ease of hybridization with fossil fuels (such as natural gas or biomass) thus increasing the capacity factor of the plant.

### **Demerits**

- Limitation in temperature with the use of HTF (synthetic oil) to less than 400°C limits the efficiency of the overall system.
- HTF leakage will lead to fire hazards.
- Complex ball joints and flexible piping are required between receiver and header pipes.
- Near flat land with less than 3° slope is required.
- Molten salt is difficult to use as HTF because of the high freezing point (freezes at 220°C) and it is difficult to drain the salts from the horizontal receiver tubes.

## 2.3 Solar Tower

### 2.3.1 Description

Solar Tower (ST), also called Central Receiver, uses a large number of heliostats, having dual axis control (one about the vertical axis and other about the horizontal axis) to reflect solar radiation to a stationary receiver located at the top of a tower. The concentrated solar energy impinging on the receiver is converted to thermal energy by the HTF passing through the receiver. The thermal energy of the HTF is transferred to the working fluid of a conventional power block to generate electrical power.

The potential advantage of ST is that a high concentration ratio from 200 to 1000 can be achieved. Consequently, temperatures of the order of 1000°C can be reached with suitable HTFs. This high temperature results in higher power cycle efficiency. Potentially, an overall conversion efficiency of around 25% can be achieved.

Thermal energy storage and hybridization can be incorporated as in PT. Further, molten salt can be used both as HTF and thermal storage medium.

Given the potential of higher efficiency, ST with molten salt/water as HTF has gained momentum in recent years. However, there are a lot of variations in the design of heliostats, receivers, HTF and even in the power block. Hence, a common description for all the power plants is not possible. Therefore, all the alternatives employed in the plants so far built have been considered. It must be pointed out that details of the components are not available in open literature. A typical ST plant (Solar Two) is shown in Figure 2.3. (Source: [http://www.sustainableworld.org.uk/solar\\_two.htm](http://www.sustainableworld.org.uk/solar_two.htm); last accessed: November, 2012)



**Figure 2.3: Solar Two – demonstration ST plant**

Basic information on ST plants in operation and under construction is given in Table 2.4 and those under planning in Table 2.5.

**Table 2.4: ST plants in operation & under construction**

Plant	Country	Developer	Capacity (MW)	No of Heliostats	Heliostat Aperture Area (m <sup>2</sup> )	Receiver Aperture (m <sup>2</sup> )	Tower Height (m)	Heliostat Supplier	Receiver to Heliostat Aperture
<b>Operational</b>									
Gemasolar	Spain	Torresol Energy	19.9	2650	120		140	Sener	
Jülich Solar Tower	Germany	Kraftan lagen	1.5	2153	8	23	60		2.88
PS-10	Spain	Abengoa Solar	11	624	120	65.22	115	Abengoa	0.54
PS-20	Spain	Abengoa Solar	20	1255	120		165	Abengoa	
Sierra Sun Tower	USA	eSolar	5	24360	1.14		55	eSolar	
Solar Energy Center	Australia		0.5	170	4.49		25		
ACME	India	ACME, eSolar	2.5	14280	1.14		46	eSolar	
<b>Under Construction</b>									
ACME Bikaner	India	ACME, eSolar	7.5	42840	1.14		46	esolar	
ISEGS	USA	Bright Source	392	214000	14.08		140		
Crescent Dunes	USA	Solar Reserve	110	17170	62.4		165	Pratt & Whitney	
Rice Solar Energy	USA	Solar Reserve	150	17170	62.4		165	Pratt & Whitney	
Bright Source (PG&E 3,4,5,6,7)	USA	Bright Source	200x5						
Khi Solar One	RSA	Abengoa Solar-IDC	50	4530	128		200		
Dahan	China	STPT &SD	1	100	100	25	64,78, 92		0.25
Supcon Solar Project	China	Supcon Solar	50	217440	2		80		
Gaskell Sun Tower	USA	eSolar; NRG Energy	245						
IEECAS	China		1						
Lake Cargelligo	Australia		3						
THEMIS (PEGASE)	France		1.4	201			100		

**Table 2.5: ST plants under planning**

Plant	Country	Developer	Capacity (MW)
Alpine Sun Tower	USA	eSolar	92
Black Rock Hill	USA	Solar Reserve	600
Bright Source SCE	USA		1200
Crossroads Solar Energy	USA		150
ESKOM	RSA		100
eSolar1	USA	NRG Energy	84
eSolar2	USA	NRG Energy	56
GD energy	China		100
Imperial Valley Solar Project	USA	Tessera Solar	709
La Paz Solar Tower	USA	Enviro Mission	200
LSR Jackrabbit	USA	LSR Jackrabbit	500
Quartzsite	USA	Solar Reserve	100
Saguache Solar	USA	Solar Reserve	200
Santa Teresa New Mexico Sun Power Tower	USA	eSolar	92
Solar Gas	Australia		4
Wildcat Harcuvar South	USA	Wildcat Harcuvar South LLC	4 x 200
Wildcat Quartzsite	USA		800

The major components involved in the Solar Tower system are explained below.

### **i. Heliostats**

Heliostats are flat or slightly curved mirrors mounted on a backup steel structure, which can be controlled about two axes, one horizontal and other vertical, so as to tilt the heliostats to reflect the solar rays to a fixed receiver on top of a tower. The aperture areas of the heliostats that have been used in various plants vary considerably from 1 to 120 m<sup>2</sup>, but all heliostats within a plant have the same aperture area.

Some developers use small heliostats and claim that the advantages are mass production, easy handling & installation, smaller wind loads because of size and proximity to ground. Heliostats of 1 m<sup>2</sup> would have a single flat mirror. However, for the total mirror aperture area required for the solar field, the number of heliostats and controllers will increase.

The heliostat of 120 m<sup>2</sup> area (William & Michael, 2001; DLR, 2005) has 28 curved facets (seven rows & four columns). When such large heliostats are used, each facet has to be canted properly, so that the receiver could be made as small as possible and to increase the concentration ratio. However, the number of heliostats and controls is reduced. But the structure of the heliostat has to withstand large wind loads and the control system has to be more powerful.

It can be seen from Table 2.4 that heliostat size is one of the important parameters in the design of the ST system.

## ii. Receivers

Since the concentration ratio in case of ST is in the range of 200 to 1000, the solar heat flux impinging on the ST receivers is also in the range from 200 to 1000 kW/m<sup>2</sup>. Thus, high temperatures of the order 1000°C are possible. Even though the temperature is high in the case of ST receiver, the thermal loss from the receiver is comparatively lower than that from the receivers of PT or LFR, since the surface area of the receiver is less.

There are mainly two types of receivers: tubular and volumetric. Tubular receivers are used for liquid HTF such as water, molten salt, thermic oil, liquid sodium and Hitec salt, whereas volumetric receivers use air as HTF. The type of receiver depends on the type of HTF and power block (Rankine or Brayton) used in the system.

### a. Tubular Receivers

In tubular receivers, the HTF passes through a number of vertical tubes and get heated by the radiant flux reflected from the heliostats. There are two types of tubular receivers: External cylindrical receivers and cavity receivers.

#### i. External Cylindrical Receivers

Here the vertical tubes are arranged side by side in a cylindrical fashion and the radiant flux from the heliostats impinges from all directions (Figure 2.4). Since the receiver is exposed to atmosphere, it is subjected to higher convection losses.



**Figure 2.4: External cylindrical receiver used in Solar Two**

#### ii. Cavity Receivers

The cavity receiver consists of welded tubes kept inside a cavity to reduce convection losses. The heliostat field is built exclusively within the range of possible incident angles onto the receiver. The photograph of the cavity receiver used in the PS 10 plant is shown in Figure 2.5.



**Figure 2.5: Cavity receiver used in PS-10**

*b. Volumetric Receivers*

Receivers which use air as HTF are made of porous wire mesh or metallic/ceramic foams. The solar radiation impinging on the volumetric receivers is absorbed by the whole receiver. Volumetric receivers are two types: open volumetric and closed/pressurized volumetric.

*i. Open Volumetric Receivers*

In open volumetric receivers, ambient air is sucked through the porous receiver where air gets heated up by concentrated solar energy. The front end of the receiver will have less temperature than inside the receiver because the incoming air from the ambient cools the surface and avoids damage to the material by maintaining low temperatures at front end of the receiver. Jülich tower plant uses a porous silicon carbide absorber module. The air gets heated up to about 700°C and it is used to generate steam at 485°C, 27 bar in the boiler to run the turbine. The schematic representation of the open volumetric receiver used in Jülich Plant is shown in Figure 2.6 (Geritt, et al., 2009).

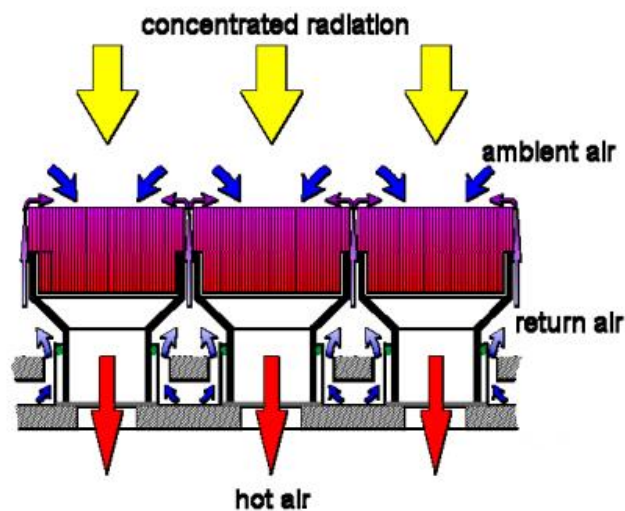


**Figure 2.6: Schematic of open volumetric receiver**

### ii. Closed Volumetric Receivers

Closed volumetric receivers are also called as pressurized volumetric receivers, in which the HTF (usually air) is mechanically charged to the receiver by a blower and the receiver aperture is sealed by a transparent window. The HTF will get heated up at the dome shaped portion of the receiver by the concentrated solar energy and the heated air will be used either in a Rankine cycle via heat exchanger or in a Brayton cycle for generating electricity. The schematic of a closed volumetric receiver is shown in Figure 2.7 (SOLGATE, 2005).

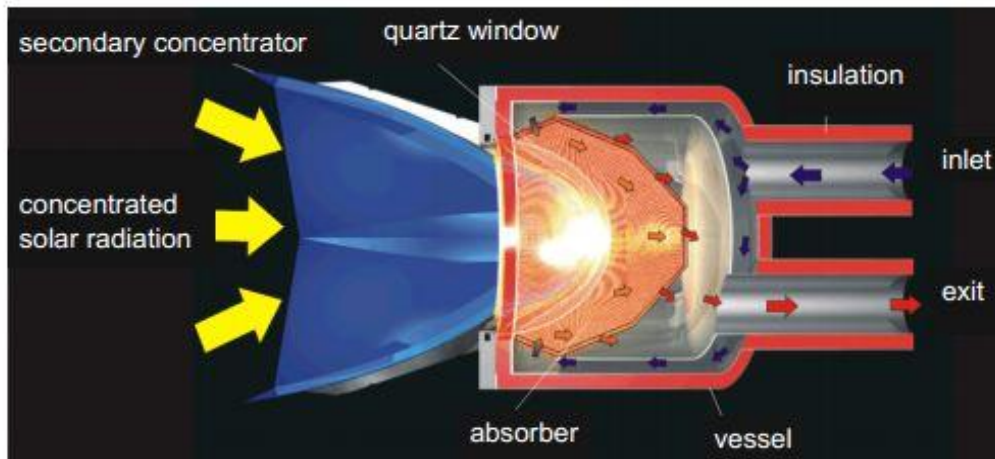


**Figure 2.7: Schematic of the pressurized volumetric receiver**

### iii. Heat Transfer Fluid and Power Cycle

Different types of HTFs can be used in ST based on the type of receiver and power cycle employed in the system. The HTF used in the operational ST plants are water, molten salt and air. Other possible candidates are liquid sodium, Hitec salt and synthetic oil. The merits and demerits of these HTFs are given in Table 2.6.

When water is used as HTF, the solar field generates steam directly and the Rankine steam cycle is used for power generation.

In the case of molten salt as HTF, a heat exchanger is used to transfer the thermal energy to water to generate steam. Rankine steam cycle is used for power generation. Use of molten salt as HTF permits easy thermal storage. When the plant is not in operation, HTF from the receiver has to be drained out.

One of the potential advantages envisaged in ST technology is use of compressed air as HTF to raise its temperature to about 1000°C to run a turbine on Brayton Cycle. This is yet to be proven commercially; however a demonstration plant is being tried out in Australia (Tania, 2011) and also at Solar Energy Centre, Gurgaon by SunBorne Energy, India. The Jülich plant (Geritt, et al., 2009) uses air as the HTF in an open cavity receiver and transfers its heat through a heat exchanger to water which is used as a working fluid in the steam Rankine cycle.

**Table 2.6: Merits & Demerits of HTF used in ST plants**

HTF	Merits	Demerits
Water	<ul style="list-style-type: none"> <li>• For steam Rankine cycle, water being the working fluid, the need for heat exchanger is eliminated.</li> <li>• Eliminates the costs associated with the salt or oil based HTFs.</li> </ul>	<ul style="list-style-type: none"> <li>• Dissimilar heat transfer coefficients in liquid, saturated vapour and superheated gas phases. Consequent problems with temperature gradient and thermal stress to be tackled</li> <li>• Flow control problems with varying solar flux</li> <li>• Thermal Storage for long hours difficult</li> </ul>
Molten Salt (KNO <sub>3</sub> + NaNO <sub>3</sub> )	<ul style="list-style-type: none"> <li>• Stable and non-toxic</li> <li>• High thermal conductivity and thermal capacity.</li> <li>• Operating temperatures can go up to 560°C.</li> <li>• Environmentally benign.</li> </ul>	<ul style="list-style-type: none"> <li>• High melting point (~222°C); Needs auxiliary heating to prevent solidification</li> </ul>
Air	<ul style="list-style-type: none"> <li>• High temperatures of the order of 1000°C can be utilized.</li> </ul>	<ul style="list-style-type: none"> <li>• Poor heat transfer properties (conductivity and film coefficient etc.) compared to other fluids.</li> <li>• Complex receiver design</li> </ul>
Liquid Sodium	<ul style="list-style-type: none"> <li>• Higher solar field outlet temperatures are possible and thus higher power cycle efficiencies</li> <li>• Low Melting Point (97.7°C)</li> <li>• High boiling point (873°C)</li> </ul>	<ul style="list-style-type: none"> <li>• Handling is difficult</li> <li>• Accidental leakage is highly hazardous</li> </ul>
Hitec Salt	<ul style="list-style-type: none"> <li>• Melting point is 142°C</li> </ul>	<ul style="list-style-type: none"> <li>• Temperatures are limited to less than 535°C</li> </ul>
Synthetic Oil	<ul style="list-style-type: none"> <li>• Freezes at 15°C</li> </ul>	<ul style="list-style-type: none"> <li>• Operating temperature is limited to about 390°C which limits the efficiency of power cycle</li> </ul>

Information about receivers, HTF and power cycle for various plants, which are in operation and under construction are given in Table 2.7 and Table 2.8 respectively (CSPToday, 2012; NREL, 2012). Among the plants in operation, three plants use cavity tubular receivers with water as HTF coupled with Rankine power cycle. Jülich solar tower uses volumetric receiver with air as HTF. Among the plants under construction (Table 2.9), information is available only for five plants. Two of them use cavity receivers and three of them use external receivers. Three of them use water as HTF while the other two use molten salt as HTF. All of these use Rankine power cycle. When water is used as the HTF, the maximum outlet temperature is only 566°C and clearly, full potential of temperatures up to 1000°C has not yet been capitalised. For the plants under planning (Table 2.5), very limited information is available.

**Table 2.7: Information on receiver, HTF & power cycle (operational plants)**

Plant	Capacity (MW)	Receiver Type	Receiver Aperture (m <sup>2</sup> )	Receiver supplier	HTF	Receiver Temperature (°C)		Power Cycle	Power Cycle inlet		Cooling Method
						Inlet	Outlet		Pressure (bar)	Temp (°C)	
Gemasolar	19.9				Molten Salt	290	565	Rankine			Wet
Jülich Solar Tower	1.5	Volumetric	23		Air	120	680	Rankine	26	485	Wet, Dry
PS-10	11.02	Cavity	65.22	Tecnicas Reunidas	Water	50	250-300	Rankine	45	250-300	Wet
PS-20	20	Cavity			Water		250-300	Rankine	45	250-300	Wet
Sierra Sun Tower	5	Dual-cavity & external		Babcock & Wilcox	Water	218	440	Rankine	60	440	Wet
ACME	2.5				Water						

**Table 2.8: Information on receiver, HTF & power cycle (under construction)**

Plant	Capacity (MW)	Receiver Type	Receiver Aperture (m <sup>2</sup> )	Receiver supplier	HTF	Receiver Temperature (°C)		Power Cycle	Power Cycle		Cooling Method
						Inlet	Outlet		Inlet Pressure (bar)	Inlet Temp (°C)	
ACME Bikaner	7.5				Water						
IGES	392	External Rectangular		Riley Power	Water	249	566	Rankine			Dry
Crescent Dunes	110	External-Cylindrical			Molten Salt	288	566	Rankine	115		Hybrid
Rice Solar Energy	150	External-Cylindrical		Pratt & Whitney	Molten Salt	288	566	Rankine	115		Dry
Bright Source PG&E 3,4,5,6 & 7	5 units of 200										
Gaskell Sun Tower	105-245										
Dahan	1	Cavity	25		Water		400	Rankine	28	400	
Supcon Solar Project	50										
IIEECAS	1										
Lake Cargelliogo	3										
Solar Brayton Cycle	0.2										
THEMIS (PEGASE)	1.4	Cavity			Molten Salt	250	450		50	430	
Khi Solar One	50				Water			Rankine			

### 2.3.2 Deployment of ST

Important information such as capacity, solar resource, land area used, total heliostat aperture area, number of hours storage etc., of the ST plants are presented in Table 2.9 for plants in operation and under development. From this data, one can observe that the mirror area and land area per MW of rated capacity vary from plant to plant due to variations in thermal storage hours. Hence it is necessary to normalise the mirror/land area requirements taking into consideration the number of hours of thermal storage.

#### *i. Mirror & Land Area per MW of Equivalent Capacity*

In order to take into account the thermal storage, it is assumed the plant with no thermal storage can nominally operate for nine hours. If  $x$  hours of thermal storage have been provided, then the mirror area and correspondingly the land area has to be increased  $(9+x)/9$  times compared to the plant with no thermal storage.

Table 2.10 and Table 2.11 give these normalised values of the mirror area and land area respectively. The values of mirror area per MW of equivalent capacity ( $\text{m}^2/\text{MW}$ ) of operating plants range from 5534 to 6750. The average value excluding Jülich plant is  $6183 \text{ m}^2/\text{MW}$ . Jülich plant has been excluded in averaging as it is a demonstration plant where air is HTF and whereas the working fluid is water used in a Rankine cycle leading to poor efficiency. The values of land area per equivalent capacity ( $\text{m}^2/\text{MW}$ ) range from 21,295 to 45,188, average value being  $35,582 \text{ m}^2/\text{MW}$ . This could be used as guidance value for plants being planned in India. ACME and Sierra use the e-Solar's technology for modular heliostat layout which requires less land area as seen in Table 2.9.

#### *ii. Overall Efficiency of Conversion of Solar to Electric Energy*

The efficiency of conversion of solar to electrical energy is as follows:

$$\eta_{s-e} = \frac{\text{Expected Annual Electricity Generation (MWh)}}{\text{Annual Solar Resource (MWh/m}^2) \times \text{Heliostat Field Area(m}^2)}$$

The values of overall efficiency are also included in Table 2.9 and range from 15.51 to 17.30%.

**Table 2.9 :Parameters of the plants (operational and under construction)**

Plant	Capacity (MW)	Incident Solar Energy (kWh/m <sup>2</sup> /yr)	Land Area (m <sup>2</sup> )	Heliostat solar Field Aperture Area (m <sup>2</sup> )	Electricity generation expected (MWh/yr)	TES (hours)	Equivalent Capacity (MW) (based on 9 hrs of nominal operation)	Total Solar Energy (MWh/yr)	Land area to Heliostat Aperture	Efficiency (%)
<b>Operational</b>										
Gemasolar	19.9	2172	1.95E6	318000	110000	15	53.07	690696	6	15.93
Jülich Solar Tower	1.5	902	1.80E5	18000	1000	1.5	1.75		10	
PS-10	11.02	2012	5.50E5	75000	23400	1	12.24	150900	7	15.51
PS-20	20	2012	8.00E5	150000	48000	1	22.22	301800	5	15.9
Sierra Sun Tower	5	2012	8.10E4	27670		0	5	72744	3	
ACME	2.5	1919	7.08E4	16279		0	2.5	31239	4.3	
<b>Under Construction</b>										
ACME Bikaner	7.5	1919	7.08E4	16279		0	2.5	31239	4.3	
Ivanpah Solar	392	2717	142E5	2295960	1079232	0	392	6238123	6.1	17.3
Crescent Dunes	110	2685	64.8E5	1071361	485000	10	232	2876604	6	16.86
Rice Solar Energy	150	2598	57.1E5	1071361	450000			2783395	5.3	16.17
Bright Source PG&E 3, 4, 5, 6, 7	5 Units of 200				573000					
Gaskell Sun Tower	245		445E4		515100					
Dahan	1									
Supcorn Solar	50		330E4	434880						
IEECAS	1									
Lake Cargelliogo	3									
THEMIS (PEGASE)	1.4									
Khi Solar One	50			580000	190000	2	61			

**Table 2.10: Mirror area based on equivalent capacity**

Plant Name	Capacity (MW)	TES (hours)	Equivalent Capacity	Mirror Area (m <sup>2</sup> )	Mirror Area (m <sup>2</sup> ) per MW of	
					Rated Capacity	Equivalent Capacity
<b>In Operation</b>						
Gemasolar	19.9	15	53.07	318000	15980	5992
PS-10	11.02	1	12.24	75000	6806	6125
PS-20	20	1	22.22	150000	7500	6750
ACME	2.5	0	2.4	16279	6512	6512
Sierra	5	0	5.0	27670	5534	5534
Jülich	1.5	1.5	1.75	18000	12000	10286
<b>Under Construction</b>						
Crescent	110	10	232.22	1071361	9740	4614
Ivanpah	392	0	392.0	2295960	5857	5857
Rice Solar	150	8	283.33	1071361	7142	3781
ACME	7.5	0	7.5	48837	6512	6512

**Table 2.11: Land area based on equivalent capacity**

Plant Name	Capacity (MW)	TES (hours)	Equivalent Capacity	Land Area (m <sup>2</sup> )	Land Area (m <sup>2</sup> ) per MW of	
					Rated Capacity	Equivalent Capacity
<b>In Operation</b>						
Gemasolar	19.9	15	53.07	1.95E6	97990	36746
PS-10	11.02	1	12.24	5.50E5	49909	44918
PS-20	20	1	22.22	8.00E5	40000	36000
ACME	2.5	0	2.4	7.08E4	28320	28320
Sierra	5	0	5.0	8.10E4	16200	16200
Jülich	1.5	1.5	1.75	1.80E5	120000	102857
<b>Under Construction</b>						
Crescent	110	10	232.22	6.48E6	58909	27904
Ivanpah	392	0	392.0	1.42E7	36224	36224
Rice Solar	150	8	283.33	5.71E6	38067	20153
ACME	7.5	0	7.5	2.12E5	28320	28320

### **iii. Heliostat Field Layout**

Layout of the heliostat field for Gemasolar, PS 10 & PS 20, Sierra Sun tower and Jülich plants are shown in Figure 2.8, Figure 2.9, Figure 2.10 and Figure 2.11.



**Figure 2.8: Heliostat field at Gemasolar, Spain**



**Figure 2.9: Heliostat field for PS 10 and PS 20, Spain**



**Figure 2.10: Heliostat field at Sierra Sun Tower, USA**



**Figure 2.11: Heliostat field of Jülich plant, Germany**

From these figures, one can infer that unlike the PT or LFR, the layout of the heliostats does not conform to any particular norm.

It is interesting to note that all these plants (except Jülich) are located at nearly the same latitude ( $34^{\circ}43'$  to  $37^{\circ}56'$ ) but the layouts are different because of different types of receivers used. At these latitudes, sun is due south throughout the year. Therefore in PS 10 and PS 20 plants, using single cavity receivers, it is appropriate to locate all heliostats to the North of the tower. Gemasolar uses an external cylindrical receiver, consequently the heliostats are located all around the tower, but greater number of heliostats is on the northern side. e-Solar uses smaller sized heliostats ( $\sim 1 \text{ m}^2$ )

and uses a modular heliostat field. Since dual cavity receivers are used, heliostats are located on both sides of the tower. Depending on the capacity of the plant, multiple modules are used and steam collected from each tower is fed to a common turbine (<http://www.esolar.com/solution.html>).

Thus the heliostat field layout is closely linked with the choice of the receiver and other design considerations.

#### iv. Tower Height

Table 2.12 gives the available information on tower heights and the distances of the farthest heliostat from tower. From Table 2.12 and Figure 2.12 no correlation is evident between the tower height and equivalent capacity of the plant. Once the capacity of the plant, the thermal storage and solar resource are known, the land and mirror area can be determined. Then based on the type of receiver and design, the heliostat field can be designed. However, the basis on which the height of the tower is fixed is not clear. From Table 2.12, the ratio of the farthest distance of the heliostat to the tower height is between 5.7 and 6.8 for most of the plants. However, for Ivanpah Solar Energy Generating Systems (ISEGS) plant, it is higher of the order of 10, while for Sierra Sun tower plant and Jülich plant, it is much smaller. As  $r/h$  increases, the blockage effect increases and also as ' $r$ ' becomes more than 1 km, attenuation losses increase. So it is a bit surprising that for ISEGS plant ' $r$ ' is of the order of 1400 m and  $r/h$  is more than 10. It is felt that, it is better to restrict  $r/h$  to less than seven and ' $r$ ' to 1 km.

**Table 2.12: Tower height and distance of the farthest heliostat from tower**

Plant	Capacity (MW)	TES (hours)	Eq. Capacity (MW)	Height (m)	$r/h$
ACME	2.5	0	2.5	46	
Sierra	5	0	5.0	55	2.3
Jülich	1.5	1.5	1.8	60	2.3
Supcon	5	0	5.0	80	
PS 10	11	1	12.2	115	6.8
Gemasolar	19.9	15	53.1	140	6.7
ISEGS	130	0	130.0	140	10.4
PS 20	20	1	22.2	165	5.7
Crescent dunes	110	10	232.2	165	
Rice Solar	150	8	283.3	165	
CrossRoads	150	10	316.7	200	
Khi Solar One	50	2	61.1	200	

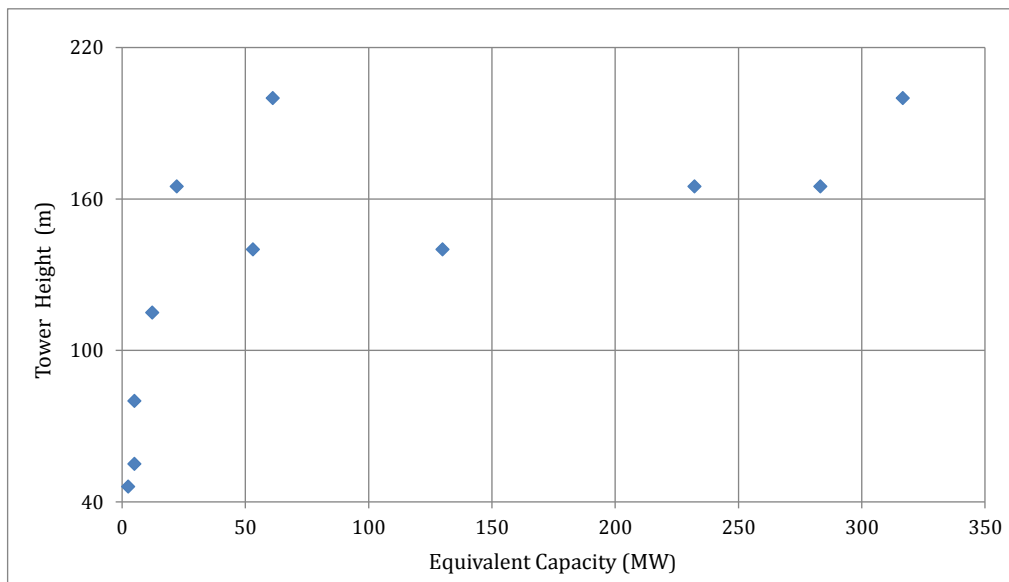


**Figure 2.12: Tower height variation with equivalent capacity for various plants**

### 2.3.3 Merits and Demerits of ST

The merits and demerits of the ST technology are given below:

#### Merits

- High concentration ratio and the consequent higher temperature (800 to 1000°C) for HTF can be achieved. High temperatures will lead to higher power cycle efficiency.
- Adverse effect on the power cycle efficiency in case of dry cooling option is less in ST compared to PT, due to higher inlet temperature.
- A slight slope of the order of 5° in land is acceptable for the heliostats, unlike the PT where near flat land is needed.
- There exists flexibility in using different type of HTFs such as water, air, thermic oil, molten salt etc.
- The use of air as working fluid in the Brayton cycle will avoid the use of water needed in wet cooling of the Rankine cycle. Even with Rankine cycle, because of higher temperature of operation, the adverse impact of air cooling is less in ST technology.
- Flat mirrors can be used in solar field which reduces the cost.
- Higher temperatures allow greater temperature differentials in the storage system. This reduces the cost of the thermal storage system.
- Combined Brayton cycle and bottoming steam Rankine or Organic Rankine Cycle (ORC) has the potential to achieve high overall efficiency.

#### Demerits

- Needs a large number of heliostats and controls
- Two axes tracking with precision control required
- Still an evolving technology compared to PT; supply chain not yet well developed

## 2.4 Linear Fresnel

### 2.4.1 Description

CSP Technology using Linear Fresnel Reflector (LFR) is a more recent development. It is also a line focusing system similar to PT. However, there are notable differences between the two technologies in the solar field and the receiver.

#### i. Solar Field

Figure 2.13 (Source: <http://www.solarpowergroup.com/>) shows the photograph of a LFR system.



**Figure 2.13: Linear Fresnel Reflector system**

It uses an array of flat or slightly curved mirrors (normally aligned in the N-S axis) to reflect solar radiation on to a linear receiver, which is stationary. Slight curvature in the mirrors is needed to reduce the receiver aperture area. The curvature is obtained by elastic bending of the flat mirror, unlike the complex process needed in case of PT mirrors. Fresnel flat mirrors are relatively small in size and are mounted closer to the ground where wind loads are much less. It is therefore likely that the overall cost of structure and solar field may be less for the LFR system compared to PT, even with the reduced optical efficiency of LFR (Buie, Dey, & Mills, 2002; Mills & Morrison, 2000).

Optical efficiency is low in the LFR due to the following reasons:

- (a) Since the receiver is stationary, the principal axes of the mirrors of LFR do not pass through the receiver, but bisects the direction of the sun's beam and the line joining the mirror and the receiver. Thus, a sharp line focus is never formed even when slightly curved mirrors are used. If slightly curved mirrors are not used, the spread will be even more, particularly if the chord of the mirror is large.
- (b) The above also means that the  $\cos \theta$  effect for LFR is more than that of PT.

It may be pointed, that these arrays of flat or slightly curved mirrors, though tilted differently with respect to each other, need the same amount of incremental rotation to track the sun. Therefore a single control system can be employed to tilting the arrays.

A modified version of LFR is the Compact Linear Fresnel Reflector (CLFR). Figure 2.14 shows the difference between LFR and CLFR. In CLFR, solar radiation is reflected to either one of the two receivers depending on the sun's position. It is claimed that this feature decreases the shadowing and blockage effects and consequently requires less land area than the LFR. This claim (Mills & Morrison, 2000) is made based on the ray diagram corresponding to noon conditions as shown in Figure 2.14.

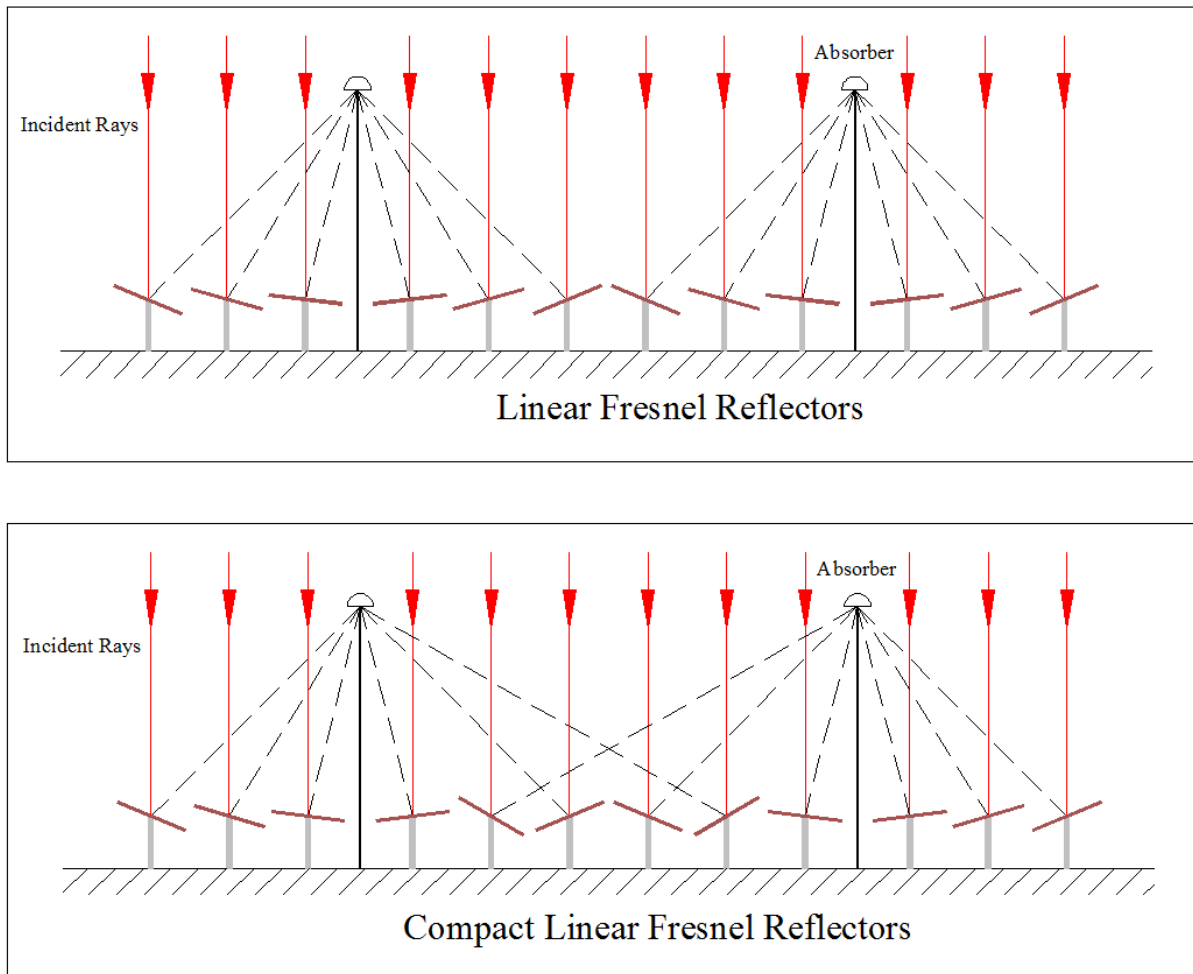


**Figure 2.14: Schematic diagram of LFR and CLFR**

## ii. Receiver

As stated earlier, unlike the PT reflector, LFR does not have a sharp line focus. Therefore, the small diameter receiver tube, similar to PT, cannot be used. Further, the width of the mirrors used varies from 0.5 m to 2 m, leading to a variation in aperture width of the receiver from 0.3 m to 1 m. Thus, a standardized receiver configuration has not yet evolved. Enclosing the receiver in a transparent tube and evacuating the annular space is complex. Hence, all receivers have a transparent cover (without evacuation) at the bottom to reduce convection losses. Also, the aperture width over which the reflected beams from the LFR impinge is wider than the width of single tube receivers. In such cases, secondary reflectors are employed to redirect the beams that do not impinge on the

receiver in the first instance. The thermal efficiency of the Fresnel receivers is less than that of the receivers in PT because of non-evacuated receivers and cosine losses. However, one great advantage of Fresnel system is that the receivers are stationary.

Some examples of the receivers that are employed in the Fresnel system are shown in Figure 2.15. Novatec Solar uses a single receiver tube with secondary reflector, whereas Ausra/AREVA uses multiple receiver tubes without secondary reflectors (Source: Novatech and Ausra/AREVA company websites).

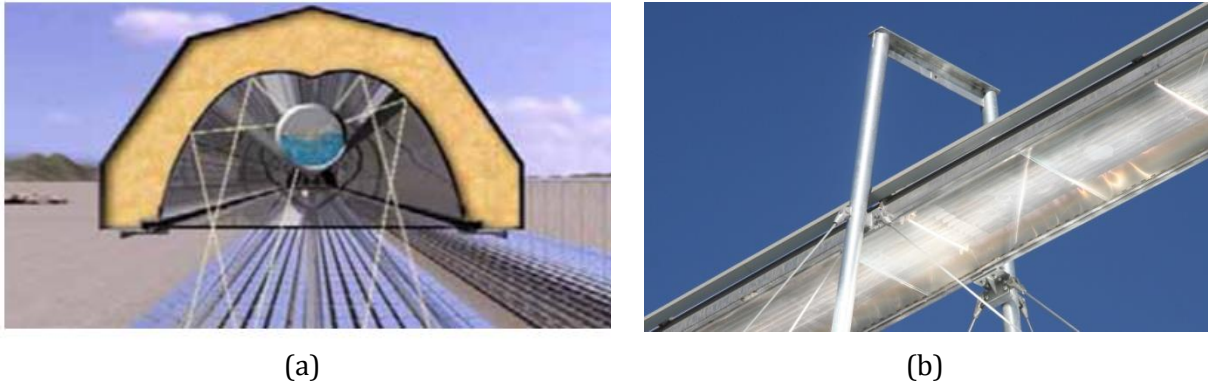


**Figure 2.15: Fresnel receiver types: (a) Novatech's design (b) Ausra's design**

### iii. Heat Transfer Fluid

Water is the HTF in all the Fresnel plants and direct steam generation is the common mode of operation. This is due to the advantage derived by elimination of HTF and heat exchanger in the system.

It must however be mentioned that in steam generation, both liquid and vapour phases coexist in the horizontal tubes with associated problems of instability due to phase change. It also causes inhomogeneous temperature distributions due to differences in heat transfer coefficients of liquid and vapour, which may lead to large thermal stresses. These problems would be severe if superheated steam is to be generated.

### iv. Thermal Storage

When direct steam generation is employed with LFR, only buffer thermal storage in the form of steam accumulator is possible. Since steam accumulator occupies large volume, extensive usage of thermal storage is not a viable option. Figure 2.16 (Tamme, 2006) shows the schematic of such a storage system. Efficiency of the system varies from 90 - 94%.

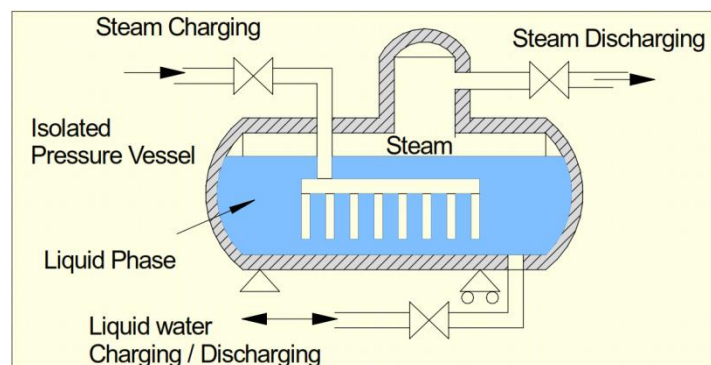


**Figure 2.16: Schematic of Ruths tank storage system**

## 2.4.2 Deployment of Linear Fresnel

Table 2.13 gives a list of Fresnel based power plants in operation, under construction and planned (CSPToday, 2012; NREL, 2012). The total capacity of all the plants in operation is only 36.65 MW. Plants under construction are 264.5 MW and plants planned about 936 MW. The present utilization of Fresnel technology is extremely small compared to that of PT or ST.

Though the indicated capacity of plants being planned is quite high, technical details are not available. Among the plants under construction also, no technical data are available for Himin Solar and Rajasthan Sun Technique power plants.

**Table 2.13: Fresnel based power plants in operation, under construction & being planned**

Sl. No	Plant	Country	Location	Developer/EPC	Capacity (MW)
<b>Operating</b>					
1	Augustin Fresnel 1*	France	Targassonne	Solar Euromed	0.25
2	Liddell	Australia	Lake Liddell, NSW	Solar Heat and Power Ltd.	1**
3	Liddell Phase 2	Australia	Lake Liddell, NSW	AREVA	3**
4	Puerto Errado 1	Spain	Sevilla	Novatec Solar Espana	1.4
5	Kimberlina	USA	Bakersfield, California	AREVA	5
6	Puerto Errado 2	Spain	Seville	Novatec Solar Espana	30
<b>Under Construction</b>					
1	Alba Nova 1*	France	Ghisonaccia	Solar Euromed	12
2	Himin Solar	China	Dezhou	Himin Solar	2.5
3	Rajasthan Sun Technique	India	Rajasthan	Reliance	2×125
<b>Under Planning</b>					
1	Collinsville Power Station	Australia	Collinsville, Queensland	Transfield Services	150
2	Kogan Creek	Australia	Kogan Creek, Queensland	Wind Prospect CWP	250
3	Kogan Creek Solar Boost	Australia	Queensland	CS Energy	23
4	Joan1	Jordan	Ma'am, Jordan	MENA Cleantech	100
5	Solar Heat and Power Ltd 1	Portugal		Solar Heat and Power Ltd	6.5
6	Solar Heat and Power Ltd 2	Portugal		Solar Heat and Power Ltd	6.5
7	Palo Verde	USA	Maricopa Country, Arizona	AREVA Solar AZ II LLC	400

\* given in NREL 2012 but not updated in CSP Today 2012

\*\* MW<sub>th</sub>

### i. Technical details of the plants

Table 2.14 gives available technical details of LFR plants in operation and under construction based on (NREL, 2012). Liddel plant is excluded since it is a solar thermal plant linked to very large fossil plant. All of them use water as HTF and saturated steam for the turbine. Except Kimberlina, all the

other plants use air cooling, probably because of scarcity of water. It is not known whether Kimberlina has thermal storage, but all the others use a small amount of thermal storage (Ruths tank) as indicated in the table. The mirrors of the Kimberlina plant have 2 m aperture and are slightly curved. Puerto Errado 1 and 2 use mirrors of 0.72 m and they are flat. Mirror size is not available for Alba Nova 1 and Augustin Fresnel 1.

**Table 2.14: Details of the Fresnel based solar thermal power plants**

<b>Power Plant Name</b>	<b>Alba Nova 1</b>	<b>Augustin Fresnel 1</b>	<b>Kimberlina Solar Thermal Plant</b>	<b>Puerto Errado 1 (PE-1)</b>	<b>Puerto Errado 2 (PE-2)</b>
Location	Ghisonaccia	Targassonne	Bakersfield	Calasparra	Calasparra
Country	France	France	USA	Spain	Spain
Status	Under Construction	Operational	Operational	Operational	Operational
Plant start year	2014	2012	2008	2011	2012
Solar Resource, kWh/m <sup>2</sup> /yr	1,800	1,800	2,725	2,100	2,095
Plant Capacity, MW	12	0.25	5	1.4	30
Total Land Area, m <sup>2</sup>	2,30,000	10,000	48,560	50,580	7,00,100
Land Area per MW	19,167	40,000	9,712	36,129	23,337
Total Mirror Area, m <sup>2</sup>	1,40,000	4,000	26,000	18,662	3,02,000
Mirror Area per MW, m <sup>2</sup> /MW	11,667	16,000	5,200	13,330	10,067
Individual Mirror width, m			2	0.72	0.72
Land to Mirror Area Ratio	1.64	2.5	1.86	2.71	2.31
Absorber Tube Height, m				7.4	7.4
Power cycle pressure, bar	65.0	100.0	40	55	55.0
Solar field inlet temperature, °C				140	140
Solar field outlet temperature, °C	300	300		270	270
Storage, hours	1	0.25	-	-	0.5

## ii. Land & Mirror usage

Table 2.14, shows the large variation in the land area/MW and mirror area/MW. This variation could be due to variations in solar resource, efficiency of the power block due to different capacities and operating conditions and thermal storage. Thus, it is difficult to draw the inferences on the nominal requirements on the mirror and land areas.

## 2.4.3 New Developments

### i. Novatec Solar's LFR (Supernova)

Novatec Solar has developed a new design of absorber tower which can generate superheated steam at 450°C it is named as Supernova. The demonstration on generating superheated steam has been done at PE-1, Spain. It uses an evacuated absorber with secondary reflector. The receiver design is jointly developed by SCHOTT Solar, German Aerospace Center (DLR) and Novatec Solar (Novatec Solar, 2011).

## ii. AREVA Solar's CLFR (SSG4)

AREVA Solar's new design SSG4 is a solar steam generator delivers superheated steam. The demonstration of SSG4 to produce a superheated steam ( $370 \pm 20^\circ\text{C}$  and  $60 \pm 3$  bar) under steady and transient conditions has been tested at Kimberlina Solar Thermal Power Station, California. SSG4 is a 400 m long and 36 m width module capable of producing a maximum thermal output of 7.3 MW with a maximum outlet temperature of  $450^\circ\text{C}$  (AREVA, 2012).

## iii. FRESDEMO loop at PSA

It is a pilot plant to demonstrate the linear Fresnel technology at PSA, Spain. It is 100 m long, having 21 m wide module with a mirror area of  $1433 \text{ m}^2$ . The receiver is at 8 m above the primary mirror area. It was designed for direct steam generation at a maximum of 100 bar and  $450^\circ\text{C}$  (PSA, 2007).

## 2.4.4 Merits & Demerits of LFR

### Merits

- Low cost of components
- Less land requirement
- Simplicity in manufacture and installation
- Amenable for indigenization

### Demerits

- The lower optical efficiency of Fresnel system requires greater mirror aperture area.
- This technology is still in developmental stage.
- LFR systems are employing DSG. Consequently, large amount of thermal storage is not possible, since steam storage is expensive.

## 2.5 Parabolic Dish

A typical Parabolic Dish (PD) system consists of a parabolic reflector, generally made up of faceted mirrors, supported on a steel structure, which is controlled in 2-axis, to track the sun and reflect the radiation to a receiver located at the focal point of the parabolic reflector. In almost all existing dish plants, a Stirling engine is mounted at the focal point of the parabolic reflector. However, in case of "India One" under construction in Rajasthan, the dish is used in conjunction with a steam Rankine cycle instead of the usual Stirling engine. Similarly at the Australian National University (ANU), a parabolic dish has been used for a similar application. Therefore, the dish system with Stirling engine and dish system with Rankine cycle are considered separately.

### 2.5.1 Parabolic Dish with Stirling Engine

#### i. Description

Figure 2.17 (Source: NREL 2012) shows a typical PD system with Stirling engine (Alex, 2010). The Stirling engines are closed cycle engines, where the working fluid is enclosed within the system and gets heated externally. Thus, they are also called external combustion engines. One end of the cylinder containing the working fluid acts as the receiver. The heat energy received by the working fluid is transformed to mechanical energy, which in turn is converted to electrical energy, all of

them happening in a self-contained unit. Since the Stirling engine is different from the conventional IC engines, a brief description of some types of Stirling engines in use is given below.



**Figure 2.17: Maricopa dish system**

## **ii. Brief description of Stirling engines**

The principle of a Stirling engine using solar thermal input is described in the website, <http://pointfocus.com/images/pdfs/eurodish.pdf>. Figure 2.18 below (taken from the same website) explains the working principle of such a Stirling engine.

As seen from Figure 2.18, the same amount of working gas is contained between the two pistons which are interconnected through a regenerator and a cooler. The two pistons which are connected by a common crankshaft is set in motion when the working gas expands when heated and contracts when cooled. The expansion of hot gas in the expansion cylinder delivers more energy than needed for the compression of the cold gas in the compression cylinder. This excess energy is used to drive an electric generator connected to the crankshaft.

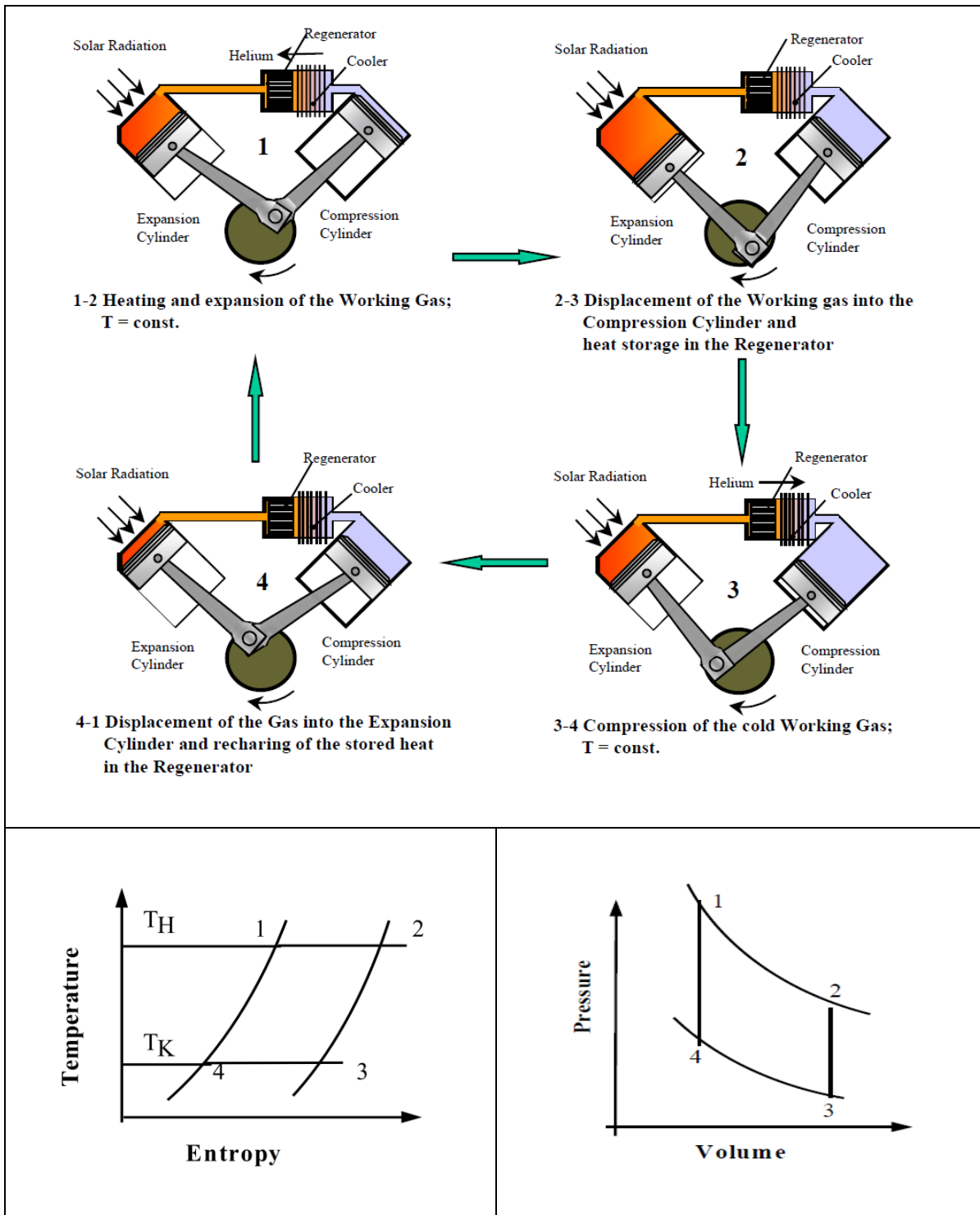


**Figure 2.18: Working principle of a simple Stirling engine**

The Stirling engine used in the power dish by Infinia is given in Figure 2.19. ([http://www.nrel.gov/csp/troughnet/pdfs/2007/smith\\_infinia\\_dish\\_stirling.pdf](http://www.nrel.gov/csp/troughnet/pdfs/2007/smith_infinia_dish_stirling.pdf), last accessed: Nov 2012). This is a free-piston type using a linear alternator to generate electric power.

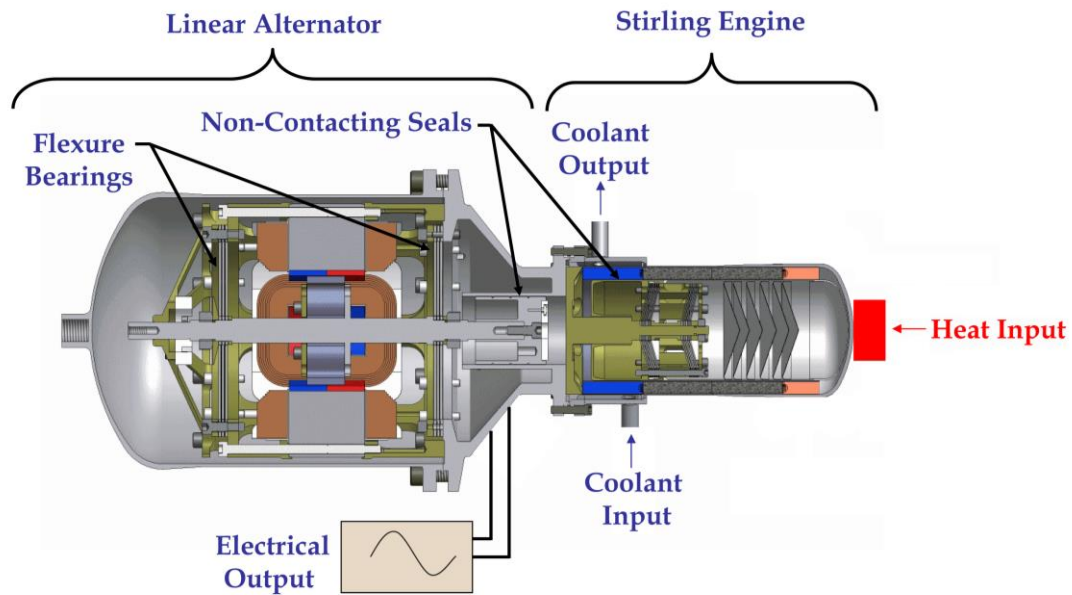


**Figure 2.19: Sectional view of Infinia's Stirling engine**

Though the configuration is different from the Stirling engine using a crank shaft, the thermodynamic principle is the same. In this arrangement, instead of two pistons, there is a single piston moving in a hermitically sealed enclosure. The ends of the enclosure on either side of the piston are connected through a regenerator and a cooler. One end of the enclosure receives the heat input from the solar energy and this region between the hot end and piston acts as an expansion cylinder. The other end of the enclosure acts as the compression cylinder. In the compression end of the enclosure there is an additional piston connected to a linear alternator for generating electrical power.

### **iii. Working fluids used in Stirling engines**

Stirling engines use gases such as hydrogen, helium and nitrogen as working fluids. The specific heats of these gases are 14.3 kJ/kg-K, 5.19 kJ/kg-K and 1.04 kJ/kg-K respectively. The higher the specific heat, higher is the efficiency. From this point of view hydrogen is the most preferred working fluid for Stirling engines. However use of hydrogen entails the risk of possible explosion. Pressure losses due to friction are low because of its low viscosity. Leakage effect needs to be addressed. Hydrogen has higher thermal conductivity. Helium and nitrogen are inert gases and are easier to handle, however their efficiencies are lower because of their lower specific heats. STM 4-120 and 4-65 Kockums Stirling engines use hydrogen as working gas. V161 Solo Stirling engine uses either hydrogen or helium as working fluid.

### **iv. Deployment of PD**

Table 2.15 gives a few details of plants in operation and under development. The total installed capacity of the dish systems around the world is just 1.51 MW. There is only one plant under development which is of 1 MW capacity. Thus dish Stirling engine is presently at an infant stage. However the total capacity of plants planned (Table 2.16) is 3273 MW (CSPToday, 2012).

**Table 2.15: Dish plants in operation & under construction**

Plant	Location	Capacity (MW)
<b>Operational</b>		
Envirodish	Spain	0.01
Maricopa Solar Project	USA	1.5
<b>Total capacity (MW)</b>		<b>1.51</b>
<b>Under Construction</b>		
Renovalia	Spain	1.0
<b>Total capacity (MW)</b>		<b>1.0</b>

**Table 2.16: Dish plants under planning**

Plant	Country	Developer	Capacity (MW)
Solar Oasis	Australia	NP Power	40
Bap Project	India	Dalmis Cements	10
PL Termosolar 8 MW Puertollano	Spain	Renovalia Energy	8
PL Termosolar 10 MW Puertollano (5 units)	Spain	Renovalia Energy	50
PL Termosolar 990 kW casas de los pinos	Spain	Renovalia Energy	1
Buckeye Landfill Project	USA	Tessera Solar	150
Calilco Solar Energy Project	USA	Abengoa Solar	663
San Luis Valley	USA	Tessera Solar	145
SES I	USA	NextEra Energy Resources	500
SES Solar One	USA	Tessera Solar/Stirling Energy System	850
SES-Solar 2	USA	Tessera Solar	750
SolarCAT pilot Plant	USA	Southwest Solar	10
Western Ranch	USA	Tessera Solar	27
Thermis	France		50
<b>Total Capacity (MW)</b>			<b>3254</b>

From Table 2.17 (ESMAP, 2010), one can infer that the diameter of the dish varies from 4.2 m to 15 m and output ranges from 3 kW to 25 kW. The mirror area/ kW varies from 3.5 m<sup>2</sup>/kW to 5.2 m<sup>2</sup>/kW. The Maricopa Solar Project (1.5 MW) uses Suncatcher dishes and each dish is able to generate 25 kW. The maximum concentration ratio of each dish mentioned in Table 2.17 is calculated based on their geometry of dish and receiver.

**Table 2.1.7: Characteristics of various parabolic dishes**

Name	Type	Aper- ture (m)	Dia (m)	Focal Length (m)	Concen tration Ratio	Receiver dia (m)	Engine	HTF	Working tempera ture (°C)	Promo- ter	Design Power (kW)	Max. Effici ency	Year	m <sup>2</sup> /kW
Sun dish	Stretched membrane	113	15	12	1558	0.38	STM 4- 120	H2	720	SAIC	22	0.23	1999	5.14
Sun Catcher	Parabola with facet	88	10.5	7.45	2756	0.2	4 - 95 kocku ms	H2	720	SAIC	25	0.23	1999	3.5
WGA	Parabola	41	8.8	5.45	2145	0.19	V161 Solo	H2 or He	650	WGA	11 or 8	0.24	1999	3.73 - 5.13
Euro dish	Parabola	57	8.5	5.45	2001	0.19	V161 Solo	H2 or He	650	SBP	11	0.23	2001	5.18
AZ-TH	Parabola with facet	56		5		0.19	V161 Solo	H2 or He	650	Abengoa	11	0.23	2007	5.09
Power Dish	Parabola	14.7	4.2				Infinia	He		Infinia	3	0.24	2007	4.90
Sun machine	Parabola	15 - 17	4 - 5				Sun Machin e	N2		Sun machine	3	0.2 - 0.25	2007	5 - 5.6

## 2.5.2 Merits and Demerits of Dish System with Stirling Engines

### Merits

- Due to its modularity, it can be used for different capacities.
- There is no requirement of water.
- It is easy to replace and repair individual small engines.
- It can be deployed in undulating terrain.

### Demerits

- There is a limitation on the maximum size of the dish that can be used from structural and wind load considerations. Therefore, the maximum capacity of a single unit is limited to about 25 kW.
- Even though the Stirling engine concept has been in existence for more than two centuries, it has not yet been perfected for commercial use.
- The leakage of working fluid requires replenishment.
- The seals wear out frequently requiring change.

## 2.5.3 Dish Technology with Steam Rankine Cycle

### i. India-One Facility

Scheffler dishes were developed essentially for mass scale cooking. India-one is a 1 MW<sub>e</sub> plant employing 770 Scheffler dishes each of 60 m<sup>2</sup> area, located in Abu Road, Rajasthan, India (India One 2011). The interesting feature of Scheffler dish (<http://www.solare-bruecke.org>) is that it concentrates the sun's rays on to a fixed focal point. At this focal point, a stationary receiver is kept which is used for producing steam for cooking. The concentration to a fixed focal point is achieved by rotating the Scheffler dish, about the earth's polar axis passing through this stationary focal point and by changing the shape of the paraboloid to account for the variation in the declination of sun. This adjustment needs to be done once in two or three days. This is illustrated in Figure 2.20.

The Scheffler dish used in India-One plant has a specially designed support structure, which uses complex control system to tilt and change the shape of reflective surface, made of mirror facets.

The receiver at the focus is a thick, hollow cast iron block as shown in Figure 2.21 (<http://www.india-one.net/photogallery.html>) and acts as a cavity receiver. The outside is insulated and during night and non-sunshine hours, the opening will be closed by an insulator to prevent heat losses.

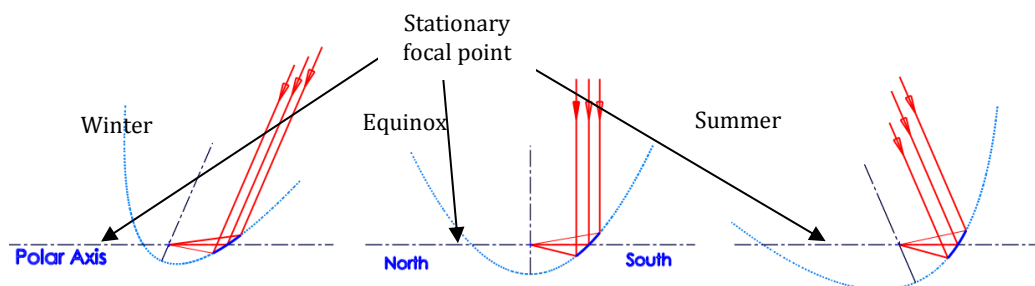


**Figure 2.20: Seasonal variation in tilt and profile needed for a Scheffler dish**



**Figure 2.21: Cast iron core cavity receiver and Scheffler dish**

Another unique feature of this receiver is that it also acts as thermal storage. The cast iron block can be heated up to 450°C. A stainless steel helically coiled tube is embedded close to the outer surface of the cast iron block. Water passing through this tube is converted to steam at 41 bar and 255°C, which runs a steam turbine to generate 1 MW electrical power.

## **ii. SG4 Dish**

SG4 dish (also referred as BIG dish) shown in Figure 2.22, at Australian National University (ANU), is one of its kind with a very large aperture area of 500 m<sup>2</sup>. This dish system comprises 380 mirror facets of size 1.17 m × 1.17 m and it is glass-on-metal laminated. The diameter of this dish is 25 m and its focal length is 13.4 m. This dish is used for direct steam generation with a cavity receiver. The cross section of the receiver is that of a top hat with a wound MS tube in a conical section and SS tube in the remaining section. The working fluid (water) enters the receiver at the beginning of conical front section and leaves at the top of the cavity. The outlet temperature of steam can be as high as 535°C at a pressure of 45 bar.

This system is able to generate power of the order of 50 kWe (Lovegrove, Burgess, McCready, & John, 2009; Greg, Lovegrove, Scott, & Jose, 2011). Investigations are going on with molten salt as HTF (DelPozo, Dunn, & Pye, 2011).



**Figure 2.22: The SG4 dish in testing for the direct steam generation**

## 2.6 Relative Assessment of CSP Technologies

The previous sections provide descriptions of the four CSP technologies along with their deployment, merits and demerits. A brief comparison of the four technologies is given below.

### 2.6.1 Technology Utilization/Maturity

PT is presently most deployed CSP technology for generating electrical power. ST comes next. Dish Stirling technology, though experimented upon for a long time has not yet reached commercial viability. LFR though a recent development is rated higher than the Dish Stirling technology. The total capacity of the plants in operation, under construction and under planning is given in Table 2.18 (CSPToday, 2012).

**Table 2.18: Comparison of the capacities of the four types of CSP plants**

Technology	Operating		Under Construction		Planning	
	No of Plants	Total Capacity (MW)	No of Plants	Total Capacity (MW)	No of Plants	Total Capacity (MW)
Parabolic Trough	28	1168	25	1377	90	23667
Solar Tower	7	60	11	2011	17	5787
Linear Fresnel	6	36.65	3	264.5	7	936
Dish Stirling	6	1.51	1	1	21	3273

From Table 2.18, it is clear that PT and the ST are way ahead of the other two technologies. It may be interesting to note that plants under construction for PT is of the same order as that the existing ones, whereas the capacity of ST plants under construction is much higher. Thus it is felt that in the near future, for large capacity power plants, ST may become the preferred choice over the PT. With regard to the dish technology, the development of Stirling engine has not yet reached a mature stage to work efficiently and reliably under varying solar thermal conditions. Therefore, it does not seem to be a viable option. The LFR is a more recent development. This has a good potential for increased use, particularly for Indian conditions, since most of the components can be indigenously manufactured.

The Scheffler dish technology that is used in the “India-One” plant is unique and if successful may merit consideration.

### 2.6.2 Mirror Area/Land Area Requirements

Taking into account the variations in efficiencies of the power cycle due to the capacity of plant, temperatures employed, DNI, etc., it appears that mirror area per MW of equivalent capacity is of the same order of magnitude for both PT and ST technologies. It is about 6000 m<sup>2</sup>/MW for equivalent capacity. The land area required is about 3.5 times the mirror area for PT whereas it is higher of the order of 6 for ST. Sufficient data for LFR plants are not available. From literature (Michael, 2012), it is found the mirror area required for this technology is 1.5 times that of PT, however the land area required is projected to be twice the mirror area in case of LFR.

## 2.6.3 Cost Comparison

The available information on cost of various plants in open literature is scanty. Table 2.19 gives the cost of various PT plants worldwide. It can be seen that the cost of a PT plant varies from ₹ 17 to 26 Cr/MW-Eq. Data are from NREL 2012 and company websites.

In case of ST, the number of plants operating are limited and data availability are less. Table 2.20 (NREL, 2012; Mustafa, Abdelhady, & Elweteedy, 2012) gives the cost of the operating ST plants. The cost per MW-Eq. is about ₹ 25.5 Cr. The cost of the PT and ST plants appears to be of the same order.

**Table 2.19: Cost of PT plants (in operation & under construction)**

Plant	Capacity (MW)	Storage (h)	Equivalent Capacity (MW)	Total Cost (Million)	Cost/MW-Equivalent	
					(Million)	(₹-Cr)
<b>In Operation</b>						
Ibersol Ciudad Real (Puertollano)	50	0	50.00	200 €	4.00 €	26.00
Martin Next Generation Solar Energy Center	75	0	75.00	476 \$	6.35 \$	31.75
Nevada Solar One	75	0.5	79.17	266 \$	3.36 \$	16.80
Alvarado - 1	50	0	50.00	250 \$	5.00 \$	25.00
Andasol -1	50	7.5	91.67	428 \$	4.67 \$	23.35
Solnova - 1	50	0	50.00	250 \$	5.00 \$	25.00
Solnova - 3	50	0	50.00	250 \$	5.00 \$	25.00
<b>Under Construction</b>						
Arcosol 50	50	7.5	91.67	320 €	3.49 €	22.69
Vallesol 50	50	7.5	91.67	320 €	3.49 €	22.69

**Table 2.20: Cost of ST plants (in operation)**

Plant	Capacity (MW)	Storage (h)	Equivalent Capacity (MW)	Total Cost (Million)	Cost/MW-Equivalent	
					(Million)	(₹-Cr)
Gemasolar <sup>a</sup>	20	15	53.33	230 €	4.31 €	28.03
PS -10 <sup>b</sup>	10	0	10.00	35 €	3.50 €	22.75

<sup>a</sup> (NREL, 2012)

<sup>b</sup> (Mustafa, Abdelhady, & Elweteedy, 2012)

Table 2.21 gives the cost data for LFR plants.

**Table 2.21: Cost of LFR plants (in operation)**

Plant	Capacity (MW)	Storage (h)	Total Cost (\$ Million)	Cost/MW (\$ Million)	Cost/MW (₹ Cr)
Kimberlina Solar Thermal Plant <sup>c</sup>	5	0	15	3	15
Puerto Errado 2 (PE 2) <sup>d</sup>	30	1	162	5.4	27

<sup>c</sup><http://www.ecoworld.com/energy-fuels/comparing-solar-technologies-to-ausras-kimberlina-solar-thermal.html>, last accessed: Nov, 2011.

<sup>d</sup> (CERC, 2010)

For the PD technology the number of plants in operation is very small and cost data are not available.

## 2.7 Salient Observations

- The CSP technology using PT has been in operation successfully for nearly three decades and has reached a reasonably mature stage. The total capacity of plants in operation and under construction with PT technology is 1168 MW and 1377 MW respectively. The total capacity of plants planned is more than 20 times the existing capacity. Some of the plants in operation and under construction have thermal storage capacity up to 7.5 hours.
- The deployment of ST to generate electrical power on a large scale appears to have gained momentum considering that the capacity of plants under construction is 2011 MW while that in operation is only 60 MW. The ST technology is yet to reach its full potential of operating temperatures of the order of 1000°C.
- The advantages of LFR with small flat or slightly curved mirrors, lower wind loads due to their proximity to the ground, lower structural weight of the mirror supports and simplicity of fixed non evacuated receivers are expected to reduce the overall cost in spite of lower optical and receiver efficiency.
- The commercial viability of CSP using dish Stirling engine has not yet been established. However, the Scheffler dish option with steam Rankine cycle that is being tried out at “India One” can be considered if it proves successful.
- The high cost of CSP power is a major deterrent for its large scale deployment at present. Abroad, the installation cost per MW of equivalent capacity is of the order of ₹ 17 to 32 crore (2.6 – 4.6 Million €). These figures may come down to ₹15 to 20 crore under Indian conditions, which is still high. However, it is hoped that through indigenization, innovation, large scale utilization and learning process, it is possible to bring down the cost, comparable to that of fossil fuel based power plants in the near future.

# 3 Model for Techno Economic Analysis of Parabolic Trough Technology

## 3.1 Introduction

In this chapter, the model developed for techno-economic analysis of PT is described and applied to a plant to be located at Jodhpur, Rajasthan.

A CSP plant based on PT is chosen for developing the model since more information is available for this system compared to others. Even with PT there is not much experience in India, though a few projects are in the pipeline. It has been difficult to get all the necessary design details in public domain.

The assessment of a CSP plant is different from that of a plant using conventional fuels. In the conventional power plant, the thermal input to the power plant for generating electrical power is usually controlled and the plant works close to the design conditions. On the other hand, the thermal input to the power block in case of CSP plants depends on the solar input received by the solar field and hence varies during the course of the day. Consequently, the power block used in CSP operates under part load conditions, often for a considerable length of time. Thermal storage and hybridization are two options to mitigate effects of transients in solar input on the performance of the power block.

The model for techno-economic analysis consists of the following main steps:

- a) Determine the reference mirror aperture area ( $A_r$ ) of the solar field, which can generate the required rated gross power (using only solar power) corresponding to maximum ( $DNI \times \cos \theta$ ) at the location.
- b) For a chosen thermal storage and hybridization, determine the total annual electrical energy generated for various values of Solar Multiple (SM - ratio of actual mirror aperture area ( $A_a$ ) to the reference mirror aperture area ( $A_r$ )).
- c) Determine the Levelised Cost of Electricity (LCOE) for the various SMs chosen and find the optimum SM for which the LCOE is minimum and then freeze the design of the solar field corresponding to the optimum SM.

For steps (a) and (b) above, hourly DNI data for the location and engineering model dealing with the technical aspects are needed. Only global and diffuse radiation data over a horizontal surface for 22 stations in India are available in open literature (IMD, 2009), but not the DNI data. So we developed a methodology to derive the hourly DNI data from the global and diffuse data and it was applied to obtain DNI data for these 22 stations. These data can be accessed at [www.cstep.in](http://www.cstep.in). For the present case study these data were used.

In the application of the above techno-economic model, various technical, economic and financial inputs are based on our best estimates. However, the user can change the inputs if required.

## 3.2 Model for Engineering Analysis

### 3.2.1 An Overview

An overview of the technical model is given below for an easier understanding of the details to follow. Various aspects of this model for PT technology can be extended to other technologies as well with suitable modifications. A schematic of a CSP plant using trough technology with thermal storage and hybridization is shown in Figure 3.1.

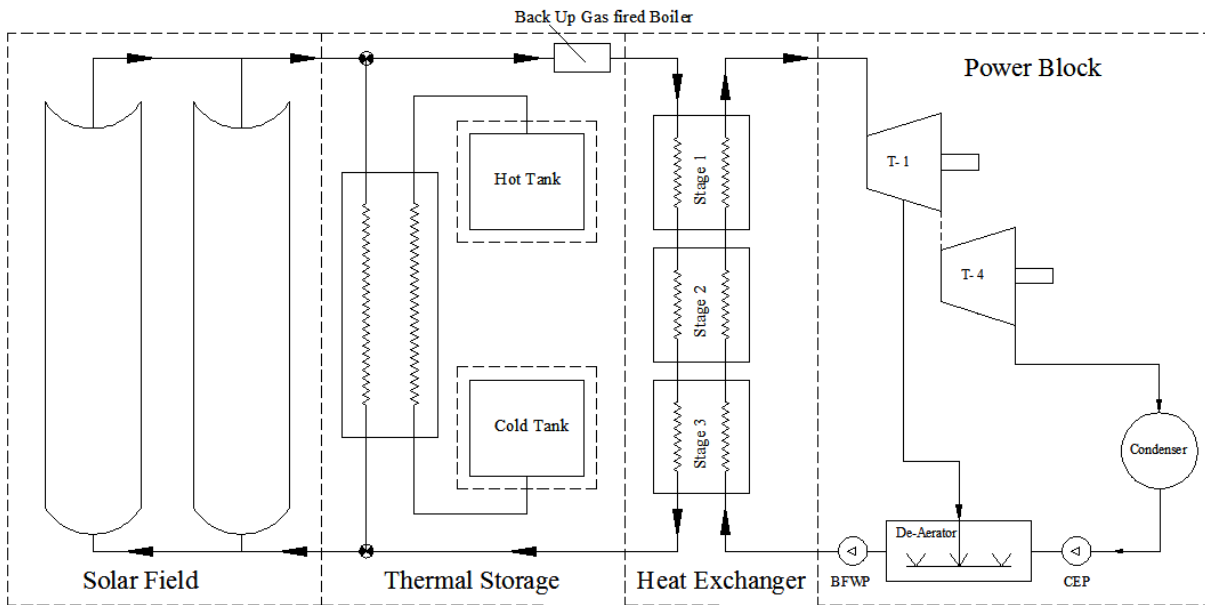


Figure 3.1: Schematic of a CSP plant - PT

The mirrors are usually mounted along the North – South axis and tilted about that axis to track the sun as it moves from East to West during the day. The receiver (absorber) tube is located at the focal axis of the parabolic mirror. The solar power impinging on the receiver tube is absorbed by the Heat Transfer Fluid (HTF) passing through it. Since the receiver tube rotates with the trough, flexible couplings are needed between the tubes and the feeder/header pipes. In order to improve the efficiency of heat transfer and reduce losses, the absorber tubes have selective coating and are enclosed in evacuated glass tubes. The thermal energy from the HTF is transferred through heat exchangers to the working fluid used in the power block. The power block uses water as the working fluid in a Rankine cycle to run the steam turbine which is coupled to the generator. Thus, the thermal energy given to the working fluid is converted to electrical energy.

The efficiency of conversion of the solar thermal power received by the solar field to electrical power depends on the efficiency of transfer of power at each of the stages mentioned above. Hence, to design the system as well as to determine annual electrical energy generated, a proper estimate of the efficiency of each of these stages, both at design and off design conditions is necessary.

In the first step, for a given location, the mirror aperture area of the solar field required to generate the rated gross capacity of the power block is estimated. This is done for the condition of maximum solar power,  $(DNI \times \cos\theta)_{max}$  incident on the mirrors. This mirror aperture area is called the Reference Mirror Aperture Area ( $A_r$ ). The reference solar field is based purely on the maximum solar power available and is independent of thermal storage or hybridization. It is obvious, that if this reference solar field is used, then the rated power is generated only for a brief period

corresponding to  $(DNI \times \cos\theta)_{max}$ . At other times, the power generated is below the rated capacity. Consequently, the annual electrical energy generated will not make the plant economically viable.

In the second step, various values of SM are considered and the corresponding annual electrical energy is computed for chosen values of storage and hybridization.

An overview of various aspects involved in steps (a) and (b) of the engineering model is given below.

### **i. Estimation of Reference Mirror Aperture Area**

The reference mirror aperture area ( $A_r$ ) is estimated as follows:

- a. For the chosen location, determine  $(DNI \times \cos\theta)_{max}$ .
- b. Consider a gross capacity of power block,  $P_{g,d}$ .
- c. Estimate the thermal power input to the working fluid ( $P_{th,d}$ ), taking into account the efficiency of the power block at design conditions ( $\eta_{p,d}$ ).
- d. Calculate the thermal power input to be given to the HTF ( $P_{htf,d}$ ) considering the efficiency of the heat exchanger ( $\eta_{he}$ ).
- e. Determine the efficiency of the absorber tube ( $\eta_{abs,d}$ ) corresponding to the solar input to the absorber tube per unit length at  $(DNI \times \cos\theta)_{max}$ .
- f. Calculate solar power ( $P_{abs,d}$ ) required to be incident on the absorber tube.
- g. Determine the reference mirror aperture area ( $A_r$ ) using  $(DNI \times \cos\theta)_{max}$  and the optical efficiency of the mirror ( $\eta_m$ ).

It may be noted that thermal storage and hybridization do not play any part in the determination of ( $A_r$ ).

### **ii. Solar Multiple (SM)**

As indicated earlier, solar multiple is defined as the ratio of the actual aperture area ( $A_a$ ) of the mirrors to the reference mirror aperture area ( $A_r$ ) to generate the rated electrical power corresponding to  $(DNI \times \cos\theta)_{max}$  for the chosen location. If  $A_a$  is equal to  $A_r$ ,  $SM = 1.0$ , then the design power is generated only over a very short period when  $(DNI \times \cos\theta)$  is maximum. At all other times, solar thermal input to the plant is lower than the design value and the plant would be working under part load. The efficiency of the plant under part load will be low. Thus the combined effect of lower solar thermal input and lower efficiency during most of the time results in a relatively low annual electrical energy.

On the other hand, if one chooses to have a solar field with higher than the optimum value of SM, then the plant will be operating most of the time at full load. However, if thermal storage is not provided, the plant will not be able to utilize the excess solar power and some mirrors will have to be defocused.

### **iii. Thermal Storage**

A major advantage of CSP is the possibility of providing thermal storage. This is to provide power during the evening and night and also to tide over intermittent periods of cloud cover. As stated above, when  $SM > 1$  and in absence of thermal storage, when  $DNI \times \cos\theta$  is close to the design value, some mirrors have to be defocused and consequently the solar thermal energy, which could

have been utilized, is wasted. Thus in CSP plants, it is a common practice to provide a few hours of thermal storage ( $t_s$ ). This means that it can deliver  $t_s$  hours of the rated electrical power, even when there is no thermal input from the sun.

#### iv. Hybridization

Hybridization refers to the use of other fuels such as natural gas, coal, lignite and biomass, to supplement the solar radiation. Hybridization in a CSP plant is generally used for taking care of transients, and hence requires a quick response. Thus, natural gas is a preferred fuel for hybridization. Here again, the maximum amount of hybridization permitted is chosen as a fraction of the design thermal power that needs to be given to the HTF to generate the rated gross power.

In other words, if  $f_{hb}$  is the hybridization permitted and if  $P_{htf,d}$  is the thermal power of HTF needed to generate the design gross power, then the natural gas burner is designed to deliver to the HTF a maximum thermal power of  $f_{hb} \times P_{htf,d}$ .

#### v. Loss Factor

When a CSP plant is not operating during night and cloud cover, the temperature of HTF in the absorber tubes will fall below the operating levels due to thermal loss. Hence, before the plant can be restarted and brought into operation, the solar energy would first be utilized to make up the thermal losses and bring back the HTF to operating conditions. Obviously, longer the period of shutdown, greater will be the thermal loss. If the insulation were perfect and there were no thermal losses, this solar energy which is now used for making up the thermal loss, would have produced electrical energy.

Thermal losses depend on ambient conditions, such as ambient temperature, wind velocity and various other design parameters of the plant. It is beyond the scope of this report to undertake a detailed analysis of the losses considering all these effects and we have chosen a relatively simple procedure to estimate the losses.

When the plant is started after a period of shut down, the thermal energy which the HTF would have lost during shutdown would have to be made up before it can be passed on to the heat exchanger of the power block to generate electrical energy. Thus there is not only a lag in electrical energy generation relative to the solar energy input but also the loss in the electrical energy generated relative to what it would have generated in the absence of thermal loss. Therefore for the assessment of CSP plant at preliminary stage we can directly consider this thermal energy loss in terms of electrical energy loss for every hour of non-operation of the plant. So we define a loss factor  $L_f$ , as the fraction of the electrical energy lost (due to thermal losses) per hour of shutdown, to the energy that the plant would have generated in one hour at rated capacity.

If the plant of rated power  $P_{g,d}$ , is shut down for  $t$  hours then the electrical energy lost will be  $L_f \times t \times P_{g,d}$ . This is discussed subsequently.

#### vi. Computation of Annual Electrical Energy Generated

We now provide a short overview of the methodology for computing the annual electrical energy for a chosen SM, thermal storage hours and fraction of hybridization. More details are given in a subsequent section. It is a usual practice to operate the power block at 10% more than the design capacity. Likewise, if the thermal power available falls below 25% of the design value, the plant is shut down.

For the hours of thermal storage chosen, the capacity of the thermal energy storage system is computed.

Starting from the 1<sup>st</sup> hour to the last hour of the year (8760), the following computations are carried out:

- a) For the chosen SM, the actual aperture area of the mirrors  $A_a$  is determined.
- b) The solar power impinging per unit length of the absorber tube ( $P_s$ ) is computed.
- c) Corresponding to this value of  $P_s$ , the thermal efficiency of the absorber tube ( $\eta_{abs}$ ) is found out. Using this information, the solar thermal power transferred to HTF ( $P_{htf,s}$ ) is computed.
- d) Fractional thermal power from solar field,  $f_{th,s}$ , the fraction of  $P_{htf,s}$  to  $P_{htf,d}$  is computed.
- e)  $f_{th}$ , is defined as the ratio of the thermal power delivered to the power block heat exchanger ( $P_{htf}$ ) to thermal power needed to generate rated gross power ( $P_{htf,d}$ ). When  $f_{th} = 1.0$ , the rated gross power is generated. Since power block is allowed to operate at 10% more than the design capacity, the maximum value of  $f_{th}$  is 1.1.
- f) Depending on the value of  $f_{th,s}$ , different options are chosen as given below.
  - i) If  $f_{th,s}$  is greater than 1.1, then HTF thermal energy equivalent to  $f_{th} = 1.1$ , (i.e.,  $P_{htf} = 1.1 \times P_{htf,d}$ ) is sent to the heat exchanger to produce electrical power. The balance thermal energy is sent to the thermal storage system.
  - ii) If  $f_{th,s}$  is less than 1.1 and if stored thermal energy is available, it is used to augment  $f_{th}$  up to a value 1.1 for electricity generation.
  - iii) If  $f_{th}$  after augmenting with available stored energy  $f_{th,sta}$ , is less than 1.1, then it is further augmented with hybrid power (limited to the maximum permissible value<sup>1</sup>). Even if  $f_{th,s}$  is zero, the plant can be run with stored thermal energy and hybridization.
  - iv) If augmented value of  $f_{th}$ , including stored thermal energy and hybridization is less than 0.25, the plant is shutdown.
  - v) When the plant is shutdown, thermal losses would occur, which would have to be made up, before the plant can generate power. For  $t$  hours of non-operation, electrical energy equivalent of thermal losses is  $e_{start} = L_f \times P_{g,d} \times t$ .
  - vi) The plant will start generating electricity only after the  $e_{start}$  compensation is completed.
  - vii) Corresponding to  $f_{th}$ , the fraction of rated gross power  $f_p$  is computed.
  - viii) Corresponding to  $f_p$  the maximum gross electrical energy  $e_g$  (in the absence of thermal losses) that could be generated is computed. However the actual electrical energy generated ( $e_{g,a}$ ) is  $(e_g - e_{start})$ . Then the corresponding fractional power generated ( $f_{pa}$ ) is  $e_{g,a}/P_{g,d}$ , as  $e_{g,a}$  is for one hour.

---

<sup>1</sup> Maximum value of  $f_{hb}$ , the fraction of thermal power that can be used is limited in our analysis to 0.2.

- ix) Then considering the auxiliary power requirements, the electrical energy supplied to grid ( $e_{grid}$ ) during that hour can be calculated.
- x) The sum of the net electrical energy generated over 8760 hours gives the annual electrical energy generated by the plant. The energy share between solar and hybridization is also computed.

### 3.2.2 Inputs for Technical Assessment of CSP

The inputs required for analysis are as follows:

- i. Hourly DNI data for a Typical Meteorological Year (TMY) for the chosen location
- ii. Efficiencies of
  - a. Solar collection
  - b. Mirror system
  - c. Absorber tube
  - d. Heat exchanger between HTF and power block
  - e. Heat exchanger between HTF and storage medium
  - f. Power block including the electrical generator
- iii. Loss factor during shutdown
- iv. Thermal storage
- v. Hybridization

Details regarding each of the above employed in our methodology, as applied to the PT system (Figure 3.1) are given below.

#### i. Solar Insolation Data

For a reliable assessment of CSP plant, DNI data at close intervals of time throughout a Representative Year (RY) or TMY derived from measured ground data over several years are required. While such data have been collected for promising locations abroad, in India DNI data are limited. But data on global and diffused radiation on a horizontal surface are available for 22 stations. Hence we developed a methodology to arrive at the hourly average DNI data from this global and diffused data and validated for a few cases. Then this methodology is used to generate DNI data for all the 22 stations in India. Details are given in (Ramaswamy, Badri, Suresh, & Thirumalai, CSTEP/E/4, 2012) and available at [www.cstep.in](http://www.cstep.in).

#### ii. Efficiency of Solar Collection

The solar collection efficiency  $\eta_c$  is defined as the ratio of actual solar power incident on the mirrors to the maximum possible power that could be captured (normal incidence).

Actual solar power,  $P_{actual}$  is given by

$$P_{actual} = \sum_{i=1}^N DNI \times A_i \times \cos \theta_i,$$

where N is the number of mirrors,  $A_i$  is the aperture area of the  $i^{th}$  mirror element and  $\theta_i$  is the angle between the normal to the  $i^{th}$  mirror element and sun's rays. Therefore

$$\eta_c = \frac{\sum_{i=1}^N A_i \times \cos \theta_i}{\sum_{i=1}^N A_i}$$

Though this report deals with CSP using parabolic trough technology, the efficiencies of collection of other systems are also described for comparison.

**a) Dish**

For a dish, which is tracked to point towards the sun,  $\theta = 0$  and  $\cos\theta = 1$ .

Hence,  $\eta_c = 1$ .

**b) Parabolic Trough**

For a parabolic trough system aligned in the North - South direction, which is the most common,  $\theta_i$  is given by

$$\cos\theta_i = \sin\phi\sin\delta\cos\beta + \cos\phi\cos\delta\cos\omega\cos\beta + \cos\delta\sin\omega\sin\beta \dots\dots\dots \text{Eqn. 3.1}$$

where,  $\phi$  is the latitude of the location

$\delta$  is the declination, which depends on the day of the year

$\omega$  is the hour angle

$\beta$  is the angle of tilt of parabolic trough

and for a tracking system  $\beta$  is given by

$$\tan\beta = \frac{\cos\delta\sin\omega}{\sin\phi\sin\delta + \cos\phi\cos\delta\cos\omega}$$

Details of parabolic trough tracking are given in (Ramaswamy, Suresh, Badri, & Ramakrishna, 2010). Since all the troughs are tilted by the same amount,  $\theta_i$  is same for all troughs. So  $\eta_c = \cos\theta_i$  and can be taken for the whole aperture area.

In NREL's SAM,  $\cos\theta$  effect, effect of end losses, shadow effects, etc. are all clubbed together and from actual field data on some existing plants, correction in form of incident angle modifier is given. It is felt that at the initial assessment stage, considering  $\cos\theta$  effect alone is sufficient.

**c) Linear Fresnel Reflector**

For a Fresnel system, aligned in the North-South direction,  $\cos\theta_i$  is given by Eqn. 3.1, but  $\beta$  of the mirror depends on its distance with respect to the receiver tube ( $d/h$ ) where,  $d$  is the horizontal distance from the projection of the receiver tube and  $h$  is the height at which the receiver tube is located. Details of the tracking of the Fresnel mirrors are given in (Ramaswamy, Badri, Suresh, Ramakrishna, & Thirumalai, Solar energy impinging on unit aperture area of a Fresnel mirror located at different positions relative to the absorber, 2010). Since  $\theta_i$  depends on the location of the Fresnel mirror, collection efficiency  $\eta_c$  depends on the details of the layout.

**d) Solar Tower**

For a tower system using heliostats,  $\theta$  depends upon the  $x/h$  and  $y/h$  location of the heliostat with respect to the tower.  $x$  and  $y$  are the horizontal coordinates of the heliostat with respect to the tower and  $h$  is the height of the tower.

Similar to Fresnel,  $\cos\theta_i$  effect is different for different heliostats and hence collection efficiency  $\eta_c$  depends on the details of the layout.

In all the systems, if there are shadow/blocking effects, they need to be taken into account. However in the parabolic trough system, we assume the spacing of the troughs is such that the effects of shadow/blockage can be neglected.

### iii. Optical Efficiency of Mirror

The optical efficiency of the mirror system,  $\eta_m$  may be defined as follows

$$\eta_m = \frac{\text{solar power incident on the absorber}}{\text{solar power incident on the mirrors}}$$

$\eta_m$  can be taken to be equal to  $(\rho \times \gamma)$

where,  $\rho$  is the specular reflectivity of the concentrator surface (typical values range from 0.93 to 0.95) and  $\gamma$  is intercept factor, the fraction of the reflected radiation intercepted by the absorber tube (typical values range from 0.9 to 0.95).

$\eta_m$  depends on the quality of the mirror and its support, (i.e., mirror, geometry, tracking accuracy, deflections due to wind loads etc.). It does not depend on DNI.

The thermal power impinging on the absorber tube is given by

$$P_{abs} = \eta_c \times \eta_m \times DNI \times A_a$$

### iv. Efficiency of Absorber Tube

Efficiency ( $\eta_{abs}$ ) is the ratio of the thermal power transferred to the HTF to the thermal power incident on the receiver. Most of the CSP plants with parabolic trough system use the SCHOTT's selectively coated 70 mm stainless steel tube enclosed in 115 mm evacuated glass tube, each segment being 4 m long. This is assumed as the benchmark for evaluation of a CSP project using trough technology. The thermal properties of the absorber tube and the glass tube are known and they can be used to evaluate the  $\eta_{abs}$  for a trough system. Also most plants use Therminol VP-1 as HTF. The inlet and outlet temperatures of the HTF using synthetic oil and steam Rankine cycle get fixed from considerations of the flash point of the synthetic oil and the saturation temperature of steam. Therefore in most plants, the maximum outlet temperature of HTF is limited to 390°C while the inlet temperature is taken to be 290°C.

The system is so designed that for the design  $[DNI \times \cos\theta]_{max}$  conditions and design mass flow, the HTF enters the absorber tube at 290°C and exits at 390°C. Hence we need to estimate the  $\eta_{abs,d}$  under design conditions of thermal input to the absorber tube. However, if due to reduced DNI, the thermal input to the absorber tube gets reduced below the design value, then the normal practice is to adjust the mass flow of HTF so as to maintain the inlet and outlet temperatures of HTF. This is because the efficiencies of the various stages of the steam turbine depend on the inlet temperature of the steam to these stages. It is desirable to keep this as high as possible. Some variations in HTF outlet temperature may be permitted in actual operation. But for our analysis, it is assumed constant. Thus, the losses remain almost constant.

Under these off-design conditions of lower solar input,  $\eta_{abs}$  will be less than  $\eta_{abs,d}$  and we need to estimate the variation of  $\eta_{abs}$  with thermal input to the absorber tube.

The details of the heat transfer analysis for an absorber tube of SCHOTT type are given in the report (Ramakrishna, Thirumalai, & Ramaswamy, 2011). The thermal loss from the absorber tube depends on the ambient conditions, viz., ambient temperature and wind velocity. Also, in this analysis, end losses and losses through conduction from the support brackets have not been taken into account. The efficiencies obtained from the steady state analysis were decreased (by 5%) to account for these losses. Based on all these considerations, efficiency of the absorber tube as a function of the thermal power input per unit length (W/m) was calculated and is shown in Figure 3.2.

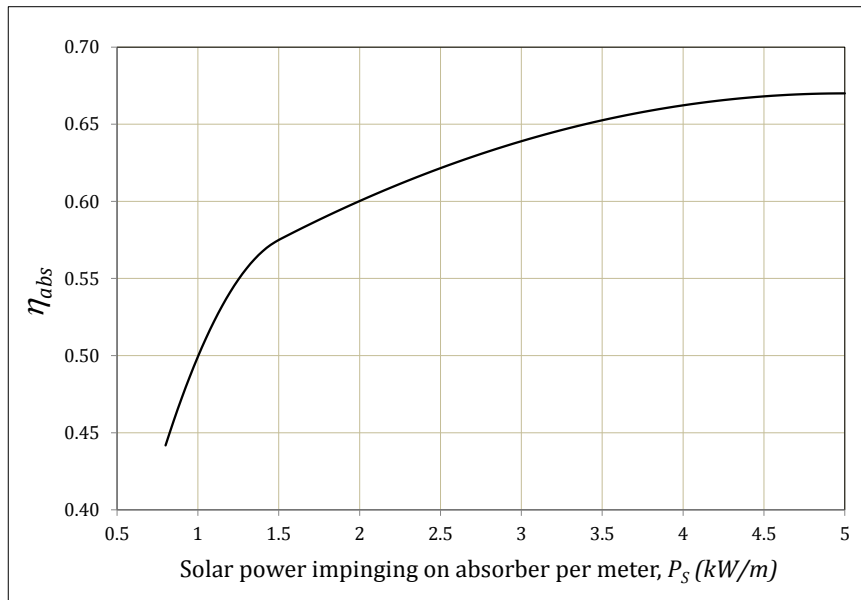


**Figure 3.2: Absorber efficiency as a function of input power**

Note that these figures are for HTF inlet temperature of 290°C and outlet temperature of 390°C. Since, most PT plants use this type of absorber tube and these range of temperatures, we have taken this as representative for carrying out the technical analysis. For a chosen chord width,  $C$  (m) of the trough and for a given location of the plant, the solar power input per meter to the absorber tube ( $P_s$ ) is given by

$$\text{Solar power input per meter, } P_s (\text{W/m}) = C \times \text{DNI} \times \cos\theta \times \eta_m$$

Corresponding to this thermal input  $\eta_{abs}$  is found out from Figure 3.2. Therefore the thermal power given to HTF is given by

$$P_{htf} = P_{abs} \times \eta_{abs}$$

#### v. Efficiency of Power Block Heat exchanger

We will not go into details of heat exchanger design. There is enough experience in the country to design such heat exchangers with an efficiency of about 95%.

#### vi. Efficiency of Power Block

We need to estimate  $\eta_{p,d}$  the efficiency of power block for the design capacity. The efficiency depends on many factors such as the inlet pressure and temperature of steam, condenser pressure, mass flow rate of steam, capacity of the power block etc. We have confined the analysis to power blocks using steam as the working fluid.

For the power blocks used in CSP plants, using synthetic oil as HTF, the variation of  $\eta_{p,d}$  with capacity is shown in Figure 3.3. This applies for plants with wet cooling option. This is based on discussions, data from manufacturers and literature. It shows that the power block efficiency is very low at low capacities. It increases with the increase in capacity and plateaus at about 37% for a

power block capacity of about 50 MW. This explains why steam cycle based CSP plants make economic sense at capacities of 50 – 100 MW.

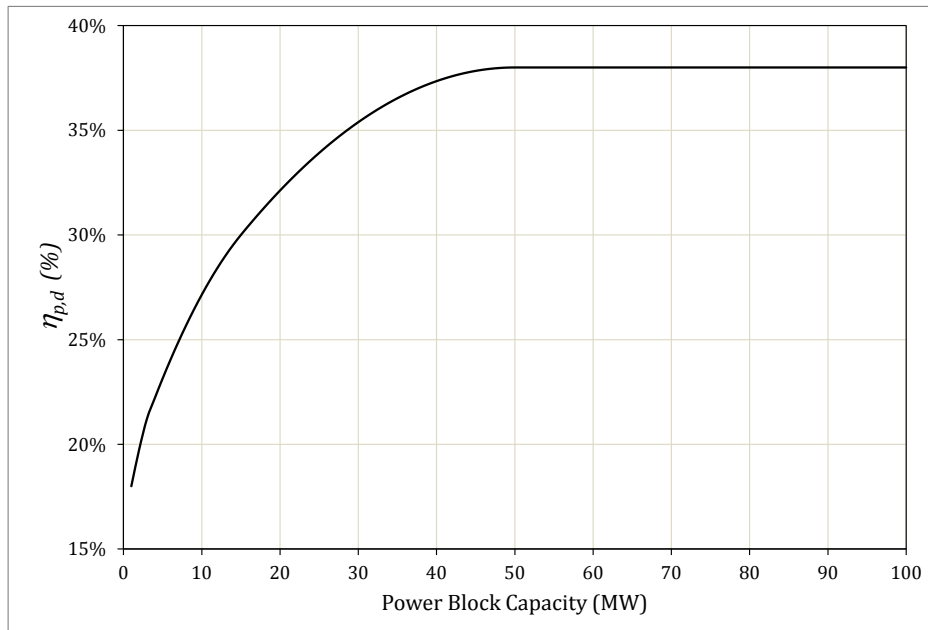


**Figure 3.3: Power block efficiency at design conditions**

Unlike conventional power plants, CSP power plants have to work under part load conditions also. Hence, we need to know the variation in efficiency,  $\eta_{pl}$ , under part load conditions. We define a relative efficiency  $\eta_r = \eta_{pl}/\eta_{p,d}$  and consider the variation of  $\eta_r$  as function of gross fractional power generated,  $f_p$ , defined as a fraction of the full load capacity. Again based on discussions and available literature (Montes, Abánades, Martínez-Val, & Valdés, 2009),  $\eta_r$  vs.  $f_p$  can be approximated as in Figure 3.4.

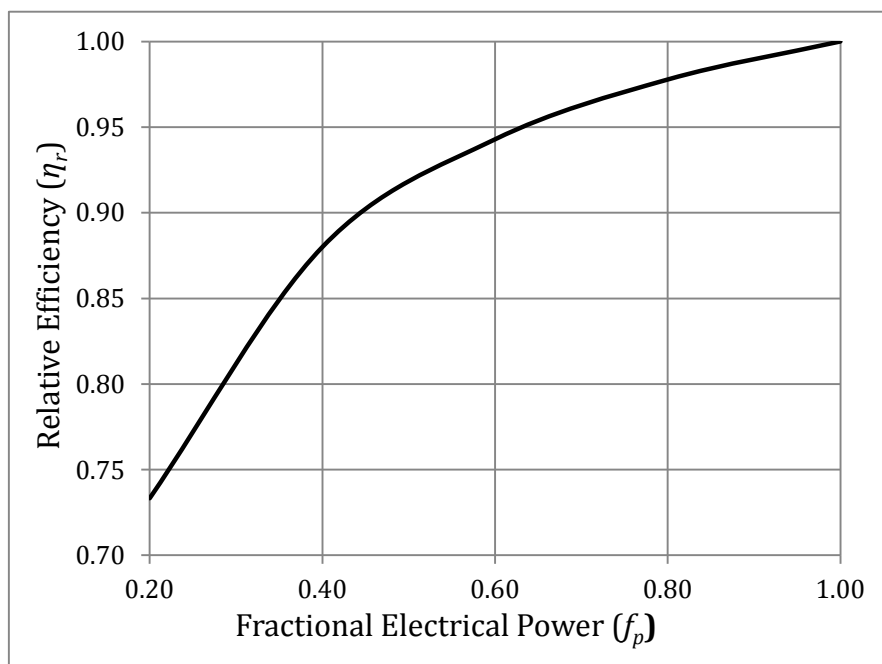


**Figure 3.4: Efficiency of power block at part load**

The variation of  $\eta_r$  vs.  $f_p$  given in Figure 3.4 can be analytically represented as

$$\eta_r = \frac{1.1 \times f_p}{f_p + 0.1} \quad \text{Eqn. 3.2}$$

To find  $f_p$  under part load conditions, we need the relation between  $f_p$  &  $f_{th}$ .

$$f_{th} = \frac{P_{htf}}{P_{htf,d}} = \frac{(P_{g,d} \times f_p) / (\eta_{p,d} \times \eta_r \times \eta_{he})}{(P_{g,d}) / (\eta_{p,d} \times \eta_{he})} = \frac{f_p}{\eta_r}$$

Substituting for  $\eta_r$  from Eqn. 3.2 and simplifying, we get

$$f_p = 1.1 f_{th} - 0.1 \quad \text{for } (0.09 \leq f_{th} \leq 1)$$

The above relationship is shown in Figure 3.5.

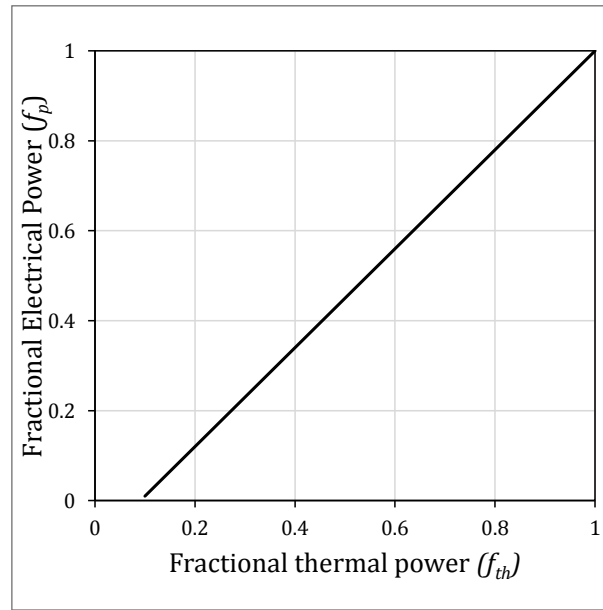


**Figure 3.5: Electrical power generated at part load conditions**

Since power block efficiency reduces with part load, the fractional thermal power generated is less than the fractional thermal power input as is evident from Figure 3.5.

### vii. Thermal Losses during Shutdown Period

An overview of how thermal losses are taken into account is given in section 3.2.1. Available literature suggests that the thermal losses that occur overnight are roughly equivalent to the energy that the plant would have generated over 3/4<sup>th</sup>s of an hour. Assuming that the plant was not operational for 15 hours overnight, we can roughly say that for every one hour of non-operation, the electrical energy, which would have to be used to make up the losses, is roughly equivalent to the energy the plant would have produced for 1/20 hour. In the above case the loss factor is 0.05 and we take that as a default value.

### viii. Thermal Storage Operation

In this study we have considered a two tank molten salt storage technology.

- a. First choose the number of hours ( $t_s$ ) of thermal storage.
- b. The efficiency of heat transfer from HTF to the molten salt is taken as  $\eta_{st}$ , during charge and discharge. The default value is taken as 0.97.

- c. Therefore, if we need  $t_s$  hours of thermal storage, the maximum amount thermal storage energy that can be collected by the storage system is

$$E_{tes,max} = \frac{P_{htf,d} \times t_s}{\eta_{st}}$$

### ix. Hybrid Operation

It is assumed that hybridization is used whenever possible to maximize the electrical energy generated. The hierarchy of usage of thermal power from solar field, thermal storage and hybridization, is in that order.

If  $P_{htf,d}$  is the thermal power required to be given to HTF to generate the rated gross power and if  $P_{hb}$  is the maximum thermal power that the natural gas boiler can augment through hybridization (Figure 3.1), then the extent of hybridization is defined by  $f_{hb}$ , which is a ratio of  $P_{hb}$  to  $P_{htf,d}$ . In other words,  $f_{hb}$  is the maximum fraction of thermal power given to HTF through hybridization to thermal power needed to generate the rated gross power.

## 3.2.3 Details of Engineering Model

Details of the methodology are given below.

### a. Reference Aperture Area

- i. Use the hourly DNI data for the whole year for the location of the CSP plant. Find the value of  $\{DNI \times \cos\theta\}_{max}$
- ii. Choose the rated gross power capacity ( $P_{g,d}$ ) of the plant.
- iii. From Figure 3.3 determine  $\eta_{p,d}$  the efficiency of the power block under design conditions. Then the design thermal input to the power block

$$P_{th,d} = \frac{P_{g,d}}{\eta_{p,d}}$$

- iv. The design thermal input to the heat exchanger by the HTF  $P_{htf,d} = \frac{P_{th,d}}{\eta_{he}}$ .
- v. Determine  $\eta_{abs,d}$  efficiency of the absorber tube under design conditions corresponding to  $P_{s,d} = (DNI \times \cos\theta)_{max} \times C \times \eta_m$  (Figure 3.2). The analytical curve fit is given in flow chart (Pg 53).
- vi. The design solar power that has to impinge on the absorber tubes ( $P_{abs,d}$ ) is given by  $P_{abs,d} = \frac{P_{htf,d}}{\eta_{abs,d}}$
- vii. The design solar power  $P_{th,s,d}$  that need to impinge on the total mirror aperture area is given by  $P_{th,s,d} = \frac{P_{abs,d}}{\eta_m}$
- viii. The reference aperture area ( $A_r$ ) of the mirrors needed to capture the solar thermal power is given by  $A_r = \frac{P_{th,s,d}}{\{DNI \times \cos\theta\}_{max}}$

This is the procedure for determining reference aperture area corresponding to SM=1. A flow chart representing the above procedure is given below.

## b. Flow Chart to arrive at the Reference Aperture Area

For a chosen location and capacity ( $P_{g,d}$  in Watts)

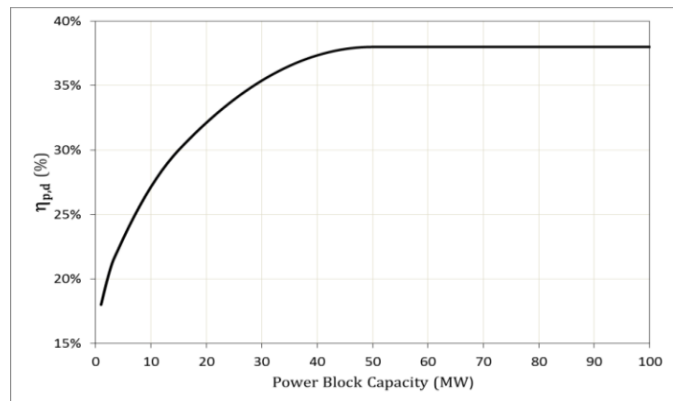
Starting from 1<sup>st</sup> hour of Jan to last hour of December 31<sup>st</sup> (i.e. for 8760 hours), compute the following corresponding to middle of every hour:

- declination of the day,  $\delta$
- hour angle,  $\omega$
- the tilt  $\beta$  needed for the troughs, taking into account  $\phi$ , the latitude of the location,
- $\theta$ , the angle between the sun's rays and the normal to the mirror aperture.
- $(DNI \times \cos\theta)$   
Find  $(DNI \times \cos\theta)_{max}$

$(DNI \times \cos\theta)_{max}$  ( $W/m^2$ )

Efficiency of Power Block ( $\eta_{p,d}$ ) under design conditions

$$\begin{aligned} \eta_{p,d} &= 0.18 + 0.011429 \times P_{g,d} - 2.286 \times 10^{-4} \times P_{g,d}^2 & \text{for } 0 \leq P_{g,d} \leq 15 \\ \eta_{p,d} &= 0.38 - 6.531 \times 10^{-5} \times (50 - P_{g,d})^2 & \text{for } 15 \leq P_{g,d} \leq 50 \\ \eta_{p,d} &= 0.38 & \text{for } P_{g,d} \geq 50 \end{aligned}$$



Other Inputs:

- Chord Length (C)
- Specular Reflectivity ( $\rho$ )
- Intercept Factor ( $\gamma$ )
- Heat Exchanger Efficiencies ( $\eta_{he}$  &  $\eta_{st}$ )

$$P_{th,d} = \frac{P_{g,d} \times 10^6}{\eta_{p,d}}$$

$$P_{htf,d} = \frac{P_{th,d}}{\eta_{he}}$$

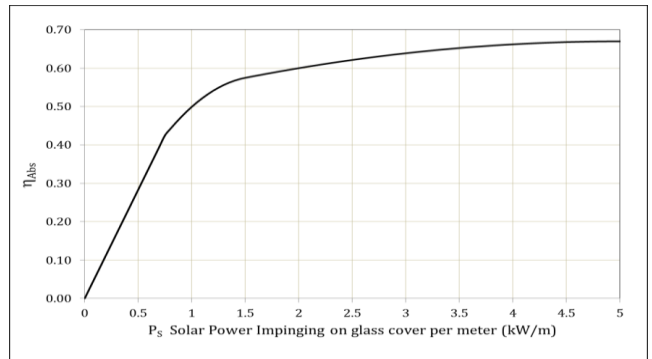
$$P_{abs,d} = \frac{P_{htf,d}}{\eta_{abs,d}}$$

$$P_{th,s,d} = \frac{P_{abs,d}}{\rho\gamma}$$

$$A_r = \frac{P_{th,s,d}}{(DNI \times \cos\theta)_{max}}$$

$$\begin{aligned} \eta_{abs} &= 0.5667 \times P_s & \text{for } 0 \leq P_s \leq 0.75 \\ \eta_{abs} &= 0.425 + 0.3457 \times (P_s - 0.75) - 0.1943 \times (P_s - 0.75)^2 & \text{for } 0.75 \leq P_s \leq 1.5 \\ \eta_{abs} &= 0.67 - 0.007755 \times (5 - P_s)^2 & \text{for } 1.5 \leq P_s \leq 5 \\ \eta_{abs} &= 0.67 & \text{for } P_s \geq 5 \end{aligned}$$

$$P_{s,d} = \frac{(DNI \times \cos\theta)_{max} \times \rho \times \gamma \times C}{1000}$$



### c. Computation of Electrical Energy Generated

We describe the procedure for computing the annual energy generated for a chosen SM, with specified thermal storage and hybridization.

Inputs:

- i.  $P_{htf,d}$  obtained from previous calculations.
- ii.  $t_s$  number of hours of thermal storage is specified.
- iii. The efficiency of heat exchanger of the storage system  $\eta_{st}$  is taken to be 0.97. The maximum amount of energy that can be stored is calculated from  $E_{tes,max} = \frac{P_{htf,d} \times t_s}{\eta_{st}}$ .
- iv. The thermal energy available  $E_{tea}$  is initialized to zero.
- v. The plant is assumed to operate at 10% overload. Therefore  $f_{th,max}$  is 1.1.
- vi.  $f_{th,min}$  is the minimum value of  $f_{th}$  below which the plant is shutdown. Default value is 0.25
- vii.  $f_{hb} = \frac{P_{hb}}{P_{htf,d}}$  is the maximum fraction of thermal power that can be delivered through hybridization. This determines the capacity of the natural gas burner.  $f_{hb}$  is limited to 0.2.

Procedure:

- i. For a chosen SM, find the corresponding mirror area ( $A_r \times SM$ ).
- ii. Start from 1<sup>st</sup> January and for each of the 8760 hours of the year, compute the electrical energy generated in the following manner.
- iii. Determine  $P_s$  (in kW/m) =  $\frac{(DNI \times \cos\theta) \times \rho \times \gamma \times C}{1000}$
- iv. Corresponding to the  $P_s$ , find  $\eta_{abs}$  from one of the following expressions:

$$\eta_{abs} = 0.5667 \times P_s \quad \text{for } 0 \leq P_s < 0.75$$

$$\eta_{abs} = 0.425 + 0.3457 \times (P_s - 0.75) - 0.1943 \times (P_s - 0.75)^2 \quad \text{for } 0.75 \leq P_s < 1.5$$

$$\eta_{abs} = 0.67 - 0.007755 \times (5 - P_s)^2 \quad \text{for } 1.5 \leq P_s < 5$$

$$\eta_{abs} = 0.67 \quad \text{for } P_s \geq 5$$

- v. The thermal power transferred to HTF during that hour is  $P_{htf} = DNI \times \cos\theta \times \rho \times \gamma \times A_r \times SM \times \eta_{abs}$
- vi. The fractional solar thermal power  $f_{th,s}$  is given by  $P_{htf}/P_{htf,d}$
- vii. Initially  $f_{th}$  is taken as equal to  $f_{th,s}$ .
- viii. Once the available  $f_{th}$  from solar field is known, the following steps are applied:
  - a. Check if  $f_{th} \geq f_{th,max}$
  - b. If so, stored energy increases

$$E_{tea} = E_{tea} + (f_{th} - f_{th,max}) P_{htf,d} \times \Delta t \times \eta_{st} \quad (\Delta t \text{ is taken as 1 hour})$$

$$\text{If } E_{tea} \geq E_{tes,max}, \text{ then } E_{tea} = E_{tes,max}.$$

$$\text{Available fractional power from stored energy, } f_{th,sta} = \frac{E_{tea} \times \eta_{st}}{P_{htf,d} \times \Delta t}.$$

The fraction of thermal energy available to power block would be made  $f_{th} = f_{th,max}$  and proceed to calculate the electrical energy for that hour. In this case,  $f_{hb,used}$  is zero.

c. If  $f_{th} < f_{th,max}$  then compute  $f_{th,m}$ , the modified  $f_{th}$ , as follows

- $f_{th,m} = f_{th} + f_{th,sta}$
- Check if  $f_{th,m}$  is  $\geq f_{th,max}$
- If  $f_{th,m} \geq f_{th,max}$  then

Fraction of thermal power used from storage:  $f_{th,st} = f_{th,max} - f_{th}$

Fraction remaining in storage:  $f_{th,sta} = f_{th,sta} - f_{th,st}$

Fraction of thermal power available to power block would be equal to  $f_{th,max}$

Proceed to calculate electrical energy output for that hour.

In this case,  $f_{hb,used}$  is zero

- If  $f_{th,m} < f_{th,max}$ , then the fraction of the total thermal power that can be delivered including hybridization is  $f_{th,T} = f_{th,m} + f_{hb}$ .

Again if  $f_{th,T} \geq f_{th,max}$ , then  $f_{hb,used} = (f_{th,max} - f_{th,m})$  and

$$f_{th} = f_{th,max}$$

If  $f_{th,T} < f_{th,max}$ , then  $f_{th} = f_{th,T}$ .

d. If  $f_{th} < f_{th,min}$  then  $f_{th} = 0$ ,  $f_{th,st} = 0$  and  $f_{hb,used} = 0$  electrical energy generated is taken as 0.

ix. When the plant is not operating, the electrical energy lost due to thermal losses is given by  $e_{start} = e_{start} + L_f \times P_{g,d} \times \Delta t$

x. When  $f_{th} > f_{th,min}$ ,  $f_p$  is found from the analytical expression:

$$\begin{aligned} f_p &= 0 && \text{for } f_{th} < 0.25; \\ f_p &= 1.1f_{th} - 0.1 && \text{for } 0.25 < f_{th} < 1; \\ f_p &= f_{th} && \text{for } f_{th} > 1; \end{aligned}$$

xi. Maximum gross electrical energy that can be generated is given by  $e_g = f_p \times P_{g,d} \times \Delta t$ , where  $\Delta t$  is 1 hour.

xii. However the actual electrical energy generated ( $e_{g,a}$ ) is  $(e_g - e_{start})$ . Then the corresponding fractional power generated ( $f_{pa}$ ) is  $e_{g,a}/(P_{g,d} \times \Delta t)$ .

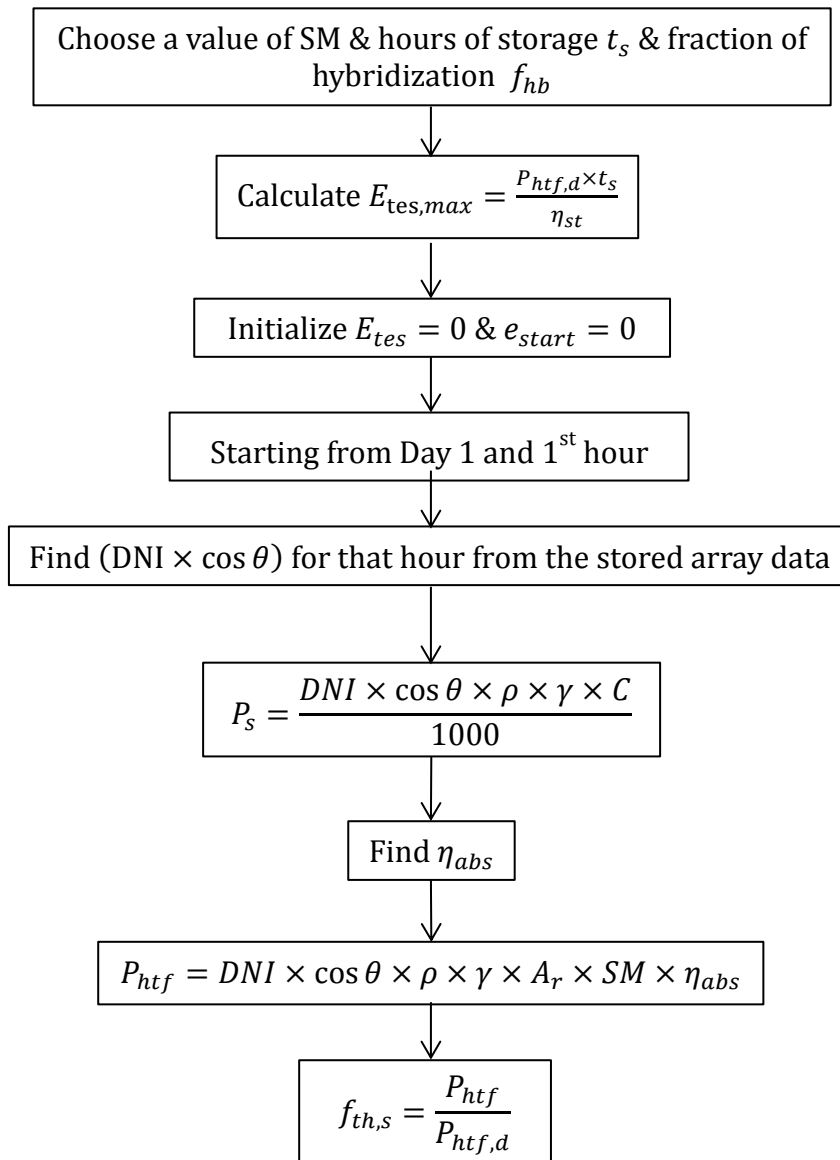
xiii. The net electrical energy supplied to grid,  $e_{grid}$ , during that interval is equal to  $e_{g,a} \times (1 - \text{Auxiliary Power Fraction})$ . Auxiliary power fraction is the ratio of power consumed by the auxiliary units to the gross power generated. The default value is 0.1.

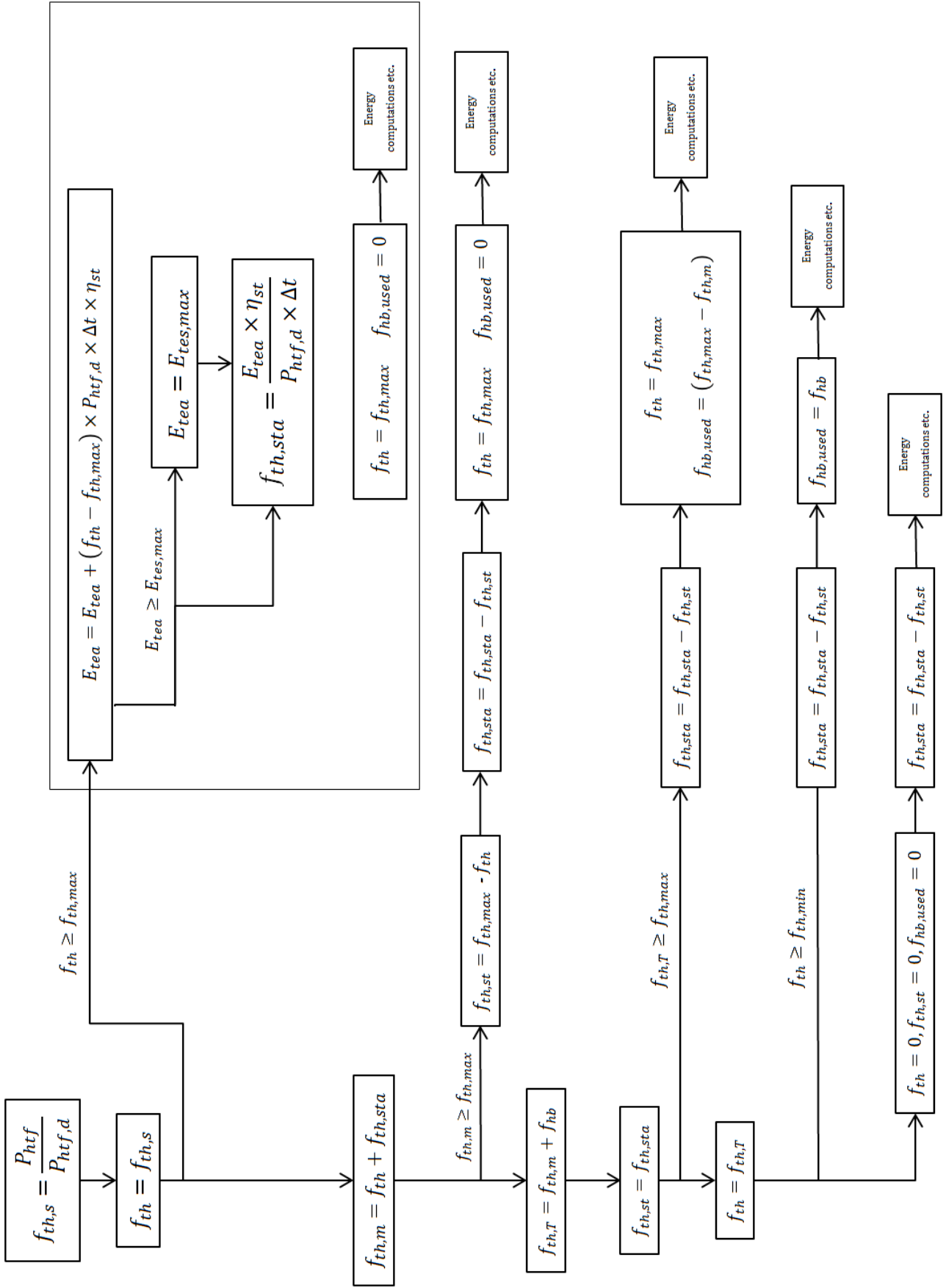
xiv. The electrical energy apportioned to hybridization ( $e_{hb}$ ) is  $\left(\frac{f_{hb,used}}{f_{th}} \times e_{grid}\right)$  and that apportioned to solar ( $e_s$ ) is  $(e_{grid} - e_{hb})$ .

- xv. On the above basis, the total net electrical energy generated over the whole year can be calculated and also the contributions from solar and hybridization are separately accounted for.
- xvi. Compute Capacity factor =  $\sum e_{g,a} / (P_{g,d} \times 8760)$
- xvii. Compute the annual efficiency of conversion from solar to electric energy as follows.  

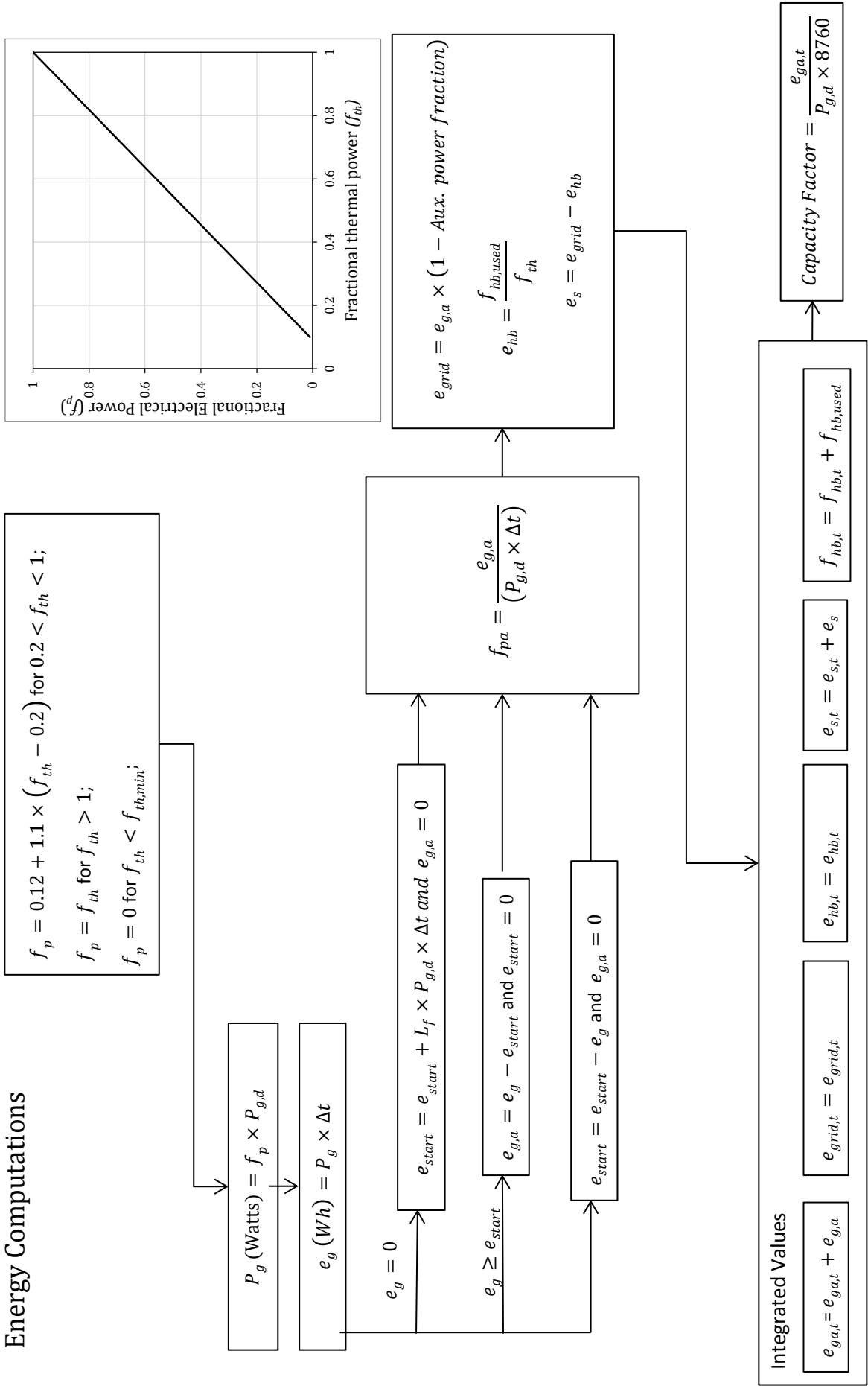
$$\sum e_{grid} / \{A_r \times SM \times \sum (DNI \times \cos \theta)\}$$

**d. Flow Chart to Compute the Annual Electrical Energy**





## Energy Computations



### 3.3 Model for Economic Analysis of PT Technology

In an economic analysis, various capital costs and Operation & Maintenance (O&M) costs are estimated. Using this information along with financial inputs, the Levelised Cost of Electricity (LCOE) for the various values of SMs chosen is computed. Then, the SM for which the LCOE is the minimum is chosen and solar field is designed for this SM.

The technical analysis is carried out for a CSP plant using the standard Euro Trough of chord width 5.75 m and the most commonly used SCHOTT absorber tube ( $\varnothing$  70 mm). If parabolic troughs having other dimensions and characteristics are used, then inputs have to be suitably modified.

#### 3.3.1 Inputs Required from Technical Model for Economic Analysis

As stated earlier, technical analysis consists of the following:

- a. The computation of the reference mirror aperture area ( $A_r$ ) for the rated capacity and chosen location of the plant.
- b. Computation of the annual electrical energy with thermal storage for various values of SM

The input and output parameters from (a) are the following:

- i. The rated capacity of the plant ( $P_{g,d}$ )
- ii. Chord width of the Mirrors ( $C$ )
- iii. Reference Mirror Aperture Area ( $A_r$ )

The input and output parameters from (b) are the following:

- i. Solar Multiple (SM)
- ii. Hours of thermal storage ( $t_s$ )
- iii. The maximum amount of thermal energy stored ( $E_{tes,max}$ )
- iv. Actual Aperture Area of Mirrors,  $A_a = A_r \times SM$
- v. Length of Absorber Tubes
- vi. Volume of HTF (including header and feeder pipes) = 4 x Volume of HTF in the absorber Tubes
- vii. Annual gross electrical energy generated accounting for shutdown losses,  $\sum e_{g,a}$
- viii. Annual electrical energy supplied to the grid,  $\sum e_{grid}$
- ix. Capacity Factor (CF)

Using these values, costs of various components of the plant are determined as follows:

#### 3.3.2 Estimation of Capital Costs

The capital cost of CSP plants has two parts.

- i. Direct Capital Cost (DCC), which refers to the cost of land and site preparation, equipment, material, components, etc. and
- ii. Indirect Capital Cost refers to the cost of Engineering Procurement and Construction (EPC), Program Management (PMG), Interest during Construction (IDC) and pre-operative expenses.

The input data are enclosed in [ ], while those derived from our analysis are enclosed in { }.

### i. Direct Capital Cost

The Direct Capital Cost (DCC) of a CSP plant using trough technology, with thermal storage and hybridization is grouped under the following categories.

- Land & Preparation
- Solar Field
- Power Block
- Thermal Storage System
- Hybridization System

#### Cost of Land & Site Preparation

The cost of land is estimated as:

$$\{A_a\} \times [\text{Land to Mirror Ratio}] \times [\text{Cost of Land per Unit Area}]$$

Cost of site preparation

$$\{A_a\} \times [\text{Land to Mirror Ratio}] \times [\text{Cost of Site Preparation per Unit Area}]$$

#### Cost of Solar Field

- a. Cost of mirror =  $\{A_a\} \times [\text{Cost of mirror per unit area}]$
- b. Cost of support structure =  $\{A_a\} \times [\text{Cost of material and fabrication/kg}] \times [\text{Support structure weight, kg/unit area}]$
- c. Cost of Foundation =  $\{A_a\} \times [\text{Cost of foundations per unit area}]$
- d. Cost of Absorber tubes =  $\{\text{Total length of Absorber tube}\} \times [\text{cost/unit length}]$ , where length of absorber tubes is given by  $\{A_a/C\}$
- e. Cost of swivel joints =  $[\text{Cost of swivel joint per unit}] \times \{A_a\} / [\text{Mirror Area per Swivel Joint}]$
- f. Cost of Hydraulic Drives & Electric Motors =  $[\text{Cost per unit}] \times (\text{Total length of Absorber Tube}) / [\text{Length of trough for each drive unit}]$
- g. Cost of HTF =  $[\text{Cost of HTF per litre}] \times \{\text{Volume of HTF}\}$
- h. Cost of HTF System =  $[\text{Cost of HTF system per unit aperture area}] \times \{A_a\}$
- i. Cost of electronics, controls, and electrical (ECE) system =  $[\text{Cost of ECE system per unit aperture area}] \times \{A_a\}$

#### Cost of Power Block System

Cost of Power Block (Turbine-Generator set and accessories) = Cost of Power Block per kW  $\times \{P_{g,d}\}$  (in Watt)/1000

where, cost of power block in ₹/kW =  $0.55 \times (\{P_{g,d}\}/10^6)^{-0.2875} \times 10^5$

The cost of balance of plant (Power block) is taken as 50% of the cost of power block.

The basis for using the above relationship is given in section 3.3.5.

#### Cost of Thermal Storage System

The cost of thermal storage system per kWh of thermal energy stored is an input value. The maximum amount thermal energy stored  $E_{tes,max}$  (in Wh<sub>th</sub>) is computed as follows.

$$E_{tes,max} = \{P_{htf,d}\} \times [t_s] / [\eta_{st}]$$

where  $\{P_{htf,d}\}$  is the design thermal input needed to generate the rated gross power,  $t_s$  is the hours of thermal storage and  $\eta_{st}$ , is the efficiency of the storage heat exchanger.

Then, the cost of the thermal storage system

$$= E_{tes,max} \times [\text{cost of thermal storage system/ kWh}_{th}]/1000$$

### Cost of Hybridization

The hybridization system consists of Natural Gas (NG) storage system and a boiler with burner for heating the HTF.

#### a. Cost of Boiler

The capacity of the boiler is generally expressed in terms of lakh kcal/h. For the chosen  $f_{hb}$ , the boiler capacity is determined as follows. Given that 1kW=860 kcal/h, the boiler capacity in lakh kcal/h is given by

$$\text{Boiler Capacity} = \{P_{htf,d}\} \times [f_{hb}] \times 860/(10^3 \times 10^5)$$

The capital cost of the boiler is taken as

$$= (\text{Boiler capacity}) \times [\text{Cost in ₹ per lakh kcal/h}]$$

#### b. Cost of NG Storage System

In order to estimate the cost of the storage system, the annual energy given by the NG boiler to HTF, volume of fuel required annually and the number of days of buffer storage is required.

The annual energy to HTF (in kcal) by the boiler is given by  $P_{htf,d} \times f_{hb,t} \times 860/1000$ . Thus, the volume of fuel required annually (in m<sup>3</sup>) is calculated by the following expression

$$V_a = \frac{\text{Annual Energy to HTF from NG boiler}/[\eta_b]}{[\text{Calorific value of NG (in kCal/m}^3\text{)}]}$$

where  $\eta_b$  = efficiency of boiler

All volumes of NG are at NTP.

Thus the storage volume of fuel required is based on the number of days one intends to have NG fuel as buffer storage at the plant location. Thus the storage volume required is given by

$$V_{st} = V_a \times \text{Buffer Storage of Fuel (in days)}/365$$

So the cost of storage system =  $V_{st} \times [\text{Cost of Storage system per cubic meter}]$

The cost of piping for this system for the storage unit has been taken as a bulk cost at 50% of the storage system cost.

### ii. Indirect Capital Cost

Indirect capital costs are taken as a percentage of the direct capital cost. The items which come under ICC are given below.

- EPC costs =  $[\text{EPC percent}] \times (\text{DCC} - \text{Cost of Land \& Site preparation})/100$
- PMG Costs =  $[\text{PMG Percent}] \times (\text{DCC} - \text{Cost of Land \& Site preparation})/100$
- Interest during Construction (IDC) =  $(\text{DCC} - \text{Cost of Land \& Site preparation}) \times [\text{Debt Percentage}] \times [\text{Loan Rate}] \times [\text{Fraction}]/10000$
- Pre-op Expenses =  $\text{DCC} \times [\text{Pre-op Expenses percent}]/100$

### 3.3.3 Methodology for Estimation of O&M Expenses

#### i. Operating Expenses

##### a. Staff Salaries

The following categories of staff are considered

- i. Senior Engineer
- ii. Plant Operators
- iii. Administrative Staff
- iv. Plant Maintenance Staff
- v. Security

Annual cost of salaries (Solar Field only) =  $\sum_{i=1}^p [N_i] \times [\text{Annual Salary/Staff } (S_i)]$

where  $N_i$  is the number of staff in category ( $i$ ), and ( $S_i$ ) is the annual salary of the staff in category ( $i$ ),  $p$  is the number of categories.

The number of staff in each category and annual salary per staff that we have used in our economic analysis are covered in Section 3.3.5.

The staff given is for a solar plant only, without thermal storage and hybridization. Thus the salary component for thermal storage system and hybridization system is given by

$$\begin{aligned} \text{Salaries (Thermal Storage)} \\ &= \text{Annual cost of salaries (Solar only)} \\ &\times \text{Percentage increase in Salary component for Storage System}/100 \end{aligned}$$

$$\begin{aligned} \text{Salaries (Hybridization)} \\ &= \text{Annual cost of salaries (Solar only)} \\ &\times \text{Percentage increase in Salary component for Hybridization System}/100 \end{aligned}$$

Thus total salary component is given by

$$\begin{aligned} \text{Total Salaries} &= \text{Annual Cost of Salaries (Solar only)} + \text{Salaries (Thermal Storage)} \\ &+ \text{Salaries (Hybridization)} \end{aligned}$$

##### b. Water

The annual cost of water used in the plant = [annual water required in  $\text{m}^3/\text{MWh}$ ]  $\times$  {  $\sum e_{g,a}$  in MWh}  $\times$  [Cost of water in  $\text{₹}/\text{m}^3$ ]

##### c. Insurance

Cost of Insurance = [Cost of insurance as percentage of DCC]  $\times$  DCC, where DCC has been computed as per Section 3.3.2.

##### d. Fuel

When hybridization is considered, the annual volume of NG ( $V_a$ ) required is known, so the operating cost of hybridization due to NG is  $\{V_a\} \times [\text{Cost of NG per } \text{m}^3]$

#### ii. Maintenance Expenses

Costs of equipment maintenance of the following components are taken into account.

- i. Mirror
- ii. Steel Structure

- iii. Heat Conduction Elements
- iv. HTF
- v. Hydraulic Drives & Electric Motors
- vi. Swivel Joints
- vii. Electronics, Controls & Electrical
- viii. Power Block
- ix. Thermal Storage
- x. Hybridization System

Maintenance cost of component = {DCC of component} × [Percentage assigned for that component]

Total Maintenance Expenses =  $\sum$  Maintenance cost of components

DCC of component is found as given in Section 3.3.5.

### 3.3.4 Financial Parameters for Computing LCOE

The inputs required for the economic analysis are as follows:

Plant Life (PL) in years, Loan Term (LT) in years, Moratorium Period (MP) in years, Debt percentage, Loan Rate, Depreciation during loan term (Dr1) and post loan term (Dr2), Return on Equity during loan term (R\_LT) and post loan term (R\_PLT) and inflation rates.

#### i. Equity Rate (average return on equity)

A weighted average value is taken for calculations as follows

$$\text{Equity Rate (in \%)} = \frac{R_{LT} \times LT + R_{PLT} \times (PL - LT)}{[PL]}$$

#### ii. Discount Rate

The discount rate is defined as

$$\text{Discount Rate (in \%)} = \frac{\text{Loan Rate} \times \text{Debt Percentage} + \text{Equity Rate} \times \text{Equity Percentage}}{[\text{Debt Percentage} + \text{Equity Percentage}]}$$

#### iii. Total Operational & Maintenance Expenses for the $i^{\text{th}}$ year

In calculating the O&M expenses for the  $i^{\text{th}}$  year, the inputs required are the inflation rates (in percentage) for each of the O&M expenses mentioned in Section 3.3.3, viz. salaries ( $Sal\_Inf$ ), water ( $Water\_Inf$ ), insurance ( $Ins\_Inf$ ), total equipment maintenance ( $EM\_Inf$ ) and fuel ( $Fuel\_Inf$ ).

Then, we have

$$\text{Total Salaries (i)} = \text{Total annual Salary} \times \left(1 + \frac{[Sal\_Inf]}{100}\right)^{(i-1)}$$

$$\text{Cost of Water (i)} = \text{Cost of water} \times \left(1 + \frac{[Water\_Inf]}{100}\right)^{(i-1)}$$

$$\text{Cost of insurance (i)} = \text{Cost of Insurance} \times \left(1 + \frac{[Ins\_Inf]}{100}\right)^{(i-1)}$$

$$\text{Cost of Fuel (i)} = \text{Cost of Fuel} \times \left(1 + \frac{[Fuel\_Inf]}{100}\right)^{(i-1)}$$

$$Total\ Equipment\ Maintenance\ (i) = Total\ Equipment\ Maintenance \times \left(1 + \frac{[EM\_Inf]}{100}\right)^{(i-1)}$$

Total O&M (i) is the sum of all the above.

#### iv. Interest on Term Loan

Interest on Term Loan at any time depends on the outstanding loan at that time, which in turn depends on the payment made up to that time towards the principal. So we should consider the mode of payment towards principal. It is also possible, that there may be a Moratorium Term [MT], the initial number of years during which no payment towards principal is made but interest on the loan is to be paid.

Hence, interest on term loan paid every month is

$$= \frac{(Debt\ Percentage \times CapitalCost)}{100} \times \frac{Loan\ Rate}{100 \times 12}$$

The payment towards principal (PPMT) after moratorium term, is made every month in equal instalments. Therefore,

$$PPMT = \frac{Debt\ Percentage \times CapitalCost}{12 \times (LT - MT) \times 100}$$

Therefore interest on term Loan (i) (for  $i \leq MT$ )

$$= (Debt\ Percentage \times CapitalCost \times Loan\ Rate)/(100 \times 100)$$

However after the moratorium, since PPMT is made, the loan amount reduces with succeeding months. However for Interest on term loan (i), during the  $i^{th}$  year of the term loan is the sum of the varying interest over the 12 months of that year. It can be shown that for the  $i^{th}$  year,

Interest on term loan (i), (for  $MT < i < LT$ )

$$= \left[ \frac{Debt\ Percentage \times CapitalCost}{100} - \frac{PPMT \times \{24(i - MT) - 13\}}{2} \right] \times \frac{Loan\ Rate}{100}$$

#### v. Depreciation

The depreciation during the term loan and for the post term loan is given below.

$$Depreciation(i) = \frac{Debt\ Percentage \times CapitalCost \times [Dr1]}{100} \quad for\ 1 \leq i \leq LT$$

$$Depreciation(i) = \frac{Debt\ Percentage \times CapitalCost \times [Dr2]}{100} \quad for\ i \geq LT$$

#### vi. Interest on Working Capital

Before considering the interest on working capital, one needs to define what constitutes the working capital. The approach we have taken in defining the working capital is based on CERC guidelines.

The working capital is taken as equivalent to cost of O&M for one month of that year (plus 15% extra to account for stock of spares) and two months of receivables from electrical energy sold to the grid. Thus for the  $i^{th}$  year

Working Capital (i)

$$= \frac{Total\ O\&M\ (i) \times 1.15}{12} + \frac{Assumed\ Tariff \times e_{grid,t}}{6 \times 1000}$$

where  $e_{grid,t} = \sum_{j=1}^{8760} e_{grid}$ . Finally,

Interest on working capital (i) =  $Working\ Capital(i) \times Loan\ rate/100$

### vii. Return on Equity

Return on equity (in %) during the loan term, and post loan term are generally taken to be different and are represented by  $R_{LT}$  and  $R_{PLT}$  respectively.

Therefore, for the year (i),  $1 \leq i \leq LT$ , the Return on Equity

$$ROE(i) = [Equity\ Percentage] \times \{Capital\ Cost\} \times [R_{LT}]/10000$$

and for the year(i),  $i > LT$ ,

$$ROE(i) = [Equity\ Percentage] \times \{Capital\ Cost\} \times [R_{PLT}]/10000$$

## 3.3.5 Cost Estimates of Components

Section 3.3.2 gives the methodology for estimation of capital cost for various components of the PT technology. In this section brief details about the inputs for various costs are discussed.

The costs are broadly divided into two sections: viz. Direct Capital costs & Indirect Capital Costs.

### i. Direct Capital Costs

Based on a detailed literature survey and discussion with vendors, the costs of various components are arrived at.

#### Land Related Costs

Cost of land varies from place to place, but in the present analysis it is taken as ₹100 per m<sup>2</sup>.

For a PT plant, the slope of the land desired is less than 3°; if not, there is a need for sufficient earth work to be done. It is estimated that the cost of site preparation would be around ₹ 110 per m<sup>2</sup>.

#### Solar Field Costs

**Mirrors:** The mirrors are imported as there is little experience in India in manufacturing these kinds of curved mirrors. It is priced around 35 €/m<sup>2</sup> (₹ 2450/m<sup>2</sup>).

**Absorber Tubes:** Absorber tubes are also imported and for the present calculations a default value of \$ 250/m is used (₹ 14250/m).

**Support Structure & Pylons:** The support structure and pylons are considered to be an indigenously designed and manufactured component, as the engineering skills and manpower required are available in India. For the present studies the Euro trough design is used as a reference. This trough structure has weight of 19 kg per unit aperture area of mirror. The material and manufacturing cost including galvanising is approximated at ₹ 150 per kg. Thus the cost of support structures per unit aperture area of the mirror is taken as ₹ 2850.

**Foundations:** It is difficult to arrive at the costing for different conditions unless the sub soil profile at the site is known. So an approximate estimate of ₹ 200/m<sup>2</sup> of mirror area is used.

**Swivel Joints:** It is assumed that, swivel joints are used for every 276 m<sup>2</sup> of aperture area of the mirror. (Considering there are four Solar Collector Assemblies in a loop of length 576 m, then the number of swivel joints required would be 12 per loop). The cost of the swivel joints is estimated to be approximately ₹ 70,000 per unit (Ernst & Young, 2011).

**Hydraulic Drives:** For the present calculations provision of a hydraulic drive for every 144 m length of the parabolic trough system is assumed. The cost of drive system is estimated to be ₹130,000 per unit (Ernst & Young, 2011).

**HTF & HTF System:** Almost all the commercial trough systems today use synthetic oil as heat transfer medium. There are several companies which manufacture this under different brand names viz. Therminol VP-1, Dowtherm, HITEC etc. The cost of HTF used in the present calculations is ₹200 per litre. The HTF system includes components like the header and feeder pipes, expansion loops, along with the necessary insulation, valves, pumps, variable speed drives, HTF to water heat exchangers, expansion vessels, nitrogen tanks etc. Since there are a lot of components involved in the HTF system, arriving at each individual cost of the component will be a challenging task, thus a bulk cost for the HTF system in terms of the aperture area is taken into consideration. The cost is taken to be ₹1900 per m<sup>2</sup> of mirror aperture area (Ernst & Young, 2011).

For the present analysis it is estimated the volume of HTF required in the complete circuit (header and feeder pipes, heat exchanger etc.) is four times the volume in the absorber tubes.

**Cost of Electronics, Controls and Electrical (ECE) system:** The electronics and controls comprise of instrumentation and controls to monitor the solar field and power block. The solar field control consists of a Supervisory Control and Data Acquisition (SCADA) system for each of the solar collectors with a closed loop feedback control system. The bulk cost has been estimated at ₹1000/m<sup>2</sup> of mirror aperture area (Ernst & Young, 2011).

### Power Block Costs

The typical power block of a CSP plant consists of turbine generator set, condenser and its auxiliaries, de-aerator, boiler feed water pump etc. Based on literature survey (Sargent & Lundy, 2003) and interaction with some of the manufacturers of steam turbines, the cost of the power block (Turbine Generator set plus accessories) has been estimated. Since the cost varies with respect to capacity an analytical fit for the cost in terms of ₹/kW vs. capacity in MW has been arrived at as given below

$$\text{Cost (₹-lakh/kW)} = 0.55 \times \left( \{P_{g,d}\} / 10^6 \right)^{-0.2875}$$

This is as represented in Figure 3.6 as shown below. The cost of balance of plant of power block has been taken to be 50% of the cost of power block.

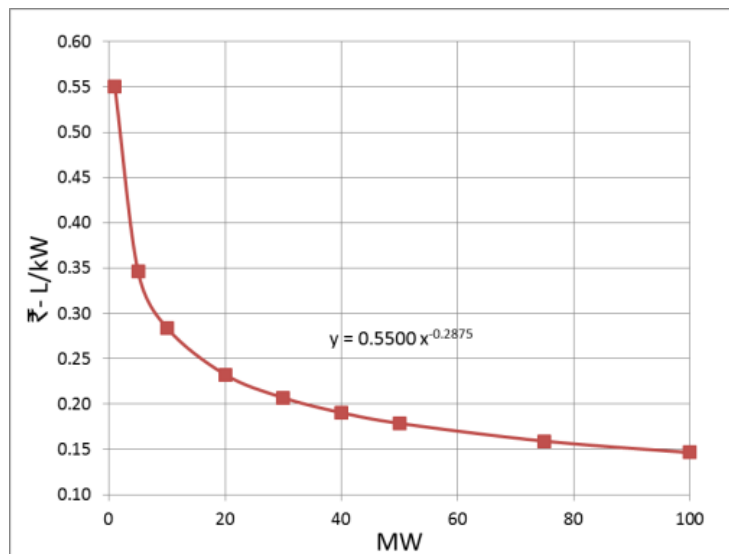


**Figure 3.6: Variation of power block cost with capacity**

### Thermal Storage System Costs

Thermal storage is a value addition in a solar thermal power plant as it increases the capacity factor of the plant. Among all the renewables, storage in solar is unique and cost effective. Molten salt (40% KNO<sub>3</sub> +60% NaNO<sub>3</sub>) is the commonly used storage medium. The other advantage with thermal storage is dispatchability to meet the peak demands.

The main components in the thermal storage system are molten salts, storage tanks, insulations for the tanks, storage heat exchangers, pumps etc. The overall cost for a two tank molten salt storage system varies between ₹ 1700 and ₹ 2280 per kWh<sub>th</sub> (\$30-40/kWh<sub>th</sub>) (Hermann-Ulf, 2004). For the present studies, a value of ₹ 1700 kWh<sub>th</sub> is used.

### Hybridization System Costs

The hybridization cost includes natural gas boiler, natural gas storage system, piping system etc. The capacity of natural gas boiler is generally expressed in terms of lakh kcal/h. The cost of the natural gas burner was estimated as ₹ 2 lakh per lakh-kcal/h, based on discussion with vendors. The cost of natural gas buffer storage system was estimated at ₹ 1000/m<sup>3</sup>; the cost of piping system for this arrangement is estimated to be 40% of the cost of NG storage system. The volumes for natural gas are considered at NTP.

Table 3.1 summarises the costs given above.

**Table 3.1: Cost break up of components used in economic assessment**

Sl. No	Component	Unit	Cost
1	Land	₹/m <sup>2</sup>	100
2	Site Preparation	₹/m <sup>2</sup>	108
3	Mirror	₹/m <sup>2</sup>	2450
4	Absorber Tube	₹/m	14,250
5	Support Structure		
	Weight per unit aperture area	kg/m <sup>2</sup>	19
	Fabrication cost per unit kg	₹/kg	150
6	Foundations	₹/m <sup>2</sup>	200
7	Swivel Joints	₹/Unit	70,000
8	Hydraulic Systems	₹/Unit	1,30,000
9	Heat Transfer Fluid	₹/liter	200
10	HTF System	₹/m <sup>2</sup>	1900
11	Electronic Controls and Electrical Systems	₹/m <sup>2</sup>	1000
12	Power Block		
	Turbine & Generator System		Ref Section
	Balance of Plant Power Block		3.3.5
13	Thermal Storage System	₹/kWh <sub>th</sub>	1710
14	Hybridization System		
	Cost of NG Burner	₹-lakh per lakh-kcal/h	2
	Cost of Fuel	₹/m <sup>3</sup>	20
	Cost NG Storage System	₹/m <sup>3</sup>	1000
	Cost of Piping System	as a % of NG Storage system	40

## ii. Indirect Capital Costs

### EPC Costs:

We have taken EPC costs as 10% of DCC excluding the cost of land & site preparation.

### Project Management:

Project management cost is taken as 5% of DCC excluding the cost of land & site preparation.

### Interest during construction (IDC):

$IDC = (DCC - \text{Land Costs} - \text{Site preparation costs}) \times \text{Debt Percentage} \times \text{Cost of debt} \times [\text{Fraction}]$ .

The value of fraction is taken to be 0.5

### Pre-Operative Expenses:

Pre-operating expenses =  $(DCC - \text{Land Costs} \& \text{Site preparation costs}) \text{ Debt Percentage} \times \text{Cost of debt} \times [\text{Pre-op Expenses percent}]$ . The value of pre-op expenses is taken to be 1%.

## 3.3.6 Estimation of O&M expenses

### i. Operating Expenses

The operating expenses relate to salaries of staff, cost of water, fuel and insurance.

#### a. Staff Salaries

The staffing was divided into five different heads viz. System Engineering, Plant Operation, Administration, Plant Maintenance and Security. The number of personnel required for a CSP plant was classified based on the gross capacity of the plant. Table 3.2 gives the number of staffing required for a solar thermal power plant with no storage and no hybridization condition. For the thermal storage and hybridization conditions the salary escalation of 10% & 5% from the base case has been considered.

**Table 3.2: Number of staff required for various capacities**

Sl. No.	Staff	$P_{g,d} \leq 5\text{MW}$	$5\text{MW} < P_{g,d} \leq 20\text{MW}$	$20\text{MW} < P_{g,d} \leq 50\text{MW}$
1	System Engineers	6	6	6
2	Plant Operators	8	10	12
3	Administrators	4	4	4
4	Plant Maintenance Personnel	8	12	16
5	Security Staff	6	8	10

The annual cost to company for the staffing based on different heads is given in Table 3.3.

**Table 3.3: Staff salaries**

Sl. No.	Staff	Cost to Company (₹-lakhs per annum per person)
1	System Engineer	4
2	Plant Operator	2.5
3	Administrator	1.8
4	Plant Maintenance Personnel	1.2
5	Security Staff	1

*b. Water*

In this analysis water cooled condensing option is considered. Water required for the power block (make up water) and for mirror cleaning purposes is estimated to be 4 m<sup>3</sup>/MWh and costed at ₹ 120/MWh.

*c. Fuel*

The cost of fuel (natural gas) is a market driven price and it is assumed to be ₹ 20/m<sup>3</sup>.

*d. Insurance*

Insurance costs are considered to be 0.5% of DCC.

**ii. Maintenance Expenses**

The maintenance costs used in the assessment studies are presented in Table 3.4.

**Table 3.4: Equipment maintenance costs**

<b>Component</b>	<b>% of DCC of Component</b>
Mirror	2.0
Steel Structure	1.5
Heat Conduction Elements	2.5
HTF	1.0
HTF System	2.0
Hydraulic Trackers & Electric Motors	0.5
Swivel Joints	1.0
Electronics, Controls & Electrical	2.0
Power Block	2.0
Thermal Storage	2.5
Hybridization System	1.0

**3.3.7 Values of the Financial Parameters**

The various metrics used in the economic analysis is tabulated in Table 3.5.

**Table 3.5: Financial metrics used in economic analysis**

Sl. No	Parameter	
1	Plant Life (PL)	25 years
2	Debt Percentage	70
3	Loan Tenure	10 years
4	Moratorium Period	0
5	Loan Rate	14%
6	Depreciation Rate	
	During Loan Term	7%
	Post Loan Term	1.33%
7	Return on Equity	
	During Loan Term	20%
	Post Loan Term	24%
8	Assumed Tariff	15 (₹/kWh)
9	Inflation Rate	
	Salary	7.5%
	Equipment Maintenance	2.5%
	Water	1%
	Insurance	0.5%
	Fuel	2.5%

### 3.3.8 Methodology for Computing LCOE & IRR

#### i. LCOE

The guidelines prescribed by Central Electricity Regulatory Commission (CERC) to compute the LCOE have been adopted (CERC, 2010).

The LCOE is defined as the ratio of Net Present Value (NPV) of all the project expenses incurred over the life time of the plant  $NPV (PE)$ , to the NPV of the total electrical energy supplied to the grid over the life time of the plant  $NPV (e_{grid,t})$ .

$$LCOE = \frac{NPV (PE)}{NPV (e_{grid,t})/1000}$$

where LOCE is in ₹/kWh

NPV of any quantity  $Q_i$  considered for the  $i^{th}$  year of the plant is given by

$$NPV (Q_i) = \frac{Q_i}{\left(1 + \frac{Discount\ rate}{100}\right)^i}$$

Project Expenses,

$$PE(i) = Total\ O\&M(i) + Depreciation(i) + Interest\ on\ Loan\ Term(i) \\ + Interest\ on\ Working\ Capital(i) + Return\ on\ Equity(i)$$

$$NPV(PE) = \sum_{i=1}^{PL} \frac{PE(i)}{\left(1 + \frac{Discount\ rate}{100}\right)^i}$$

The  $e_{grid,t}(i) = \sum_{j=1}^{8760} e_{grid(j)}$ , where  $e_{grid(j)}$  is the energy generated during the  $j^{th}$  hour of the  $i^{th}$  year. Therefore  $e_{grid,t}(i)$  is the total energy supplied to the grid in the  $i^{th}$  year.

$$NPV(e_{grid,t}) = \sum_{i=1}^{PL} \frac{e_{grid,t}(i)/1000}{\left(1 + \frac{Discount\ rate}{100}\right)^i}$$

Since  $e_{grid,t}(i)$  is taken to be same for all years,

$$NPV(E) = e_{grid,t} \sum_{i=1}^{PL} \frac{1}{\left(1 + \frac{Discount\ rate}{100}\right)^i}$$

$$NPV(E) = e_{grid,t} \times A_f$$

where  $A_f$  is defined as the Annuity factor

$$A_f = \sum_{i=1}^{PL} \frac{1}{\left(1 + \frac{Discount\ Rate}{100}\right)^i} = \frac{1 - (1 + Discount\ Rate/100)^{-PL}}{Discount\ Rate/100}$$

## ii. LCOE for Solar & Hybridization Component

In case of hybridization, the LCOE is apportioned between the solar component and natural gas component. The electrical energy supplied to grid from solar and from hybridization is separately estimated (section 3.2.3). Similar to the energy estimation,  $NPV(PE\_Solar)$  and  $NPV(PE\_Hyb)$  are determined. Using these,  $LCOE(Solar)$  and  $LCOE(Hyb)$  are determined as given below.

### LCOE - Solar Component

**Direct Capital Costs - Solar:** The capital costs for the solar component is arrived by excluding the cost of hybridization system from the overall cost.

**Indirect Capital Costs - Solar:** The indirect capital cost is calculated similarly as discussed in 3.3.2, except that the DCC used here would be DCC of solar component.

The O&M expenses for the solar component are estimated by excluding the hybridization component in each of the items discussed in section 3.3.3. The annual O&M expenses for each year with corresponding inflation rates are estimated as discussed in the same section.

The project expenses attributed to solar ( $PE\_Solar(i)$ ), are calculated for each of the items discussed in section 3.3.3 excluding hybridization component wherever applicable. Finally the  $NPV(PE\_Solar)$  of project expenses is calculated as given below.

$$NPV(PE\_Solar) = \sum_{i=1}^{PL} \frac{PE\_Solar(i)}{\left(1 + \frac{Discount\ rate}{100}\right)^i}$$

The NPV of electrical energy from solar is given by,

$$NPV(e_{s,t}) = e_{s,t} \times A_f, \text{ where } e_{s,t} = \sum_{j=1}^{8760} e_s$$

$$LCOE(Solar) = \frac{NPV(PE\_Solar)}{NPV(e_{s,t})/1000}$$

### LCOE - Hybridization Component

Similar to the estimation of LCOE for the solar component, LCOE of hybridization is estimated considering the cost of hybridization system alone. The following section describes the steps involved.

The cost of the hybridization system forms the Direct Capital Cost. The indirect capital cost is calculated using DCC of hybridization system as discussed in 3.3.2

The O&M expenses for the hybridization component are estimated by taking into account the hybridization component alone in each of the items discussed in section 3.3.3. The annual O&M expenses for each year, considering corresponding inflation rates are estimated similarly as discussed in the same section.

The project expenses attributed to hybridization  $PE_{Hyb}(i)$ , are calculated for each of the items discussed in section 3.3.3. Finally the  $NPV(PE_{Hyb})$  of project expenses is calculated as given below.

$$NPV(PE_{Hyb}) = \sum_{i=1}^{PL} \frac{PE_{Hyb}(i)}{\left(1 + \frac{Discount\ rate}{100}\right)^i}$$

The NPV of electrical energy from hybridization system is given by,

$$NPV(e_{hb,t}) = e_{hb,t} \times A_f, \text{ where } e_{hb,t} = \sum_{j=1}^{8760} e_{hb}$$

$$LCOE(Hyb) = \frac{NPV(PE_{Hyb})}{NPV(e_{hb,t})/1000}$$

### iii. Internal Rate of Return

Internal Rate of Return (IRR) is that rate at which the difference between the NPV of the net income and capital cost is zero. The net income is the income obtained from the tariff minus the O&M expenses for each year. Thus the rate ' $r$ ' for which the equation below is satisfied will be the Internal Rate of Return.

$$Capital\ Costs - \sum_{i=1}^{PL} \frac{(Income(i) - Total\_O\&M\_yr(i))}{(1+r)^i} = 0$$

## 3.4 Technical Assessment – Case Study at Jodhpur

We discuss the results of the application of engineering model (section 3.2) for locating a PT plant at Jodhpur. The parameters chosen for the study are given in Table 3.6 below.

**Table 3.6: Parameters considered**

Gross capacity (MWe)	1, 5, 10, 20, 35, 50
Hours of thermal energy storage	0, 3, 6
Fraction of hybridization	0.0, 0.1, 0.2

The annual electrical energy generated, capacity factor, overall efficiency etc. have been computed for different combinations of the above parameters for a range of SM from one to four.

### 3.4.1 No Thermal Storage and No Hybridization

#### i. Effect of Capacity of the Plant

Table 3.7 gives the variation of

- Power Block Efficiency  $\eta_{p,d}$  under design conditions
- Reference Mirror Aperture Area  $A_r$
- Reference Mirror Aperture Area per MW.

**Table 3.7: Variation in power block efficiency & reference aperture area with capacity**

Capacity (MW)	$\eta_{p,d}$	$A_r$ ( $m^2$ )	$A_r$ per MW ( $m^2/MW$ )
1	0.19	10444	10444
5	0.23	43141	8628
10	0.27	73568	7357
20	0.32	124328	6216
35	0.37	191318	5466
50	0.38	262743	5255

It can be seen that the design efficiency of the power block increases with capacity and consequently the reference aperture area/MW decreases with increase in capacity. This trend is illustrated in Figure 3.7. From this it is obvious, that lower capacity plants will be expensive.

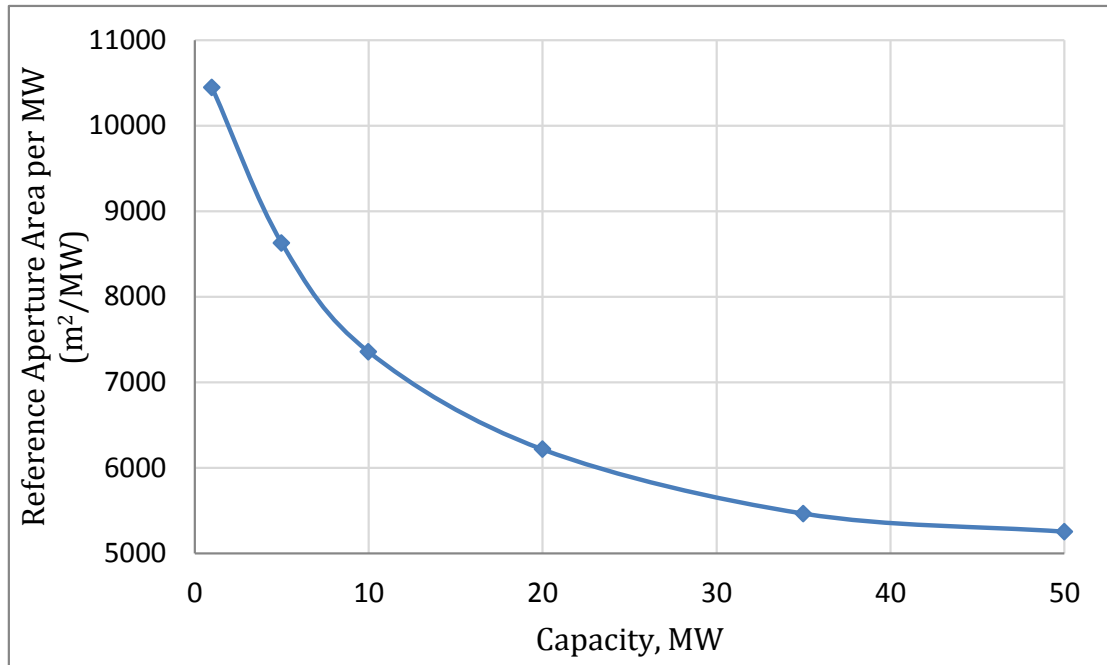


**Figure 3.7: Variation of reference mirror aperture area per MW with capacity**

## ii. Effect of Solar Multiple

For a given SM, the annual electrical energy supplied to the grid is directly proportional to the rated gross capacity of the plant (Table 3.8). Therefore, the variation of the annual electrical energy generated can be expressed in terms of annual energy per MW capacity. Figure 3.8 shows this variation with SM. It can be inferred from the table that the capacity factor is independent of the plant capacity. The variation of capacity factor with SM is shown in Figure 3.9. From these figures, it is clear that increasing SM beyond three is only marginally beneficial.

**Table 3.8: Annual electrical energy generation with SM for various capacities**

Annual Electrical Energy - MWh ( $t_s=0, f_{hb}=0$ )						
SM	1 MW	5 MW	10 MW	20 MW	35 MW	50 MW
1	1218	6088	12176	24352	42615	60900
1.25	1672	8362	16725	33450	58537	83600
1.5	2034	10168	20337	40673	71178	102000
2	2428	12140	24281	48561	84982	121000
3	2718	13589	27177	54355	95120	136000
4	2835	14174	28300	56697	99220	142000

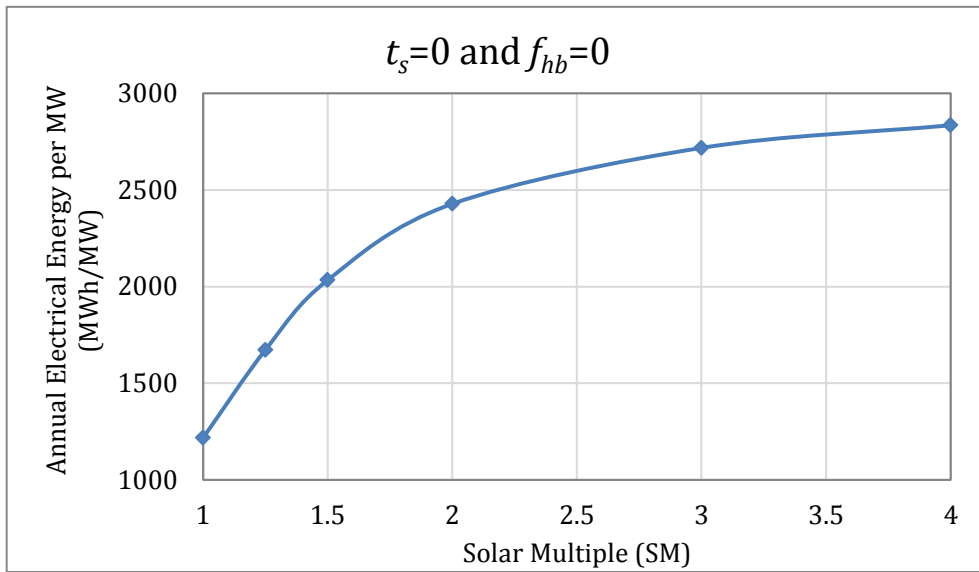


**Figure 3.8: Variation of annual electrical energy generated per MW with SM**

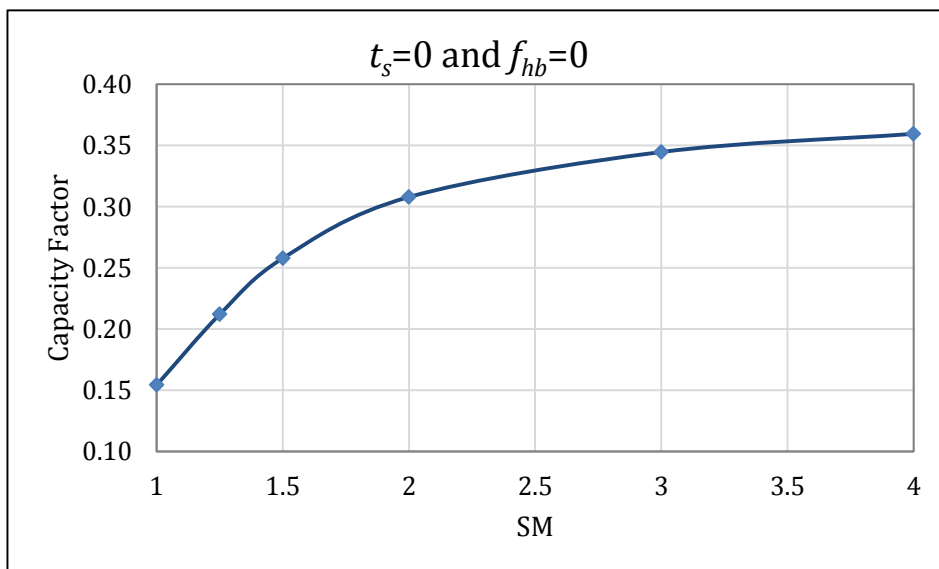


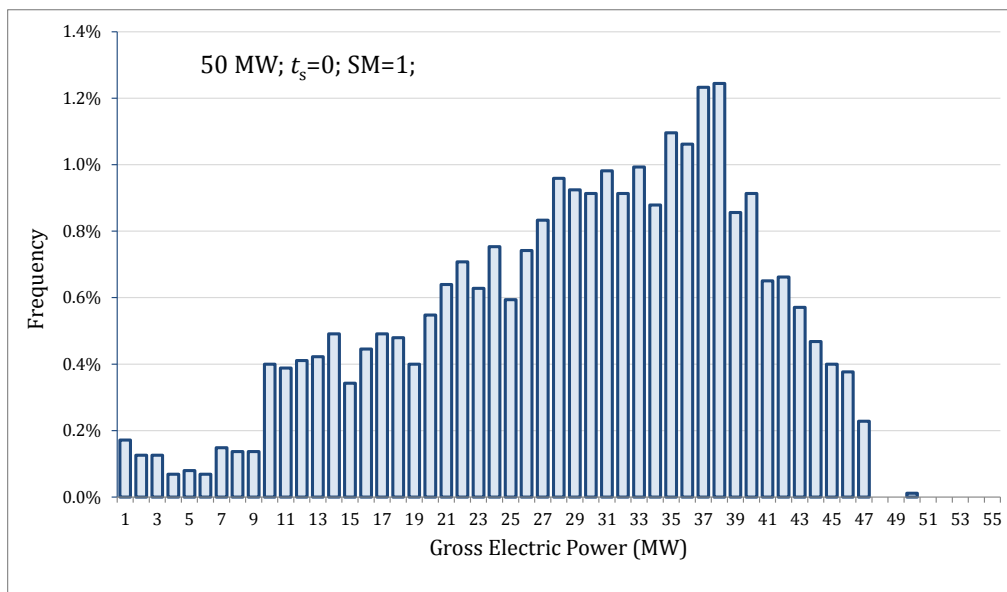
**Figure 3.9: Variation of capacity factor with SM for all capacities**

### Frequency Distribution of Power Generation

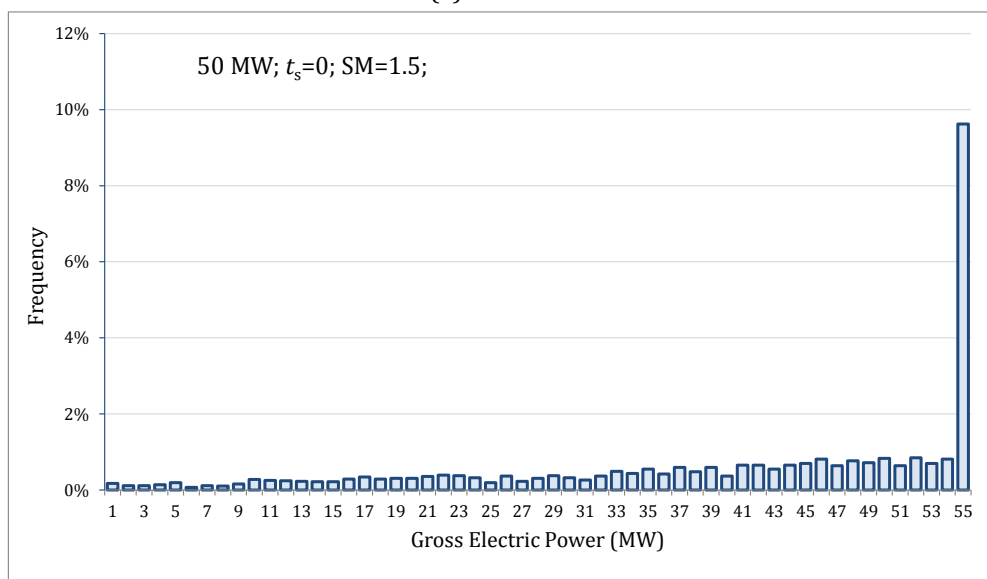
In order to understand the frequency distribution of power generated by the plant over the year, a frequency distribution graph for a 50 MW plant is presented in Figure 3.10 for SM=1 and SM=1.5. The x value corresponding to the bar indicates the power range between x and (x-1) MW. The corresponding bar indicates the percentage of hours in a year that the plant is generating power in that range (The percentage of hours the plant is not operating is not shown).

For example, for SM=1, the power generated in the range between 37 and 38 MW corresponding to a frequency of 1.24% implies that the power in that range is being produced for 109 hours ( $1.24 \times 8760 \text{ hours}/100 = 109 \text{ hours}$ ). It also shows that the full rated power of 50 MW is generated for a very short time.

When the SM is increased to 1.5, the plant operates at 1.1 times the full load condition for nearly 10% (843 hours). The plant operates beyond full load for 13.45% (1178 hours). These examples indicate that our tool has the capability of presenting this frequency data also.



(a) SM=1



(b) SM=1.5

Figure 3.10: Frequency distribution graph

### iii. Solar to Electrical Conversion Efficiency

To get an idea of the optimum SM, the annual efficiency of conversion of solar energy to electrical energy was computed as follows.

$$\text{Annual solar energy impinging} = A_r \times SM \times \left( \sum DNI \times \cos\theta \right)$$

$$\text{Annual Efficiency} = \frac{\text{Gross annual energy generated}}{\text{Annual solar energy impinging}}$$

This annual efficiency vs. SM is plotted in Figure 3.11 for various capacities of the plant. From this figure, one can infer that the maximum efficiency occurs around SM = 1.5 for all capacities and this overall efficiency increases with capacity.

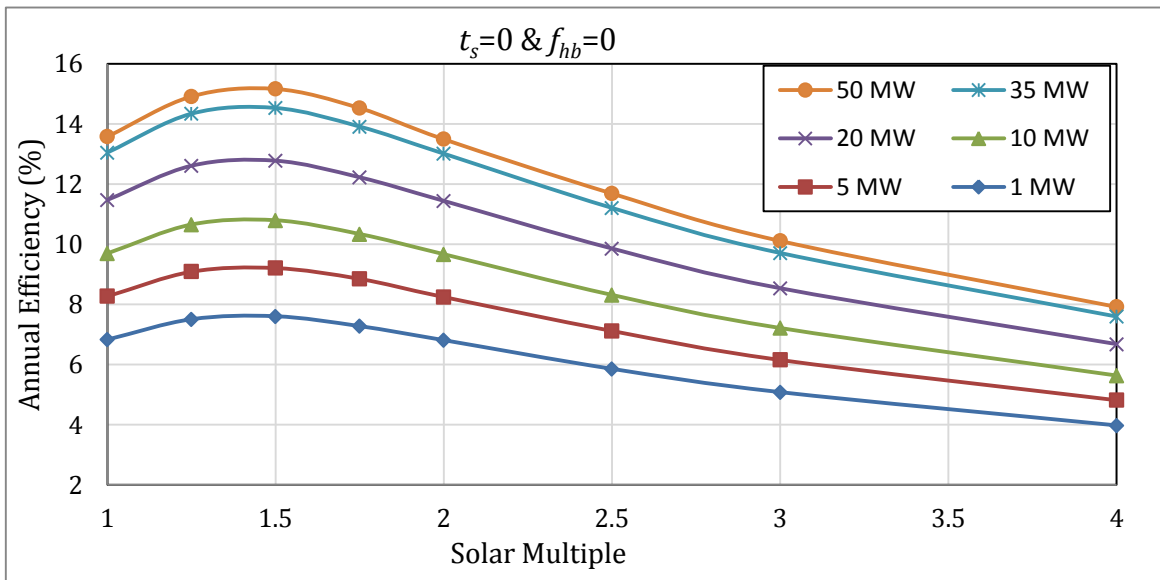
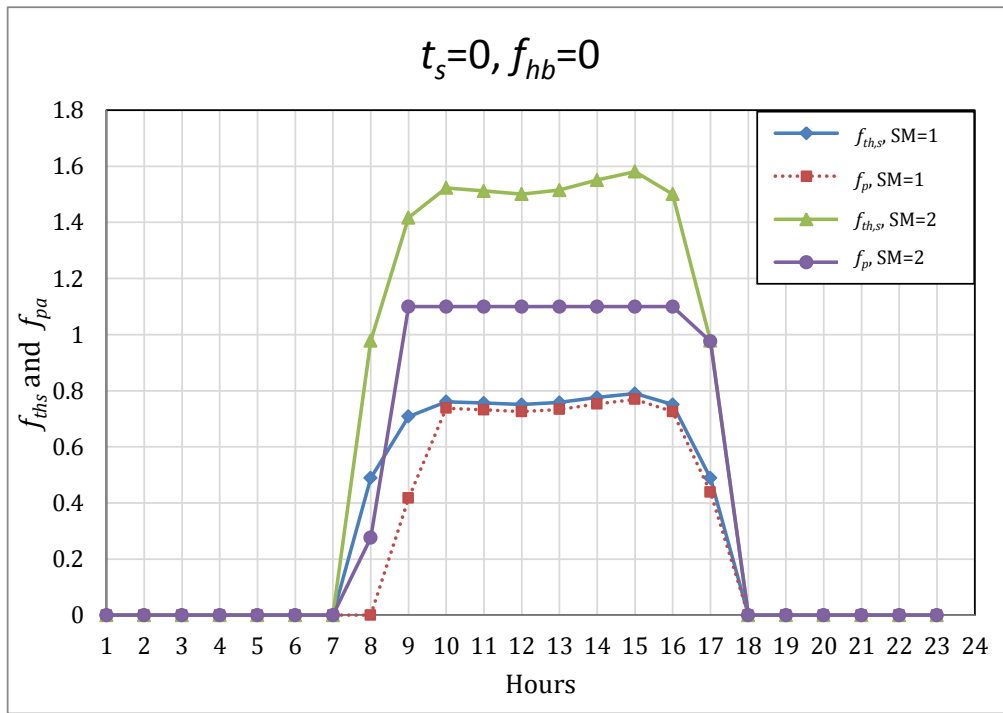


Figure 3.11: Variation of annual efficiency with SM for various capacities

### iv. Electrical Power Generation during a Typical Day

Figure 3.12 gives the variation of  $f_{th,s}$  and  $f_p$  during a typical day (21<sup>st</sup> January), for SM = 1.0 and SM = 2.0. The advantage of representing the data in terms of  $f_{th,s}$  and  $f_p$  is that, it is independent of the capacity of the plant.



**Figure 3.12: Variation of the fractional solar thermal power and fractional electrical power generated during a typical day**

One can notice the lag in the generation of electric power relative to the solar power, to account for making up of the thermal losses that would have occurred overnight. The solar power over the initial period is used up to make good these losses and bring the HTF to operating conditions, before the power generation can occur.

For  $SM = 1.0$ ,  $f_p$  is slightly less than  $f_{th,s}$ , due to lower efficiency of the power block during part load conditions ( $f_p = 1.0$ , when  $f_{th,s} = 1.0$ ).

For  $SM = 2.0$ ,  $f_{th,s}$  is twice the value corresponding to  $SM = 1.0$ . However, the  $f_p$  gets limited to 1.1, as the plant is permitted to work with 10% overload. So the excess solar power cannot be utilized and the mirrors have to be suitably defocused to limit  $f_p = 1.1$ .

### 3.4.2 Thermal Storage without Hybridization

We have considered three hours and six hours of thermal storage with no hybridization for plants of capacity 1, 5, 10, 20, 35 and 50 MW. The effect of SM and thermal storage on the annual electrical energy generated is discussed below.

#### i. Effect of Solar Multiple

Variation of annual electrical energy generated with SM, with three hours and six hours of thermal storage for various capacities of the plant were computed. It was found that the annual electrical energy generated is proportional to rated capacity even with storage. The variations in annual electrical energy per MW capacity with SM, for thermal storage of zero, three and six hours, are given Table 3.9 and shown in Figure 3.13. This information is presented in terms of capacity factor in Table 3.10 and Figure 3.14. Capacity factor is also presented in terms of its variation with thermal storage for various SM in Figure 3.15. From Figure 3.13 and Figure 3.14, one can infer that providing thermal storage without sufficient SM is not beneficial. Higher requirement of thermal storage hours implies the need for higher SM.

**Table 3.9: Variation of annual electrical energy per MW with SM, for  $t_s= 0, 3$  &  $6$**

Annual Electrical Energy in MWh ( $f_{hb}=0$ )			
SM	$t_s=0$	$t_s=3$	$t_s=6$
1.00	1218	1218	1218
1.25	1672	1676	1676
1.50	2034	2120	2120
2.00	2428	2904	3005
3.00	2718	3628	4194
4.00	2835	3888	4694

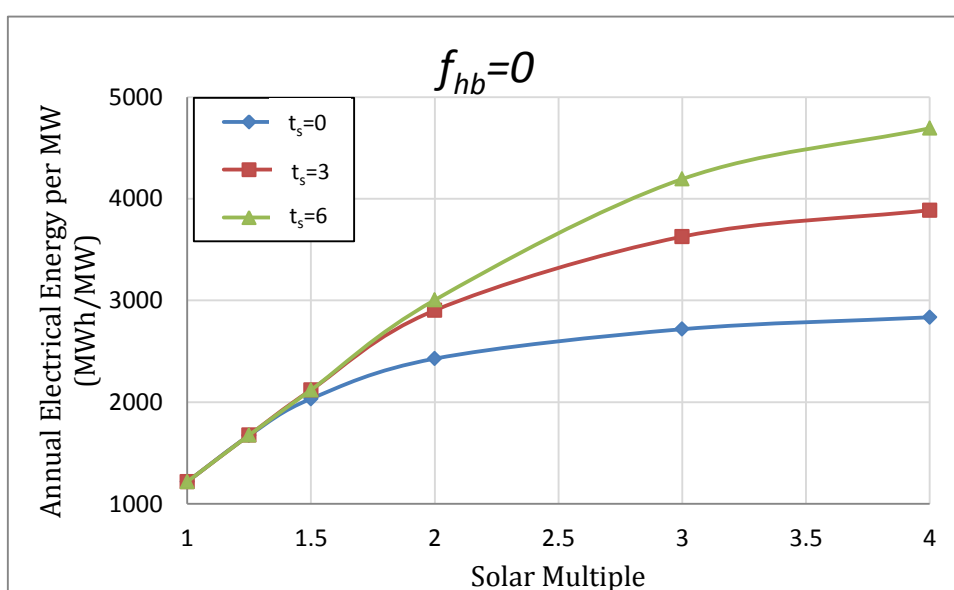


**Figure 3.13: Variation of annual electrical energy/MW with SM for  $t_s= 0, 3$  and  $6$  hours**

**Table 3.10: Variation of capacity factor with SM for  $t_s= 0, 3$  and  $6$  hours**

Capacity Factor ( $f_{hb}=0$ )			
SM	$t_s= 0$	$t_s= 3$	$t_s= 6$
1.00	0.15	0.15	0.15
1.25	0.21	0.21	0.21
1.50	0.26	0.27	0.27
2.00	0.31	0.37	0.38
3.00	0.34	0.46	0.53
4.00	0.36	0.49	0.60

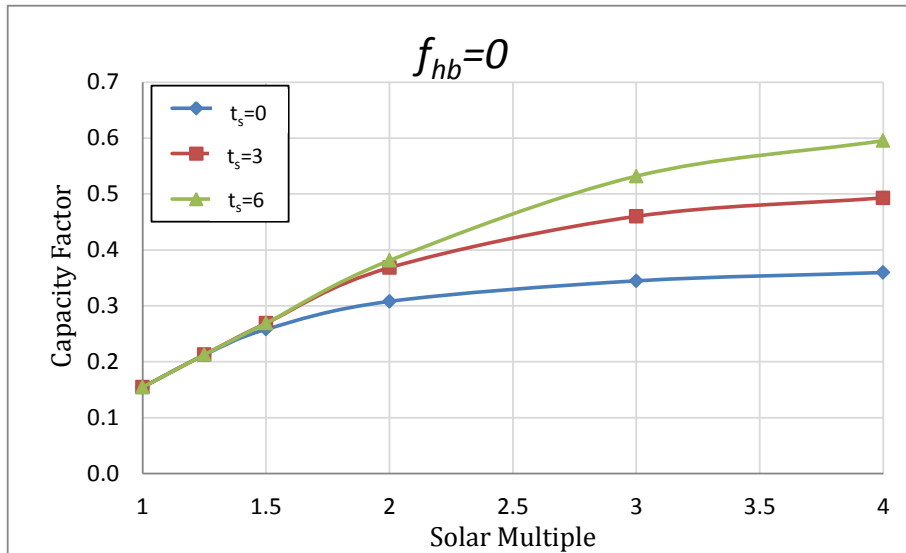


Figure 3.14: Variation of capacity factor with SM, for  $t_s = 0, 3$  and 6 hours

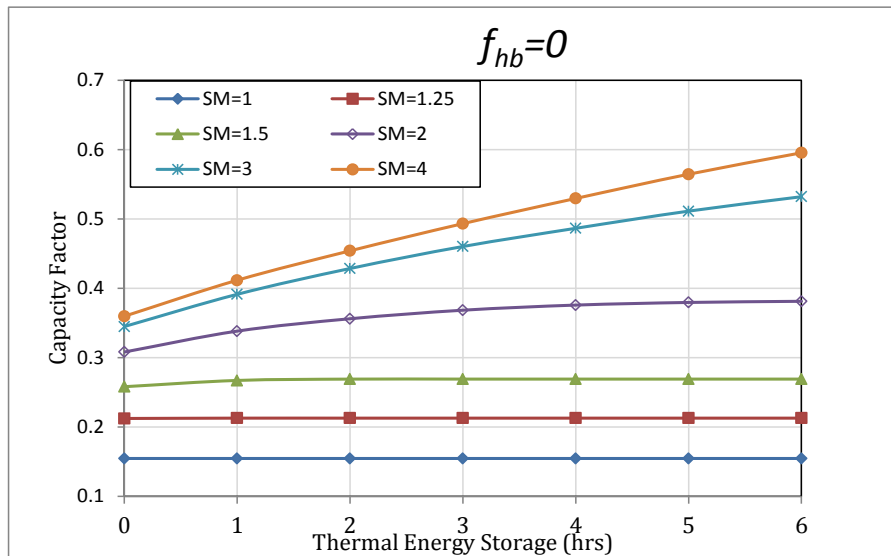


Figure 3.15: Variation of capacity factor with thermal energy storage for various SMs and no hybridization

## ii. Annual Conversion Efficiency from Solar to Electrical Energy

The variations of annual efficiency of conversion of solar energy to electrical energy with SM, for various capacities, are shown in Figure 3.16 and Figure 3.17 for thermal storage of three hours and six hours respectively. From these figures, one can infer that with three hours of thermal storage, the highest efficiency occurs around SM = 1.9 whereas for six hours of thermal storage, the highest efficiency occurs around SM = 2.2. These optimum values of SM are from an energy efficiency point of view. However, from economical point of view, the optimum SM has to be determined based on least LCOE. But, the present information does indicate the trend and gives some physical insight into why one can expect a minimum LCOE around these values of SM. Here again, the overall efficiency increases as the plant capacity increases.

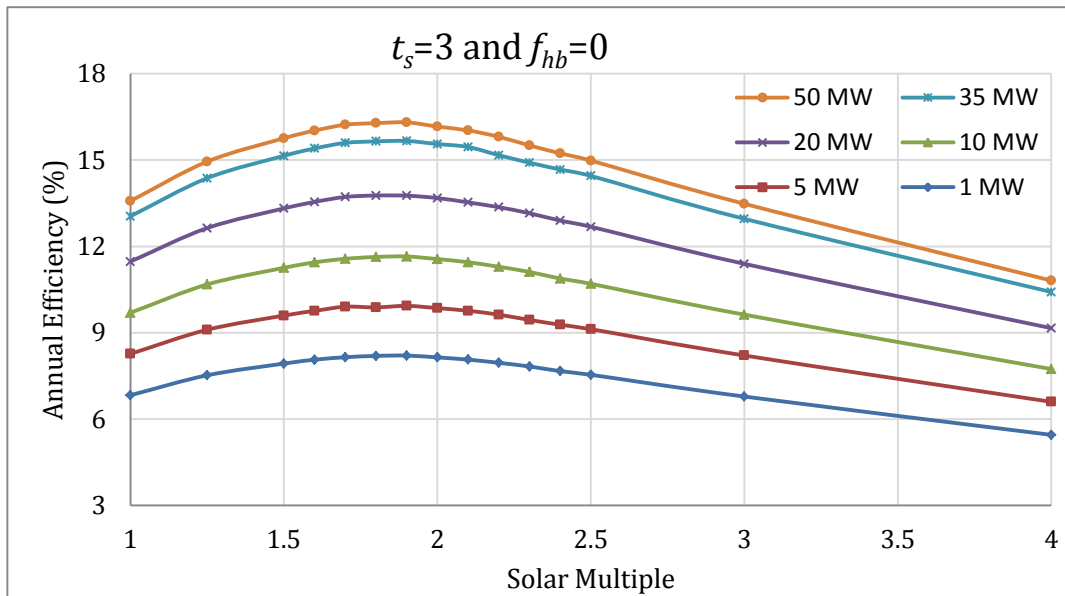


Figure 3.16: Variation of annual efficiency with SM for various capacities for  $t_s=3$  hours and no hybridization

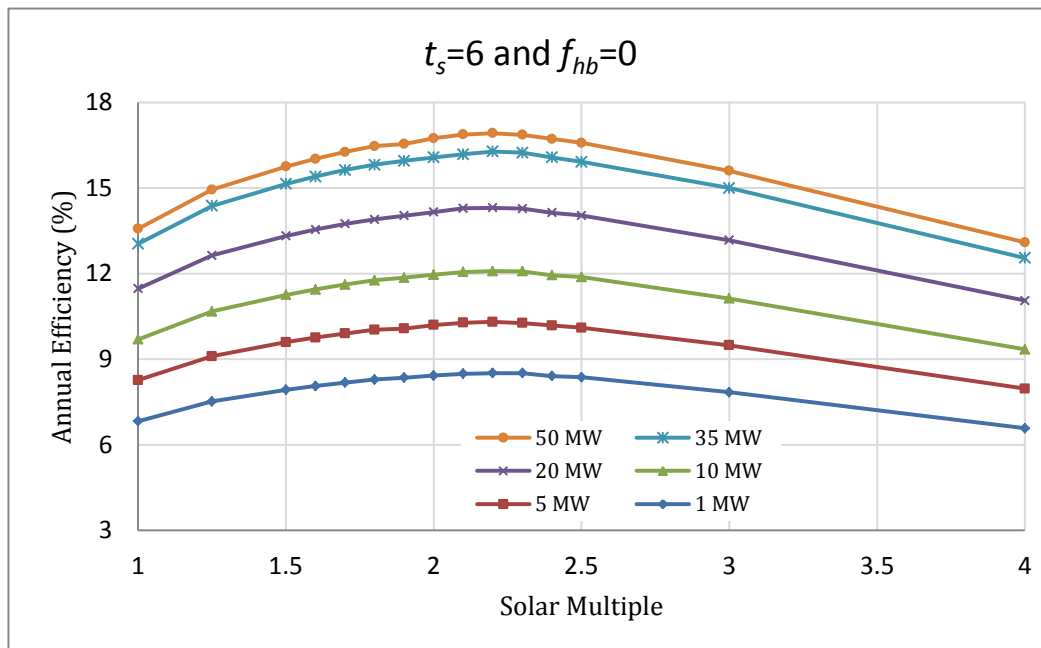


Figure 3.17: Variation of annual efficiency with SM for various capacities for  $t_s=6$  hours and no hybridization

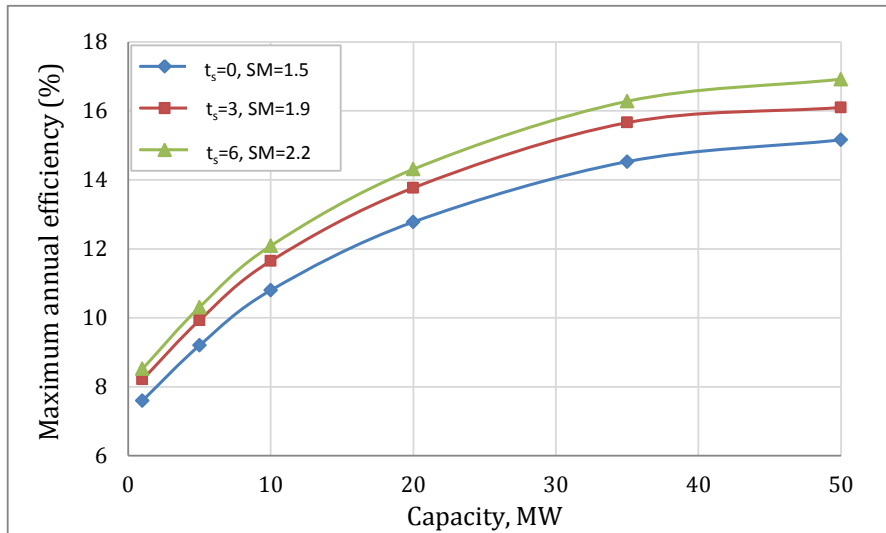
### iii. Variation of Maximum Annual Efficiency with Plant Capacity

Table 3.11 shows the variation of the maximum annual efficiency of solar to electrical energy with plant capacity for zero, three and six hours of thermal storage with no hybridization. This information is also presented in Figure 3.18. From this, one can infer that the annual efficiency increases with plant capacity and also with thermal storage.

**Table 3.11: Variation of maximum annual efficiency and corresponding SM with plant capacity for  $t_s= 0, 3$  and 6**

Capacity (MW)	$t_s= 0$		$t_s= 3$		$t_s= 6$	
	SM	$\eta_{annual}(\%)$	SM	$\eta_{annual}(\%)$	SM	$\eta_{annual}(\%)$
1	1.5	7.60	1.9	8.21	2.2	8.52
5		9.20		9.93		10.31
10		10.80		11.65		12.09
20		12.78		13.77		14.31
35		14.53		15.66		16.28
50		15.16		16.10		16.92

The optimum SM at which the maximum annual efficiency occurs increases with the hours of thermal energy storage and it is shown in Figure 3.19. This optimum value of SM is independent of the plant capacity.



**Figure 3.18: Variation of maximum annual efficiency with plant capacity**

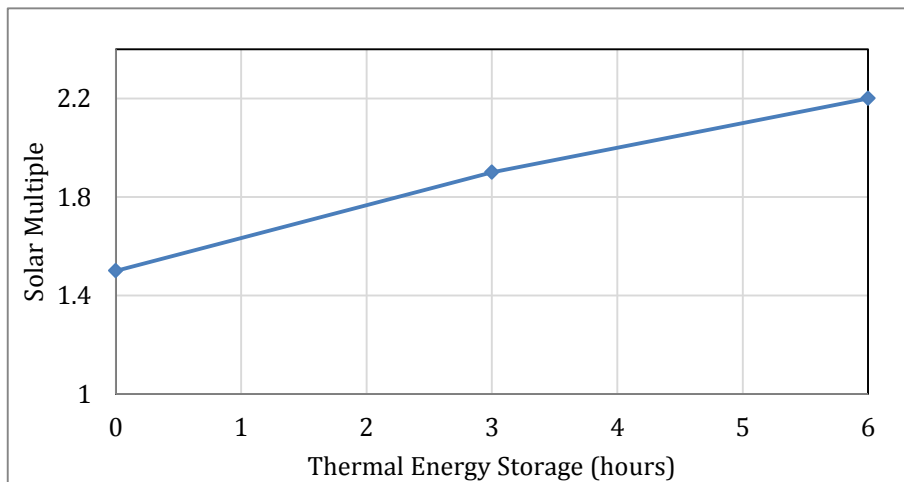


**Figure 3.19: Optimum SM for maximum annual efficiency with thermal storage**

#### iv. Solar Power Input and Electrical Power Generated during a Typical Day

Figure 3.20 shows the variation of  $f_{th,s}$  and  $f_p$ , during a typical day for SM=2 and with three hours of thermal storage. From this figure it is seen that the full electrical power is generated for about 3 hours even after sunset and the excess solar energy is efficiently utilized.

Figure 3.21 shows the variation of  $f_{th,s}$  and  $f_p$  during a typical day for SM=2 & 2.2 and for 6 hours of thermal storage. For SM=2 and six hours of thermal storage provided, the electrical power generated does not go for six hours after the sun sets, but slightly more than three hours and indicating that SM = 2.0 is not sufficient to cater for six hours of thermal storage. With SM=2.2, the thermal storage capacity is better utilized and power is generated for about four hours. It must however be stated that such inferences should not be based on the performance over a single day, but must be based on the overall annual efficiency as indicated earlier. The data on the variation of  $f_{th,s}$  and  $f_p$  during a day have been shown to give some physical idea of how thermal storage, with appropriate SM, helps in extending the power plant operation beyond sunshine hours.

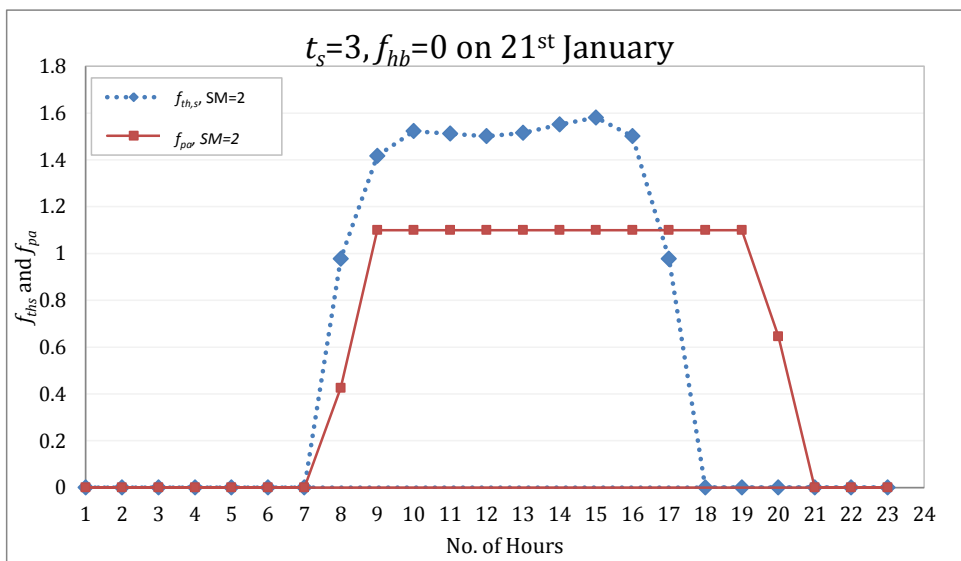


Figure 3.20: Variations in  $f_{th,s}$  and  $f_{pa}$  during a typical day for  $t_s=3$  hours

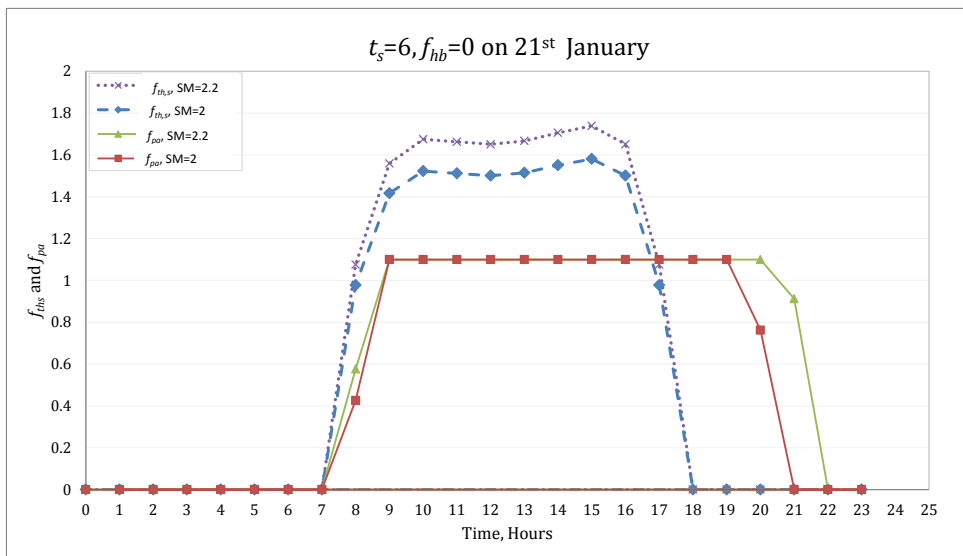


Figure 3.21: Variations in  $f_{th,s}$  and  $f_{pa}$  during a typical day for  $t_s=6$  hours

### 3.4.3 Hybridization without Thermal Storage

We have used hybridization to augment the thermal power to HTF to the extent of 0.1 and 0.2 times the design thermal power, so that the electrical energy produced is as high as possible.

#### i. Effect of Solar Multiple

$SM = 1.0$

Figure 3.22 shows for  $SM = 1.0$ , the variation in  $f_{pa}$  during a day for  $f_{hb} = 0, 0.1$  and  $0.2$  along with  $f_{th,s}$ . Figure 3.23 gives the value of  $f_{hb,used}$  during the day. It may be noticed that  $f_{pa}$ , the fractional gross power generated increases with  $f_{hb}$ .  $f_{hb,used}$  is equal to  $f_{hb}$  through-out the day.

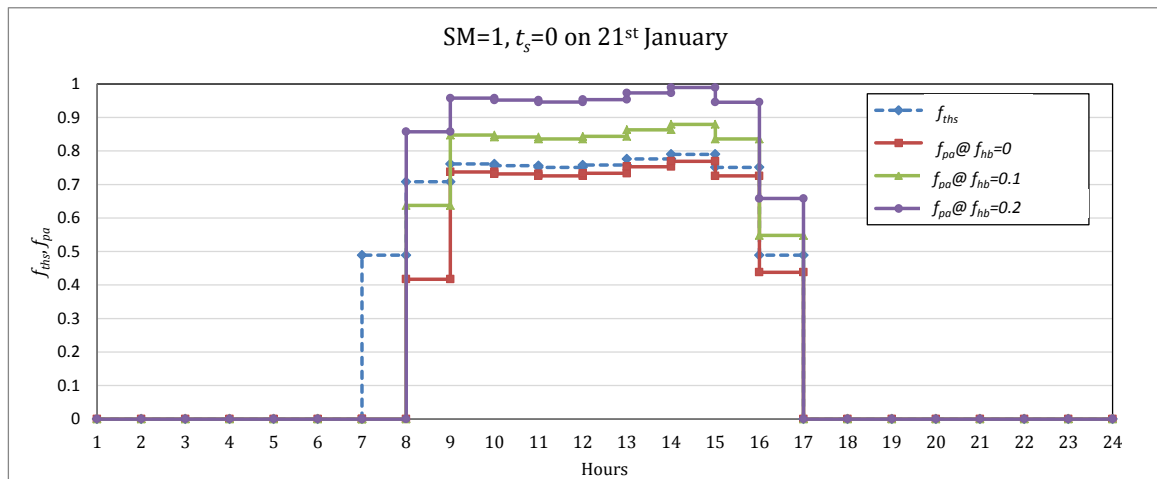


Figure 3.22: Effect of hybridization on the electrical power generated during a typical day for  $SM=1$

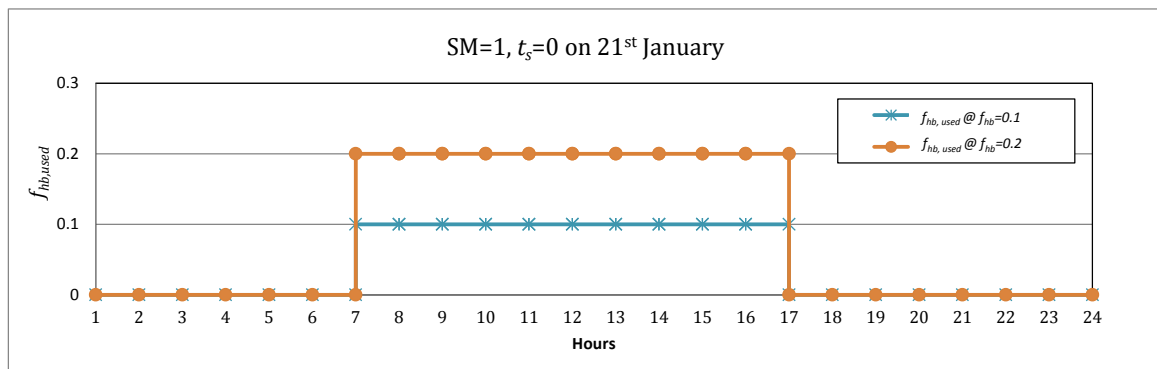


Figure 3.23: Fraction of hybridization used during a typical day for  $SM=1$

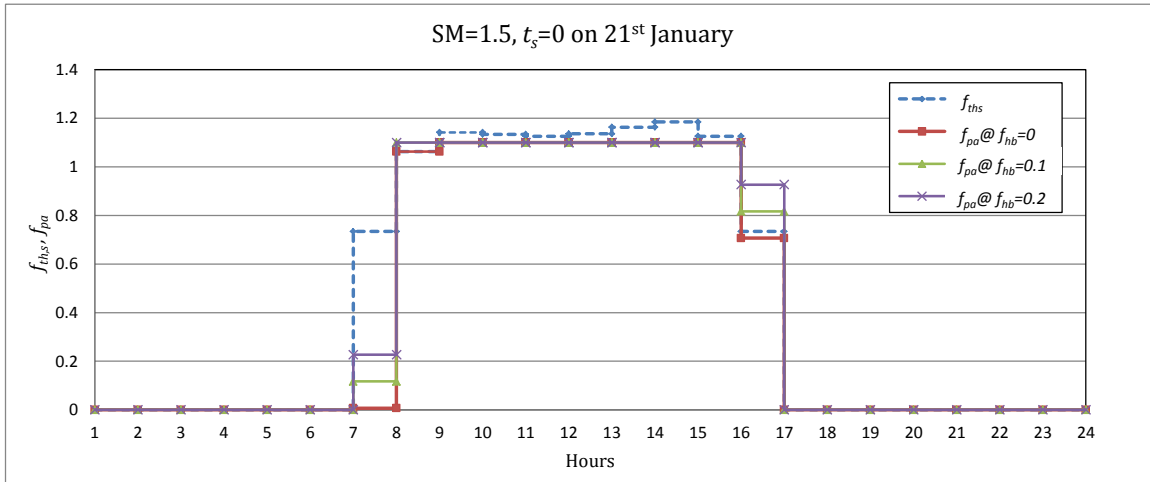
$SM = 1.5$

Figure 3.24 shows the variation in  $f_p$  during a typical day for  $f_{hb} = 0, 0.1$  and  $0.2$  along with  $f_{th,s}$ . Figure 3.25 gives the value of  $f_{hb,used}$  during the day. It may be noticed that the power generated  $f_p$  is nearly the same for all the three cases except during the first hour in the morning and the last hour in the evening. With  $SM=1.5$ , the solar power  $f_{th,s}$  available during most of the day is more than that required to generate even 10% more than rated electrical power. Therefore hybridization

is not required for most of the time. Thus hybridization is utilized during the first hour in the morning and during the last hour in the evening.

It is observed from Figure 3.24 that in the first hour  $f_{th,s}$  and hybridization contribute towards making up the thermal losses that would have occurred overnight. So  $f_{pa}$  is very small during the first hour in the morning, whereas it is much higher in the last hour.

Since hybridization does not contribute much for even  $SM=1.5$ , higher values of  $SM$  were not considered.



**Figure 3.24: Effect of hybridization on the electrical power generated during a typical day for  $SM=1.5$**

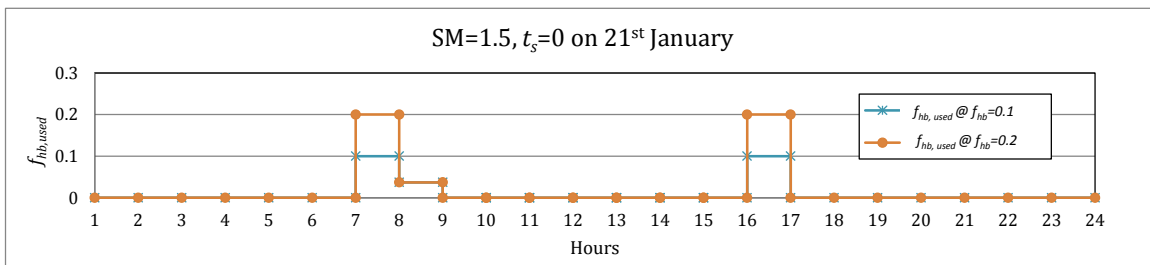


**Figure 3.25: Fraction of hybridization used during a typical day for  $SM=1.5$**

## ii. Effect of Hybridization Fraction

The benefit of hybridization is maximum for  $SM=1$ , the annual electrical energy generated for this case only is discussed. With hybridization, the annual electrical energy generated is partly attributable to solar energy and partly to thermal energy from fossil fuel. These are found to be proportional to the rated capacity. Figure 3.26 plots the annual energy from solar per MW, the annual energy from hybridization per MW and the total annual energy generated per MW for varying  $f_{hb}$ .

It is interesting to note that the electrical apportioned to solar increases with  $f_{hb}$  though there is no increase in solar field. The reason for this is that with hybridization, the thermal power to HTF increases and consequently the power block operates at higher part load conditions with consequent higher efficiency. Thus the electrical energy from solar field increases indicating that hybridization is beneficial when there is no thermal storage.

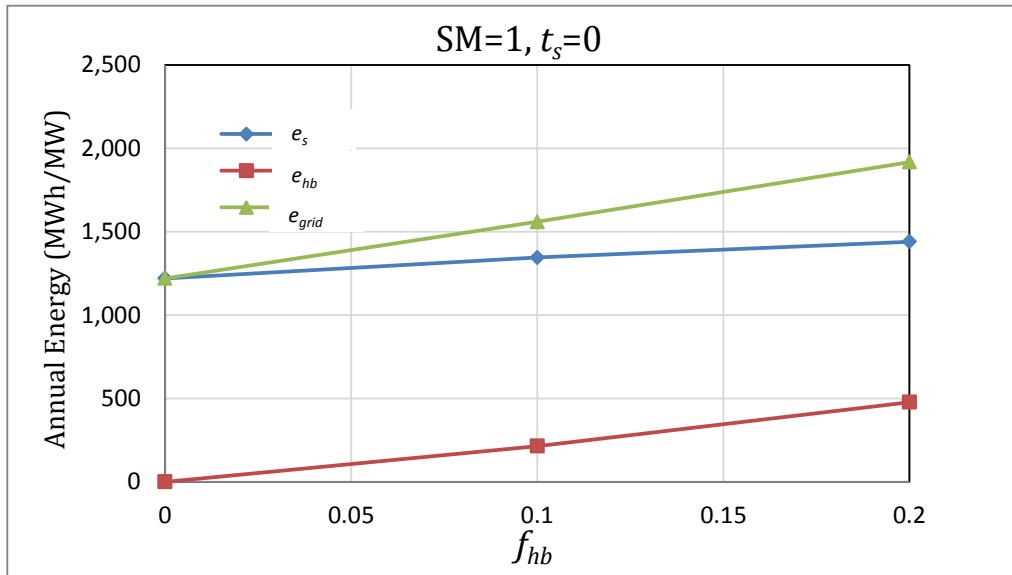


Figure 3.26: Variation of annual energy per MW with hybridization

### iii. Effect of Hybridization on Annual Efficiency Attributed to Solar Field

As seen in Section 3.4.3 hybridization not only increases the electrical energy generated due to additional thermal energy input but also increases the electrical energy attributable to the solar field because of higher efficiency at higher part load operation. The overall efficiency of the solar field with hybridization can be defined as the ratio of annual electrical energy generated (attributable solar field) to the total annual solar energy input. The variation of this annual efficiency with SM for  $f_{hb}=0, 0.1$  and  $0.2$  is shown in Figure 3.27 for 1 MW and 50 MW capacities. From this figure, it is clear that the overall efficiency increases with  $f_{hb}$  but the benefit of hybridization decreases as SM increases.

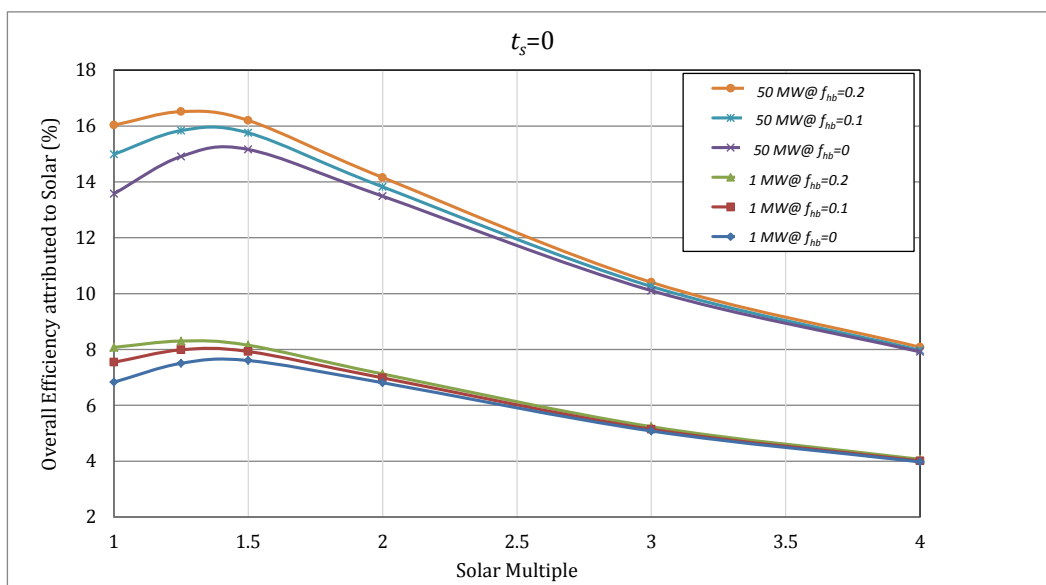


Figure 3.27: Variation of annual efficiency with SM for  $f_{hb}=0, 0.1$  and  $0.2$

### 3.4.4 With Thermal Storage and Hybridization

It was mentioned earlier that the capacity factor is independent of the rated capacity of the plant. Figure 3.28 to Figure 3.30 show respectively the variation of capacity factor with SM for zero, three and six hours of thermal storage. In each figure, hybridization values of 0, 0.1 and 0.2 are considered. It is seen that CF increases with SM but the benefit of hybridization is maximum for SM=1 and decreases as SM increases.

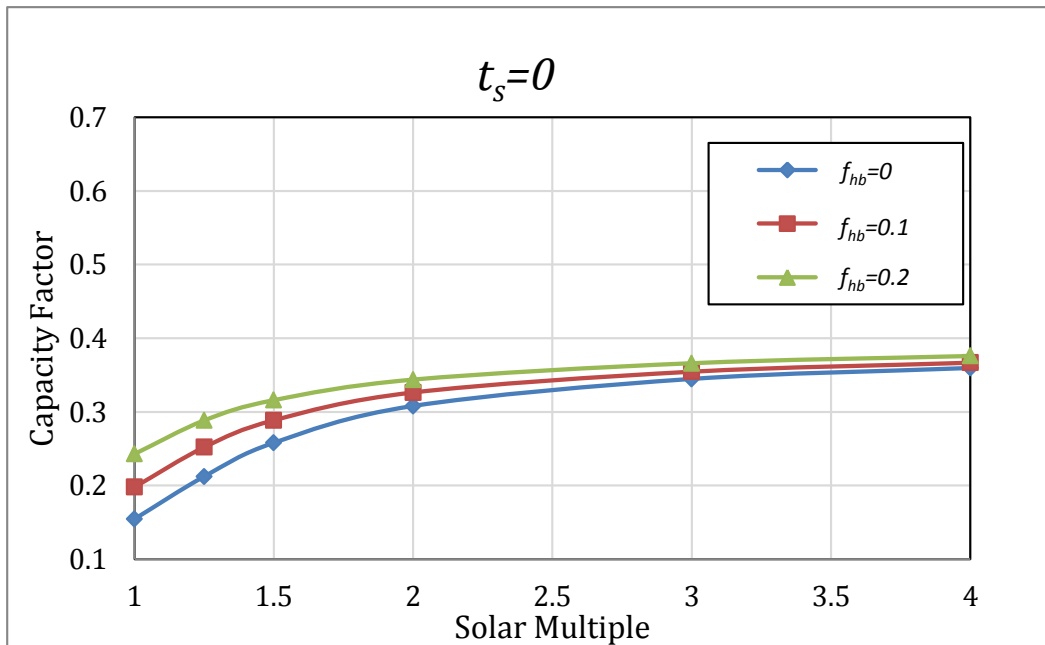


Figure 3.28: Variation of capacity factor with SM for  $t_s=0$  hours

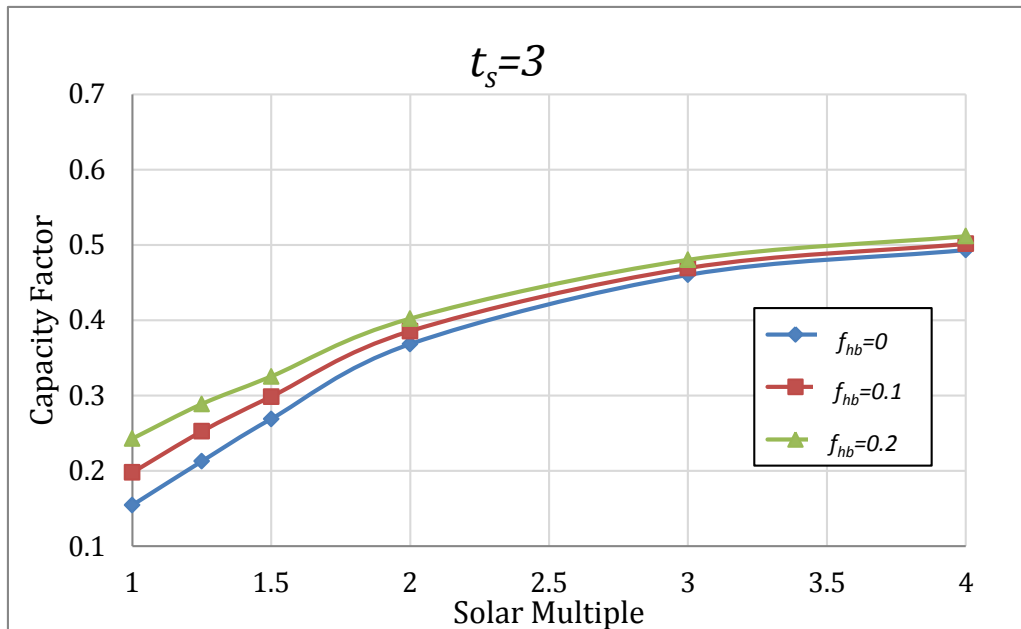


Figure 3.29: Variation of capacity factor with SM for  $t_s=3$  hours

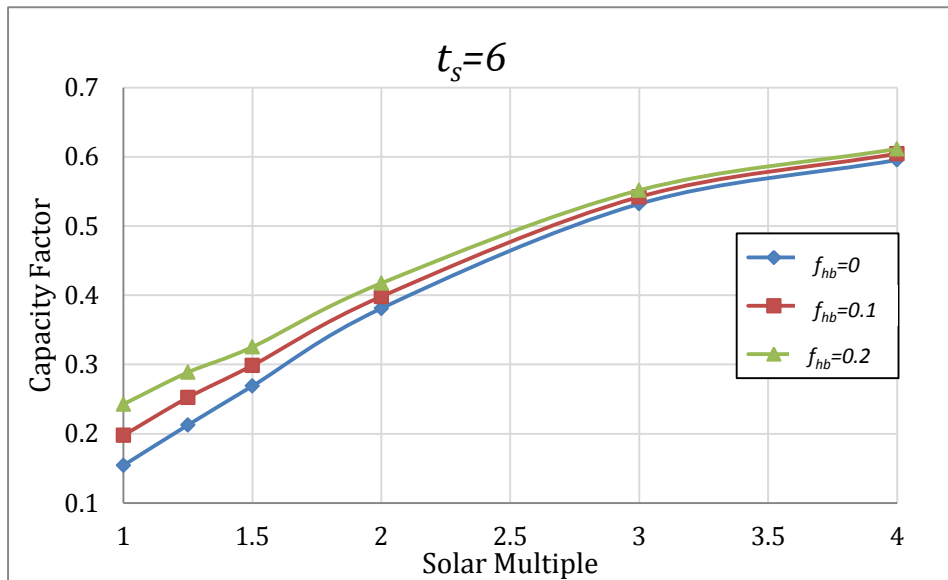


Figure 3.30: Variation of capacity factor with SM for  $t_s=6$  hours

### 3.5 Economic Assessment – Case Study at Jodhpur

An economic analysis is carried out using the methodology and inputs given in section 3.3 for a PT plant at Jodhpur. For easy reference, the parameters chosen are repeated below.

Design Gross Capacity (MWe)	1, 5, 10, 20, 35, 50
Hours of Thermal Energy Storage	0, 3, 6
Fraction of Hybridization	0, 0.1, 0.2

The objective of this exercise is to determine the LCOE and IRR for several combinations of input parameters such as plant capacity, thermal storage, hybridization and SM.

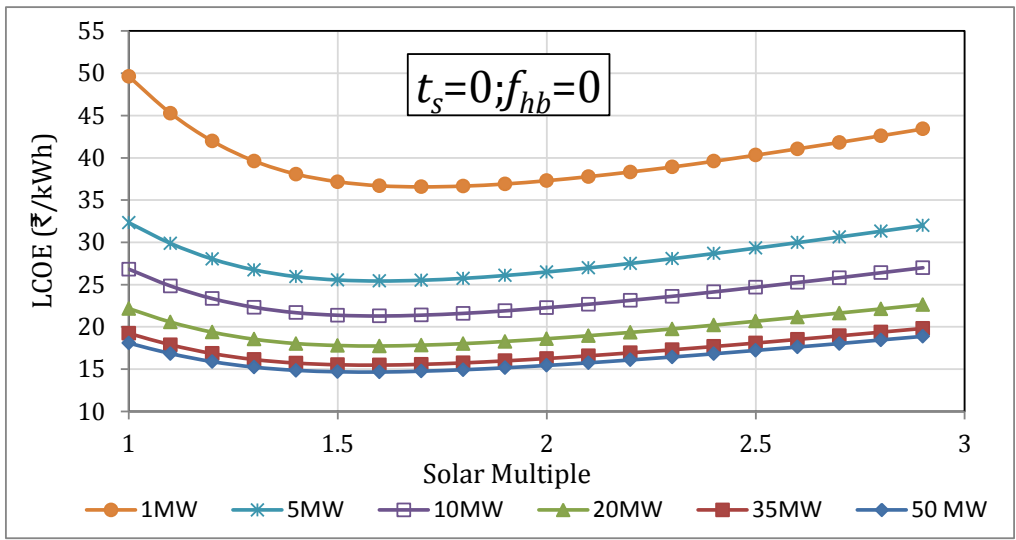
#### 3.5.1 Determination of Optimum SM based on LCOE

The design of a CSP plant requires the determination of optimum solar multiple for which the LCOE is minimum. Therefore the variation of LCOE with SM for various cases is first considered.

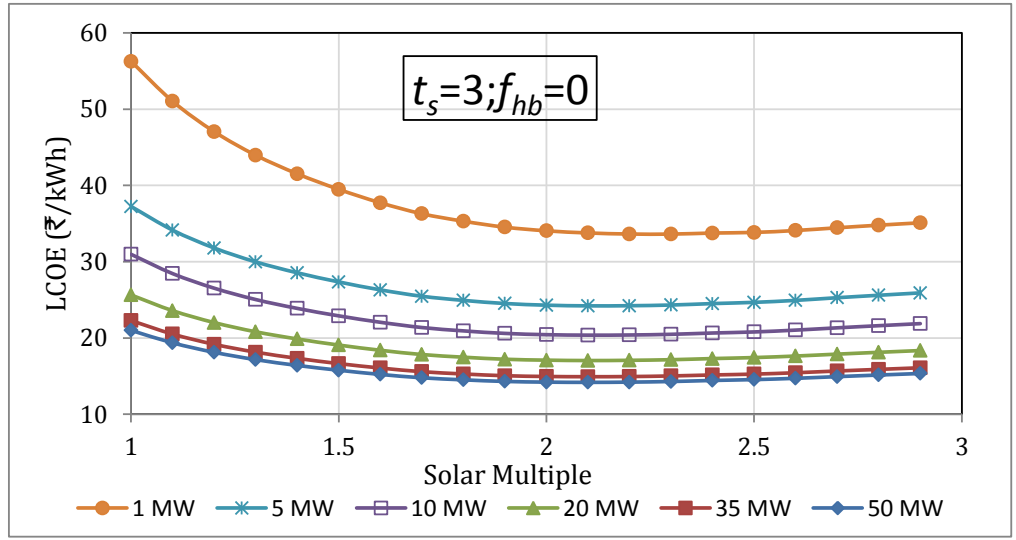
Variations in LCOE with SM for  $f_{hb}=0, 0.1$  and  $0.2$  for various plant capacities are shown in Figure 3.31, Figure 3.32 and Figure 3.33 respectively. In each of these figures, (a), (b) and (c) correspond to  $t_s=0, 3, 6$  hours of thermal storage. Similarly variations of IRR with SM are presented in Figure 3.34, Figure 3.35 and Figure 3.36. It may be mentioned that, for some plants of lower capacities, the IRR turned out to be negative and results of IRR for such cases have not been included in these figures.

In all cases, the optimum value of SM for which LCOE is minimum and IRR is maximum is the same. The CSP plant is then designed for this optimum SM.

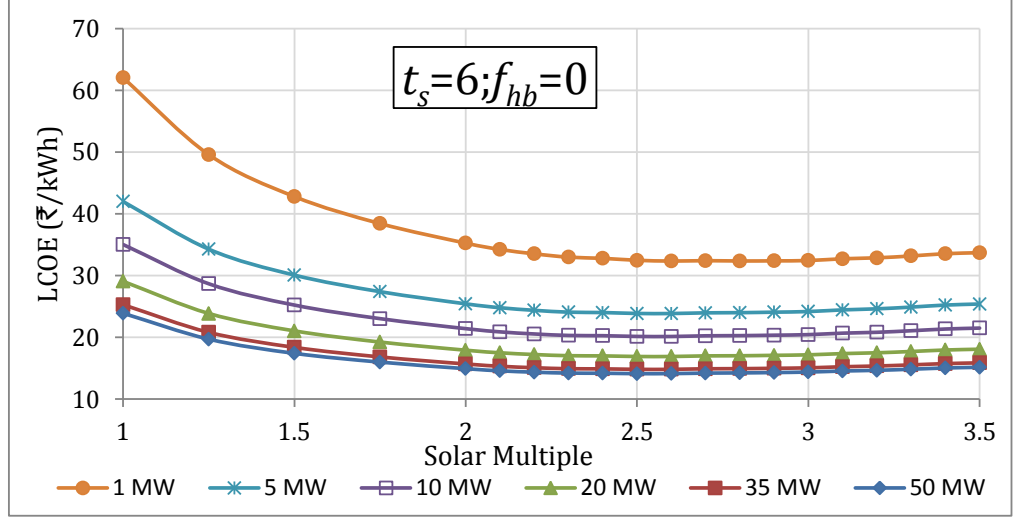
The variations in both LCOE and IRR are very small around the optimum SM. The solar field cost, O&M expenses increase with SM but it also generates more electrical energy. However one can choose an SM close to the optimum based on other considerations such as capital cost, IRR etc.



(a)

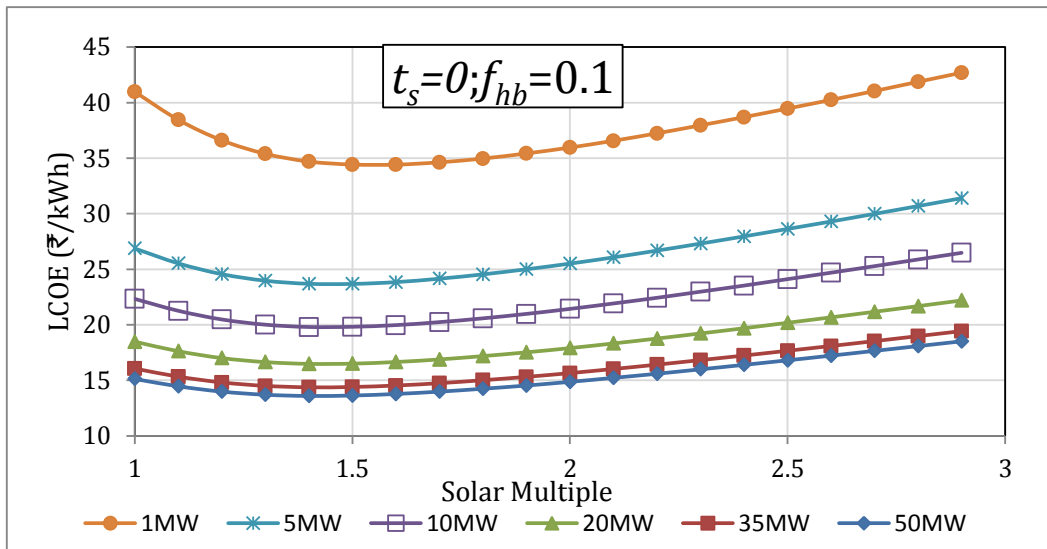


(b)

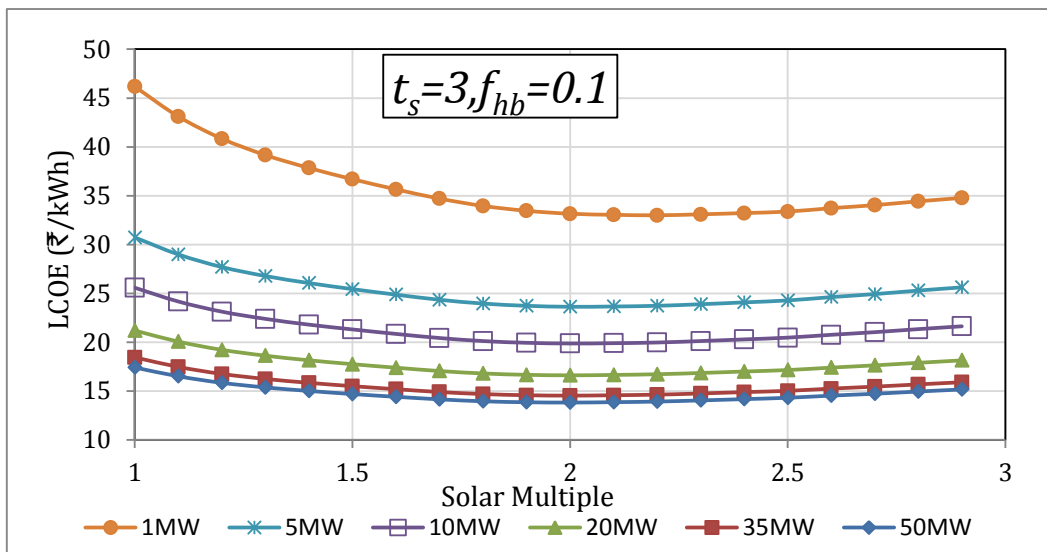


(c)

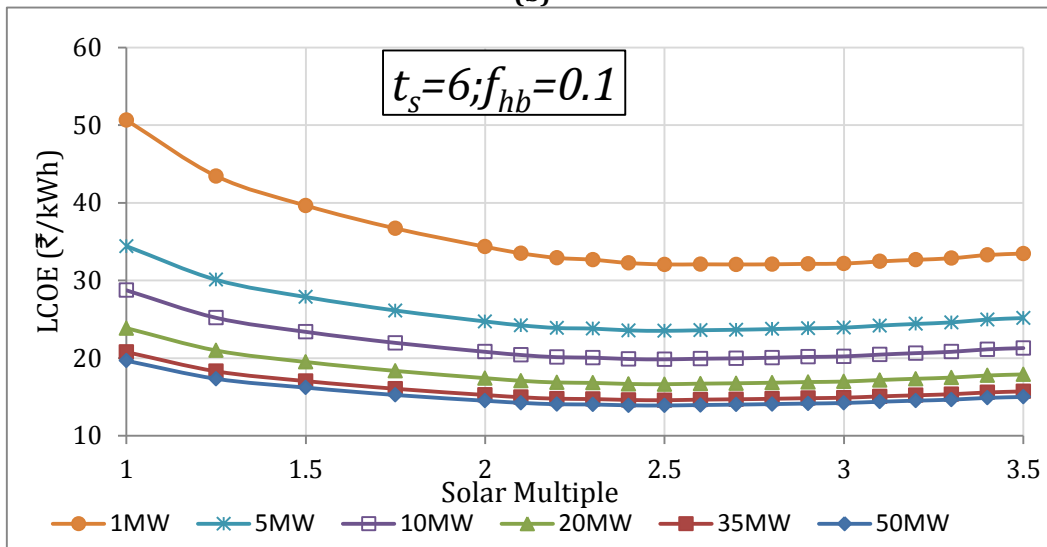
Figure 3.31: Variation of LCOE with SM for different thermal storage hours with  $f_{hb}=0$



(a)

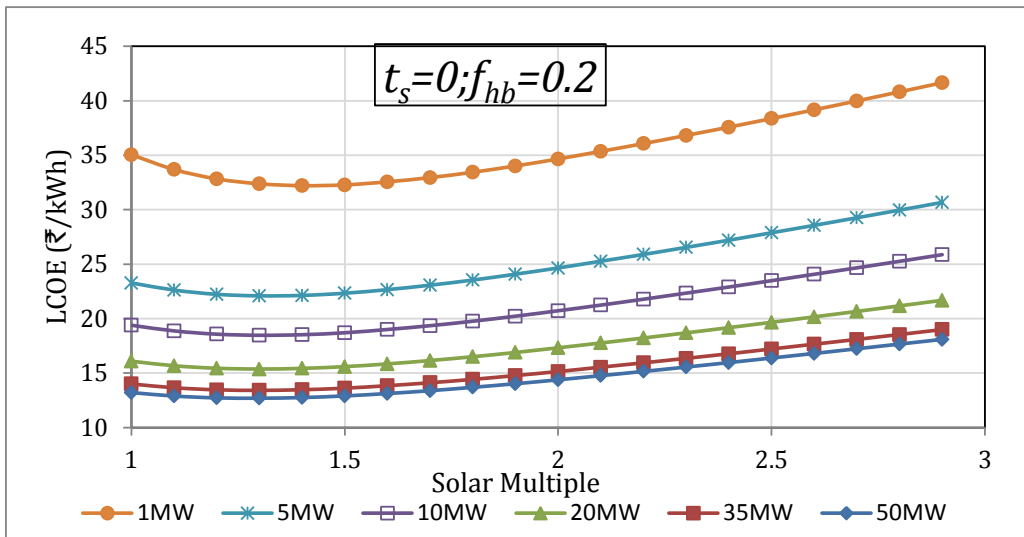


(b)

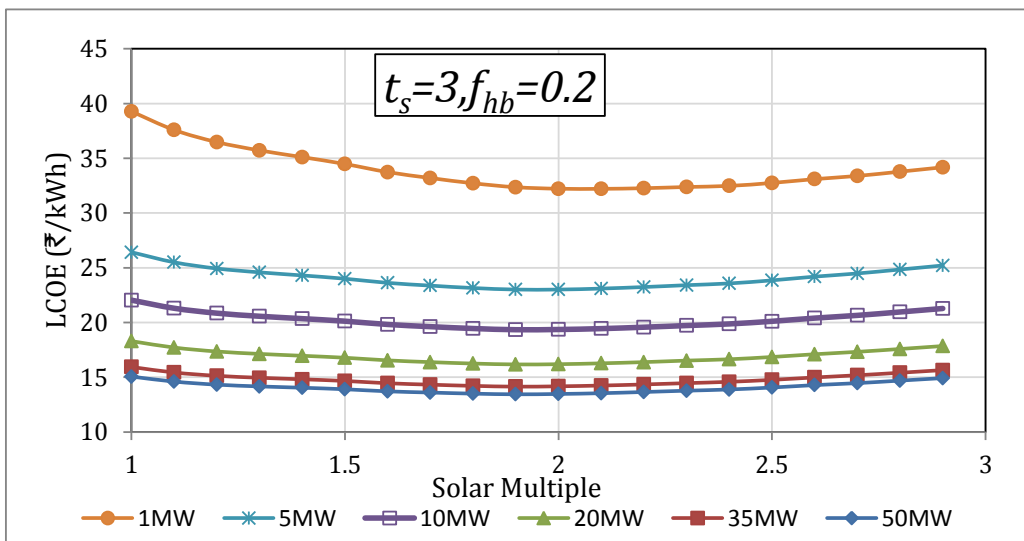


(c)

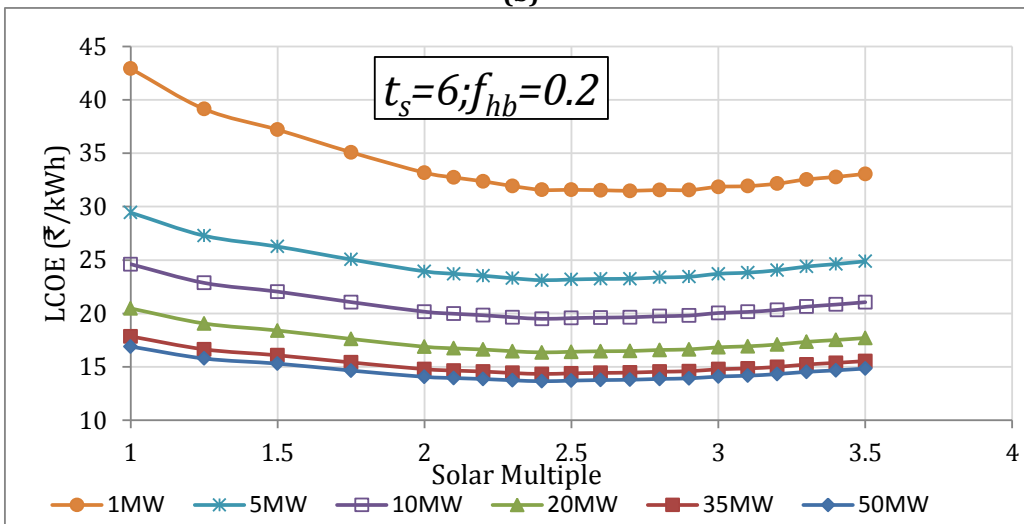
Figure 3.32: Variation of LCOE with SM for different thermal storage hours with  $f_{hb}=0.1$



(a)

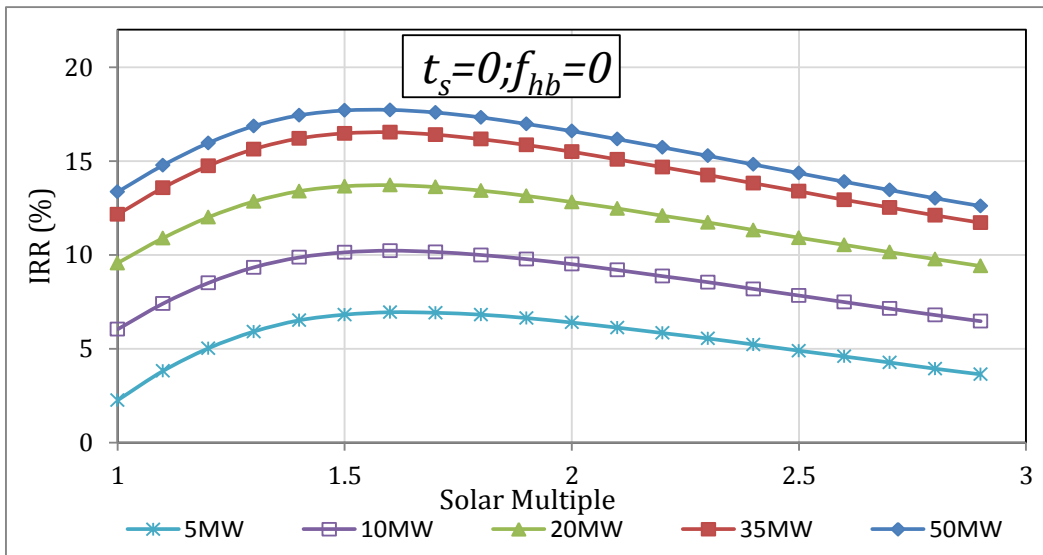


(b)

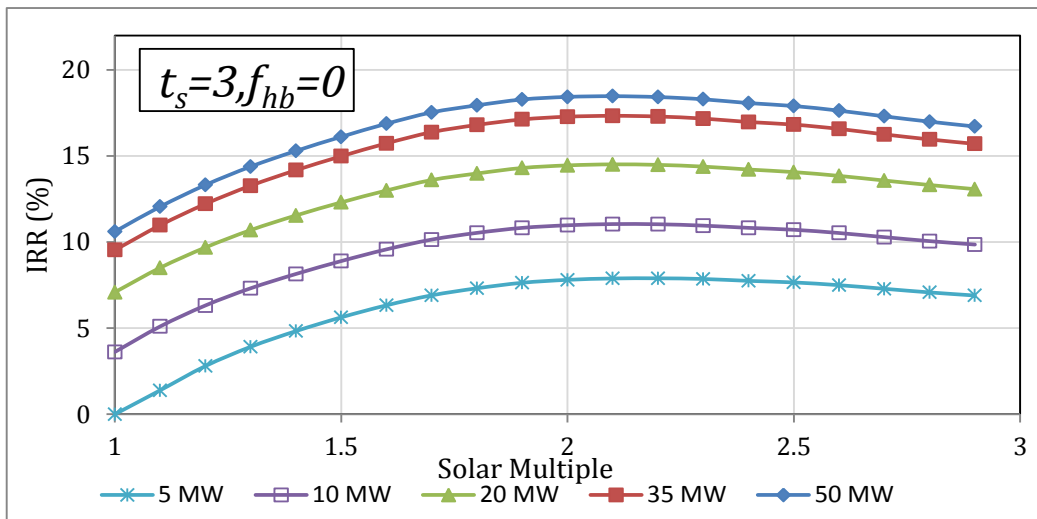


(c)

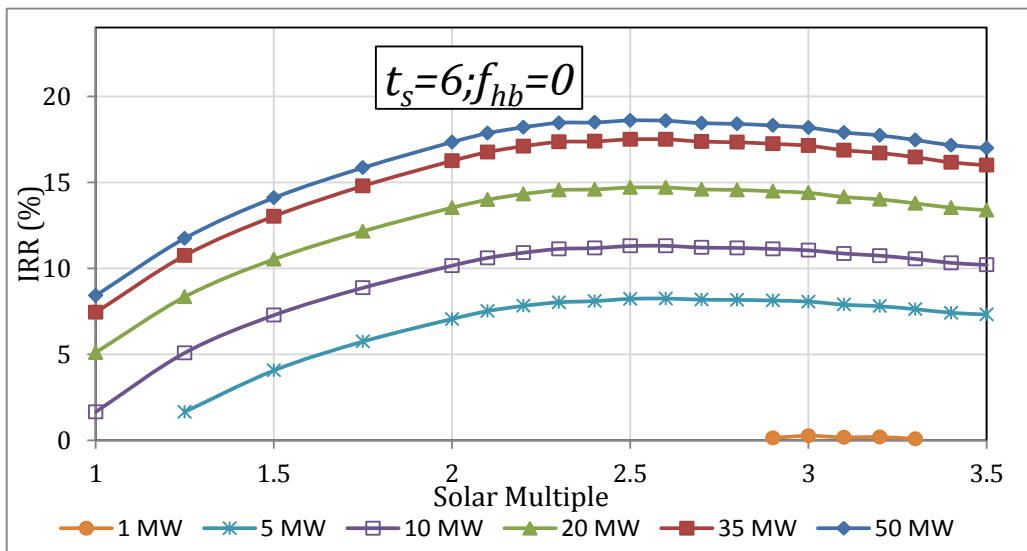
Figure 3.33: Variation of LCOE with SM for different thermal storage hours with  $f_{hb}=0.2$



(a)

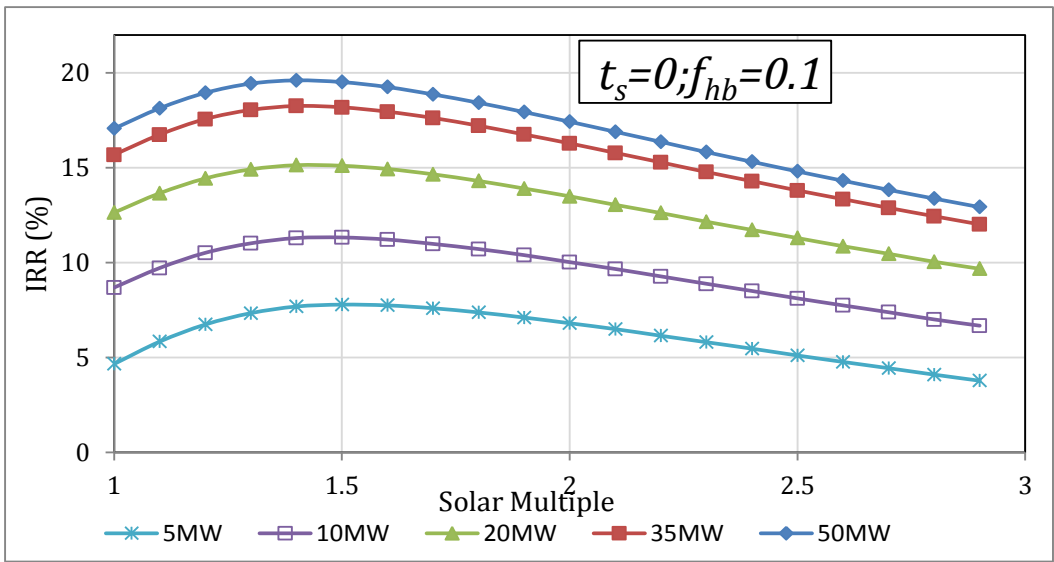


(b)

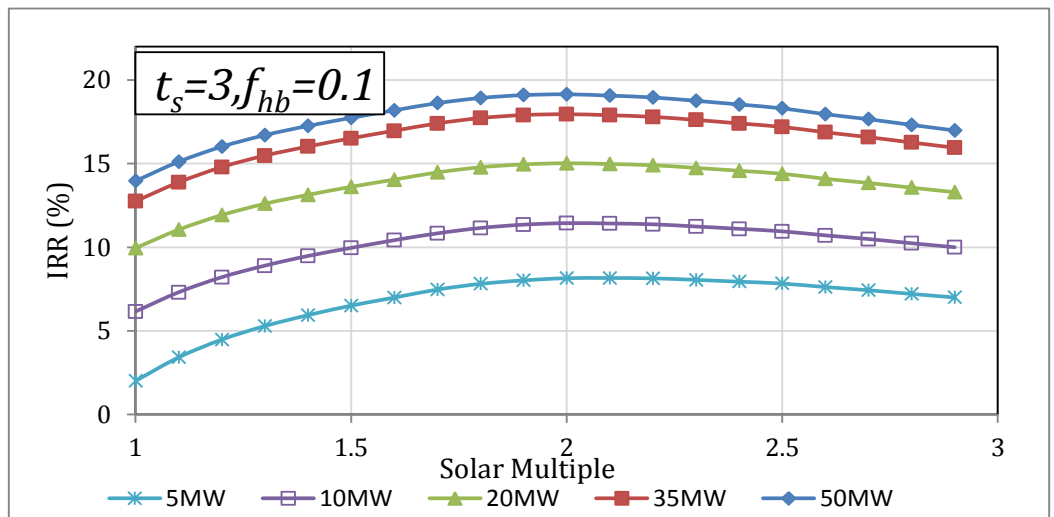


(c)

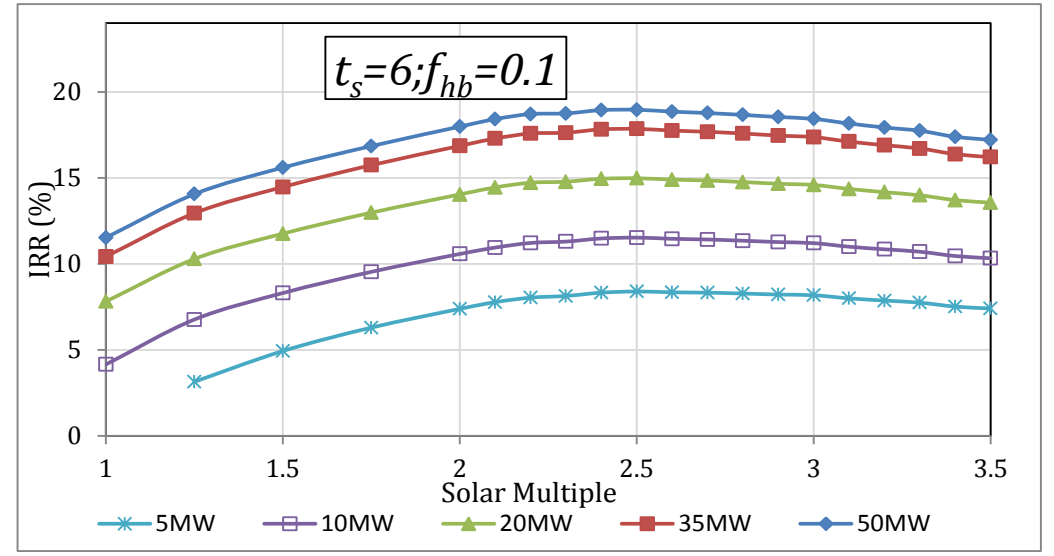
Figure 3.34: Variation of IRR with SM for different thermal storage hours with  $f_{hb}=0$



(a)

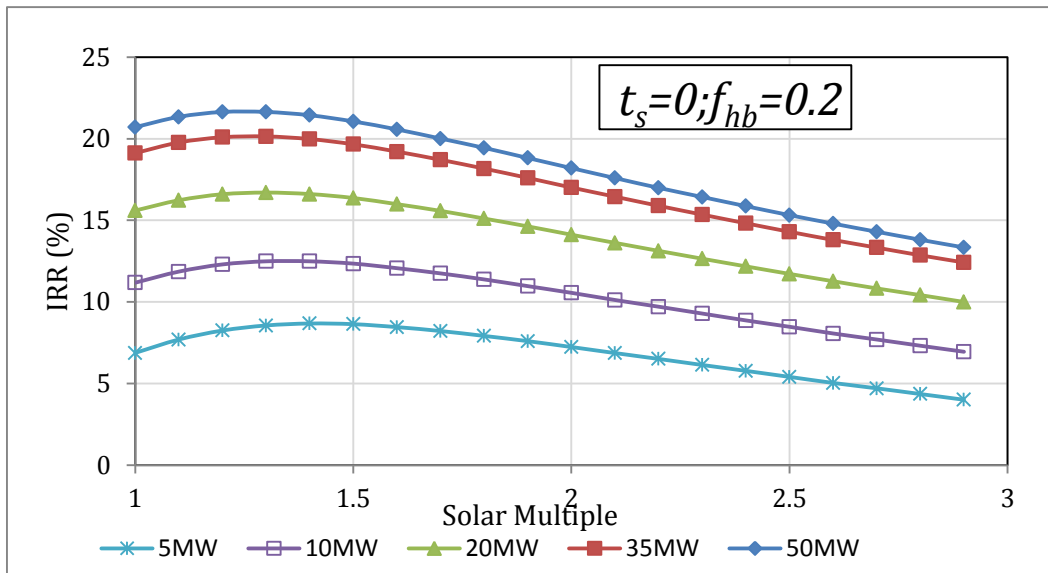


(b)

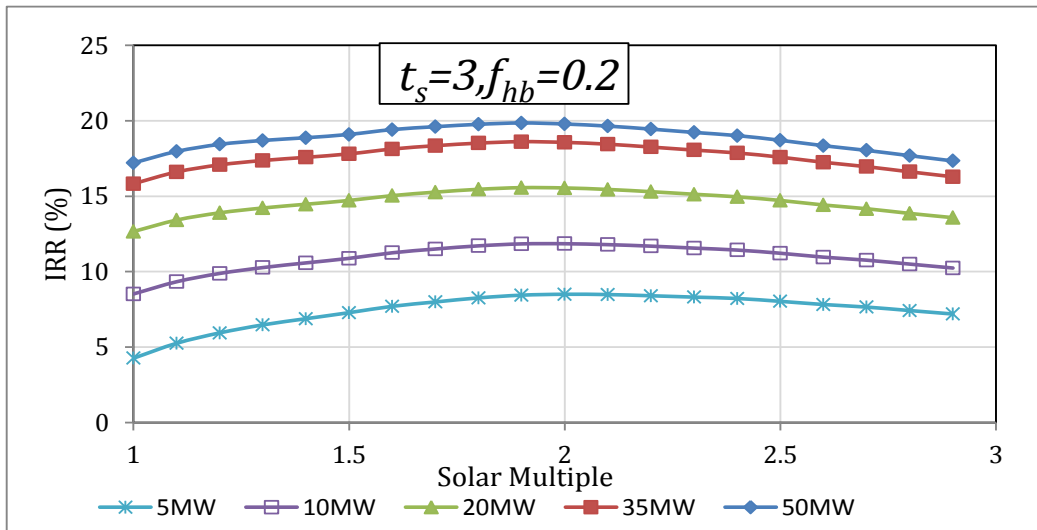


(c)

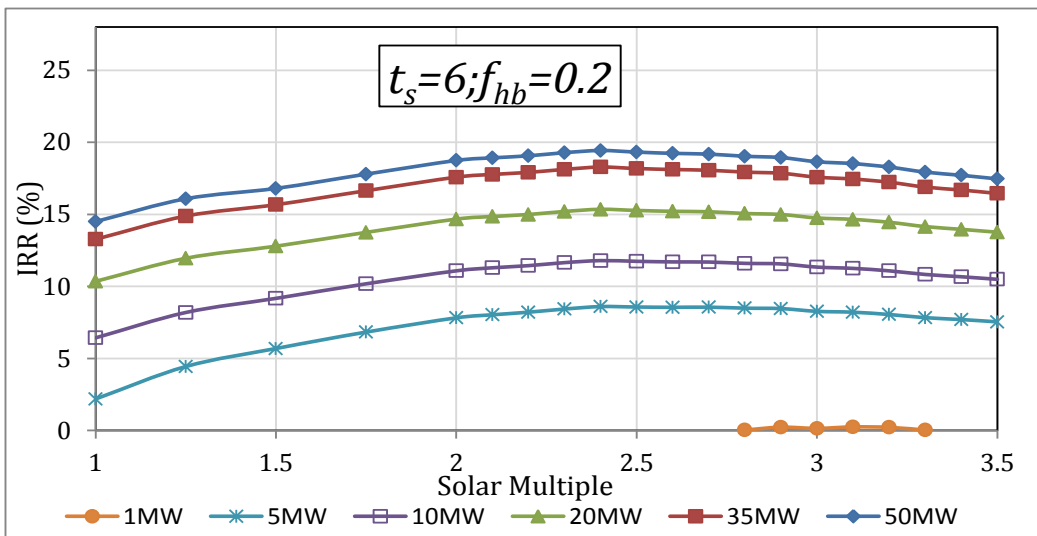
Figure 3.35: Variation of IRR with SM for different thermal storage hours with  $f_{hb}=0.1$



(a)



(b)



(c)

Figure 3.36: Variation of IRR with SM for different thermal storage hours with  $f_{hb}=0.2$

**i. Effect of Thermal Storage on Optimum SM for Different Hybridization Fractions**

Table 3.12 gives data of the optimised SMs for different thermal storage conditions and hybridization fractions. It can be seen that there is no significant variation in optimum SM with plant capacities, but the optimum SM increases with thermal storage.

**Table 3.12: Optimized SMs under different conditions**

<b>Thermal Storage (Hours)</b>	<b>Capacity (MW)</b>	<b><math>f_{hb} = 0</math></b>	<b><math>f_{hb} = 0.1</math></b>	<b><math>f_{hb} = 0.2</math></b>
$t_s=0$	1	1.7	1.6	1.4
	5	1.6	1.5	1.3
	10	1.6	1.4	1.3
	20	1.6	1.4	1.3
	35	1.6	1.4	1.3
	50	1.6	1.4	1.3
$t_s=3$	1	2.3	2.2	2.1
	5	2.1	2.0	1.9
	10	2.1	2.0	1.9
	20	2.1	2.0	1.9
	35	2.1	2.0	1.9
	50	2.1	2.0	1.9
$t_s=6$	1	2.8	2.7	2.7
	5	2.6	2.5	2.4
	10	2.6	2.5	2.4
	20	2.5	2.5	2.4
	35	2.5	2.5	2.4
	50	2.5	2.5	2.4

**3.5.2 Economic Parameters of PT plants**

For various plant capacities, thermal storage and hybridization, the values of optimum SM and other corresponding parameters like LCOE, IRR, capital cost, O&M expenses and CF are given in the following tables. Table 3.13, Table 3.14 and Table 3.15 correspond to  $f_{hb}=0, 0.1$  and  $0.2$  respectively. In each of them (a), (b) and (c) correspond to  $t_s=0, 3$  and  $6$  hours respectively. IRR values for 1 MW capacity for all the thermal storage and hybridization values considered were negative and hence, not shown. When hybridization is used, the values of LCOE for solar and hybridization components are also presented.

**Table 3.13: Data corresponding to optimum SM for  $f_{hb}=0$**

<i>a. <math>f_{hb} = 0; t_s = 0</math></i>						
Capacity	Optimum SM	LCOE	LCOE (Solar)	IRR	Capital Cost	Capacity Factor
(MW)		( $\text{₹}/kWh$ )		(%)	( $\text{₹-lakh}/MW$ )	
1	1.7	36.56	36.56	-	3610	0.28
5	1.6	25.42	25.42	6.95	2660	0.27
10	1.6	21.28	21.28	10.23	2247	0.27
20	1.6	17.73	17.73	13.72	1885	0.27
35	1.6	15.47	15.47	16.54	1646	0.27
50	1.6	14.65	14.65	17.73	1561	0.27
<i>b. <math>f_{hb} = 0; t_s = 3</math></i>						
1	2.3	33.62	33.62	-	4884	0.41
5	2.1	24.21	24.21	7.89	3585	0.38
10	2.1	20.37	20.37	11.05	3036	0.38
20	2.1	17.04	17.04	14.52	2552	0.38
35	2.1	14.92	14.92	17.34	2232	0.38
50	2.1	14.18	14.18	18.48	2125	0.38
<i>c. <math>f_{hb} = 0; t_s = 6</math></i>						
1	2.8	32.36	32.36	-	6005	0.51
5	2.6	23.85	23.85	8.25	4511	0.49
10	2.6	20.13	20.13	11.31	3825	0.49
20	2.5	16.89	16.89	14.7	3128	0.47
35	2.5	14.81	14.81	17.5	2738	0.47
50	2.5	14.11	14.11	18.6	2611	0.47

**Table 3.14: Data corresponding to optimum SM for  $f_{hb}=0.1$**

<i>a. <math>f_{hb} = 0.1; t_s = 0</math></i>							
Capacity	Optimum SM	LCOE	LCOE (Solar)	LCOE (Hyb)	IRR	Capital Cost	Capacity Factor
(MW)		( $\text{₹}/kWh$ )			(%)	( $\text{₹-lakh}/MW$ )	
1	1.6	34.42	35.4	18.1	-	3473	0.30
5	1.5	23.68	24.5	12	7.79	2546	0.29
10	1.4	19.8	20.7	9.8	11.3	2042	0.28
20	1.4	16.48	17.2	8.2	15.14	1712	0.28
35	1.4	14.37	15	7.2	18.26	1494	0.28
50	1.4	13.59	14.2	6.9	19.61	1415	0.28
<i>b. <math>f_{hb} = 0.1; t_s = 3</math></i>							
1	2.2	32.99	33.1	26.9	-	4747	0.41
5	2	23.62	23.8	15.4	8.15	3472	0.39
10	2	19.86	20	12.8	11.44	2940	0.39
20	2	16.6	16.8	10.6	15.02	2470	0.39
35	2	14.52	14.7	9.3	17.95	2161	0.39
50	2	13.81	13.9	8.9	19.14	2056	0.39
<i>c. <math>f_{hb} = 0.1; t_s = 6</math></i>							
1	2.7	32.06	32.1	30.9	-	5867	0.51
5	2.5	23.51	23.6	18.2	8.4	4397	0.49
10	2.5	19.84	19.9	15	11.53	3728	0.49
20	2.5	16.64	16.7	12.3	14.98	3137	0.49
35	2.5	14.58	14.6	10.7	17.85	2747	0.49
50	2.5	13.9	13.9	10.2	18.96	2620	0.49

**Table 3.15: Data corresponding to optimum SM for  $f_{hb}=0.2$**

a. $f_{hb} = 0.2; t_s = 0$							
Capacity	Optimum SM	LCOE	LCOE (Solar)	LCOE (Hyb)	IRR	Capital Cost	Capacity Factor
(MW)		(₹/kWh)			(%)	(₹-lakh/MW)	
1	1.4	32.21	35.2	14.7	-	3182	0.31
5	1.3	22.09	24.4	10.8	8.56	2306	0.30
10	1.3	18.47	20.4	9.2	12.49	1945	0.30
20	1.3	15.37	16.9	7.8	16.7	1630	0.30
35	1.3	13.41	14.8	6.9	20.14	1422	0.30
50	1.3	12.69	13.9	6.6	21.64	1346	0.30
b. $f_{hb} = 0.2; t_s = 3$							
1	2.1	32.21	32.7	20.9	-	4609	0.41
5	1.9	23.01	23.6	13.9	8.44	3358	0.39
10	1.9	19.34	19.8	11.7	11.84	2842	0.39
20	1.9	16.17	16.6	9.8	15.57	2389	0.39
35	1.9	14.14	14.5	8.6	18.62	2089	0.39
50	1.9	13.44	13.8	8.3	19.86	1987	0.39
c. $f_{hb} = 0.2; t_s = 6$							
1	2.7	31.48	31.7	23.8	-	5883	0.52
5	2.4	23.11	23.3	16	8.6	4284	0.49
10	2.4	19.49	19.7	13.4	11.79	3632	0.49
20	2.4	16.35	16.5	11.2	15.35	3055	0.49
35	2.4	14.33	14.5	9.8	18.28	2675	0.49
50	2.4	13.65	13.8	9.4	19.43	2550	0.49

**i. Variation of Plant Characteristics with Capacity and Thermal Storage without Hybridization**

*Capital Cost*

Figure 3.37 shows the variation of capital cost per MW for various capacities under different thermal storage conditions. The capital costs given are for optimized SMs. At 50 MW the capital cost varies from 1561 to 2611 ₹-lakhs/MW for zero to six hours of thermal storage.

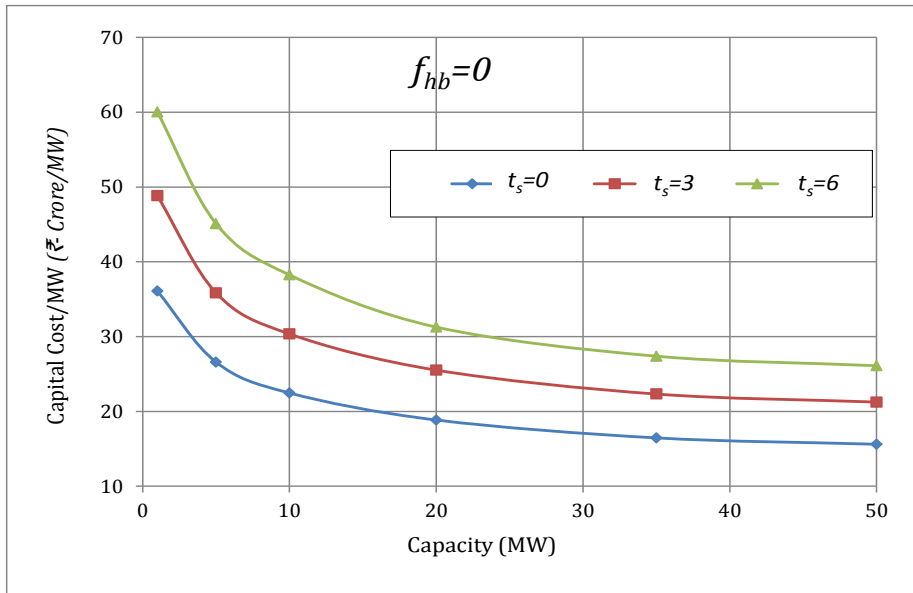


**Figure 3.37: Variation of capital cost for various thermal storage conditions**

*Mirror Area/ Land Area*

The mirror area required per MW for various capacities under different storage conditions are presented in Figure 3.38 and Table 3.16. Since land to mirror area ratio is a constant (3.8) in the present analysis, the variation of land area required is similar to that of the mirror area.

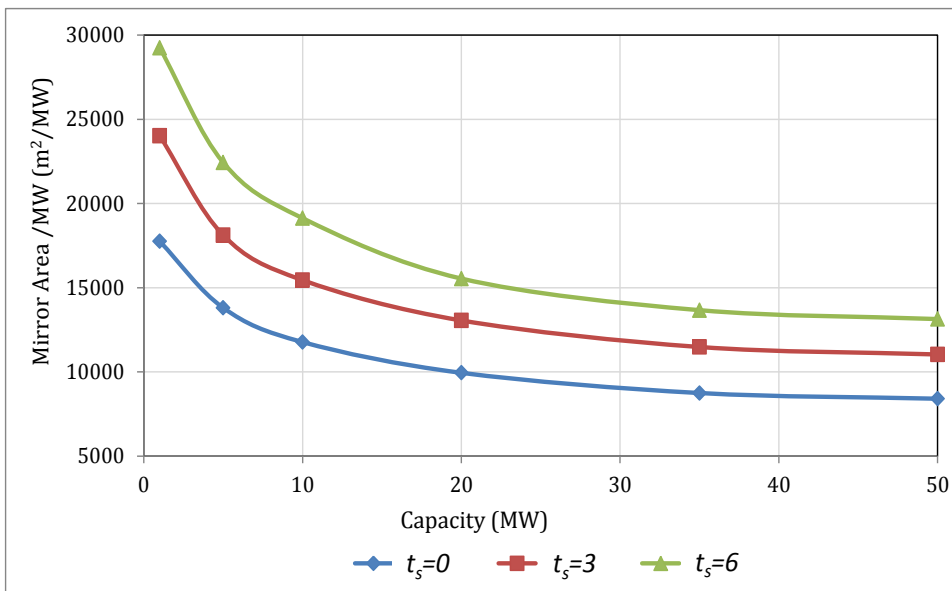


**Figure 3.38: Variation of mirror area per MW under different thermal storage conditions**

**Table 3.16: Mirror area and land area details for various thermal storage conditions**

$f_{hb}=0; t_s=0$				
Capacity (MW)	Optimum SM	Actual Aperture Area (m <sup>2</sup> )	Mirror Area (m <sup>2</sup> /MW)	Land Area (m <sup>2</sup> /MW)
1	1.7	17755	17755	67468
5	1.6	69026	13805	52459
10	1.6	117709	11771	44729
20	1.6	198925	9946	37796
35	1.6	306109	8746	33235
50	1.6	420389	8408	31950
$f_{hb}=0; t_s=3$				
1	2.3	24021	24021	91281
5	2.1	90596	18119	68853
10	2.1	154493	15449	58707
20	2.1	261089	13054	49607
35	2.1	401768	11479	43621
50	2.1	551760	11035	41934
$f_{hb}=0; t_s=6$				
1	2.8	29243	29243	111124
5	2.6	112167	22433	85247
10	2.6	191277	19128	72685
20	2.5	310820	15541	59056
35	2.5	478295	13666	51929
50	2.5	656858	13137	49921

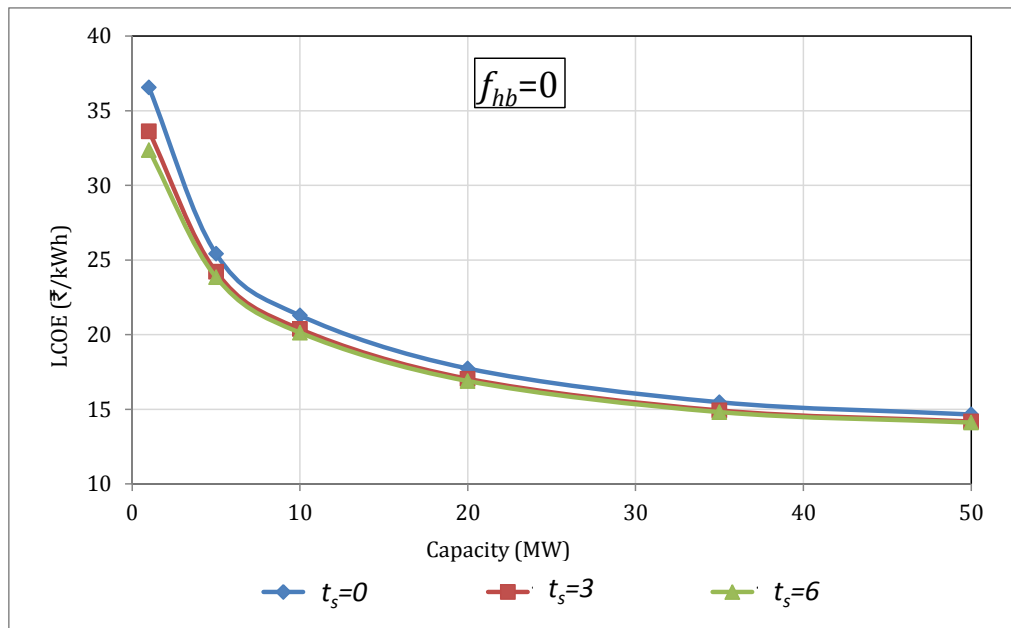


**Figure 3.39: Variation of LCOE for various thermal storage conditions**

### LCOE

Figure 3.39 shows the variation of LCOE for various capacities under different thermal storage conditions. It can be seen that the increase in thermal storage has minimal effect on LCOE. The benefit of thermal storage on LCOE at a 50 MW level is found to be just around 4% for 6 hours storage compared to no storage condition.

### IRR

Figure 3.40 shows the variation of IRR for various capacities under different thermal storage conditions. Similar to LCOE the increase in thermal storage has minimal effect on IRR. The benefit of thermal storage on IRR at a 50 MW level is found to be just around 5% for six hours storage compared to no storage condition.

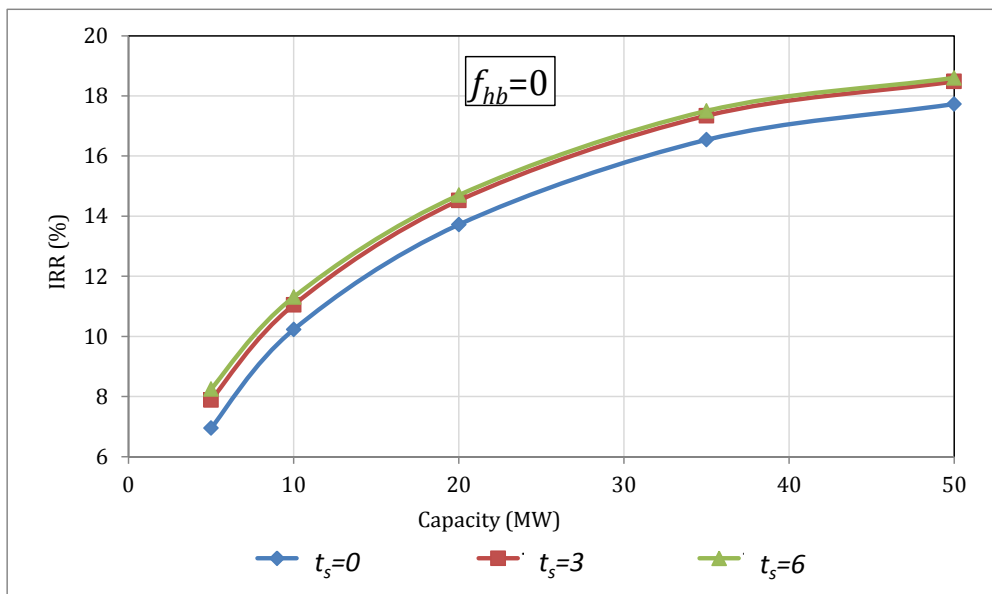


Figure 3.40: Variation of IRR for various thermal storage conditions

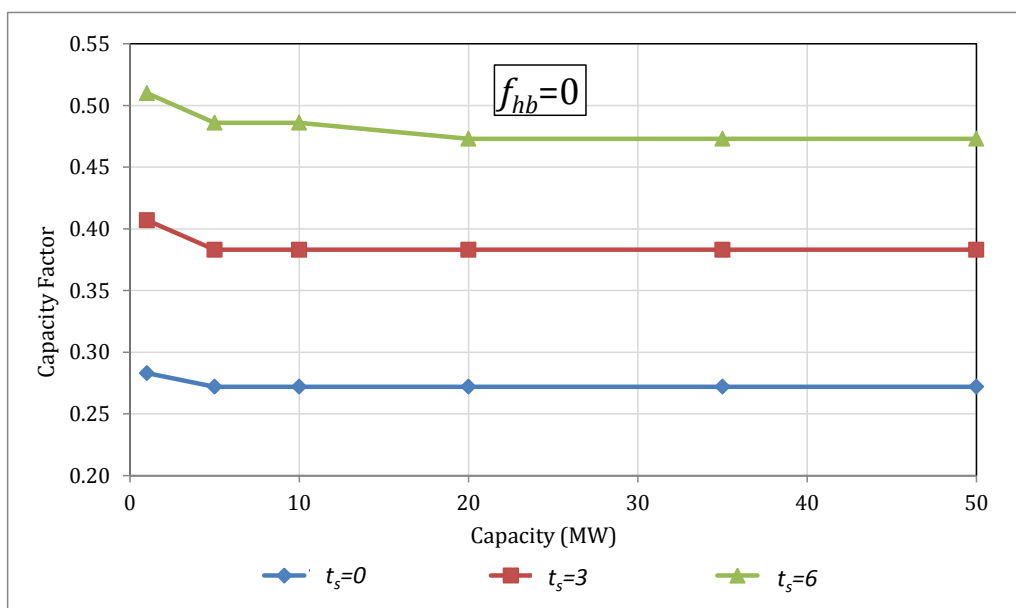


Figure 3.41: Variation of capacity factor for various thermal storage conditions

### Capacity Factor

Figure 3.41 shows the variation of capacity factor with plant capacities under different thermal storage conditions. Unlike LCOE & IRR, the increase in thermal storage has significant impact on capacity factor. It can be seen that the capacity factor increases substantially and found to be uniform over all capacities.

### ii. Variation of Capital Cost and Capacity Factor with Thermal Storage (no Hybridization Condition) for 50 MW plant

Figure 3.42 shows the variation of capital cost per MW and capacity factor at optimized SMs for a 50 MW plant with thermal storage. The optimum values of SM are also indicated. This information is in fact presented in the previous section, but here the effect of thermal storage can be more easily perceived. As expected the capital cost increases with thermal storage but the capacity factor also increases.

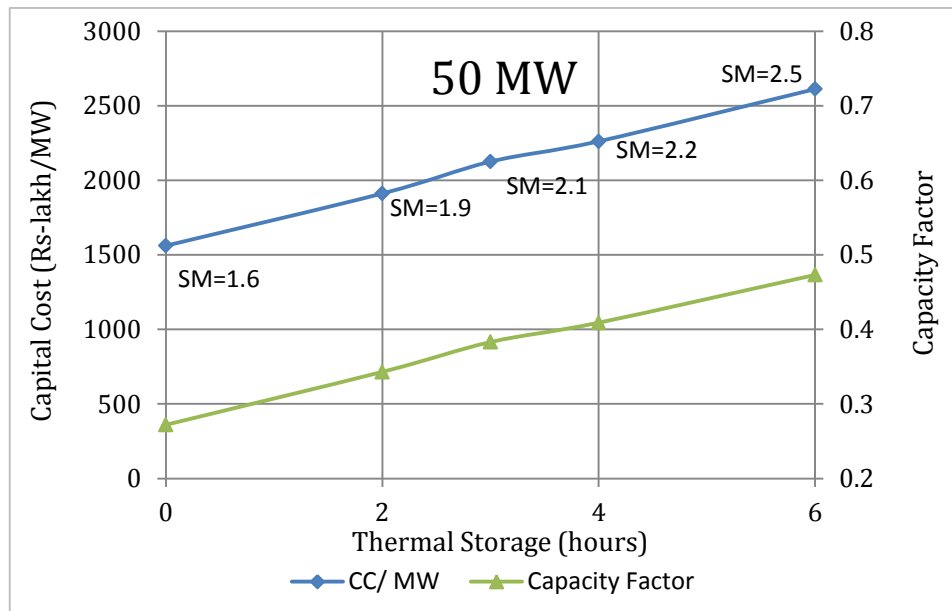


Figure 3.42: Effect of thermal storage on capital cost and capacity factor

### iii. Effect of Hybridization

As seen earlier in Section 3.4.3, the highest benefit of hybridization on energy generated can be seen at SM = 1 with no thermal storage. The impact of hybridization on LCOE, is presented in Table 3.17. Apart from the benefit on overall LCOE, it can be observed that the LCOE of solar with hybridization is less than that of LCOE of solar without hybridization.

**Table 3.17: Hybridization benefit for case of  $f_{hb}=0.2$  and  $t_s=0$**

	$f_{hb}=0.2; t_s=0$			$f_{hb}=0; t_s=0$	<b>Benefit of Hybridization</b>
<b>Capacity</b>	<b>LCOE (Solar)</b>	<b>LCOE (Hyb)</b>	<b>LCOE (Overall)</b>	<b>LCOE</b>	<b>(%)</b>
<i>(MW)</i>	<i>(₹/kWh)</i>				
1	35.2	14.7	32.21	36.56	11.90
5	24.4	10.8	22.09	25.42	13.10
10	20.4	9.2	18.47	21.28	13.20
20	16.9	7.8	15.37	17.73	13.31
35	14.8	6.9	13.41	15.47	13.32
50	13.9	6.6	12.69	14.65	13.38

Effect of thermal storage on the benefit of hybridization is presented in Table 3.18 and Figure 3.43 and Figure 3.44. It is seen that the benefit of hybridization on LCOE is maximum without any thermal storage.

**Table 3.18: Effect of storage on benefit of hybridization**

<b>Benefit of Hybridization on LCOE (%)</b>						
<b>Capacity (MW)</b>	$f_{hb}=0.1$			$f_{hb}=0.2$		
	$t_s=0$	$t_s=3$	$t_s=6$	$t_s=0$	$t_s=3$	$t_s=6$
1	5.85	1.87	0.93	11.90	4.19	2.72
5	6.85	2.44	1.43	13.10	4.96	3.10
10	6.95	2.50	1.44	13.20	5.06	3.18
20	7.05	2.58	1.48	13.31	5.11	3.20
35	7.11	2.68	1.55	13.32	5.23	3.24
50	7.24	2.61	1.49	13.38	5.22	3.26

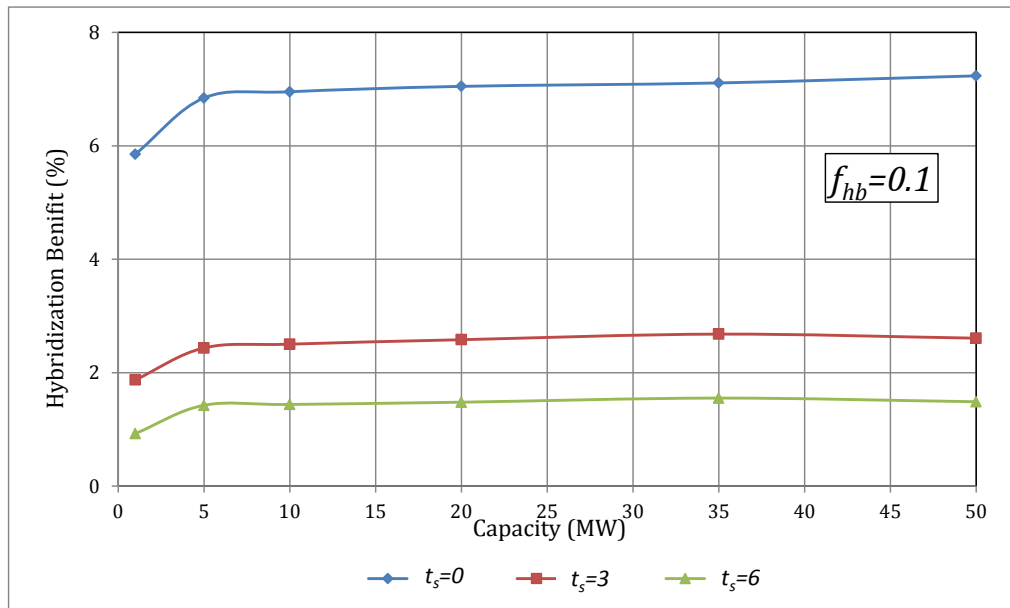


Figure 3.43: Hybridization benefit for LCOE when  $f_{hb}=0.1$

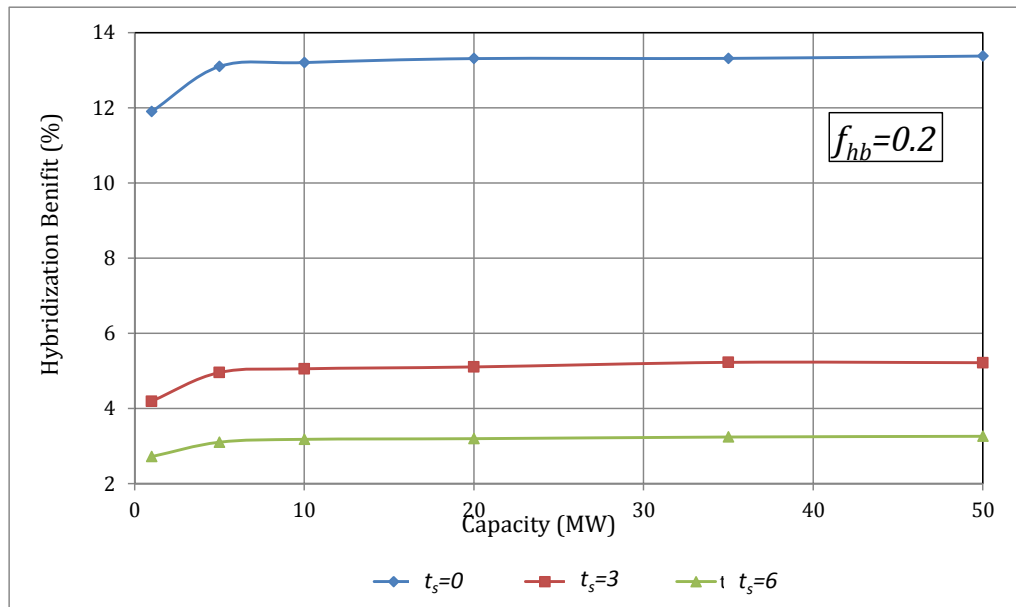


Figure 3.44: Hybridization benefit for LCOE when  $f_{hb}=0.2$

### 3.6 Salient Observations

An engineering economic model for analysis of CSP plants using PT technology has been developed. It takes into account the hourly variation of DNI, variation in the efficiencies of power block with part load & absorber tube with solar input, lag between the power generation and solar input due to thermal losses, use of thermal storage and hybridization.

This model was then applied to locating a PT plant at Jodhpur, for different plant capacities, thermal storage and hybridization.

The results indicate that the estimated capital cost for a 50 MW plant with no thermal storage is around ₹ 15.6 Cr/MW with an LCOE of 14.65 ₹/kWh and a capacity factor of 27%. If six hours of

thermal storage is provided, then the capital cost increases to ₹ 26.11 Cr/MW with LCOE of 14.11 ₹/kWh and a capacity factor of 47.3%.

These figures look reasonable but are dependent on the inputs used in this analysis which have certain uncertainties. Further refinements would lead to more reliable estimates. It is relevant to note that even NREL's Solar Advisory Model states that there are uncertainties in their estimates.

## 4 Interactive Desktop Tool

### 4.1 Introduction

An interactive desktop tool for the application of the model for engineering-economic analysis for PT plants described earlier has been developed. This tool takes inputs from the user, and displays the results based on assumptions made in the model. The user of this tool is expected to be aware of CSP technology and economics involved. This tool presents a complete set of basic design information needed for establishing a PT plant at a chosen location and also the financial parameters such as the total capital cost, LCOE and IRR.

### 4.2 Overview of the Tool

This tool is designed using the concept of “tab” similar to that of tabs present in any of the contemporary web browsers. The user has the advantage of switching between tabs at any time as required. All the tabs present in this tool have been categorized into two types:

- a. Tabs for entering/modifying default input values needed to run a simulation, known as Input Tabs.
- b. Tabs for displaying the results/outputs of the latest simulation executed, known as Output Tabs.

Simulation considers all the inputs entered by the user and applies the techno-economic model and presents the user the results obtained. Simulation in this tool is of two types.

- a. Base Case Simulation: This is considered to be a particular case that is executed for a chosen SM.
- b. Parametric Simulation: In this type of simulation, the tool executes more than one case simultaneously depending on the various SMs entered by the user. The tool takes all the input variables, other than SMs, to be the same and executes the simulation for the all the SMs chosen sequentially. A detailed explanation of parametric simulation is provided in section 4.4.

The tool on start-up, displays default values for all the variables present under input tabs. These variables are known as input variables, which are essential to run a simulation. All input variables have pre-defined ranges. The default values and ranges for the input variables have been chosen based on the existing literature.

The variables in the input tabs have been categorized as listed below:

- i. Location Details
- ii. Plant Details
- iii. Capital Costs
- iv. O&M Expenses
- v. Financial Parameters
- vi. Simulation and Results

As mentioned earlier, all these input tabs have several text fields with default values displayed which can be modified.

Figure 4.1 shows all the input tabs present in the tool. The details of the input variables for the highlighted tab will also be shown.

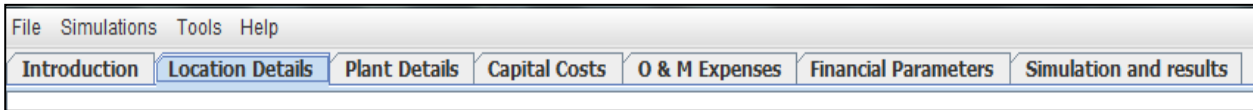


**Figure 4.1: Input tabs**

Similarly after successful execution of a simulation, the tool prompts a tab named “Outputs”, which again contains several tabs under it categorized as output tabs as mentioned earlier. The outputs have been categorized into following tabs:

- i. Summary
- ii. Technical Outputs
- iii. Equipment Cost Outputs
- iv. Other Costs Outputs
- v. Monthly Profile Graphs
- vi. Time Series Graph
- vii. Parametric Simulation Graph (This tab is shown only when simulation chosen is parametric).

The variables present under these tabs are called as output variables. All the tabs highlighted under “Outputs” are as shown in Figure 4.2.

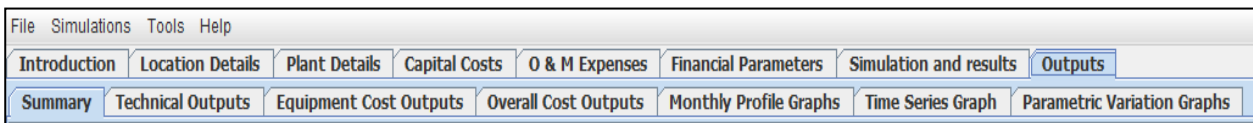


**Figure 4.2: Output tabs**

### 4.3 Start of the Application

The following procedure describes the basic steps to run a simulation. At the start of the application it displays introduction page (Figure 4.3) that gives a general description of the tool and assumptions made in building the tool.

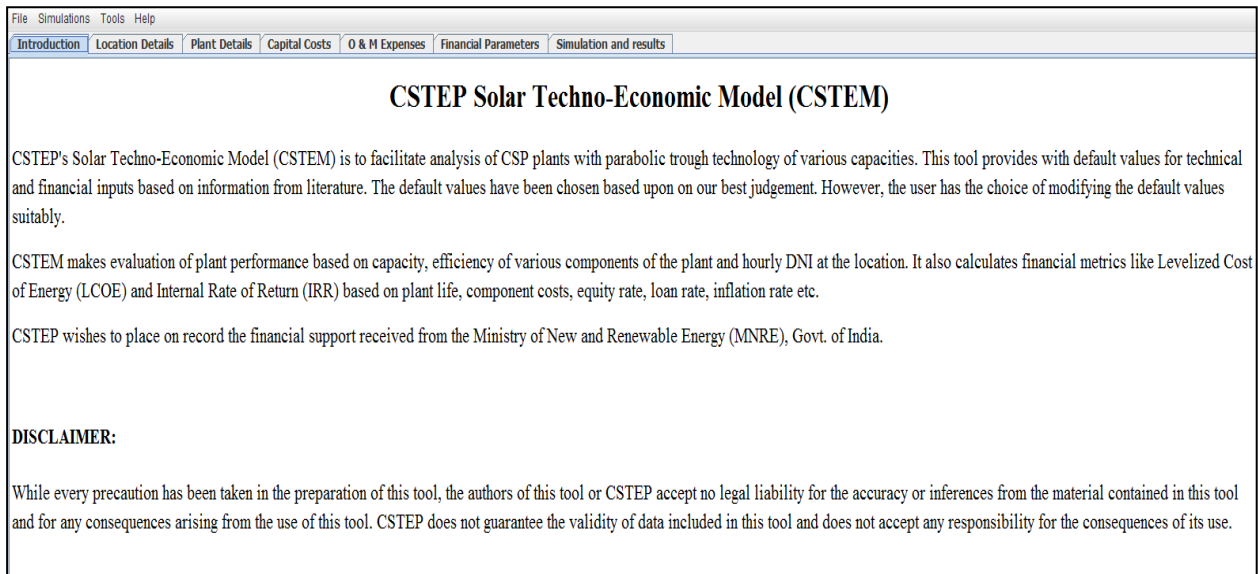


**Figure 4.3: Start page of the tool**

Before exploring the tool, the user needs to know the various menu options in the tool (Figure 4.4).

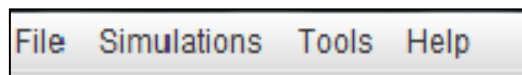


**Figure 4.4: Menu options in the tool**

The “File” menu contains option to exit the tool.

The “Simulations” menu contains options for enabling and removing parametric simulation.

The “Tools” menu provides the user, the feature of adding a new location.

The “Help” menu provides the user manual and it also contains details of the developers of the tool.

## 4.4 Input Tabs

Details of the input tabs listed below are discussed.

### 4.4.1 Location Details

This tab allows the user to choose a particular location from the existing 22 locations presented as drop down menu, for which DNI data are available. For a chosen location, the user is provided with the complete information about the location, such as Latitude, Longitude, Elevation, and Annual DNI. Apart from these the user has the option of visualizing the monthly profiles of DNI data and also the variations of DNI over the complete year as step graphs, by clicking on the “DNI Profiles” button available on this page. This information provided is not editable by the user. Figure 4.5 shows the contents under location details tab.

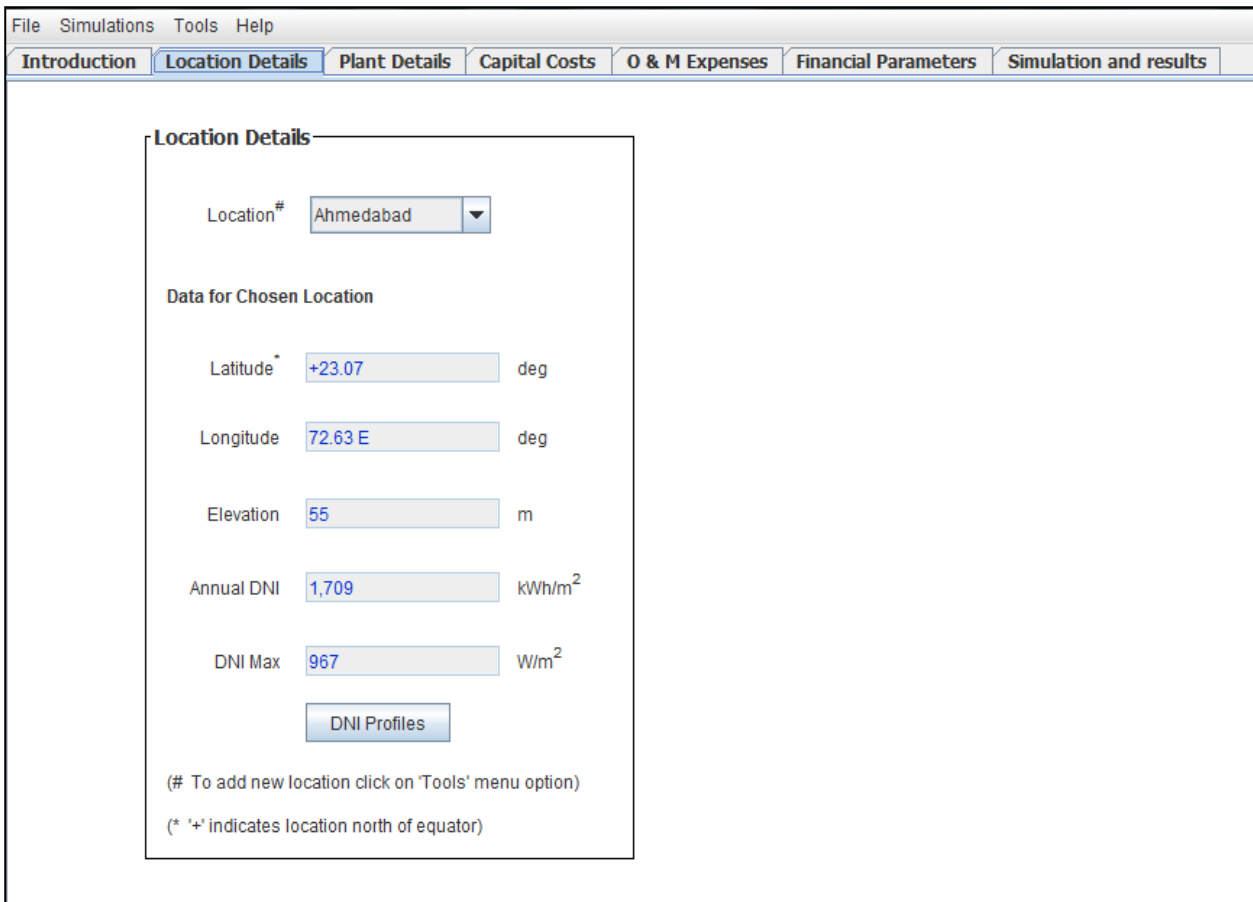


**Figure 4.5: Location details tab**

**Adding a new location:**

The tool can be run only for the locations present in the drop down menu. However, the user can add a new location to the drop down menu as mentioned below.

For adding a new location, the user needs to have the hourly DNI data over a complete year for the desired location and also other information like latitude, longitude and elevation. To add a new location the user needs to click on the “Tools” menu bar option and then click on the “Add DNI data for new location” as depicted in Figure 4.6. Upon clicking this button, the user is shown the excel workbook where the information of existing 22 locations is available. The user needs to enter the data in a new sheet within the same excel workbook. An important point to be noted here is that, the user needs to plug in the data in the same format as that of other existing locations. Also the data should be placed exactly in the same cells as that of data for default locations. Once the user ensures proper data input, the excel workbook can be saved. The user needs to restart the tool to choose the newly added location.

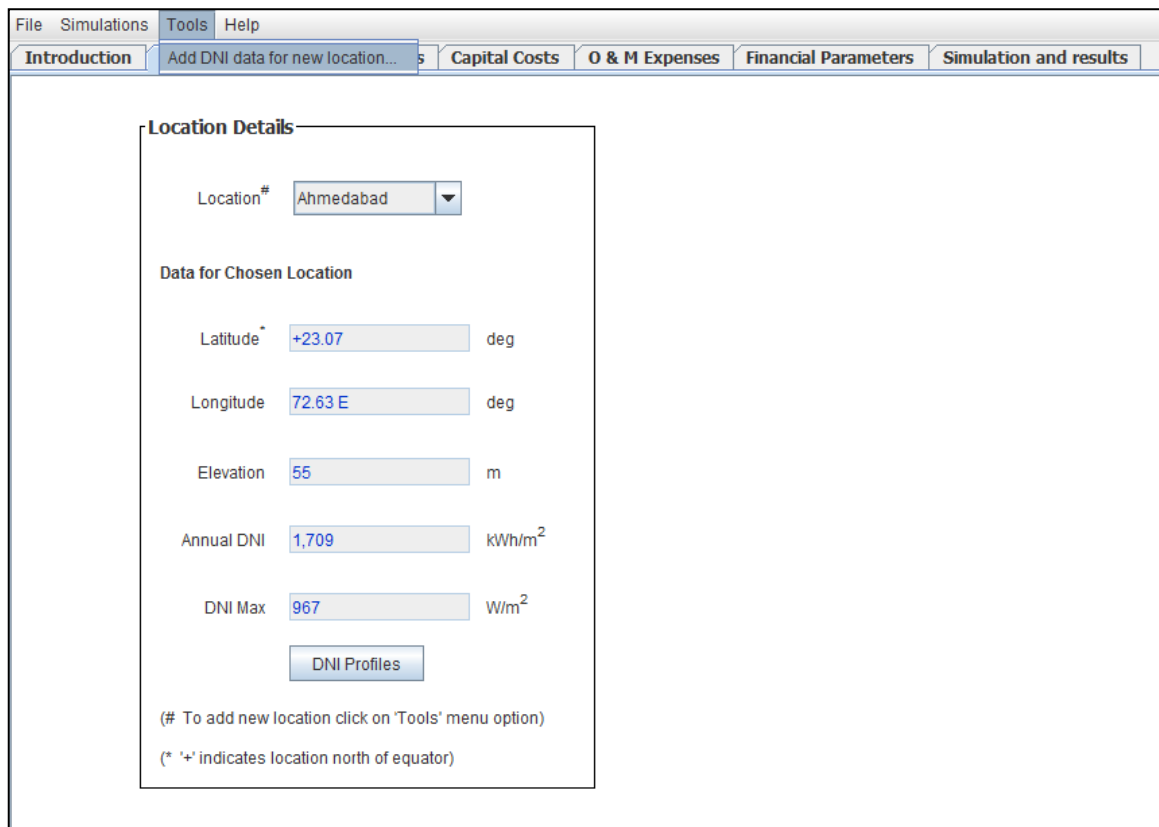


**Figure 4.6: Steps for adding new location of user choice**

### 4.4.2 Plant Details

When the user clicks on this tab the screenshot shown in Figure 4.7 is presented.

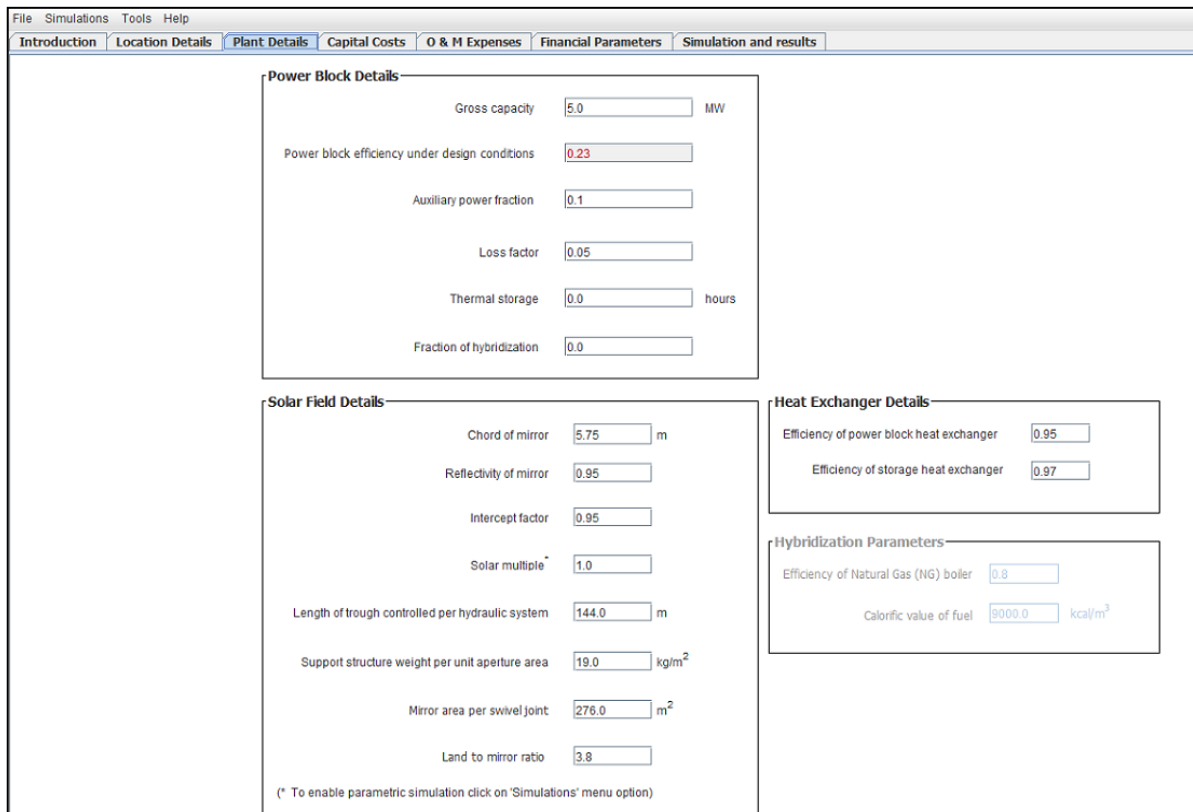


**Figure 4.7: Plant details tab**

The input variables in the “Plant Details” tab are divided into Power Block Details, Solar Field Details, Heat Exchanger details and Hybridization parameters.

The ‘Power Block Details’ subsection contains input information on the gross capacity of the plant, hours of thermal storage, fraction of hybridization, auxiliary power requirements and loss factor associated with the plant.

The ‘Solar Field Details’ subsection consists of input variables that provide information needed for designing and deciding the size of solar field. One of the important inputs is the SM. For base case simulation only one value of solar multiple is given as input. However, initially one would be interested to run simulation for various values of SM to determine the optimum SM for which LCOE is minimum. In such a case, one has to use the parametric simulation which is described in detail below.

The ‘Heat Exchanger’ subsections provide the efficiencies of the power block heat exchanger and the storage heat exchanger.

Depending on the fraction of hybridization entered by the user the ‘Hybridization parameters’ subsection is enabled (Figure 4.7). The main aim of hybridization is to augment the short fall in thermal energy delivered by the solar field. In our analysis, hybridization is limited to the usage of natural gas. So this subsection provides information about the efficiency of the natural gas boiler and the calorific value of the fuel used.

### **Parametric Simulations**

As explained in section 3.3.1, there is an optimum SM for which LCOE is a minimum. So, user needs to run a parametric simulation for different SMs.

In order to enable the parametric simulation, user needs to click on ‘Simulations’ menu option and then click on ‘Parametric’ as shown in Figure 4.8. Then, the screen shown in Figure 4.9 appears where the user needs to enter the number of SM values and individual solar multiples separated by commas. After clicking the OK button, the tool returns to the Input screen. At this stage, if the user wishes to disable the parametric simulation and switch back to base case simulation, then user needs to click on simulation menu option and then click on ‘Remove Previous Simulation’ as shown in Figure 4.10. If user wishes to run the parametric simulation, the user needs to click on the ‘Simulation and results’ tab and then click on the ‘Run Simulation’ button available on the page. For user entered SMs the tool considers each SM as a single case and runs all the cases as a batch and presents the results for each individual SM in the outputs tab. Under outputs, in summary tab, there exists a variable named solar multiple, which has a drop down menu with all SMs chosen by the user. Results for the chosen SM from the drop down menu are displayed. Also under ‘Parametric Variations Graph’ tab the user is shown plots of LCOE and IRR vs. SM. From the graph user can determine the optimum SM and corresponding LCOE and IRR.

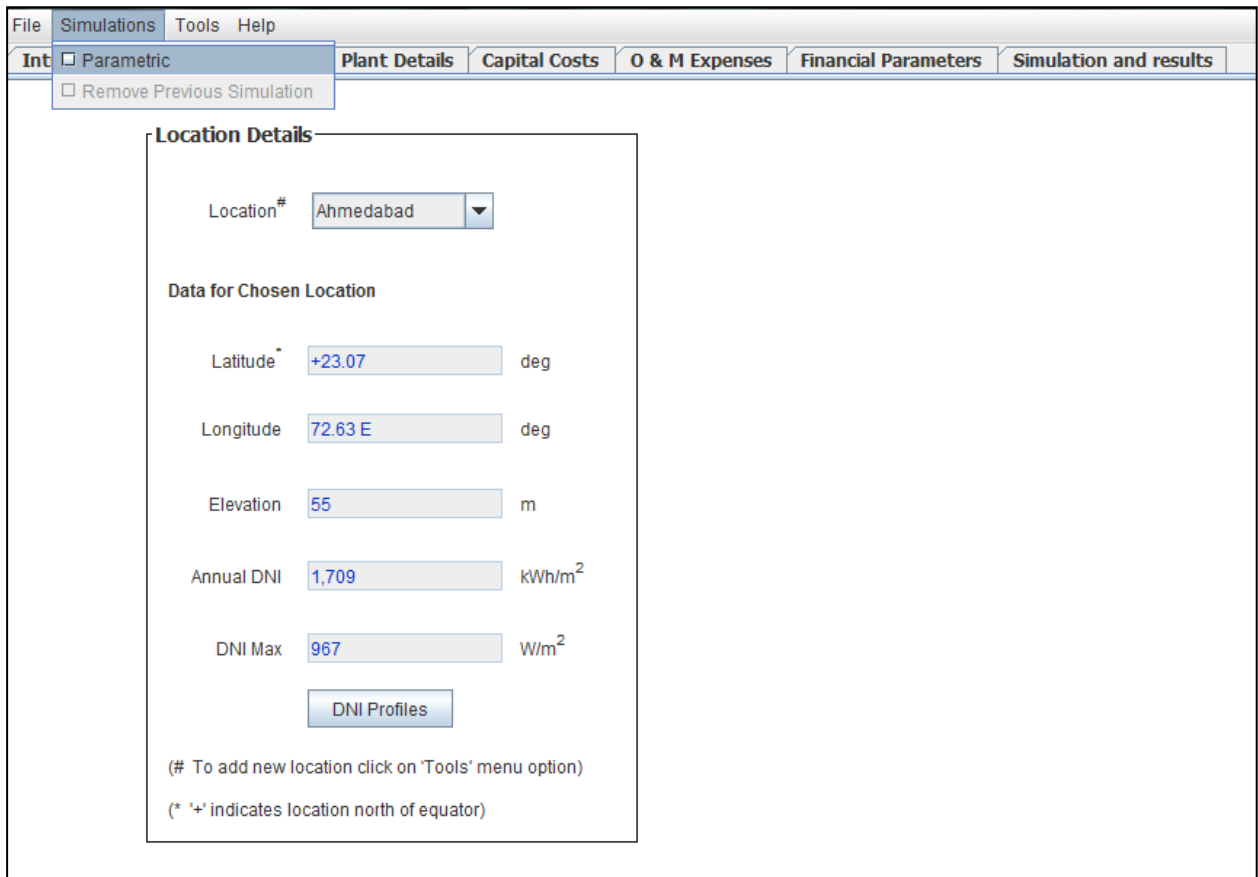


**Figure 4.8: Enabling parametric simulation**

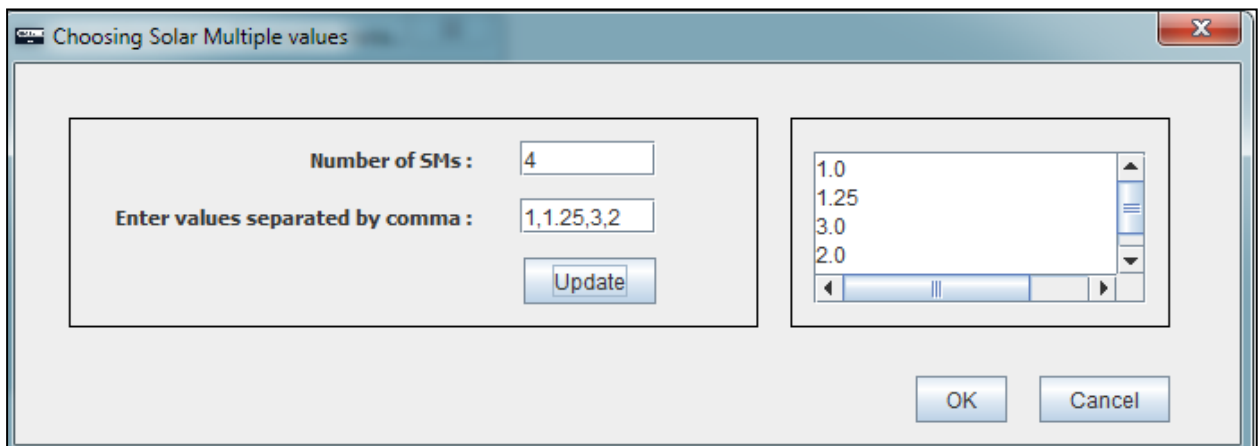


**Figure 4.9: Entering SM values for parametric simulation**

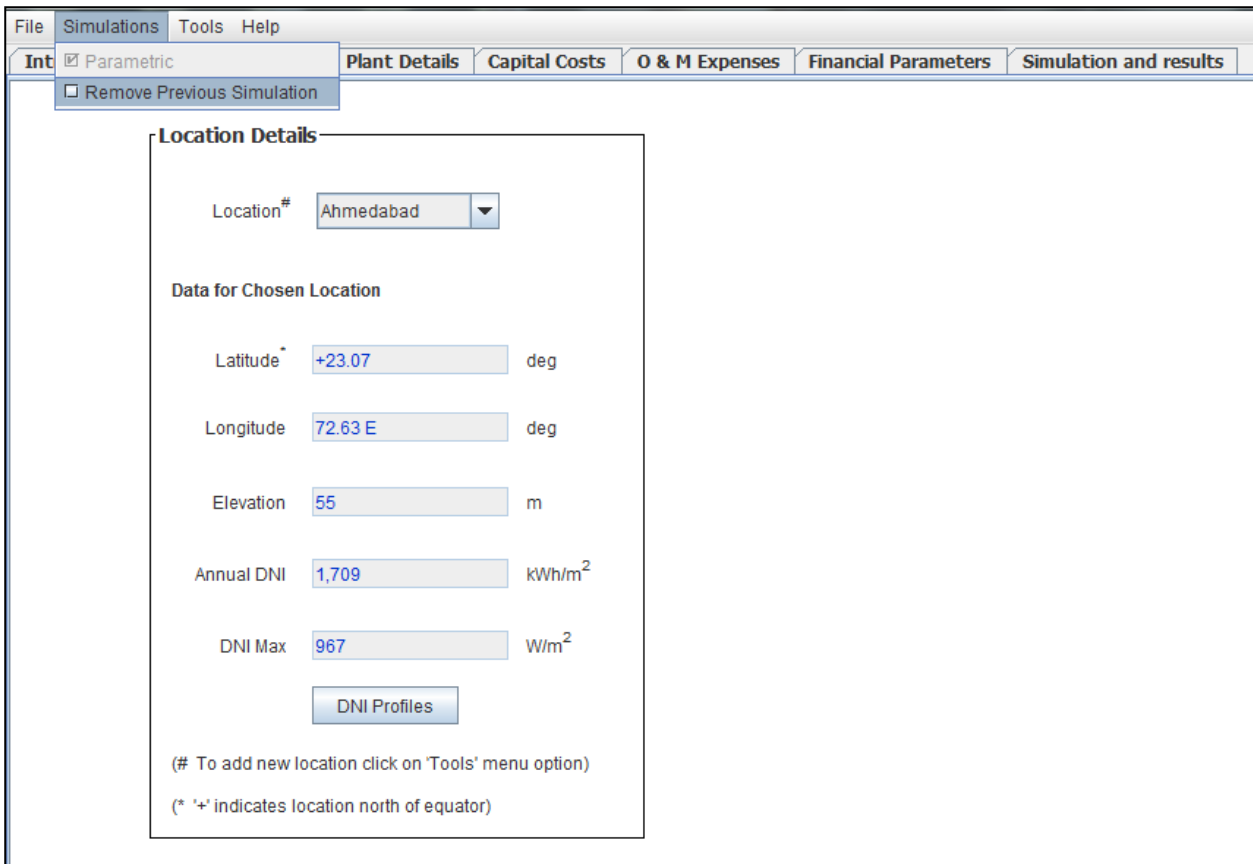


**Figure 4.10: Procedure to remove the parametric simulation**

### 4.4.3 Capital Costs

The capital costs tab provides information about the variables that can be segregated into DCC and ICC as shown in Figure 4.11. This tab takes into consideration all the costs associated with the PT power plant. Default values are provided for each individual variable under this tab. However, the user has the option of modifying these values.

Description of capital costs are described below:

- i. **DCC:** The direct capital cost includes land related costs, solar field components, power block, thermal storage system and hybridization system costs. Under each of these categories, there are several variables for which default values have been provided.
- ii. **ICC:** These costs include EPC costs, PMG costs, pre-operative expenses and IDC. All these variables are provided as a percentage of DCC.

The screenshot displays the 'Capital Costs' tab of a simulation software. The interface is organized into several sections with input fields for various cost parameters:

- Direct Capital Costs**
  - Solar Field Components**
    - Cost of mirror per unit aperture area: 2450.0 Rs/m<sup>2</sup>
    - Support structure material & fabrication cost: 150.0 Rs/kg
    - Support structure cost per unit aperture area: 2,850 Rs/m<sup>2</sup>
    - Cost of absorber tube: 14250.0 Rs/m
    - Cost of HTF: 200.0 Rslitre
    - Cost of HTF system per unit aperture area of mirror: 1900.0 Rs/m<sup>2</sup>
    - Cost of hydraulic trackers & electric motors: 130000.0 Rs/unit
    - Cost of swivel joints: 70000.0 Rs/unit
    - Cost of foundation for support structure per unit aperture area: 200.0 Rs/m<sup>2</sup>
    - Cost of electronics, controls & electrical system per unit aperture area: 1000.0 Rs/m<sup>2</sup>
  - Land Related Costs**
    - Cost of land: 100.0 Rs/m<sup>2</sup>
    - Cost of site preparation: 107.6 Rs/m<sup>2</sup>
- Power Block System**
  - Cost of Turbine Generator (TG) set and accessories (Estimated value based on power block capacity): 1,731.33 Rs Lakh
  - Cost of balance of plant - Power block (as % of cost of TG set): 50.0 %
- Thermal Storage**
  - Cost of thermal storage system: 1710.0 Rs/kWh-th
- Hybridization System**
  - Cost of thermic oil heater: 2.0 Rs Lakh per Lakh kcal/h
  - Cost of NG storage tank per m<sup>3</sup>: 5.0 Rs
  - Buffer storage of fuel (no. of days): 15.0
  - Cost of piping (as % of cost of Thermic oil heater): 40.0 %

**Figure 4.11: Capital costs tab**

As seen from Figure 4.11, the variables under ‘Thermal Storage’ and ‘Hybridization System’ are available for editing only for non-zero values of hybridization and thermal storage.

#### 4.4.4 O&M Expenses

O&M expenses of the plant include maintenance and replacement of mechanical, electrical and hybridization systems, water required for cooling, employee salaries, fuel used in case of hybridization etc.

The salaries are computed based on the number of people required at various levels to operate and maintain the plant. If thermal storage and hybridization are considered, a slight increase in number of personnel is needed. The expenses towards this are accounted for, by increasing the expenses towards salaries by a certain percentage.

The subsection ‘Equipment Maintenance’ provides a default value as a percentage of each individual component costs. This tab also provides the inflation rates for all O&M components, which need to be taken into consideration over the duration of plant life. Figure 4.12 shows the screen shot of the O&M expenses tab.

File Simulations Tools Help

Introduction Location Details Plant Details Capital Costs O & M Expenses Financial Parameters Simulation and results

**Salaries**

Staff	Number required	Cost to company (Rs Lakh-per person per annum)
Systems engineers	6	4.0
Plant operators	8	2.5
Administrators	4	1.8
Plant maintenance personnel	8	1.2
Security staff	6	1.0

Percentage increase in salaries due to inclusion of thermal storage  Percentage increase in salaries due to inclusion of hybridization

**Equipment Maintenance**

Component	O & M (% Component cost)
Mirror	2.0
Steel structure	1.5
HCE	2.5
HTF	1.0
HTF system	2.0
Hydraulic trackers	0.5
Swivel joints	1.0
Electronics, Control & Electrical	2.0
Thermal storage	2.5
Power block	2.0
Hybridization system	2.5

**Hybridization Fuel**

Cost of fuel  Rs/m<sup>3</sup>

**Water**

Water cost  Rs/m<sup>3</sup>

Water requirement per MWh  m<sup>3</sup>/MWh

**Insurance**

Insurance (as % of DCC \*)  %

\*DCC - Direct Capital Cost

**Inflation Rates**

Salary  %

Equipment maintenance  %

Water  %

Insurance  %

Fuel  %

Figure 4.12: O&M expenses tab

#### 4.4.5 Financial Parameters

The financial parameters tab shown in Figure 4.13 contains values for financial metrics for the calculation of LCOE and IRR. The input variables under this tab are categorized into:

- Financing - Finance parameters related to the project
- Return on equity - Return expected on the equity portion.
- Depreciation rate – Depreciation during loan and post loan term.
- Tariff - Expected tariff per unit of electrical energy supplied to the grid.

File Simulations Tools Help

Introduction Location Details Plant Details Capital Costs O & M Expenses Financial Parameters Simulation and results

**Financing**

Debt percentage  %

Equity percentage  %

Plant life  years

Moratorium  years

Loan rate  %

Loan tenure  years

**Return on Equity**

During loan term  %

For rest of plant life  %

**Depreciation Rate**

During loan term  %

For rest of plant life  %

**Tariff**

Tariff per kWh  Rs

Figure 4.13: Financial parameters tab

#### 4.4.6 Simulation and Results

In this tab, options of executing a simulation, saving results and clearing results are available. For running a particular simulation, click the button “Run Simulation”. The “Clear Simulation” button clears any existing results from previous simulation. The function of “Save Results” is described below.

##### **Saving the results of simulation:**

Whenever any simulation, either base case simulation or parametric simulation is executed, an excel workbook for each SM containing all the inputs and outputs is generated and stored in temporary memory. Upon selection of ‘Save Results’ user is shown a window to save the results where all the excel sheets pertaining to the latest simulation are saved. One important point to be noted is that, if the user clicks ‘Clear Simulation’ button before saving the results, all the results stored in the temporary memory will be deleted and ‘Save Results’ button is disabled.

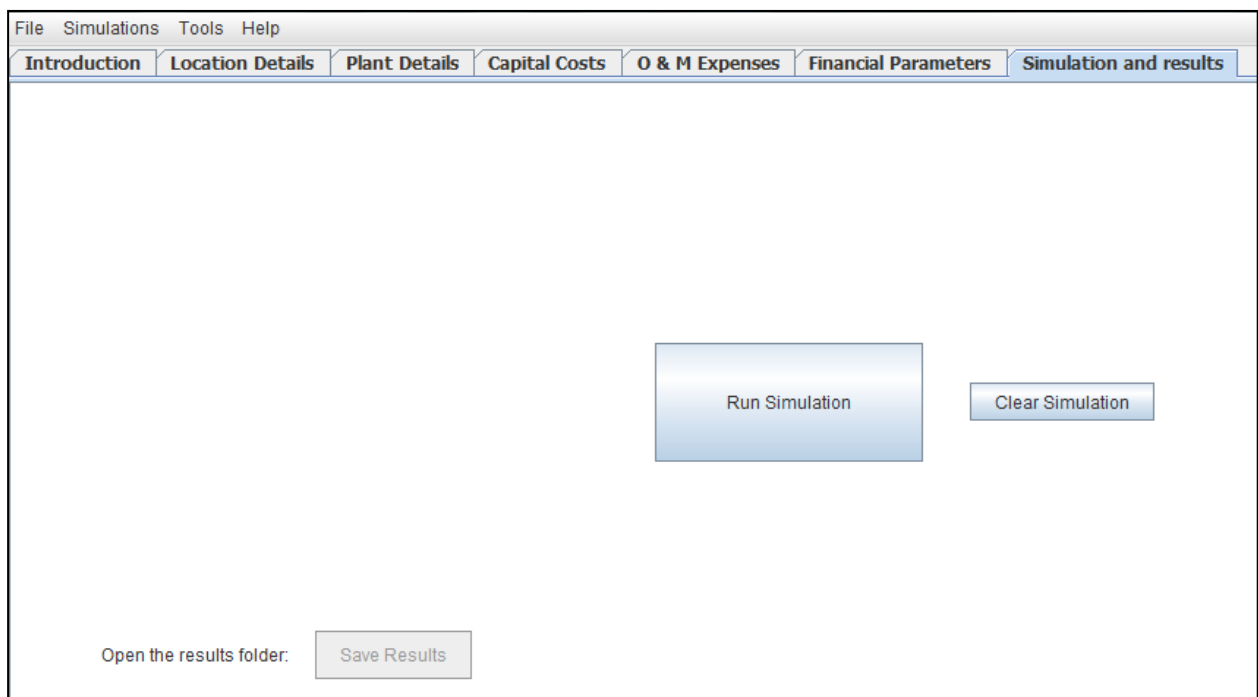


**Figure 4.14: Simulation and results tab**

#### 4.5 Output Tabs

After completion of a simulation, the user is prompted with the ‘Outputs Tab’. There are several tabs under the output section as mentioned earlier:

All the output variables are segregated into various tabs depending on the information they convey. All the variables under different tabs of outputs are non-editable and just display the value for that particular variable. A detailed explanation of each tab is given below:

## 4.5.1 Summary

The summary tab gives the overview of the results of the latest simulation executed. It presents the important inputs chosen for the simulation, energy outputs, solar field related terms, financial metrics and LCOE values.

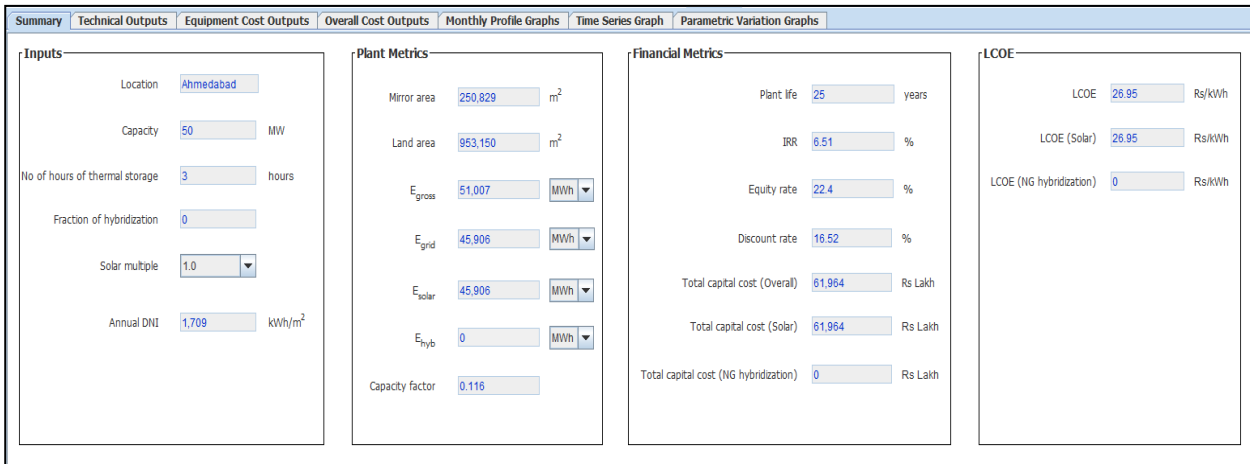


Figure 4.15: Summary tab

## 4.5.2 Technical Outputs

As shown in Figure 4.16, the technical outputs tab provides the user with the detailed technical information about various major components like solar field, hybridization and energy related information.

The solar field details contain important variables like reference aperture area, amount of energy transferred between components of solar field and heat exchangers, thermal storage details and land area required. The hybridization subsection gives information on capacity of thermic oil heater, annual thermal energy transferred from thermic oil heater, volume of fuel used and volume of buffer storage tank.

The energy related variables give information about annual energy produced by the solar field, by hybridization and annual energy transferred to the grid.

Under this tab, values of the variables like land area, capacity of thermic oil heater and annual energy from thermic oil heater are provided with a drop down menu permitting change in units of measurement.

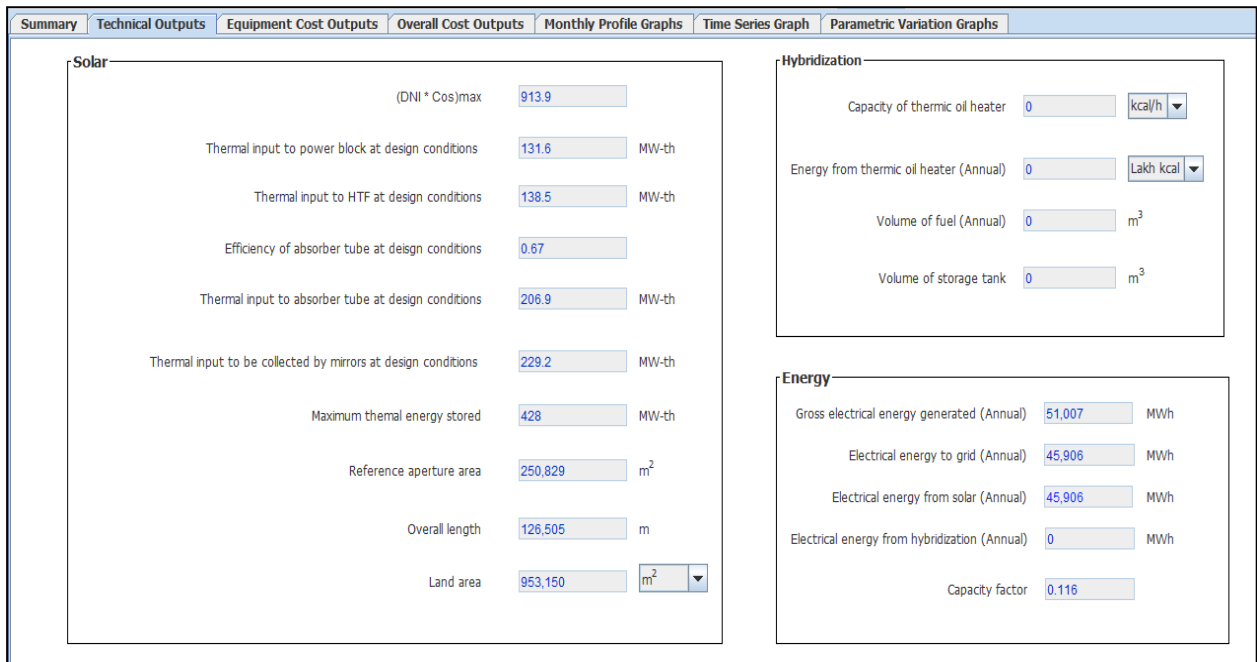


**Figure 4.16: Technical outputs tab**

### 4.5.3 Equipment Cost Outputs

This tab gives detailed cost information about solar field, land, hybridization components and thermal storage and power block. All these costs constitute direct capital costs.

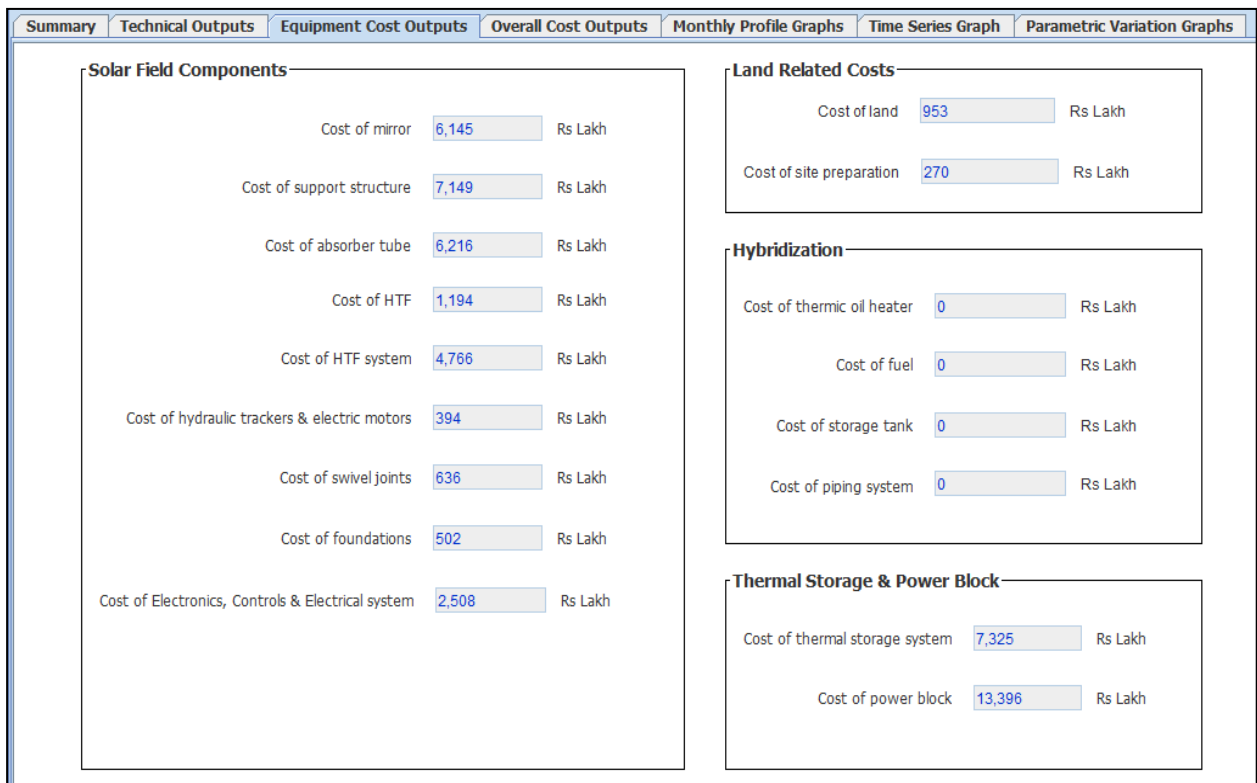


**Figure 4.17: Equipment cost tab**

### 4.5.4 Overall Costs

This tab gives information about various costs contributing to indirect capital costs. It displays the overall costs by taking into account DCC as well. The LCOE and IRR computed are also displayed (Figure 4.18).

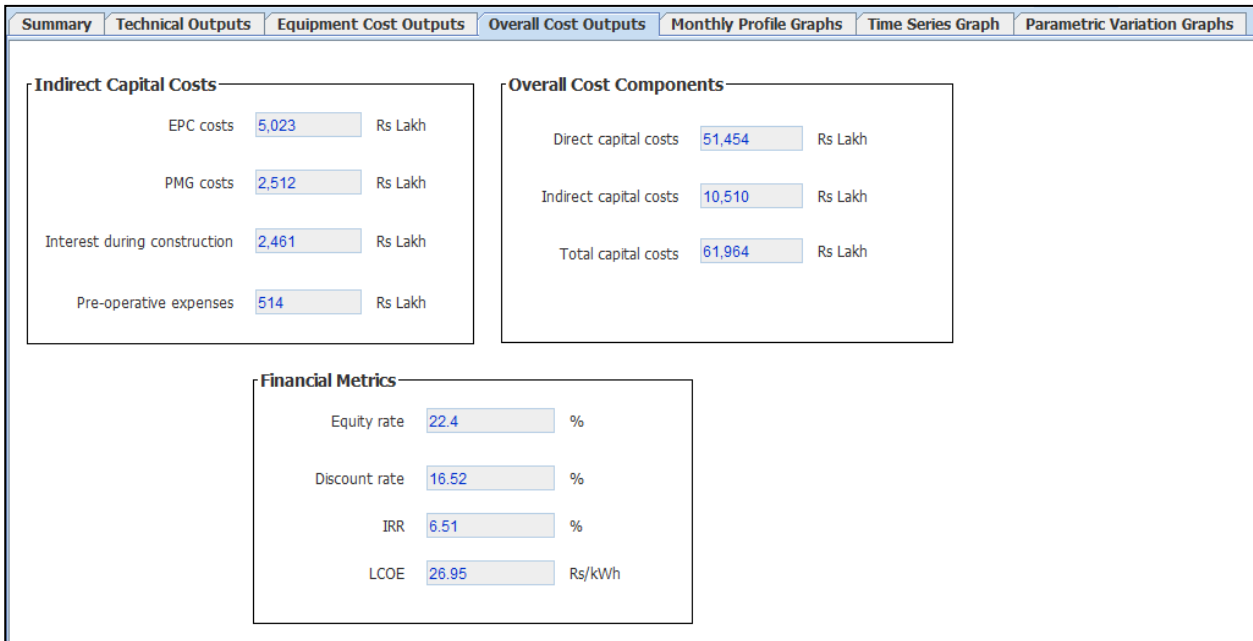
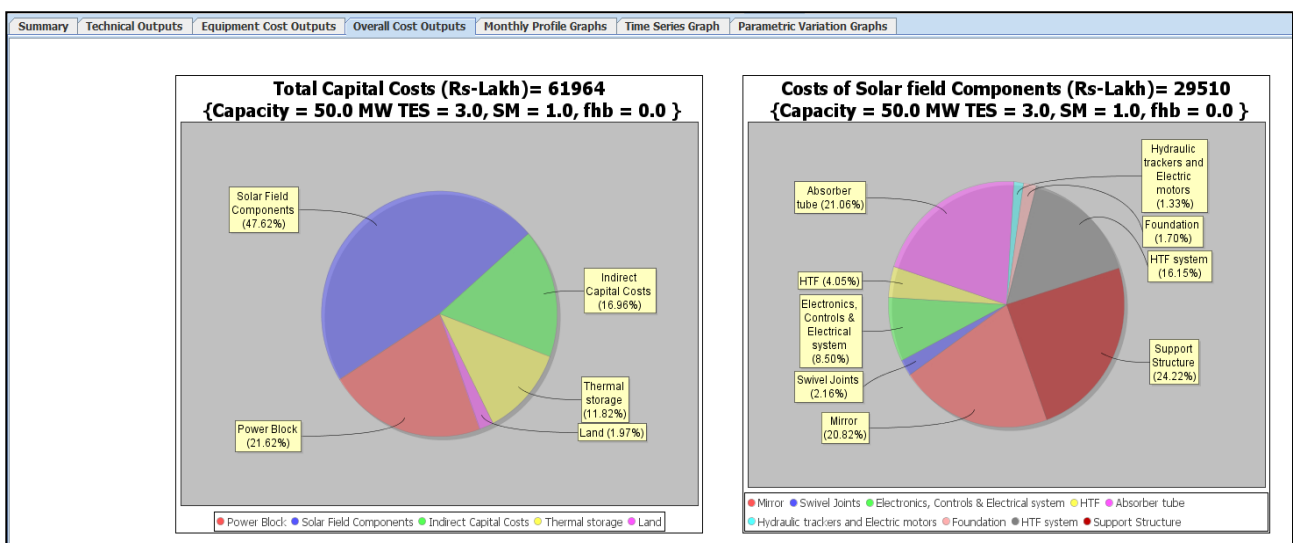


Figure 4.18: Overall costs tab

This tab also provides pie charts (Figure 4.19) for the user to visualize the costs for various important components. The pie chart titled 'Total Capital Costs' gives the percentage break-up of various components of the capital costs. A split up of the solar field costs is also given as a pie chart titled 'Cost of solar field components'.



Total Capital Costs

Solar Field Costs

Figure 4.19: Other costs tab

### 4.5.5 Monthly Profile Graphs

This tab provides the user with the option of viewing hourly variation of monthly average gross energy generated or net energy supplied to the grid (Figure 4.20). These data can be also stored in an excel file.

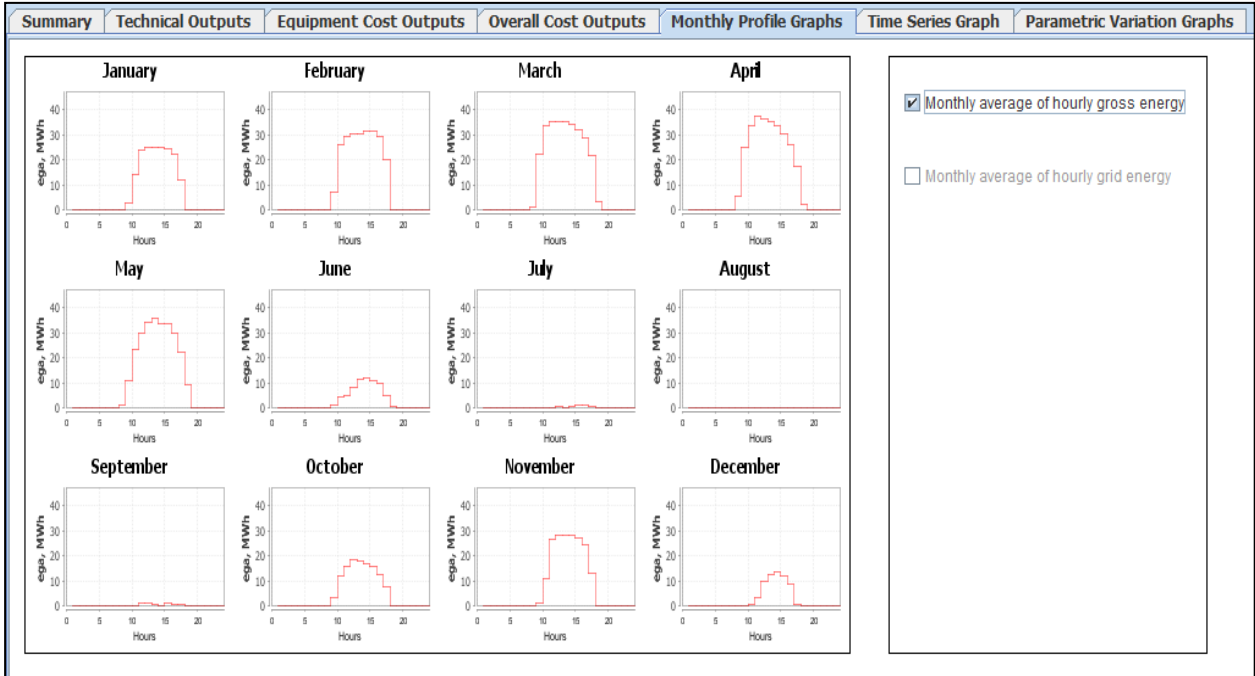


Figure 4.20: Monthly profile graphs tab

### 4.5.6 Time Series Graph

Time series graphs (Figure 4.21) provide the user with the information of hourly energy generated over the year. The graphs under this tab are also step graphs and provide the user with the option of saving the graph data in excel. The step nature of the graph becomes apparent when the portion of a graph is zoomed in (Figure 4.22).

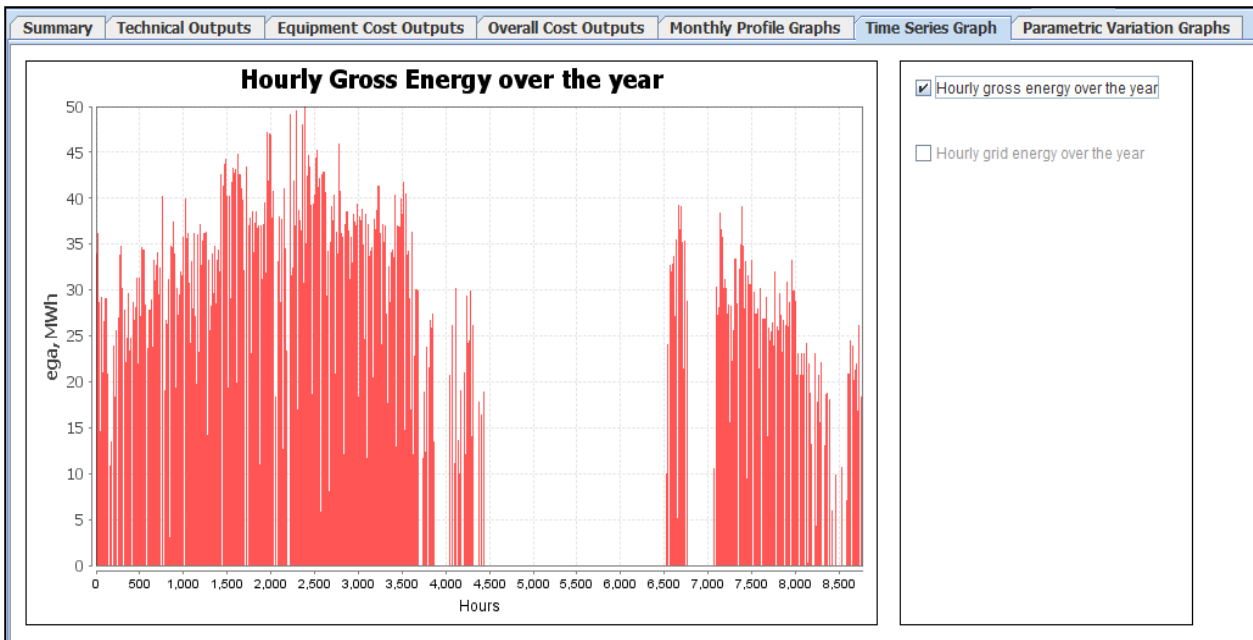


Figure 4.21: Time series graph tab

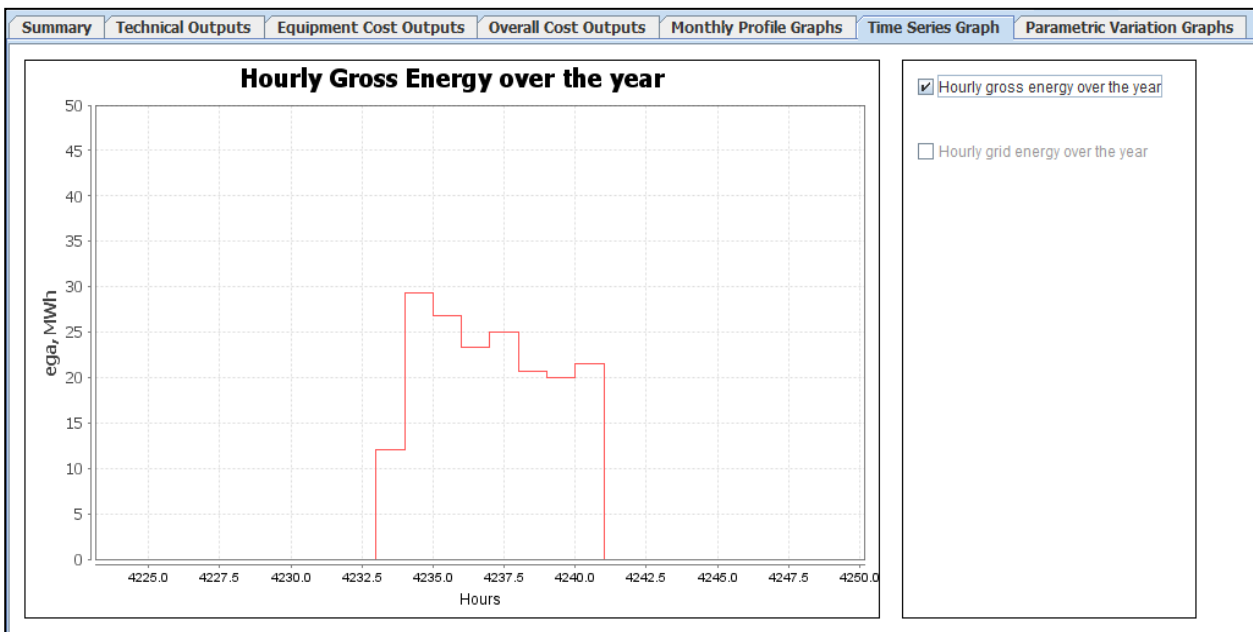


Figure 4.22: Zoomed in step graph

### 4.5.7 Parametric Variation Graphs

If the simulation is a base case simulation then parametric variation graph tab is not shown under outputs tab. If the simulation is a parametric simulation then this tab is enabled under outputs tab.

This tab plots two important parameters namely LCOE and IRR for various SMs chosen by the user as shown in Figure 4.23. From this graph user can determine the least LCOE and find the corresponding SM and IRR. The SM for which the LCOE is least is called the optimum solar multiple. It is found that the SM for which LCOE is least gives the highest IRR.

The graph displayed under this tab provides the user with the option of saving the graph data to excel.

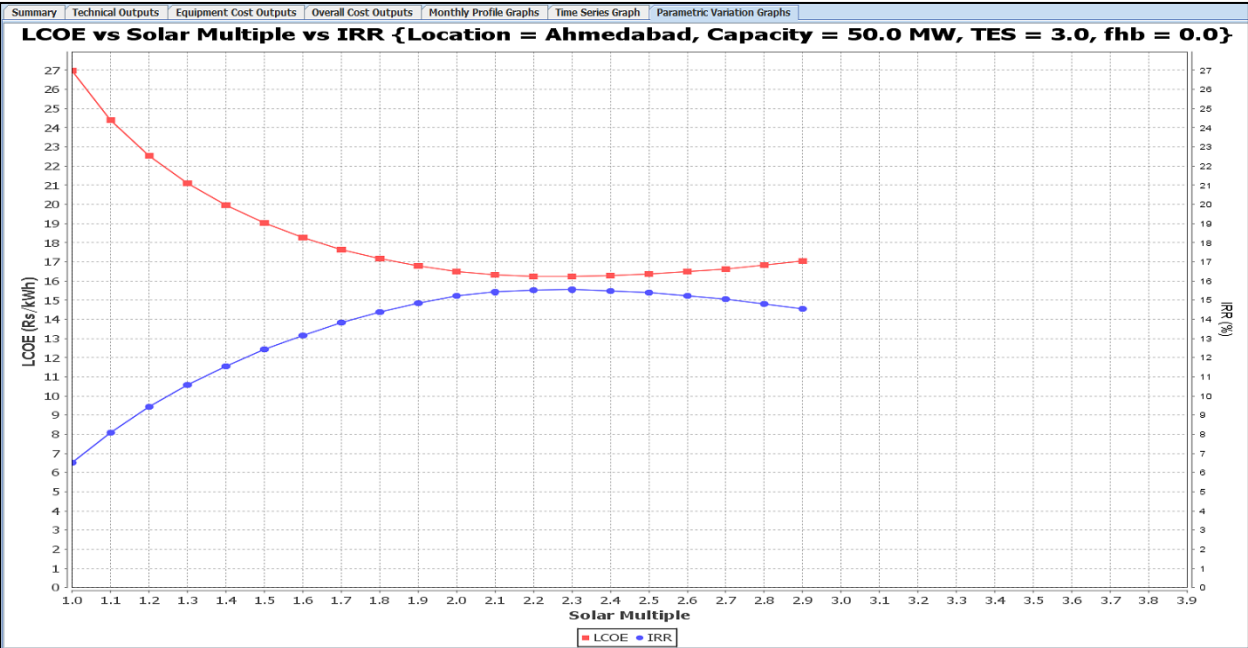


Figure 4.23: Parametric variation graphs tab

# 5 Sensitivity Analysis of PT Plant Parameters

## 5.1 Introduction

Sensitivity analysis shows how sensitive an output metric is to variations in the input values. This kind of analysis helps in making decisions on important parameters of the project.

As the number of output and input parameters is large, there could be several sensitivity studies. Here we have limited the sensitivity analysis to a 50 MW plant with three hours of thermal storage and without hybridization. The sensitivity analyses that have been carried out are with respect to:

- a) Capital cost, LCOE and IRR due to variation in efficiency of power block.
- b) LCOE and IRR in relation to capital cost and loan rate.
- c) Capital cost, capacity factor, LCOE and IRR with respect to deviations from optimum value of SM.

## 5.2 Sensitivity to Power Block Efficiency

For the chosen 50 MW plant, the efficiency of the power block is 38% (Figure 3.3). The power block efficiency was varied by 5% on either side of this reference value and its impact on capital costs, LCOE and IRR are determined. The results are presented in Table 5.1 and shown in Figure 5.1, Figure 5.2 and Figure 5.3.

**Table 5.1: Sensitivity of capital costs, LCOE and IRR to efficiency of power block**

$\eta_{p,d}$ as % of reference value	$\eta_{p,d}$ (%)	Capital Cost		LCOE		IRR	
		(₹-crore)	% change from reference value	(₹/kWh)	% change from reference value	(%)	% change from reference value
-5.0	36.1	1110	+4.46	14.79	+4.15	17.53	-5.24
0	38	1062	0	14.2	0	18.5	0
+5.00	39.9	1020	-4.04	13.63	-4.01	19.41	+4.92

From Table 5.1 we see that a 5% increase/decrease in the efficiency of power block results in:

- Capital cost decreases/increases approximately by 4.25%. This change in the capital costs can be attributed to the fact that as efficiency of the power block increases, the size of solar field decreases.
- LCOE decreases/increases approximately by 4.1%. This change is directly attributable to the change in capital costs.
- IRR increases/decreases approximately by 5%.

From the above we infer that the efficiency of power block has a significant effect on the capital cost and hence on LCOE and IRR. It should also be mentioned that the change in efficiency had hardly any effect on optimum value of SM.

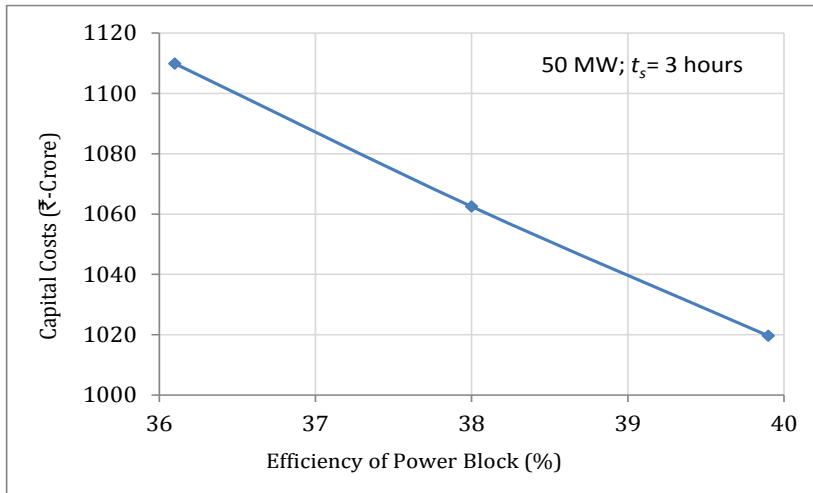


**Figure 5.1: Effect of efficiency of power block on capital cost**

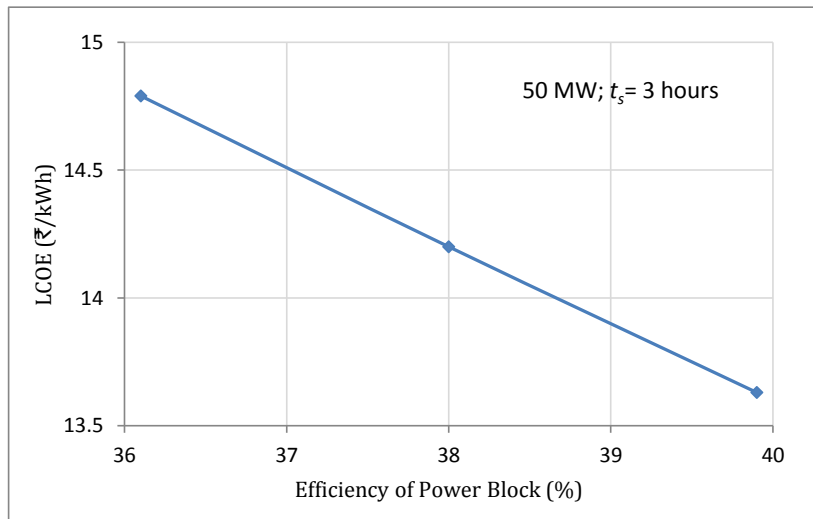


**Figure 5.2: Effect of efficiency of power block on LCOE**

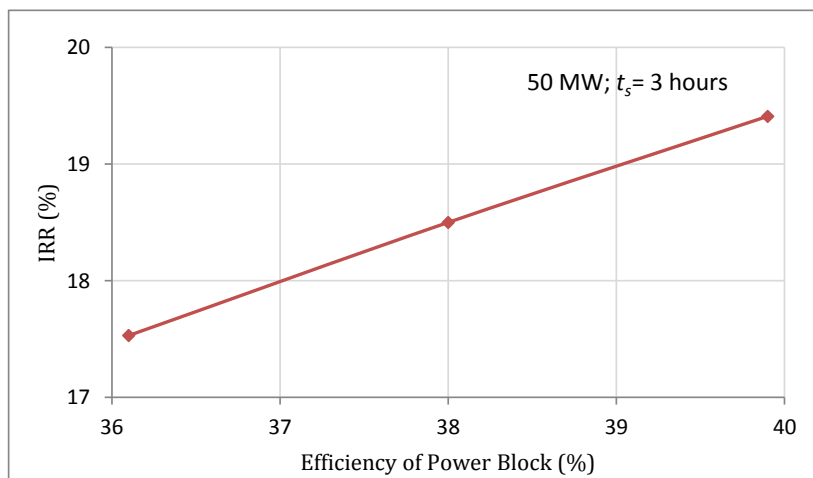


**Figure 5.3: Effect of efficiency of power block on IRR**

### 5.3 Sensitivity to Capital Cost

The capital cost is varied by 5% on either side of the reference value and its impact on LCOE and IRR are presented in Table 5.2 and shown in Figure 5.4 and Figure 5.5.

**Table 5.2: Sensitivity of LCOE and IRR to capital cost**

Capital cost as % change from reference value	Capital cost (₹-crores)	LCOE		IRR	
		(₹/kWh)	% change from reference value	(%)	% change from reference value
-5.0	1009	13.58	-4.37	19.52	+5.51
0	1063	14.2	0	18.5	0
+5.00	1116	14.78	+4.08	17.53	-5.24

From Table 5.2 we can see that for 5% increase/decrease in capital cost results in:

- LCOE increases/decreases approximately by 4.2%.
- IRR decreases/increases approximately by 5.4%.

From the above analysis we infer that IRR is slightly more sensitive to capital cost than LCOE. Here also, there was no effect on optimum SM.

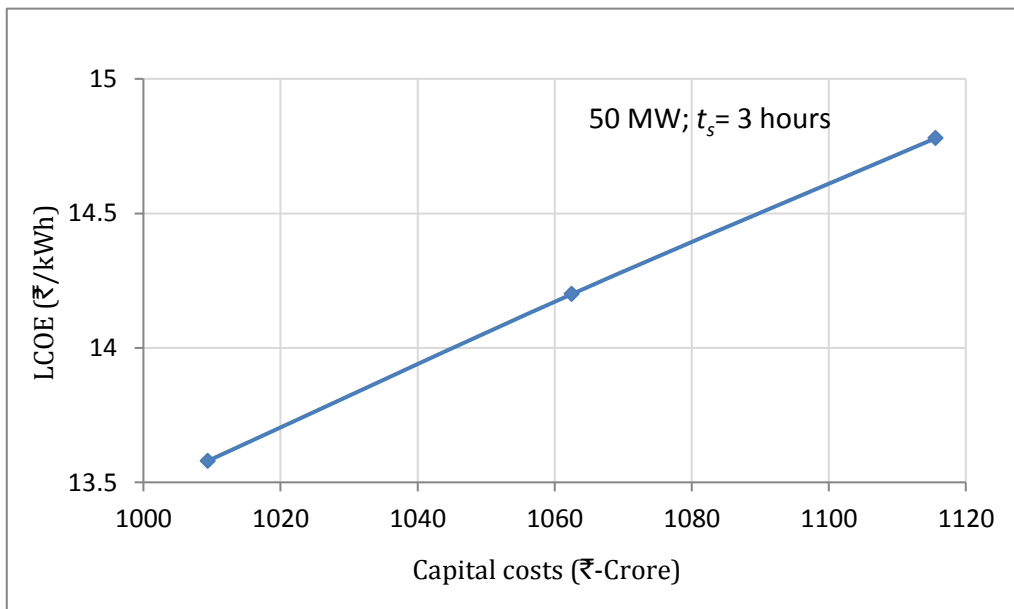


**Figure 5.4: Variation of LCOE with capital costs**

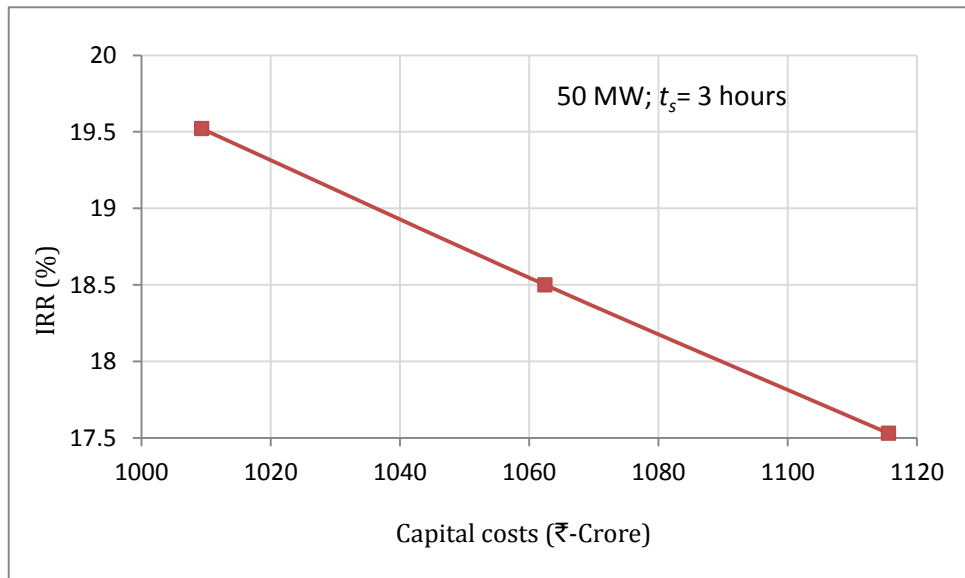


**Figure 5.5: Variation of IRR with capital costs**

## 5.4 Sensitivity to Loan Rate

Loan rate is one of the parameter which can vary considerably depending upon the source from where capital cost is borrowed. The loan rate has a direct impact on discount rate which affects the LCOE & IRR. The loan rate has been varied from 6% to 18% to see its effect on LCOE and IRR. Results are presented in Table 5.3 and Figure 5.6.

**Table 5.3: Sensitivity of LCOE and IRR to loan rate**

Loan rate (%)	Discount rate (%)	LCOE (₹/kWh)	IRR (%)
6	10.92	11.27	18.93
8	12.32	11.93	18.82
10	13.72	12.64	18.71
12	15.12	13.39	18.59
14	16.52	14.18	18.48
16	17.92	15.01	18.37
18	19.32	15.86	18.26

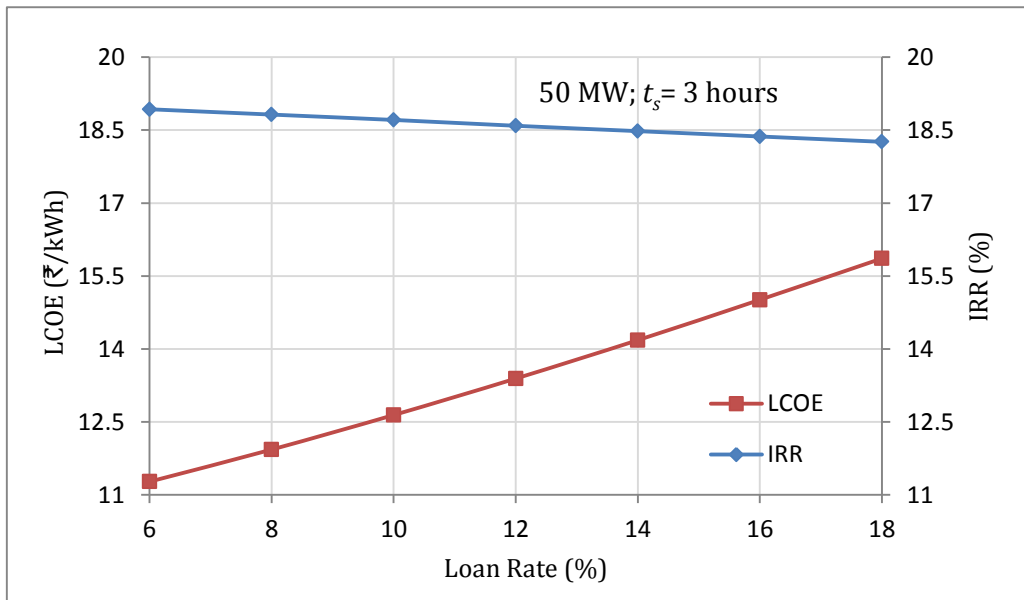


**Figure 5.6: Variation of LCOE & IRR with loan rate**

From the results one can infer that the LCOE is sensitive to loan rate whereas its effect on IRR is marginal. It was found that there was no change in optimum SM.

LCOE changes from ₹ 11.27 to ₹ 15.86 per kWh for a change in loan rate from 6 to 18%. The variation is slightly non-linear, but as an approximation one can state that for every 1% change in loan rate, LCOE changes approximately by 0.38 ₹/kWh.

## 5.5 Sensitivity to Assumed Tariff

Assumed tariff is the rate at which energy is sold to the grid. The assumed tariff is varied from ₹ 9 to ₹ 18 per kWh to see the effect on IRR. Results are presented in Table 5.4 and Figure 5.7.

**Table 5.4: Sensitivity of IRR to assumed tariff**

Assumed Tariff (₹/kWh)	IRR (%)
9	8.83
12	13.85
15	18.48
18	22.92

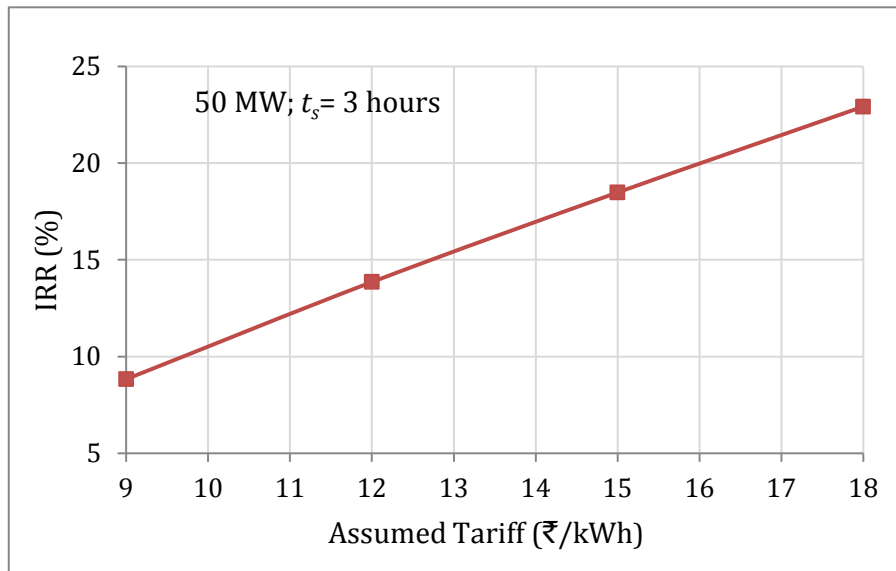


**Figure 5.7: Variation of IRR with assumed tariff**

From the results it is seen that for a change in tariff from 9 to 18 ₹/kWh, IRR varies from 8.8% to 22.9%. The variation is slightly non-linear, but as an approximation one can state that for every change of Re 1 per kWh in tariff, IRR changes approximately by 1.56%.

## 5.6 Deviation from Optimum SM

The variation of LCOE and IRR with SM in the vicinity of optimum SM is found to be very small (section 3.5.1). Thus, one has a freedom to choose values of SM near the optimum value. Therefore, the effect of deviation of 5% in SM from optimum value of 2.1 on capital cost, capacity factor, LOCE and IRR is carried out. The results are presented in Table 5.5 and Figure 5.8 and Figure 5.9.

**Table 5.5: Sensitivity of parameters to deviation of SM from optimum**

SM as % of reference value	SM	Capacity Factor		Capital Costs		LCOE (₹/kWh)	IRR (%)
		(Value)	as % change from reference value	(₹-crore)	as % change from reference value		
-5.0	1.995	0.367	-4.18	1022	-3.82	14.22	18.42
0	2.100	0.383	0	1063	0	14.20	18.5
+5.0	2.205	0.396	+3.39	1103	+3.82	14.22	18.42

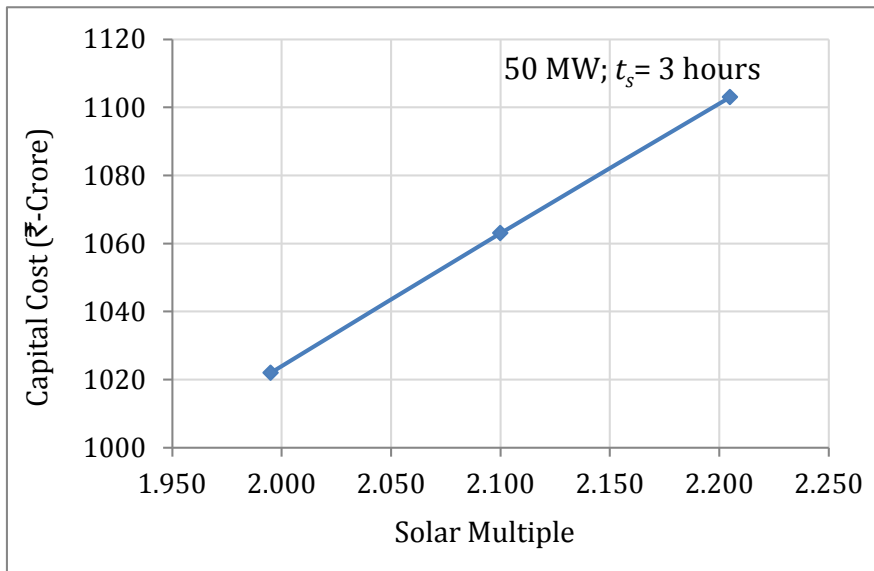


**Figure 5.8: Variation of capital cost for deviation with optimum SM**

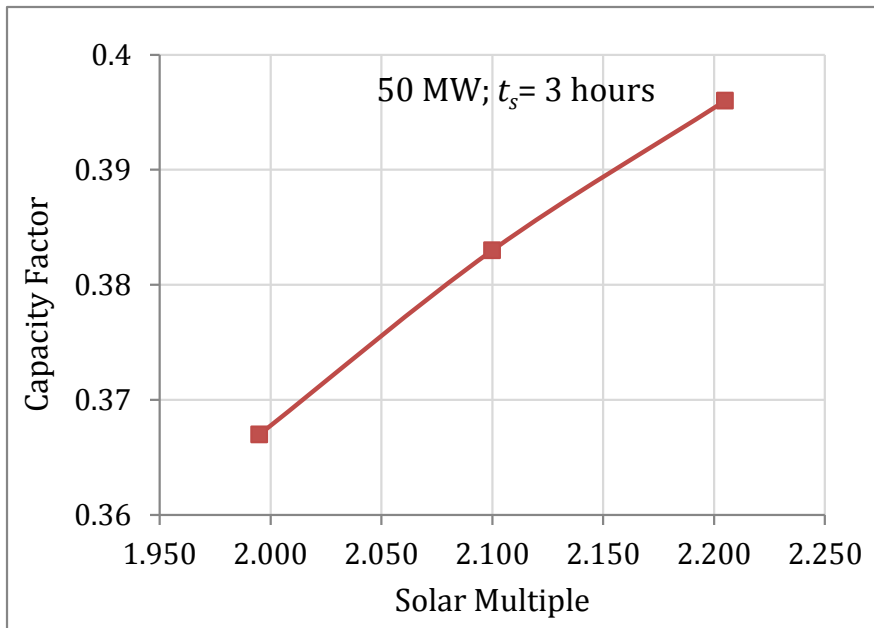


**Figure 5.9: Variation of capacity factor with deviation from optimum SM**

## **6 Techno Economic Viability of Solar Tower Technology in India**

### **6.1 Introduction**

As mentioned in chapter 2 the CSP plants using ST, though not in operation to the same extent as PT (PT-1168 MW, ST-60 MW), seem to have gained momentum. More ST plants are under construction (2011 MW) than PT plants (1377 MW). In view of this an assessment of the techno-economic viability of this technology is relevant for India.

However, the design variations in presently operating ST plants are wide in terms of HTF, receivers and power cycle employed. The choice of the type of ST system most suited technically and economically, under Indian conditions is discussed. Then, a methodology for the techno-economic assessment for the chosen type of ST technology is presented. LCOE and IRR are computed adopting the procedure given in chapter 3 for PT.

### **6.2 Choice of Type of ST Technology in India**

We shall now discuss the pros and cons of the various types of ST technology in use so as to arrive at the most suitable technology that can be adopted in India.

#### **6.2.1 Direct Steam Generation with Rankine cycle**

DSG with super-heated steam has not reached the stage of commercial maturity and hence all existing plants are using saturated steam only. Also, with DSG, it is extremely difficult to have reasonable extent of thermal storage. The main advantage of CSP over a PV system is its ability to have thermal storage. If that advantage is not utilized, then one can as well use a PV system which is cheaper and simpler. Therefore a ST system using DSG is not recommended.

#### **6.2.2 Air as HTF Coupled with Brayton Cycle**

In principle, using air heated up to 1000°C as HTF in a gas turbine Brayton cycle having a high efficiency is very attractive. However, heat transfer co-efficient of air being low, design of a suitable volumetric receiver is still in R&D stage and is not a proven technology. Therefore, though this type of technology needs to be pursued in a R&D mode, it cannot be considered for immediate large scale utilization.

#### **6.2.3 Molten Salt as HTF with Rankine Cycle**

ST technology using molten salt as HTF has been a commercial success and many plants of this type are coming up on a large scale globally. A schematic arrangement of this system is shown in Figure 6.1 ([www.solarpaces.org/CSP\\_Technology/docs/solar\\_tower.pdf](http://www.solarpaces.org/CSP_Technology/docs/solar_tower.pdf)). The advantages of this technology are given below:

- a) Since molten salt is used as HTF, one can reach temperatures of HTF up to 560°C.
- b) Molten salt solidifies at 220°C. So using molten salt as HTF in PT technology poses problems of draining it from long receiver tubes, when not in operation. On the other hand, the

receivers in case of ST technology, are compact and located high above. So draining the HTF in the receiver to the storage tanks below, by gravity, is much simpler.

- c) Using molten salt as HTF, permits it to be used as a storage medium also, so the additional heat exchanger between the synthetic oil and molten salt, which is needed in PT technology, when molten salt thermal storage system is used is avoided.
- d) Superheated steam at high pressure and temperature up to 540°C can be generated resulting in high Rankine cycle efficiency.
- e) Since the inlet temperature is high, the adverse effect of air cooling option is less for ST. Hence, where water availability is scarce, ST technology is better suited.
- f) The large difference in operating temperatures of 270°C (560°C – 290°C) for ST compared to only 100°C (390°C - 290°C) for PT, results in lesser quantity of molten salt to be used in thermal storage for the same stored thermal energy. So cost of thermal storage system is less.

In view of the above advantages and the global trend of utilization of this technology, it is recommended that this type of ST technology be seriously considered for large scale utilization in India. Therefore an assessment of the techno-economic viability of this type of ST technology for India is being attempted here.

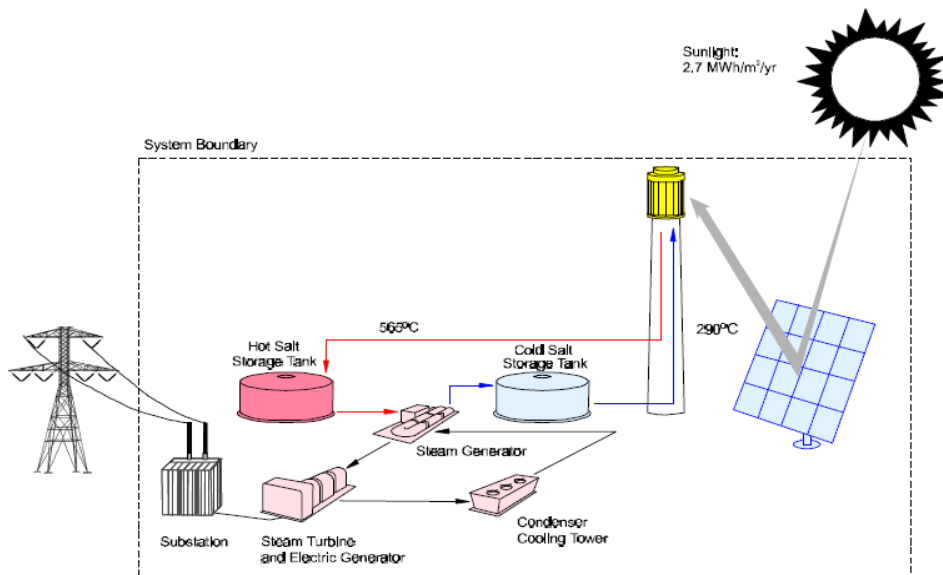


**Figure 6.1: Schematic of ST system**

### 6.3 Techno-Economic Assessment of ST Technology using Molten Salt as HTF

The gross capacity of the plant and the number of hours of thermal storage are the input parameters. Based on hours of thermal storage and data from operating plants the capacity factor is arrived at. Using this and the gross capacity the annual gross electricity generated is determined. Based on data from the existing ST plants (PS 10, PS 20 and Gemasolar), the efficiency of annual solar to electrical energy is approximated. This is used to determine the annual solar energy to be collected. Considering the annual solar resource ( $DNI_{annual}$ ), the size of the heliostat field is calculated. The land area is computed assuming a ratio of land area to heliostat field area (literature survey). The maximum thermal energy stored is determined, based on the gross capacity

of the plant, number of hours of storage and the efficiencies of the power block and power block heat exchanger.

Considering the gross capacity of the power block and using the technical assessment data the direct capital cost, indirect capital cost, O&M expenses, etc. of the CSP plant are estimated. LCOE and the IRR are computed adopting the procedure given in chapter 3 for PT.

### 6.3.1 Procedure to Determine Solar Field Area and Stored Thermal Energy

The design requirements are the gross capacity of the plant ( $P_{g,d}$ ) and the hours of the thermal energy storage ( $t_s$ ).

#### i. Input Parameters

The following input parameters needed to determine the heliostat field area ( $A_a$ ) and maximum thermal energy stored ( $E_{tes,max}$ ).

- a. Plant capacity,  $P_{g,d}$  (Watts)
- b. Hours of thermal energy storage,  $t_s$  (hours)
- c. Capacity factor,  $CF$
- d. Annual solar resource,  $DNI_{annual}$  (kWh/m<sup>2</sup>)
- e. Annual efficiency of solar to electric energy conversion,  $\eta_{s-e}$
- f. Efficiency of the receiver,  $\eta_r$
- g. Efficiency of power block at design conditions,  $\eta_{p,d}$
- h. Efficiency of power block heat exchanger,  $\eta_{he}$

#### ii. Computation of Heliostat Field Area

The following steps are adopted to estimate the heliostat field area:

- a. Annual gross electrical energy ( $e_{g,t}$ ) generated is estimated as,

$$e_{g,t} = P_{g,d} \times 8760 \times CF$$

- b. Annual solar energy ( $e_{solar}$ ) to be captured by the heliostat field,

$$e_{solar} = \frac{e_{g,t}}{\eta_{s-e}}$$

- c. The heliostat field area ( $A_a$ ) is estimated as,

$$A_a = \frac{e_{solar}/1000}{DNI_{annual}}$$

#### iii. Thermal Capacity of the Receiver

The thermal capacity of the receiver ( $P_{rec,th}$  in  $MW_{th}$ ) is given by

$$P_{rec,th} = \frac{P_{g,d}/10^6}{\eta_{p,d} \times \eta_{he} \times \eta_r}$$

#### iv. Stored Thermal Energy

The maximum capacity of thermal energy stored ( $E_{tes,max}$ ),

$$E_{tes,max} = \frac{P_{g,d} \times t_s}{\eta_{p,d} \times \eta_{he}}$$

where,  $E_{tes,max}$  is maximum thermal energy stored ( $Wh_{th}$ )

## 6.3.2 Inputs and Assumptions in Economic Assessment

### i. Direct Capital Costs (DCC)

The DCC of a CSP plant using ST technology, with thermal storage can be categorized as follows:

- Land & site preparation cost
- Solar Field cost
- Power Block cost
- Thermal Storage System cost

#### a. Land and site preparation cost

The land cost is taken as ₹ 100 per m<sup>2</sup>. The site preparation cost is ₹ 80 per m<sup>2</sup>, which is slightly less than that required for the PT systems since a land slope of up to 5° is acceptable for the ST system.

#### b. Solar Field cost

The solar field costs are broadly categorized into heliostat field costs and receiver & tower cost.

**Heliostat Field Cost:** The heliostat field cost comprises of various components such as mirror modules, drives, pedestal, mirror support structure, foundation, controls, wired connections, installation etc. All these costs vary based on the individual size of the heliostats installed. Heliostat field cost for larger size heliostats is lesser than that of the smaller size heliostats. It has been reported in the literature that the heliostat field cost for a 148 m<sup>2</sup> size heliostat is \$ 137/m<sup>2</sup> and for a 30 m<sup>2</sup> size heliostat is \$ 237/m<sup>2</sup> (IRENA, 2012; Gregory, Clifford, Thomas, & Jesse, 2011). For our cost analysis, an average value is taken as \$ 187/m<sup>2</sup>. i.e. ₹ 9350/m<sup>2</sup>.

**Receiver & Tower Cost:** The capital cost of the receiver and tower reported in the literature for various receiver thermal capacities is shown in Figure 6.2 (Gregory, Clifford, Thomas, & Jesse, 2011; Csaba, Reiner, Robert, & Hans, 2010; ECOSTAR, 2003). A second order polynomial fit for the data is given by

$$C_{RT} = 196.2 - 0.165 \times P_{rec_{th}} + 0.000095 \times P_{rec_{th}}^2$$

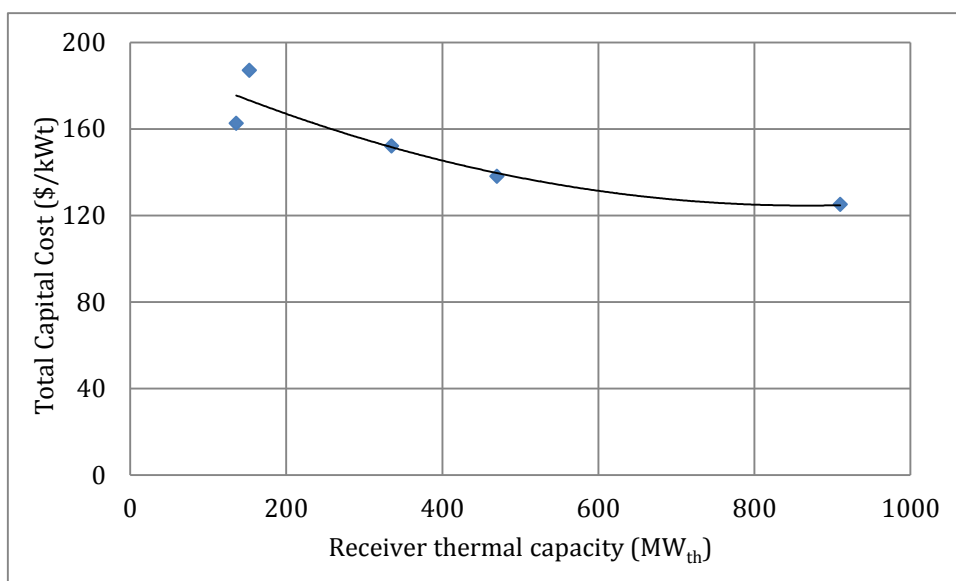


Figure 6.2: Capital cost for receiver and tower corresponding to receiver capacity

### c. Thermal Energy Storage System

The thermal energy storage system cost is approximated based on the two-tank molten salt storage system. This cost for the PT system is taken as ₹ 1710 per kWh<sub>th</sub> and it is approximated for the ST system as half of this cost. The reasons are mentioned below.

- In the PT system, HTF operating temperature is from about 290°C to 390°C. In ST system, molten salt operating temperature is from 290°C to 560°C. So for the same amount of thermal storage, the quantity of molten salt required is inversely proportional to temperature difference. So the amount of molten salt required in ST is less than half of that in PT.
- An additional heat exchanger to transfer the heat from HTF to molten salt as in case of PT is not required in ST.

Therefore, taking above considerations into account, the cost of storage for ST system is taken to be ₹ 855 per kWh<sub>th</sub>.

### d. Power Block Cost

Cost of power block and cost of Balance of Power for ST system are taken to be the same as that used in PT analysis, since, both are using same working fluid but the operating temperatures are more than that of PT. The variation of cost with design capacity is given by equation

$$\text{Cost of PB (Rs/kW)} = 55000 \times (\text{Capacity in MW})^{-0.288}$$

## ii. Indirect Capital costs

The methodology used for determining the components of ICC is identical to that used for PT analysis (Section 3.3.2).

## iii. O&M Expenses

The annual O&M expenses will vary from 2 to 3% of DCC. In the PT analysis, we have found O&M expenses are 2.7% of the DCC. We have assumed the O&M as 2.5% of DCC. It includes all the expenses for the plant operation and maintenance (salaries, equipment maintenance, water requirements and insurance).

## 6.4 Assessment of 50 MW ST Plant with 3 Hours of Thermal Storage

This section illustrates the application of the above methodology for an ST plant of 50 MW with 3 hours of thermal storage located at Jodhpur with an annual DNI of 1920 kWh/m<sup>2</sup>.

### 6.4.1 Determination of Various Technical Parameters

#### i. Capacity Factor

The capacity factor has to be estimated for the chosen hours of thermal storage. The variation of CF with storage hours for PT and ST technologies, from literature, is shown in Figure 6.3 (ITP, 2012). From this it is seen that the CF for PT and ST are of the same order. In our earlier analysis of PT, the CF for 3 hours thermal storage was computed as 0.37 which is higher compared to that shown in Figure 6.3. In order to compare the techno-economic assessment of ST with PT, it may be appropriate to take the CF value of ST to be also 0.37. However to be conservative the CF for ST is taken as 0.35 which is in between that computed for PT and that given in literature.

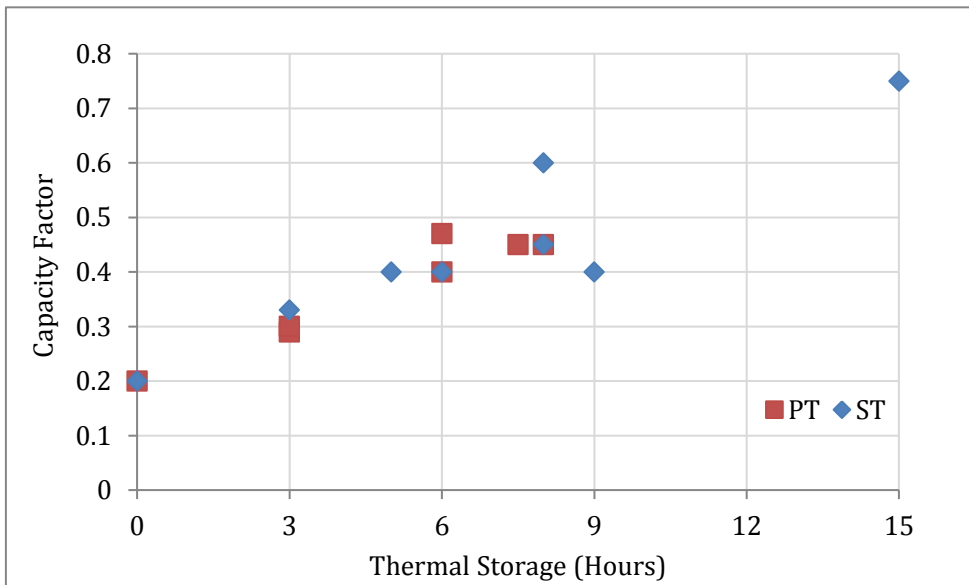


**Figure 6.3: Capacity factor with thermal energy storage for the ST system**

**ii. Annual Solar Resource**

We have considered Jodhpur as the location of the plant which has annual DNI of 1920 kWh/m<sup>2</sup>.

**iii. Solar to Electric Conversion Efficiency**

The overall efficiency of solar energy to electric energy is estimated for various ST plants based on the data of annual solar resource, solar field area and the expected electricity generation (Table 2.9). It can be observed that the efficiency varies from 15.4% to 17.3%. For the existing plants, the efficiency is roughly around 15% whereas for the plants under development it is around 17%. Therefore, the annual solar to electric efficiency is taken as 16% in the analysis.

**iv. Annual Gross Electrical Energy Generated**

The gross electrical energy generated by a 50 MW capacity plant with a 35% CF is 1,53,300 MWh.

**v. Annual Net Electrical Energy Generated**

It is assumed that the auxiliary power utilized is 10% of the gross power. Thus the net electrical energy generated is 0.9 times of the gross electrical energy generated, i.e., 1,37,970 MWh.

**vi. Annual Solar Energy to be Collected**

$$e_{solar} = \frac{153300}{0.16} = 958125 \text{ MWh}_{th}$$

**vii. Heliostat Field Area**

Taking annual solar resource as 1920 kWh/m<sup>2</sup>, the aperture area required is given by

$$\text{Heliostat Field area, } A_a \text{ (m}^2\text{)} = \frac{958125 \times 1000}{1920}$$

$$A_a = 499023 \text{ m}^2$$

### viii. Land Area

It is assessed in Section 2.3 that the ratio of land area to mirror area is about 6. Therefore, land area is 29,94,141 m<sup>2</sup> (299 hectares).

### ix. Thermal Capacity of Receiver

A 50 MW plant with  $\eta_{p,d}$  of 0.42,  $\eta_{he}$  of 0.95 and external cylindrical receiver efficiency  $\eta_r$  of 0.83 (William & Michael, 2001), requires a receiver thermal capacity

$$P_{rec\_th}(MW_{th}) = \frac{P_{g,d}/10^6}{\eta_{p,d} \times \eta_{he} \times \eta_r} = \frac{50/10^6}{0.42 \times 0.95 \times 0.83} = 153 MW_{th}$$

### x. Stored Thermal Energy

The efficiency of the power block for the ST system is taken to be 0.42, slightly more than PT system since the operating temperatures of the power block for the ST is about 540°C. The efficiency of the power block heat exchanger is taken to be 0.95, same as that of PT. Thus for  $t_s = 3$  hours, the stored thermal energy is 3,75,940 kWh<sub>th</sub>.

## 6.4.2 DCC, ICC & O&M Expenses

### i. Direct Capital Costs

#### a. Cost of land & site preparation

$$\text{Cost of Land} = \text{Land Area (m}^2\text{)} \times \text{Cost/m}^2$$

$$= 29,94,141 \times 100 \text{ ₹/m}^2 = 2994 \text{ ₹-lakhs}$$

$$\text{Cost of Site preparation} = \text{Land Area (m}^2\text{)} \times \text{Cost of site preparation/m}^2$$

$$= 29,94,141 \times 80 = 2395 \text{ ₹-lakhs}$$

#### b. Cost of solar field

*Cost of Heliostat:*

$$\text{Cost of Heliostat} = \text{Mirror Area} \times \text{Cost /m}^2$$

$$= 4,99,023 \times 9350 = 46,659 \text{ ₹-lakhs}$$

*Cost of Receiver and Tower:*

The cost of the receiver and tower (in \$/kW<sub>th</sub>) is given by

$$C_{RT} = 196.19 - 0.165P_{rec\_th} + 10^{-4}P_{rec\_th}^2$$

Thus for  $P_{rec\_th}$  of 152.8 MW<sub>th</sub>,  $C_{RT}$  is equal to \$173/ kW<sub>th</sub>

Therefore cost of receiver and tower =

$$(173 \times 50 \times 152.8 \times 10^3)/10^5 = 13,219 \text{ ₹-lakhs}$$

The cost of solar field = 46,659 + 13,219 = 59,878 ₹-lakhs.

#### c. Cost of power block of 50 MW capacity

$$= P_{g,d} \times 1000 \times 26,792 \text{ ₹/kW} = 13,396 \text{ ₹-lakhs}$$

#### d. Cost of thermal storage system

$$= E_{tes,max}(kWh_{th}) \times \frac{\text{Cost}}{kWh_{th}} = \frac{3,75,940 \times 855}{10^5} = 3214 \text{ ₹-lakhs}$$

Therefore, the total DCC is 81,877 ₹-lakhs.

## ii. Indirect Capital Costs

Following the same procedure as indicated in section 3.3.2, ICC is 16,040 ₹-lakhs.

## iii. O&M Expenses

Here O&M expenses are taken to be 2.5% of the DCC. So it is 2046 ₹-lakhs.

### 6.4.3 LCOE & IRR

Using the same procedure as for PT for computing LCOE and IRR based on DCC, ICC, O&M expenses and financial assumptions (same as in PT analysis), the LCOE is 14.17 ₹/kWh and IRR is 18.48%.

### 6.4.4 Comparison of ST with PT of 50 MW with 3 Hours Storage

The techno-economic comparison of ST with PT is shown in Table 6.1.

**Table 6.1: Comparison of 50 MW ST system and PT analysis**

Technical Parameters	ST	PT
Gross Capacity, MW	50	50
Hours of thermal Storage, hour	3	3
Capacity Factor	35%	38.30%
Solar Resource, kWh/m <sup>2</sup> /year	1920	1920
Annual Solar to Electric Efficiency	16%	15.8%
Solar Field Area, m <sup>2</sup>	499023	551760
Ratio of land to mirror area	6	3.8
Land Area, ha	287	210
Gross Electricity Generated, MWh	153300	1,67,616
Net Electricity to grid, MWh	137970	1,50,855
<b>Component Costs</b>		
Heliostat Field Cost, ₹/m <sup>2</sup>	9350	11765
Receiver and Tower, ₹/m <sup>2</sup>	8650	-
Power Block Cost, ₹/kW	26792	26792
Thermal Storage Cost, ₹/kWh <sub>th</sub>	855	1710
<b>Overall Costs</b>		
Land Cost, ₹-lakhs	2994	4361
Direct Capital Cost (DCC), ₹-lakhs	81877	88,325
Indirect Capital Cost (ICC), ₹-lakhs	16040	17,925
O&M Expenses, ₹-lakhs	2046	2403
Capital Cost, ₹-lakhs	97917	106250
Capital Cost per MW, ₹-crores	19.58	21.25
LCOE, ₹/kWh	14.17	14.2
IRR, %	18.48	18.5

Based on the assumptions, it may be seen that ST looks competitive with PT systems. In our assessment ST system is more amenable for indigenization when compared to PT. Therefore, it is worthwhile to consider this option for large scale utilization in India.

## 6.5 Sensitivity Analysis for ST Plant Parameters

In the previous section, we have done a techno-economic assessment of a 50 MW ST plant with three hours of thermal energy storage. As, there are considerable uncertainties in the inputs used in the analysis, we have attempted a sensitivity analysis to understand the sensitivity of CC, LCOE and IRR to the following input parameters.

- i. Percentage variation of capital cost
- ii. Tariff (₹/kWh)
- iii. Annual solar to electric efficiency ( $\eta_{s-e}$ )
- iv. Percentage variation of solar field cost

It may be note that, the above listed parameters are varied one at a time, the other parameters being held at their reference values used in section 6.4.

### 6.5.1 Sensitivity to Capital Cost

The capital cost is varied by 5% from reference value and its impact on LCOE and IRR are presented in Table 6.2 and shown in Figure 6.4 and Figure 6.5.

**Table 6.2: Sensitivity of LCOE & IRR to capital cost**

Capital cost as % change from reference value	Capital cost (₹ crores)	LCOE		IRR	
		(₹/kWh)	% change from reference value	(%)	% change from reference value
-5.0	930	13.47	-4.94	19.66	+6.39
0	979	14.17	0	18.48	0
+5.00	1028	14.86	+4.87	17.4	-5.84

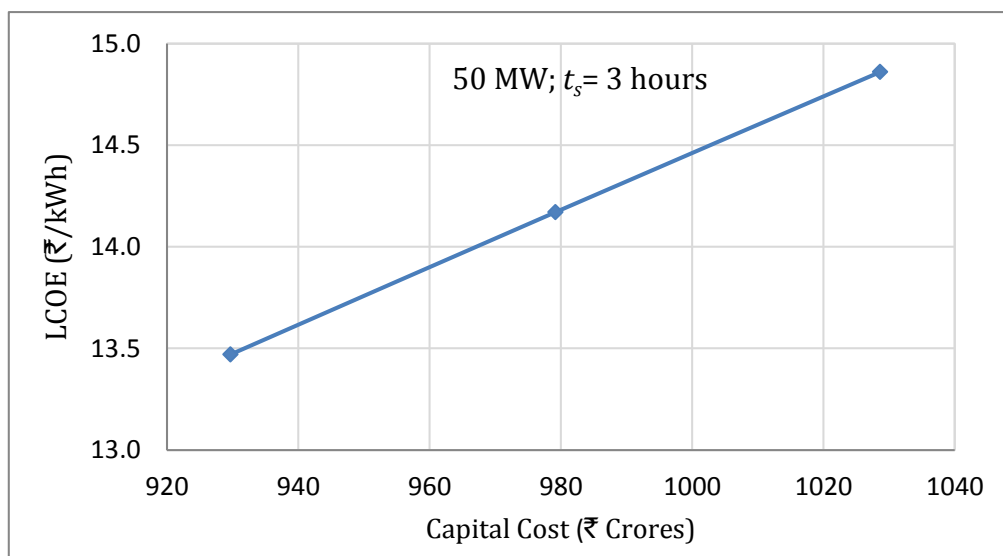


**Figure 6.4: Variation of LCOE with capital costs**

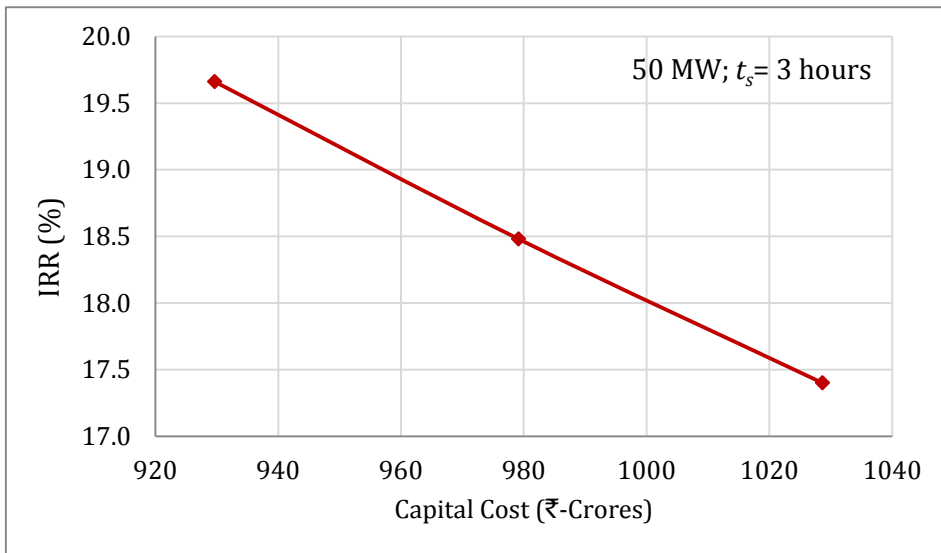


**Figure 6.5: Variation of IRR with capital costs**

From Table 6.2 it is seen that a 5% increase/decrease in capital cost results in:

- LCOE increases/decreases approximately by 4.9%
- IRR decreases/increases approximately by 6.1%

From the above analysis, we infer that the IRR is slightly more sensitive to CC than LCOE.

## 6.5.2 Sensitivity to Tariff

### i. Impact on CC

CC is independent of tariff. Hence, tariff has no impact on CC.

### ii. Impact on IRR

Figure 6.6 shows the variation of IRR due to variation in tariff from ₹ 8 to 18 per kWh. It can be seen that the IRR is a strong function of tariff.

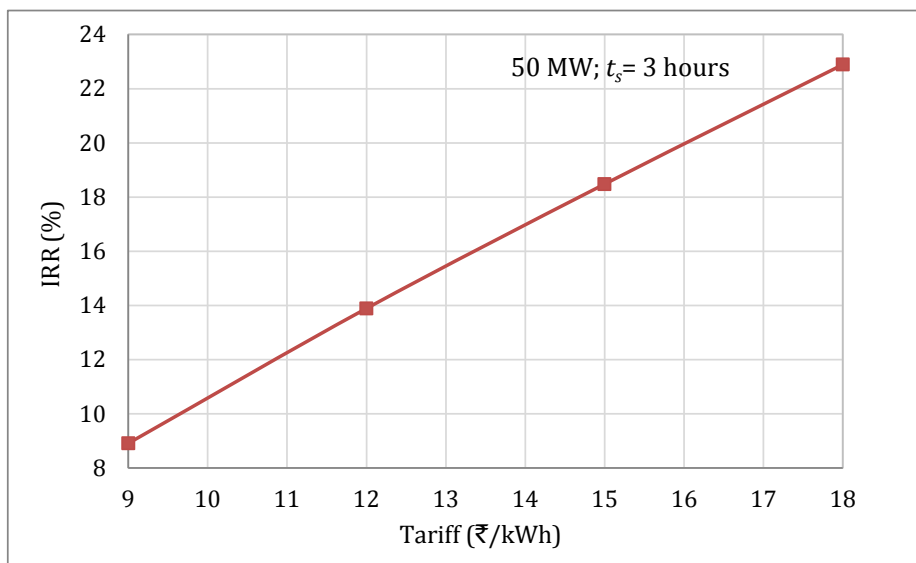


**Figure 6.6: Variation of IRR with tariff**

### 6.5.3 Sensitivity to Annual Solar to Electric Efficiency

#### i. Impact on Capital Cost

Table 6.3 and Figure 6.7 show the variation of capital cost due to the variation of annual solar to electric efficiency ( $\eta_{s-e}$ ). It is seen that capital cost per MW is a strong function of  $\eta_{s-e}$  and it decreases as  $\eta_{s-e}$  increases.

**Table 6.3: Variation of capital cost with annual solar to electric efficiency**

Solar to Electric Efficiency (%)	Capital Cost per MW (₹ crores)
12	23.71
14	21.35
16	19.58
18	18.21
20	17.11

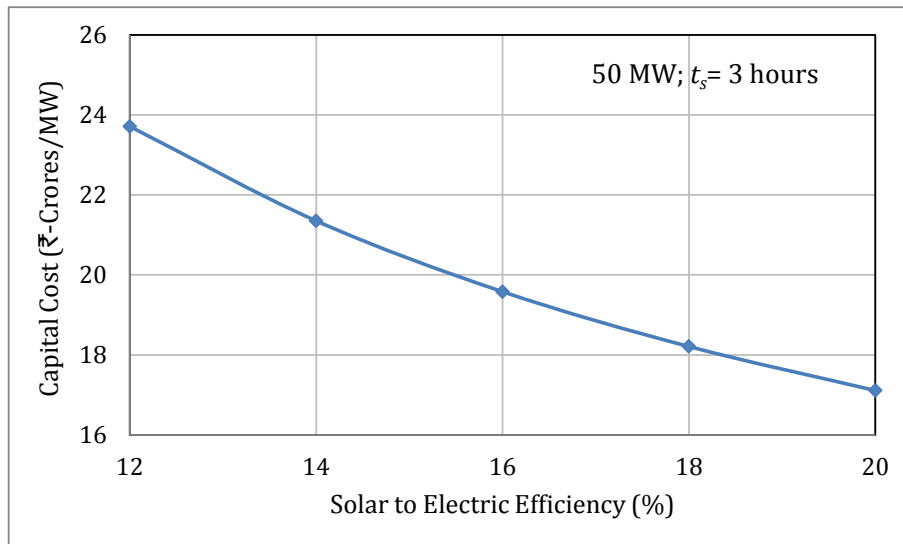


**Figure 6.7: Variation of capital cost with annual solar to electric efficiency**

#### ii. Impact on LCOE & IRR

Table 6.4 and Figure 6.7 show the variation of LCOE and IRR due to the variation of annual solar to electric efficiency ( $\eta_{s-e}$ ). It may be noted that, IRR is more sensitive to  $\eta_{s-e}$  than LCOE.

**Table 6.4: Variation of LCOE & IRR with annual solar to electric efficiency**

Solar to Electric Efficiency (%)	LCOE (₹/kWh)	IRR (%)
12	17.08	14.5
14	15.41	16.61
16	14.17	18.48
18	13.2	20.16
20	12.42	21.68

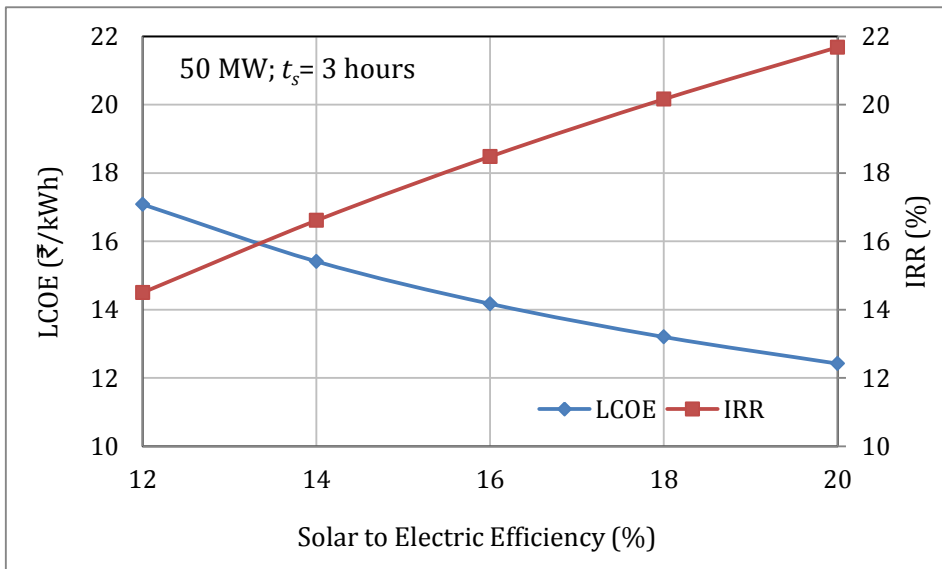


Figure 6.8: Variation of LCOE and IRR with annual solar to electric efficiency

### 6.5.4 Sensitivity to Solar Field Cost

The solar field cost is varied by 5% from reference value and its impact on LCOE and IRR are presented in Table 6.5 and shown in Figure 6.9.

Table 6.5: Sensitivity of LCOE and IRR to solar field cost

Solar Field cost as % change from reference value	Solar Field Cost (₹ crores)	LCOE		IRR	
		(₹/kWh)	% change from reference value	(%)	% change from reference value
-5.0	569	13.66	-3.6	19.33	+4.6
0	599	14.17	0	18.48	0
+5.0	623	14.68	+3.6	17.68	-4.3

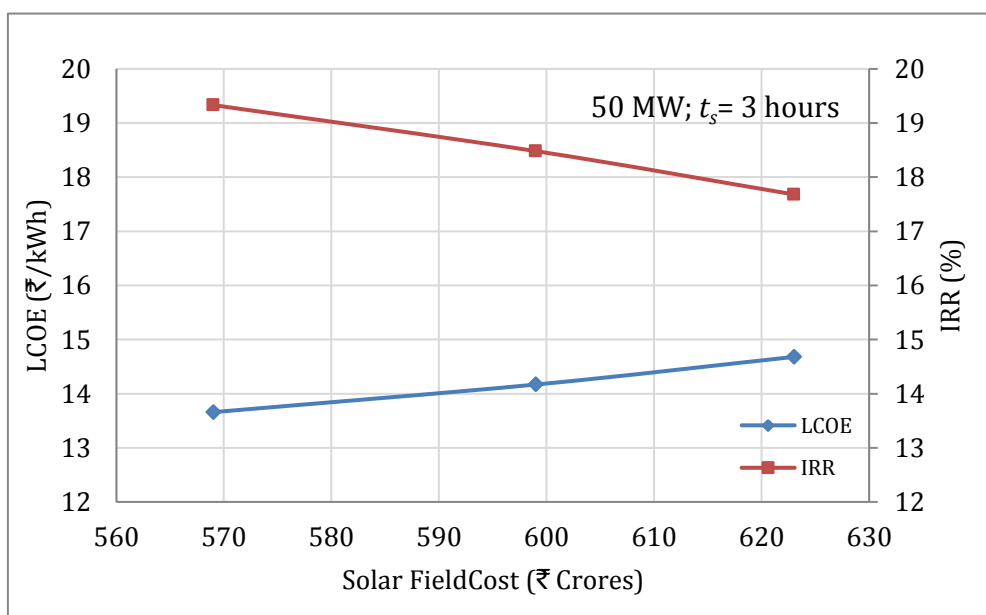


Figure 6.9: Variation of LCOE with solar field cost

From Table 6.5 it is seen that a 5% increase/decrease in solar field cost results in:

- LCOE increases/decreases approximately by 3.6%
- IRR decreases/increases approximately by 4.5%

Since solar field cost is a part of the total capital cost, it is to be expected that its effect on LCOE and IRR is slightly less than the effect due to capital cost.

# 7 Techno Economic Viability of Linear Fresnel Technology in India

## 7.1 Introduction

The global review of CSP plants in Chapter 2 indicates a limited deployment of Linear Fresnel Reflector (LFR) systems. As a result, the information and data availability are sketchy. The largest LFR plant of 100 MW is being built in Rajasthan by Reliance Power, but hardly any data are available. Therefore, it is difficult to make a reliable assessment of the techno-economic viability of a LFR plant. However, possible reasons for low deployment of LFR are indicated and a possible option to make LFR an alternative candidate to PT or ST is suggested.

With the present PV prices, it is difficult for CSP to compete with PV. However, CSP would be an attractive proposition with hybridization and storage. CSP using LFR has so far opted for Direct Steam Generation (DSG) with which significant thermal storage is not viable. This is probably one of the main reasons for this technology not picking-up momentum.

Therefore, we suggest that LFR should also follow PT in using synthetic oil as HTF instead of water. This would then require an additional heat exchanger to generate steam for the power block. But the technology of the heat exchanger and thermal storage using molten salt has been well established in PT and they can easily be adopted for LFR. One might argue that it negates the advantage of LFR in avoiding the heat exchanger. On the other hand, the receiver tubes need to be pressurized to 10 bar only with synthetic oil as HTF, unlike when water used as HTF, the absorber tubes have to withstand the higher steam pressures.

In this chapter the viability of using synthetic oil as HTF in the LFR is covered. Then the techno-economic assessment of a LFR system with thermal storage is described. This method is applied for a 50 MW capacity plant with 3 hours of thermal storage to demonstrate its viability in India.

## 7.2 Viability of Using Synthetic Oil as HTF in LFR Systems

At present, all LFR systems built so far have used water as HTF for DSG. However, the problems in generating superheated steam along with thermal storage have not been fully addressed. Hence, a natural extension would be to use synthetic oil as HTF along with thermal storage. This was probably not considered earlier since it was felt that with LFR, temperatures that could be attained is less than that in PT.

Many technological improvements have taken place in LFR during 2008 – 2012. Novatec Solar and AREVA Solar have demonstrated LFR systems for superheated steam at high pressures and temperatures (100 bar and 450°C). The pilot plant in PSA, Spain also demonstrated that superheated steam at 100 bar and 450°C could be generated. AREVA Solar is attempting to use molten salts as HTF and also as a thermal storage medium (Section 2.4.3). Since molten salts freeze at 220°C and its use even in PT is not fully proven, it is felt that LFR system using synthetic oil as HTF will be a better option.

We shall call this LFR using synthetic oil as HTF, as Modified LFR (MLFR).

## 7.3 Techno-Economic Assessment of a LFR using Synthetic Oil as HTF

The gross capacity of the plant and the number of hours of thermal storage are the input parameters. Based on hours of thermal storage, capacity factor is arrived at. Using this and the gross capacity, the annual gross electricity generated is determined. Based on the estimated efficiency of annual solar to electrical energy conversion and annual DNI, the size of the solar field is determined.

Considering the gross capacity of the power block and using the technical assessment data the direct capital cost, indirect capital cost, O&M expenses, etc. of the CSP plant are estimated. LCOE and the IRR are computed adopting the procedure given in chapter 3 for PT.

### 7.3.1 Determination of Solar Field Area and Stored Thermal Energy

#### i. Input Parameters

To determine the mirror aperture area ( $A_a$ ), maximum thermal energy stored ( $E_{tes,max}$ ) and volume of HTF ( $V_{htf}$ ), the following parameters are required:

- Plant capacity,  $P_{g,d}$  (Watts)
- Hours of thermal energy storage,  $t_s$
- Capacity factor,  $CF$
- Annual solar resource,  $DNI_{annual}$  (kWh/m<sup>2</sup>)
- Annual solar to electric conversion efficiency,  $\eta_{s-e}$
- Efficiency of power block at design conditions,  $\eta_{p,d}$
- Efficiency of power block heat exchanger,  $\eta_{he}$
- Efficiency of thermal storage heat exchanger,  $\eta_{st}$
- LFR module configuration details

#### ii. Computation of Mirror Aperture Area

$A_a$  is calculated as given below:

- Annual Gross Electrical Energy generated,

$$e_{g,t} = P_{g,d} \times 8760 \times CF$$

- Annual solar energy to be captured,

$$e_{solar} = \frac{e_{g,t}}{\eta_{s-e}}$$

- Calculate the solar field area ( $A_a$ )

$$A_a = \frac{e_{solar}/1000}{DNI_{annual}}$$

#### iii. Stored Thermal Energy

The maximum stored thermal energy ( $E_{tes,max}$ ) is computed as below

$$E_{tes,max} = \frac{P_{g,d} \times t_s}{\eta_{p,d} \times \eta_{he} \times \eta_{st}}$$

where,  $E_{tes,max}$  is the maximum thermal energy stored ( $Wh_{th}$ )

#### iv. Volume of HTF

In order to calculate the volume of HTF ( $V_{htf}$ ), we have considered Novatec Solar's LFR module configuration. The module configuration details are given in Table 7.1.

**Table 7.1: Novatec Solar's LFR module configuration**

Parameters	Value	Units
Mirror module width, $W_{mod}$	16.56	$m$
Module length, $l$	44.8	$m$
Number of mirrors in a module, $n$	16	-
Height of the absorber above the primary reflector level, $H$	7.4	$m$
Height of primary reflector level, $H_0$	1.0 - 1.3	$m$
Mirror width	0.7165	$m$
Absorber tube diameter, $D_i$	0.07	$m$

The length of absorber tube ( $L_{abs}$ ) is given by

$$L_{abs} = \frac{A_a}{W_{mod}}$$

To account for the HTF contained in the header & feeder pipes and piping in the heat exchanger, we have assumed that the total volume of HTF required is approximately four times the volume of HTF in the absorber tubes. Thus the total volume of HTF needed

$$V_{htf} = \frac{A_a}{W_{mod}} \times \pi D_i^2 \times 1000 = (1.345) \times A_a, \text{ litre}$$

Therefore, the volume of HTF required per  $m^2$  of mirror aperture area,  $v_{htf} = 1.345 \text{ litre}/m^2$ .

### 7.3.2 Inputs and Assumptions in Economic Assessment

#### i. Direct Capital Cost

The DCC of a CSP plant using LFR technology, with thermal storage can be categorized as follows:

- Land & site preparation cost
- Solar field cost
- Power block cost
- Thermal storage system cost

##### a. Land & site preparation cost

Cost of the land and cost for site preparation are taken as  $100 \text{ ₹}/m^2$  and  $108 \text{ ₹}/m^2$ , respectively, the same as that used for PT analysis. However, the ratio of land area to mirror area is taken to be 2.0 for LFR.

##### b. Solar Field Cost

At present, costs of various components of the solar field for LFR are not available in open literature. But, some information on bulk solar field cost per unit mirror area is available. Even this is for conventional LFR and not for MLFR. It was felt that from the costs used for PT, a reasonable estimate for MLFR can be made.

The cost of the PT components used earlier has been reproduced in Table 7.2 for easy reference.

**Table 7.2: Cost of the PT components**

Components	Value	Unit
Mirror	2450	₹/m <sup>2</sup>
Support Structure		
- Weight per unit aperture area	19	kg/m <sup>2</sup>
- Material and fabrication cost per kg	150	₹/kg
- Cost of support structure	2850	₹/m <sup>2</sup>
Absorber tube	14250	₹/m
HTF	200	₹/litre
HTF system	1900	₹/m <sup>2</sup>
Hydraulic drive & Electrical Motor	130000	₹/unit
Foundation	200	₹/m <sup>2</sup>
Electronics, Controls and Electricals	1000	₹/m <sup>2</sup>
Thermal Storage	1710	₹/kWh <sub>th</sub>

Based on the above, costs for LFR are estimated as described below.

Mirror cost is taken as 1400 ₹/m<sup>2</sup> (20 €/m<sup>2</sup>) since mirrors are flat and cheap compared to parabolic mirrors.

For PT (Euro Trough) 19 kg/m<sup>2</sup> of material is used. For the LFR, it will be less and it is taken as 10 kg/m<sup>2</sup>. The cost of material and fabrication is assumed as 150 ₹/kg. So the cost of support structure is taken as 1500 ₹/m<sup>2</sup>.

Absorber tube for the LFR systems is non-evacuated and therefore it should cost less than that of the SCHOTT tube. However, non-evacuated absorber tube has secondary reflector, insulation on the top of the secondary reflector, glass cover at bottom etc. So as a first approximation, cost of absorber system for LFR is taken to be same as the cost of evacuated absorber tube. Since 1 meter length of absorber tube in LFR corresponds to 11.46 m<sup>2</sup> of mirror area, we can take the LFR absorber tube cost as 1243 ₹/m<sup>2</sup> of mirror area.

$$\text{Cost of HTF} = v_{htf} \times 200 = 269 \text{ ₹/m}^2$$

The cost of HTF system is taken to be same as in PT.

Hydraulic drives are used in PT systems whereas for LFR systems electrical motors are used. In the PT analysis, each hydraulic drive has been assumed to control 862.5 m<sup>2</sup> of aperture area and its cost is taken as ₹ 1,30,000. Therefore the cost of drive system per unit area is approximately 150 ₹/m<sup>2</sup> of aperture area. Same cost has been used for the LFR drive systems.

It may be noted that the loads on the foundation of LFR will be less compared to PT, as LFR systems are closer to ground and are subjected to lesser wind loads. However, the number of foundations would be more for LFR. So we have assumed the same cost per m<sup>2</sup> for foundation of LFR systems.

Electronics, Controls and Electrical (ECE) systems include all necessary equipment for operating the plant. It is taken as ₹ 1000 per unit aperture area for PT systems. We have assumed the same for LFR systems.

The cost of various components arrived at on the above basis are summarized in Table 7.3.

**Table 7.3: Cost of components for LFR**

Components	Value (₹/m <sup>2</sup> )
Mirror	1400
Support Structure	1500
Absorber system	1243
HTF Fluid	269
HTF system	1900
HT & EM	150
Foundation	200
ECE System	1000

Based on Table 7.3, the total solar field cost was arrived at ₹ 7662 per m<sup>2</sup>.

*c. Power Block Cost*

Cost of power block and cost of Balance of Plant of power block for LFR are taken to be the same as that used in PT analysis.

The variation of cost of power block with capacity is given by equation

$$\text{Cost of PB (Rs/kW)} = 55,000 \times (\text{Capacity in MW})^{-0.2875}$$

The cost of BOP of power block is taken as 50% of the cost of power block.

Therefore, the total cost is 1.5 times the cost of power block.

*d. Cost of Thermal Storage*

The specific cost of a two-tank molten salt thermal storage is also taken to be same as that used in PT analysis.

**ii. Indirect Capital Cost**

The methodology used for determining the components of ICC are identical to that used for PT analysis (Section 3.3.2).

**iii. O&M Expenses**

The annual O&M expenses will vary from 2 to 3% of DCC. In the PT analysis, O&M expenses have been computed in detail, and total O&M expenses were found to be 2.7% of the DCC. Here, we have assumed the O&M expenses as 2.5% of DCC. It includes all the expenses for the plant operation and maintenance (salaries, equipment maintenance, water requirements and insurance).

## **7.4 Assessment of 50 MW LFR Plant with 3 Hours Storage**

This section illustrates the application of the above methodology for a LFR plant of 50 MW with three hours of thermal storage located at Jodhpur with an annual DNI of 1920 kWh/m<sup>2</sup>.

## 7.4.1 Determination of Various Technical Parameters

### i. Capacity Factor

Capacity factor has to be estimated for  $t_s$  hours of thermal storage. To determine  $CF$  we take the guidance from results obtained for PT in Section 3.4 and also from information available in open literature. In our analysis for PT,  $CF$  varies linearly from 27% for  $t_s = 0$  to 47% for  $t_s = 6$ . The variation of  $CF$  with  $t_s$  for PT reported in (ITP, 2012) is shown in Figure 7.1. It is seen that the values obtained from our analysis are slightly more than that given in Figure 7.1. It was felt that for MLFR, one can consider slightly lower values than PT, namely 25% for zero hours of  $t_s$  and 45% for six hours of  $t_s$ . On this basis the  $CF$  for three hours of thermal storage is 35%.

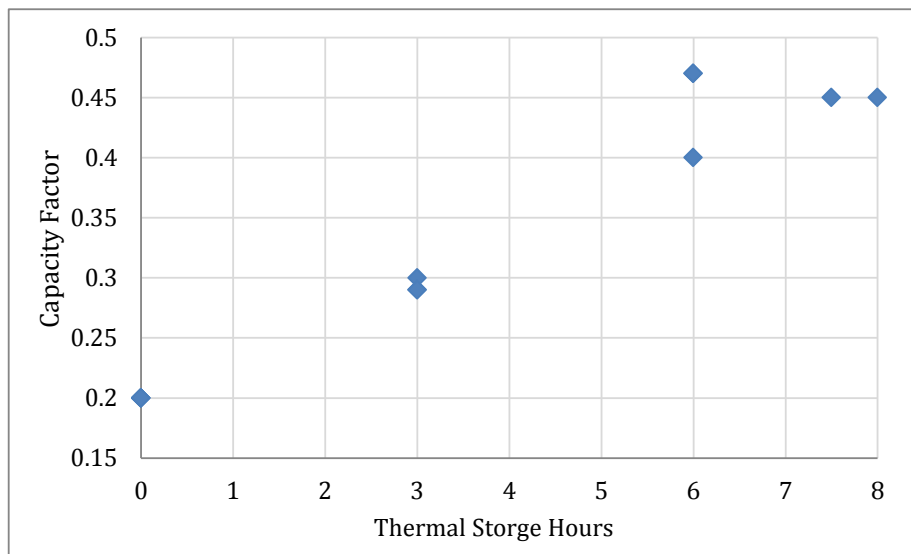


Figure 7.1: Variation of capacity factor with storage for PT

### ii. Annual Solar Resource

We have considered Jodhpur as the location of the plant which has annual DNI of 1920 kWh/m<sup>2</sup>.

### iii. Solar to Electric Conversion Efficiency

Annual solar to electric conversion efficiency ( $\eta_{s-e}$ ) for LFR system can vary from 8% to 10% (Robert-Pitz-Paal, 2012; Fichtner, 2010). It can increase up to 12% by the technology improvements mainly due to achieving higher temperatures (EASAC, 2011). For the analysis, we have considered annual solar to electric efficiency of 10%.

### iv. Annual Gross Electrical Energy Generated

The annual gross electrical energy generated for 50 MW capacity and 35% capacity factor is 1,53,300 MWh.

### v. Annual Net Electrical Energy Generated

It is assumed that the auxiliary power utilized is 10% of the gross power. Thus the net electrical energy generated is 0.9 times of  $e_{g,t}$ , i.e., 1,37,970 MWh.

#### vi. Annual Solar Energy to be Collected

$$e_{solar} = \frac{153300}{0.1} = 15,33,000 \text{ MWh}_{th}$$

#### vii. Total Mirror Aperture Area

Assuming 10% overall efficiency of solar to gross electrical energy and taking annual solar resource as 1920 kWh/m<sup>2</sup>, the aperture area required is given by

$$A_a = \frac{15,33,000 \times 1000}{1920} = 7,98,438 \text{ m}^2$$

#### viii. Land Area

$$= 2 \times 7,98,438 = 15,96,875 \text{ m}^2 (\sim 160 \text{ hectares})$$

#### ix. Stored Thermal Energy

Efficiency of power block at design ( $\eta_{p,d}$ ) conditions, used in PT analysis, is shown in Figure 3.3. It may be noted that it is a function of capacity. For a 50 MW plant, it is 0.38.

Efficiency of the power block heat exchanger and the thermal storage heat exchanger are taken as 0.95 and 0.97, respectively. The same values were used in PT assessment.

The stored thermal energy,  $E_{tes,max} = 4,28,363 \text{ kWh}_{th}$

### 7.4.2 DCC, ICC and O&M Expenses

#### i. Direct Capital Cost

a. Cost of land & site preparation:

$$= \text{Land Area (m}^2\text{)} \times \text{Cost/m}^2 \\ = 15,96,875 \times 208 \text{ ₹/m}^2 = 3322 \text{ ₹-lakhs}$$

b. Cost of solar field:

$$= A_a \text{ (m}^2\text{)} \times 7662 \text{ ₹/m}^2 = 61,177 \text{ ₹-lakhs}$$

c. Cost of power block of 50 MW capacity:

$$\text{The total cost of power block per kW is } 55000 \times 50^{-0.2875} \times 1.5 = 26,792 \text{ Rs/kW}$$

Therefore, the total cost of power block for 50 MW capacity

$$= P_{g,d} \times 1000 \times 26,792 \text{ ₹/kW} = 13,396 \text{ ₹-lakhs}$$

d. Cost of thermal storage:

$$= E_{tes,max}, \text{ kWh}_{th} \times 1710 \text{ ₹/ kWh}_{th} = 428363 \times 1710 = 7325 \text{ ₹-lakhs}$$

Therefore the Total DCC = 3322 + 61177 + 13396 + 7325 = 85220 ₹-lakhs

#### ii. Indirect Capital Cost

Following the same procedure as indicated in section 3.3.2, the ICC come out to be 17150 ₹-lakhs.

#### iii. O&M Expenses

Here O&M expenses are taken to be 2.5% of the DCC. So it becomes 2130 ₹-lakhs.

### 7.4.3 LCOE and IRR

Using the same procedure as for PT for computing LCOE and IRR based on DCC, ICC, O&M expenses and financial assumptions (same as in PT analysis), the LCOE is 14.79 ₹/kWh and IRR is 17.51%.

### 7.4.4 Comparison of MLFR with PT of 50 MW with 3 Hours Storage

Table 7.4 shows the comparison of the results for MLFR and PT.

**Table 7.4: Techno-economic comparison of a 50 MW capacity MLFR and PT plants**

<b>Technical Parameters</b>	<b>MLFR</b>	<b>PT</b>
Capacity Factor	35%	38.30%
Solar Resource, kWh/m <sup>2</sup> /year	1920	1920
Annual Solar to Electric Efficiency	10%	15.8%
Solar Field Area, m <sup>2</sup>	7,98,438	5,51,760
Land Ratio	2	3.8
Land Area, ha	160	210
Gross Electricity Generated, MWh	15,33,000	1,67,616
Net Electricity to grid, MWh	1,37,970	1,50,855
<b>Component Costs</b>		
Solar Field Cost, ₹/m <sup>2</sup>	7,662	11,765
Power Block Cost, ₹/kW	26,792	
Thermal Storage Cost, ₹/kWh <sub>th</sub>	1710	
Total cost of Land & site preparation, ₹-lakhs	3322	4361
<b>Economics</b>		
Direct Capital Cost (DCC), ₹-lakhs	85,220	88,325
Indirect Capital Cost (ICC), ₹-lakhs	17,150	17,925
Total Capital Cost (TCC), ₹-lakhs	1,02,369	1,06,250
Capital Cost (CC) per MW, ₹-crores	20.47	21.25
LCOE, ₹/kWh	14.79	14.2
IRR in %	17.51	18.5

Based on our assumptions, it is seen that the MLFR appears comparable to PT. Advantage of MLFR over PT is that all the solar field components can be made by local industry. It is therefore suggested that though the MLFR has not been tried out, it may be worthwhile for India to build a demonstration plant to verify the techno-economic viability of such a system.

## 7.5 Sensitivity Analysis for MLFR Parameters

In the previous section, we have done a techno-economic assessment of a 50 MW LFR plant with 3 hours of thermal energy storage. As, there are considerable uncertainties in the inputs used in the analysis, we have attempted a sensitivity analysis to understand the sensitivity of capital costs, LCOE and IRR to the following input parameters.

- i. Percentage variation of capital cost
- ii. Tariff (₹/kWh)
- iii. Annual solar to electric efficiency ( $\eta_{s-e}$ )
- iv. Percentage variation of solar field cost

It may be noted that, the above listed parameters are varied one at a time, the other parameters being held at their reference values used in section 7.4.

### 7.5.1 Sensitivity to Capital Cost

The capital cost was varied by 5% on either side of the reference value and its impact on capital costs, LCOE and IRR are determined. The results are presented in Table 7.5 and shown in Figure 7.2 and Figure 7.3.

**Table 7.5: Sensitivity of LCOE & IRR to capital cost**

Capital Costs		LCOE		IRR	
% change from reference value	(₹-crore)	(₹/kWh)	% change from reference value	(%)	% change from reference value
-5.0	972	14.06	-4.91%	18.6%	6.50%
0	1024	14.79	0	17.5%	0
+5.0	1075	15.51	4.91%	16.5%	-5.94%

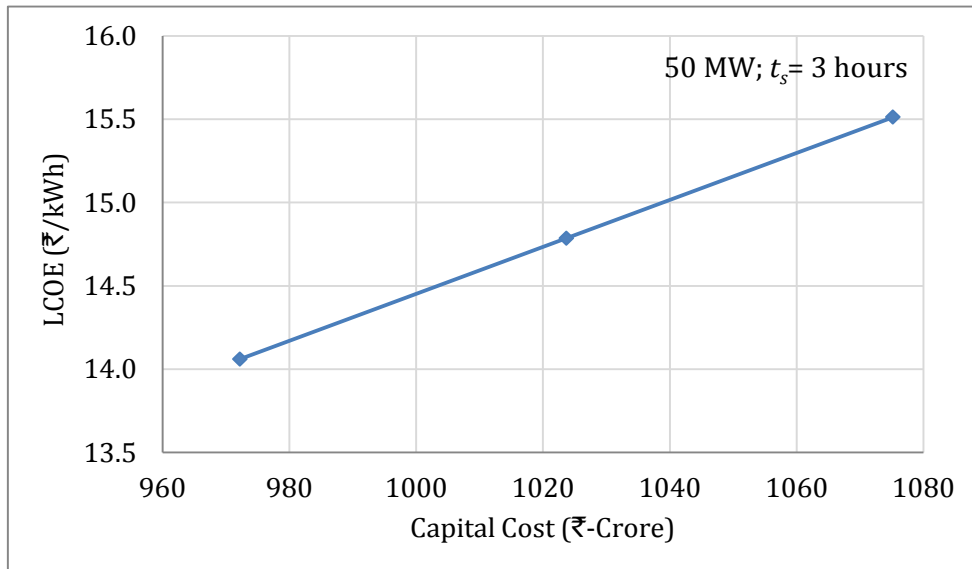


**Figure 7.2: Variation of LCOE with capital costs**

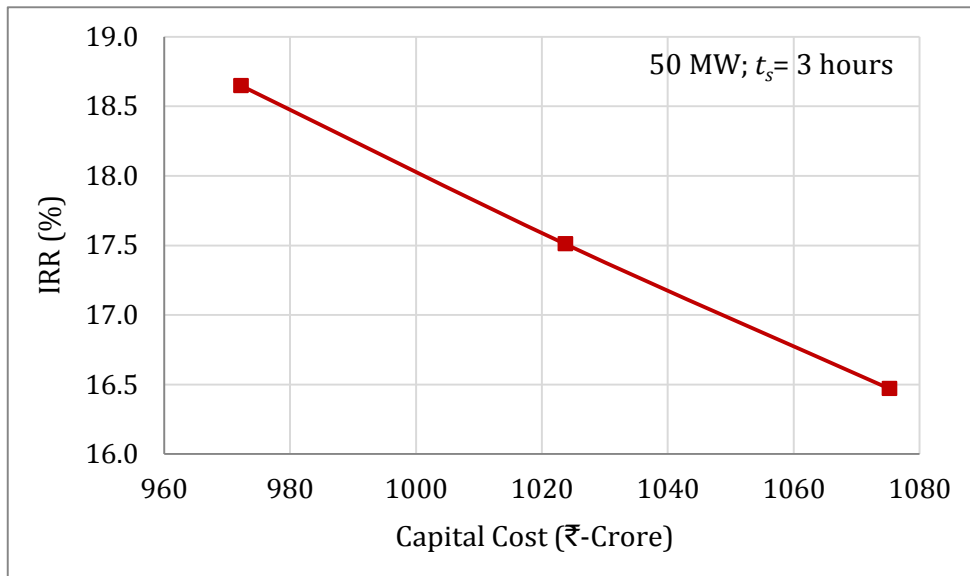


**Figure 7.3: Variation of IRR due to variation of DCC**

From Table 7.5 we can see that a 5% decrease/increase in the capital costs results in:

- LCOE decreases/increases approximately by 4.9%.
- IRR increases/decreases approximately by 6%.

### 7.5.2 Sensitivity to Tariff

The assumed tariff is varied from ₹ 9 to 18 per kWh to see its impact on IRR. Results are presented in Table 7.6 and shown in Figure 7.4.

**Table 7.6: Sensitivity of IRR to assumed tariff**

Assumed Tariff (₹/kWh)	IRR (%)
9	8.23
12	13.07
15	17.51
18	21.76

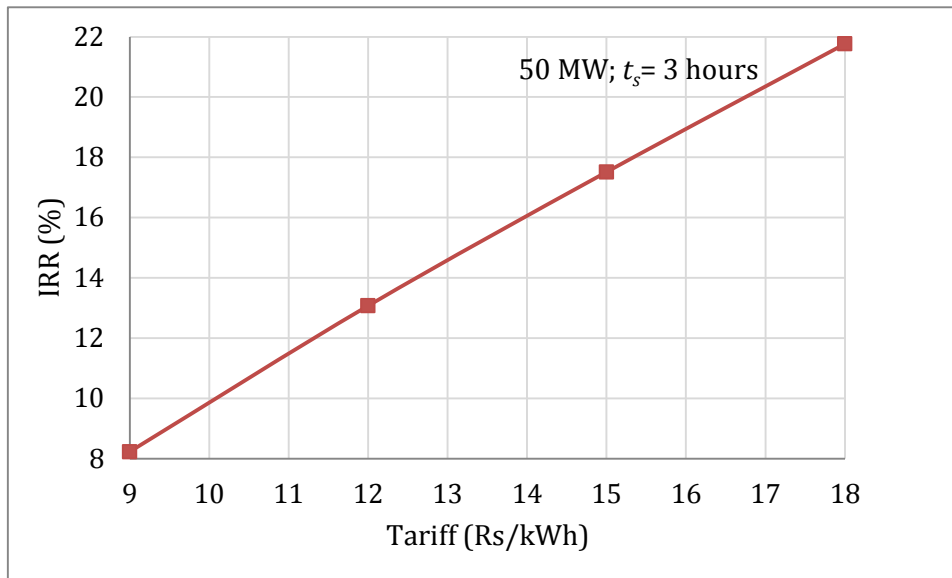


**Figure 7.4: Variation of IRR with assumed tariff**

It may be seen that for a change in tariff from 9 to 18 ₹/kWh IRR changes from 8.23% to 21.76%.

### 7.5.3 Sensitivity to Annual Solar to Electric Efficiency

Annual solar to electric efficiency is the overall efficiency of the CSP system. It is varied from 6% to 14% to see the impact on capital costs, LCOE and IRR. The results are presented in Table 7.7 and shown in Figure 7.5 and Figure 7.6.

**Table 7.7: Sensitivity of capital costs, LCOE and IRR to solar to electric efficiency**

Solar to electric efficiency, $\eta_{s-e}$ (%)	Capital costs		LCOE		IRR	
	(₹-crores)	% change from reference value	(₹/kWh)	% change from reference value	(%)	% change from reference value
6	1539	50.35	22.06	49.17	9.87	-43.63
8	1217	18.88	17.51	18.44	14.01	-20.01
10	1024	0.0	14.79	0.00	17.51	0.00
12	895	-12.59	12.97	-12.29	20.59	17.56
14	803	-21.58	11.67	-21.07	23.34	33.27

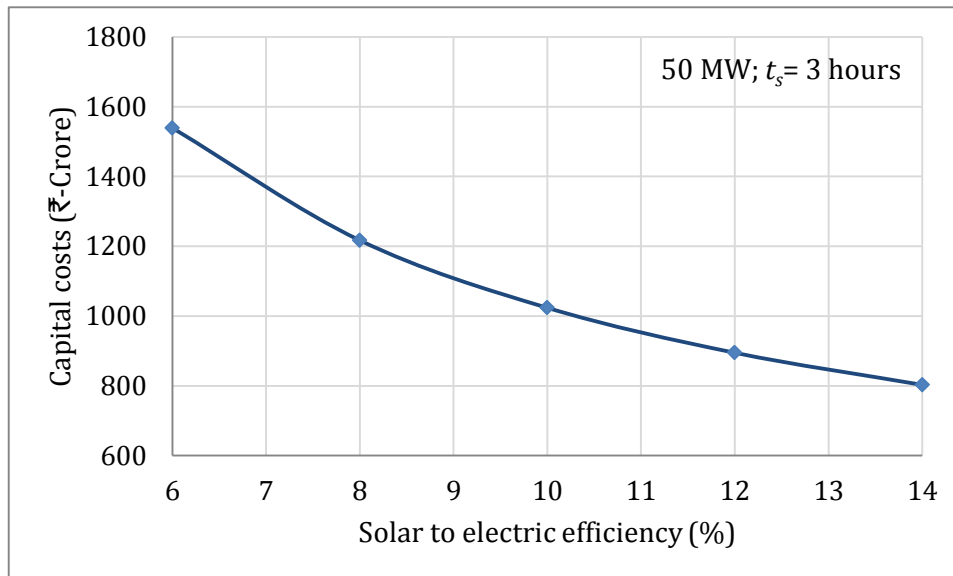


**Figure 7.5: Variation of capital cost with solar to electric efficiency**

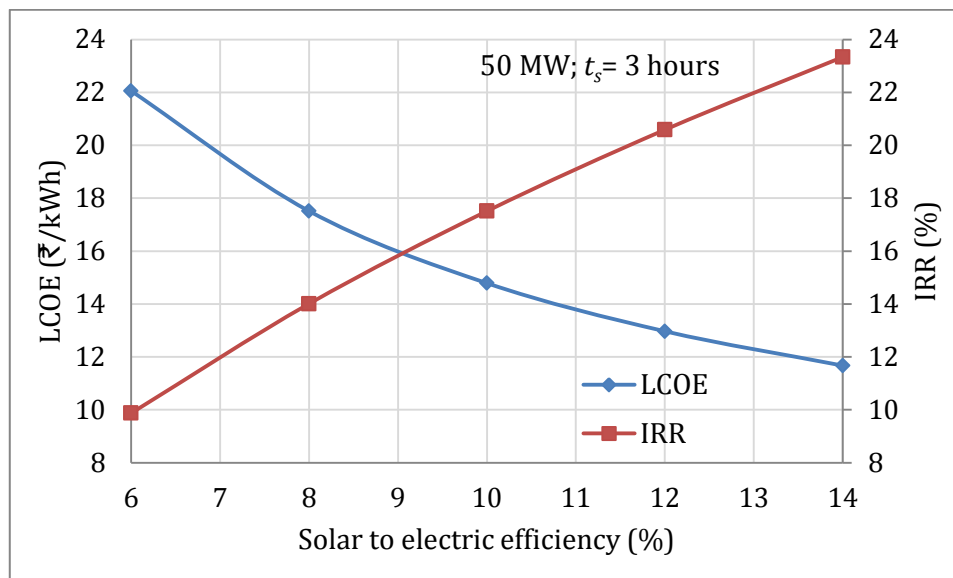


**Figure 7.6: Variation of LCOE and IRR with conversion efficiencies**

From Table 7.7 it is seen that:

- When annual solar to electric efficiency decreases by 4%, capital cost increases by 50% of the reference value. Capital cost decreases over 20% due to 4% increase in annual solar to electric efficiency.
- LCOE decreases non-linearly from ₹ 22.06 to 11.67 per kWh.
- IRR increases non-linearly from 9.87 to 23.34%.

#### 7.5.4 Sensitivity to Solar Field Cost

Solar field cost includes all the component costs corresponding to the solar field. It is varied 5% from reference value to see its impact on capital cost, LCOE and IRR. The results are presented in Table 7.8 and shown in Figure 7.7 and Figure 7.8.

**Table 7.8: Sensitivity of capital costs, LCOE and IRR to solar field cost.**

% change of Solar Field Cost	Solar Field Cost (₹/m <sup>2</sup> )	Capital Costs		LCOE		IRR	
		(₹-crore)	%change from reference value	(₹/kWh)	% change from reference value	(%)	% change from reference value
-5.0	7279	987	-3.61	14.26	-3.52	18.3	+4.61
0	7662	1024	0.00	14.79	0.00	17.5	0.00
+5.0	8045	1061	+3.61	15.31	+3.52	16.8	-4.32

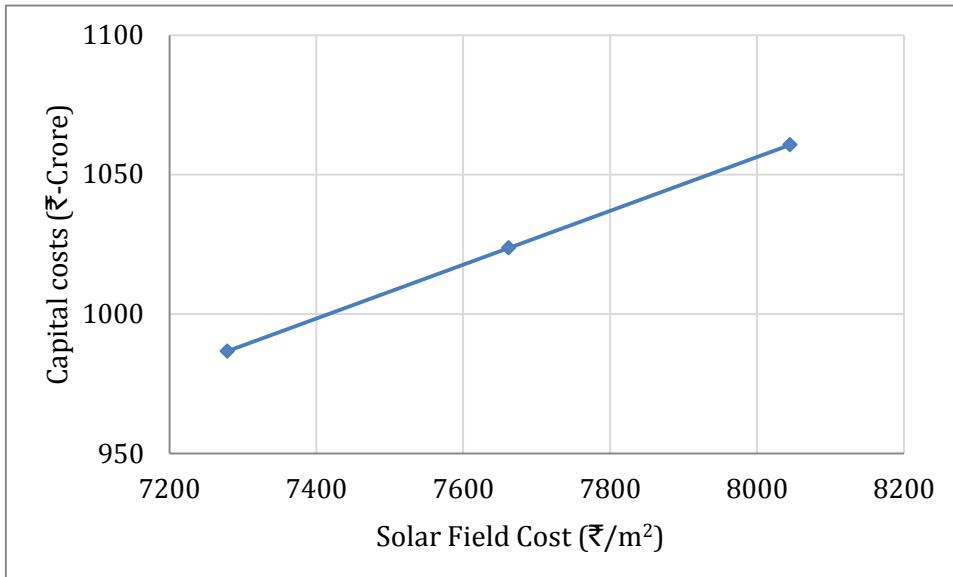


**Figure 7.7: Variation of capital cost with solar field cost**

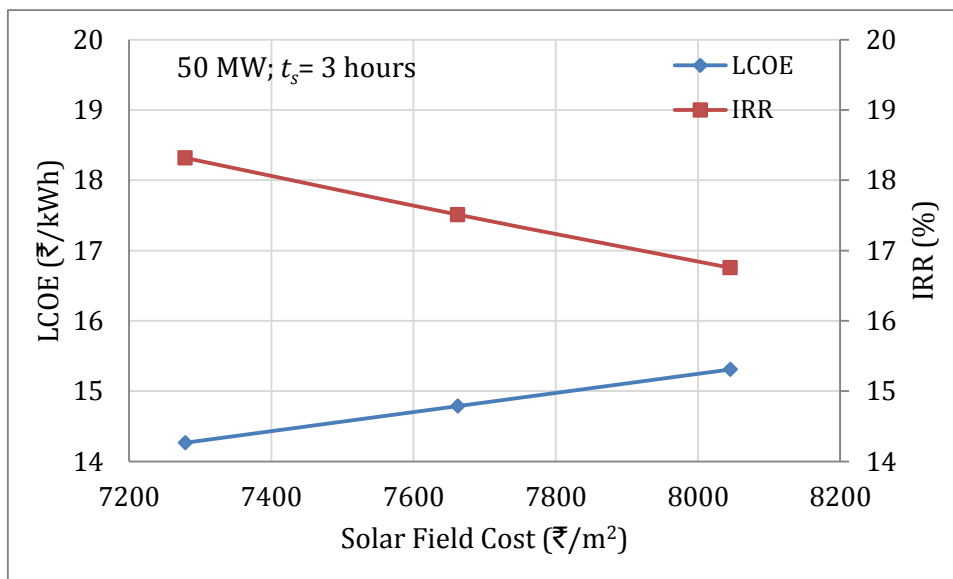


**Figure 7.8: Variation of LCOE and IRR with solar field cost**

## 7.6 Salient Observations

CSP plant without thermal storage cannot compete with PV system. The LFR systems presently in use are based on DSG and consequently reasonable amount of thermal storage is not viable (only some small buffer storage is feasible). Adoption of DSG avoids HTF and heat exchanger and consequently one expects LFR costs to compete with that of PV.

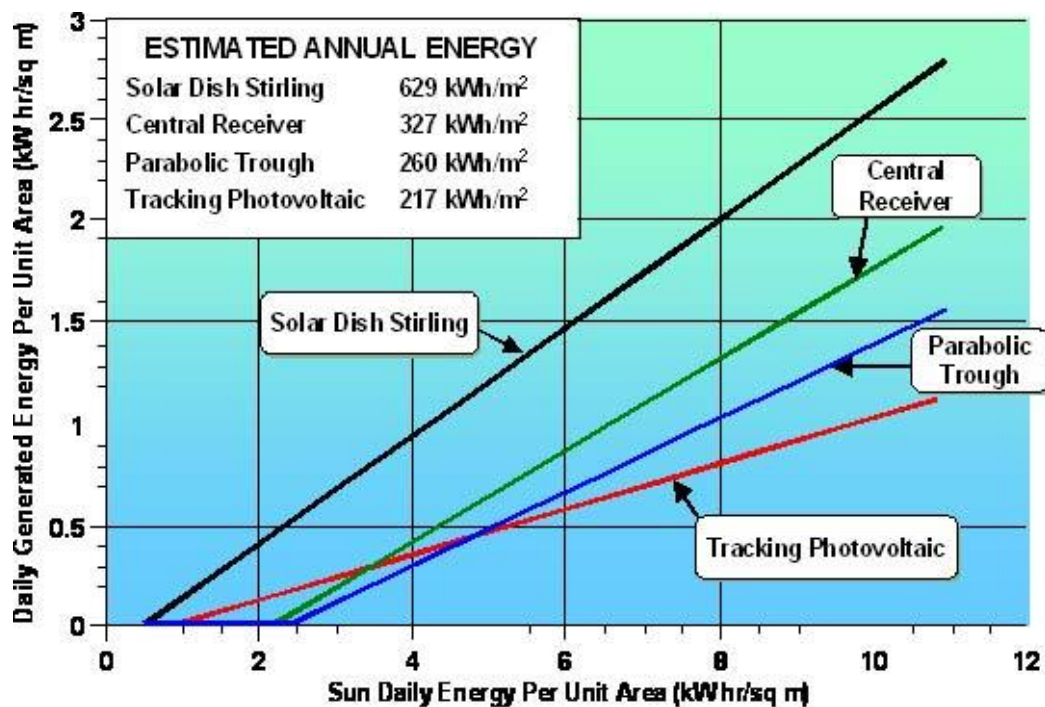
It is again believed, that technically it is feasible to use synthetic oil as HTF in the LFR system also, just as in PT and with that two tank molten salt storage system become feasible. Obviously the addition of HTF and heat exchanger would add to the cost of the system. However, LFR system being considerably simpler than either PT or ST systems, it is amenable for total indigenization. Consequently, despite the additional costs, the MLFR system could compete with PT and ST. The techno-economic analysis carried out on such a MLFR system confirms that such a system can be competitive against PT and ST systems. Therefore, it is recommended that pilot plants using this MLFR system be built in India to demonstrate the techno-economic viability of such MLFR systems.

# 8 Techno Economic Viability of Dish Technology in India

## 8.1 Introduction

In this chapter the techno-economic aspects of Dish technology are discussed. Parabolic dish systems track the sun without any cosine loss. For this reason, they have the highest energy reflected on to the receiver per unit mirror aperture area. The high temperature achievable in this system can lead to higher efficiency with regard to solar - electric conversion. The prime mover adopted for this technology usually is a Stirling engine mounted at the focus of the dish. The maximum solar to electric conversion efficiency obtained for this technology is about 30%, which is the highest among the CSP technologies. An attempt to identify the areas of future R&D which could improve the techno-economics is made.

Basics of Stirling engine and its operation have been described earlier in section 2.5. The comparative performance of various CSP technologies in converting solar energy to electrical energy is shown in Figure 8.1.



Source: Southern California Edison and Sandia National Laboratories

Figure 8.1: Conversion efficiencies of various solar technologies

There is also a possibility to use gas turbines as the prime mover with parabolic dish. The schematic of this concept is shown in Figure 8.2 (Source: <http://me1065.wikidot.com/solar-thermal-electric-power-plants>). The main components of this system are parabolic dish concentrator, solar receiver, combustor and a recuperated gas turbine using air as the working fluid. A 30 kW system would require about 120 m<sup>2</sup> of mirror area. The system is amenable for hybridization. This option may

hold promise in future dish systems leading to better techno-economics. However, no pilot plant is operating using this technology.

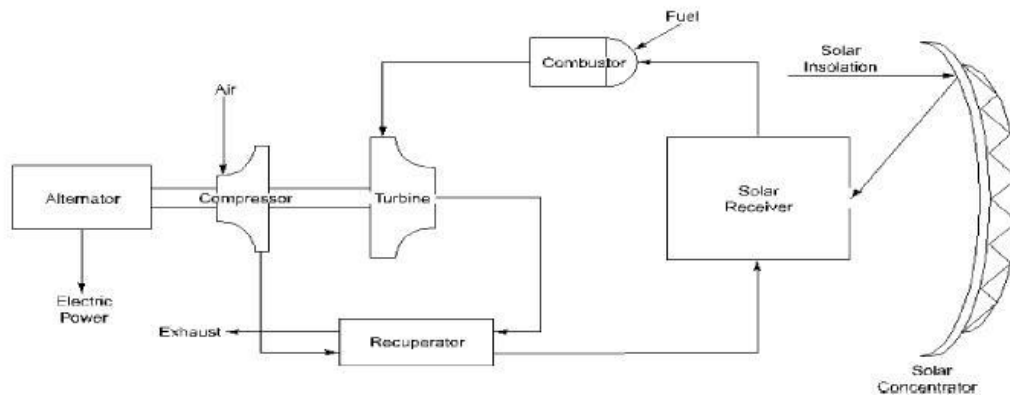


**Figure 8.2: Dish with gas turbine**

In a variant of this technology known as “Scheffler Dish”, direct steam generation is used for power production in a Rankine cycle. This was discussed previously in section 2.5.3. Results and data from a project of this kind being implemented in Mount Abu, Rajasthan are awaited. The cost of this project for 1 MW plant with 16 hours of storage (using cast iron blocks) is about ₹ 64 crores.

## 8.2 Dish with Stirling Engine

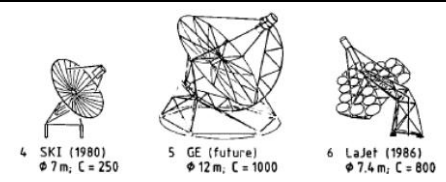
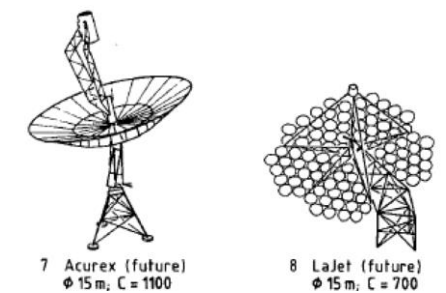
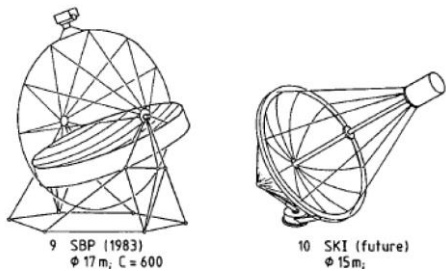
The dish Stirling engine systems have undergone experimental trials and a few pilot plants are under evaluation. The dish engines can be used in a cluster of units in distributed mode, producing electricity in hundreds of kW range or in a solar farm comprising of large number of units in utility mode supplying power to the grid in MW range. They also have the advantage of being deployed in slightly undulating terrain. They do not require water in their power cycle. However, storage technology is not yet available for this system. This is a major drawback unless the generated power can be directly used in applications such as irrigation pumps.

### 8.2.1 Limited Techno-Economic Data

#### i. Earlier Dish Systems

Many dish engine systems have been studied for more than 35 years. Some of the earlier attempts are listed in Table 8.1 (Winter, Sizmann, & Vaut Hull, 1991).

**Table 8.1: Earlier dish systems**

Technology	Name		Diameter (m)	Concentration	Dish Weight (kg/m <sup>2</sup> )	Cost (\$/m <sup>2</sup> )
Glass/Metal	TBC(1977)	 <p>1 TBC (1977) φ 11m, C = 3000</p> <p>2 Vanguard (1980) φ 11m, C = 2800</p> <p>3 MDAC (1984) φ 11m, C = 2400</p>	11	3000	162	1300
	Vanguard (1980)		11	2800	118	650
	MDAC(1984)		11	2400	73	300-200
Aluminized film	SKI(1980)	 <p>4 SKI (1980) φ 7m, C = 250</p> <p>5 GE (future) φ 12m, C = 1000</p> <p>6 LaJet (1986) φ 7.4m, C = 800</p>	7	250	74	1000
	GE(future)		12	1000	56	300
	LaJet (1986)		7.4	800	37	190-160
Polymer-Silver/Steel-Silver	Acurex (future)	 <p>7 Acurex (future) φ 15m, C = 1100</p> <p>8 LaJet (future) φ 15m, C = 700</p>	15	1100	67	127
	LaJet (future)		15	700	55	80
Stretched Membrane	SBP(1983)	 <p>9 SBP (1983) φ 17m, C = 600</p> <p>10 SKI (future) φ 15m,</p>	17	600	52	180
	SKI (future)		15	-	30	140

**ii. Recent Systems**

Table 8.2 summarizes the dish systems which have been recently built.

**Table 8.2: Summary of dish systems**

	<b>Sundish</b>	<b>Suncatcher</b>	<b>WGA</b>	<b>Eurodish</b>	<b>AZ-TH</b>	<b>Power Dish</b>	<b>Sunmachine</b>
<b>Type</b>	<b>Stretched membrane</b>	<b>Parabola with facets</b>	<b>Parabola</b>	<b>Parabola</b>	<b>Parabola with facets</b>	<b>Parabola</b>	<b>Parabola</b>
Aperture (m <sup>2</sup> )	113	88	41	57	56	14.7	15-17
Diameter (m)	15	10.5	8.8	8.5		4.2	4-5
Reflectivity (%)	95	91	94	94	94		
Focal length (m)	12	7.45	5.45	4.5	5		
Concentration Ratio	2500	7500	11000	12700			
Receiver Diameter (m)	0.38	0.2	0.19	0.19	0.19		
Engine	STM 4-120	4-95 Kockums	V161 Solo	V161 Solo	V161 Solo	Infinia	Sunmachine
Engine Type	Kinematic	Kinematic	Kinematic	Kinematic	Kinematic	Free Piston	
Working fluid	H <sub>2</sub>	H <sub>2</sub>	H <sub>2</sub> /He	H <sub>2</sub> /He	H <sub>2</sub> /He	H <sub>2</sub>	N <sub>2</sub>
Working Temperature	720 °C	720 °C	650 °C	650 °C	650 °C		
Promoter	SAIC	SEC	WGA	SBP	Abengoa	Infinia	Sunmachine
Year	1999	1998	1999	2001	2007	2007	2007
Design Power (kW)	22	25	11/8	11	11	3	3
Efficiency (%)	23	29	24	23	23	24	20-25

### 8.3 Commercial Ventures

There are two commercial projects, which are underway in Spain and in the USA.

The Spanish 1 MW project is promoted by Renovalia energy. It has more than 300 units of 3 kW each developed by Infinia. It uses a parabolic dish of 4.2 m diameter to capture the solar energy in conjunction with a free piston Stirling engine to produce 3 kW power when the DNI is 850 W/m<sup>2</sup>. When the DNI is 500 W/m<sup>2</sup> the electricity generated is about 1.5 kW. The dish performance under partial load is given in Figure 8.3.

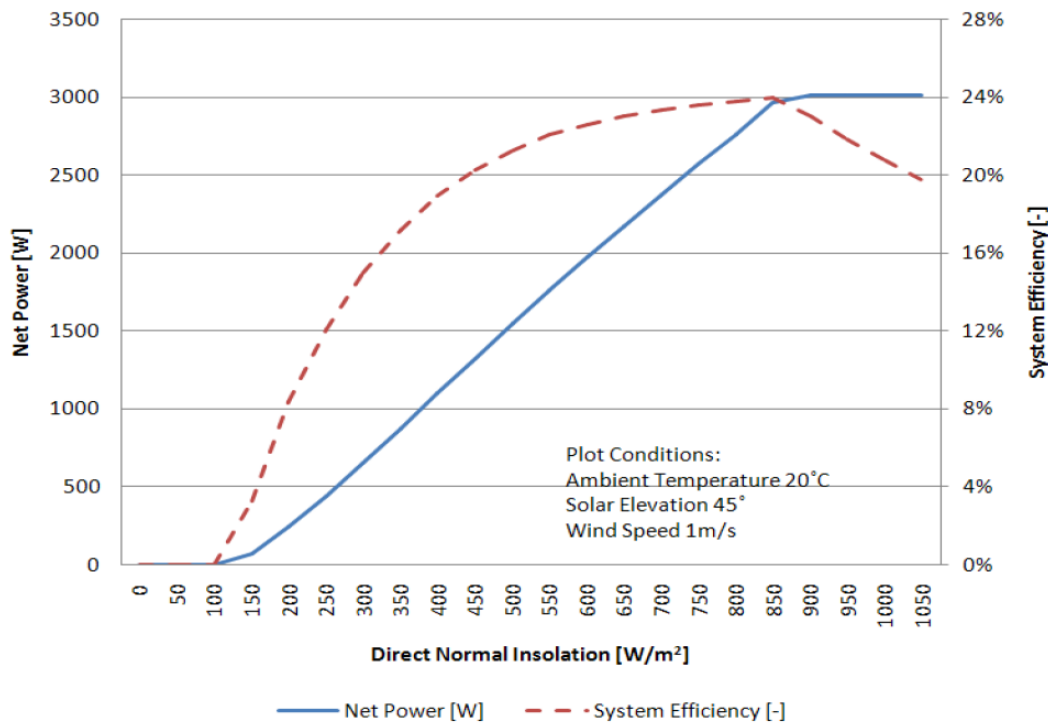


**Figure 8.3: Infinia dish performance**

In the second commercial venture in Arizona, USA, Suncatcher units developed by Stirling Energy Systems (SES) are used. Tessera Solar have promoted this project of 1.5 MW capacity using 60 units each of 25 kW. However it is learnt that SES, the technology partner in this project has filed for bankruptcy (Jennifer, 2011).

It may be noted that attempts made so far have not resulted in successful commercialization of this technology. It is therefore worthwhile to examine the underlying reasons.

### 8.4 Plant Cost

The cost input for dish Stirling system of 50 MW capacity for Seville (Spain) as worked out by (ECOSTAR, 2003) is given in Table 8.3. This is based on a conversion rate of 1 €=₹ 80. The cost for Jodhpur, India is arrived at as follows: Solar field cost is reduced by 20% as structures manufactured in India will be cheaper due to reduced cost of labour in India. Also mirrors made in India may cost less. Power block and receiver costs are assumed to be same. Land cost in India is assumed to be ₹ 100/m<sup>2</sup> and a land area of 2.8 hectares per MW is used. 20% reduction in indirect costs is also assumed under Indian conditions. With these assumptions, the cost of dish Stirling

system works out to ₹ 57.0 crores per MW. This capital cost per MW is very high as compared to other solar technologies.

**Table 8.3: Cost break-up of dish Stirling plant**

Component	Plant in Seville(Spain)		Plant in Jodhpur(India)	
	Cost in ₹ crores	Percent of total cost	Cost in ₹ crores	Percent of total cost
<b>Solar field</b>	1232	38.3	986	34.6
<b>Power Block</b>	1200	37.3	1200	42.1
<b>Receiver</b>	224	7.0	224	7.8
<b>Land</b>	22	0.7	10	0.5
<b>Indirect costs</b>	536	16.7	429	15.0
<b>Plant cost</b>	3214		2849	

## 8.5 Discussion

According to (ECOSTAR, 2003), the dish cost and the lack of Stirling engine industry are the two major bottlenecks in commercialization of dish Stirling concept. Stirling engine performance over a period of time is affected by high maintenance cost due to leakage of working fluid and poor seal performance. The fact that its performance reliability has not been demonstrated in any plant for a length of time spanning a few years also deters investors in adopting this technology.

The proponents of this technology consider that the Stirling engine assembly can be produced on a mass scale similar to automobile components thereby bringing about sizable cost reduction and more importantly ensure reliability of performance of the engine for solar use. At present, the manufacture of Stirling engine for solar use is limited to very few companies and there is very little information sharing on the performance of the engines or on the technical problems faced. While there is scope for improving the performance with hybridization, the possibility of incorporating storage provision appears less.

# 9 Air Condensing for CSP Plants

## 9.1 Introduction

CSP plants with wet cooling require large quantity of water for steam condensing. Since most plants are likely to be located in hot arid regions, water availability would pose a problem. Under these circumstances, it is worthwhile considering air cooling/hybrid cooling options. Therefore it is necessary to understand the impact of air cooled condensing. Air cooled condensing option for CSP plant has the following adverse effects:

- a. The gross efficiency of the power block reduces. Therefore, for the same gross capacity, the solar field has to be increased to compensate for the reduced gross efficiency.
- b. The auxiliary power used for the fan in air cooling system is higher than the combined power consumed by cooling water circulating pump and cooling tower fan of the wet cooled system. Consequently there is a reduction in net efficiency of the power block.
- c. If the net electrical energy generated has to be maintained the same, then the increase in solar field necessary would be even higher. However since the annual electrical energy generated by a CSP plant depends on the varying solar inputs over the year and consequent varying part load operation, to design the solar field to get the same annual electrical energy generated would be difficult.
- d. The balance of plant costs of the power block for the air cooled condenser is higher than that of a wet cooled system.
- e. The adverse technical impacts indicated above increase the capital cost of the CSP plant and LCOE.

A description of the methodology which enables one to estimate the gross efficiency of the plant and auxiliary load for both wet cooling and air cooled condensing options are given. To start with, the gross efficiency of steam turbine as function of turbine inlet and outlet temperatures and gross capacity is estimated. The reduction in gross efficiency due to higher turbine outlet temperatures in air cooling is brought out. Then, the auxiliary power requirements of wet cooling and dry cooling systems are discussed. We have chosen a 50 MW PT plant for this evaluation.

## 9.2 Gross Efficiency of the Power Block

The gross efficiency of steam turbine/generator power block of utility capacity of the order 50 MW or higher is given by

$$\eta_{gross-max} = 0.7 \times \left(1 - \frac{T_{turb,out}}{T_{turb,in}}\right) \dots\dots\dots Eqn. 9.1$$

where  $T_{turb,in}$  and  $T_{turb,out}$  are turbine inlet and outlet temperature in Kelvin. The relative gross efficiency of lower capacity plants, as fraction of  $\eta_{gross-max}$  has been represented by the relation (ITP, 2012).

$$\eta_{rel} = \left(1 - 0.59 \times e^{(-0.06 \times P_{g,d})}\right)$$

The above function is shown in Figure 9.1 where  $P_{g,d}$  is in MW. While theoretically  $\eta_{rel}$  reaches 1 for  $P_{g,d} = \infty$ , for practical purposes, it is approximated to 1 for a 50 MW plant. Thus, one can approximately obtain the gross efficiency

$$\eta_{gross} = (\eta_{gross-max} \times \eta_{rel}) \dots\dots\dots Eqn.9.2$$

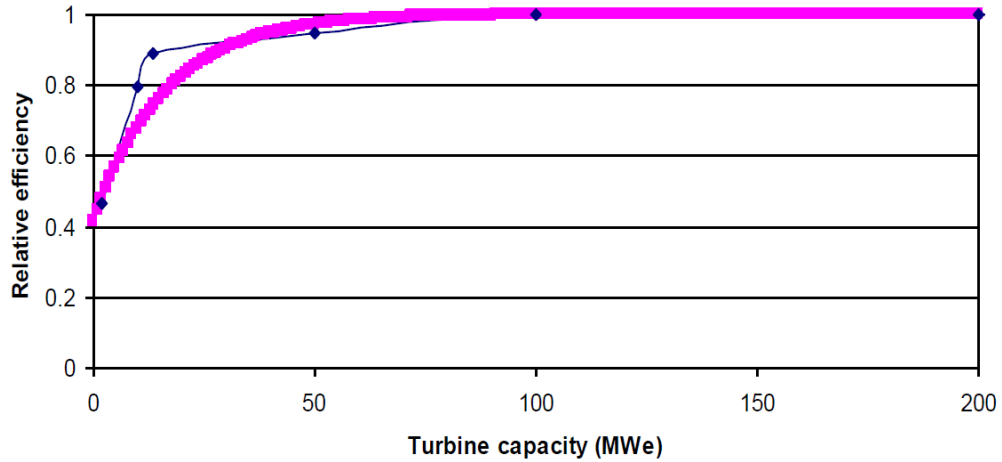


**Figure 9.1: Relative efficiency of turbines against a 100 MWe baseline**

Table 9.1 gives the values of the  $\eta_{gross-max}$  as function of  $T_{turb,in}$  for various values of  $T_{turb,out}$  and same data are plotted in Figure 9.2. In this figure, the nominal turbine inlet temperatures used in Fresnel (270°C), PT (370°C) and the ST system (560°C) are also indicated.

**Table 9.1: Variation of  $\eta_{gross-max}$  for different turbine inlet and outlet temperatures**

Turbine Inlet Temp (in °C)	Turbine outlet temperature (in °C)				
	30	40	50	60	70
240	0.286	0.273	0.259	0.246	0.232
260	0.302	0.289	0.276	0.263	0.249
280	0.316	0.304	0.291	0.278	0.266
300	0.330	0.318	0.305	0.293	0.281
320	0.342	0.330	0.319	0.307	0.295
340	0.354	0.342	0.331	0.320	0.308
360	0.365	0.354	0.343	0.332	0.321
380	0.375	0.364	0.354	0.343	0.332
400	0.385	0.374	0.364	0.354	0.343
420	0.394	0.384	0.374	0.364	0.353
440	0.402	0.393	0.383	0.373	0.363
460	0.411	0.401	0.391	0.382	0.372
480	0.418	0.409	0.400	0.390	0.381
500	0.426	0.416	0.407	0.398	0.389
520	0.432	0.424	0.415	0.406	0.397
540	0.439	0.430	0.422	0.413	0.405
560	0.445	0.437	0.428	0.420	0.412
580	0.451	0.443	0.435	0.427	0.418
600	0.457	0.449	0.441	0.433	0.425

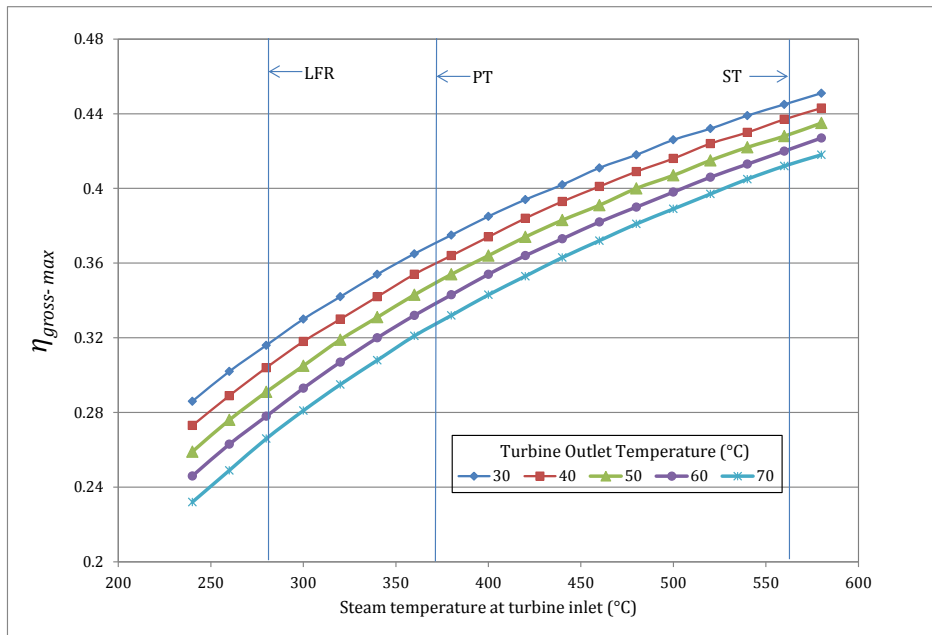


**Figure 9.2: Variation of  $\eta_{gross-max}$  with turbine inlet temperature**

### 9.2.1 Impact of Higher Turbine Outlet Temperature on Gross Efficiency

From equation 9.1, the difference in gross efficiencies for a difference in turbine outlet temperatures is given by

$$\Delta\eta_{gross-max} = -0.7 \left( \frac{\Delta T_{turb.out}}{T_{turb.in}} \right)$$

where  $\Delta T_{turb.out}$  is difference between two different turbine outlet temperatures

The negative sign indicates that as turbine outlet temperature increases, the gross efficiency reduces. Due to the use of air cooling option (as explained later) one can expect an increase in turbine outlet temperature of about 20°C (.i.e.  $\Delta T_{turb.out} = 20$ ). Figure 9.3 gives the variation of this decrease in the gross efficiency with respect to turbine inlet temperature for this 20°C increase in turbine outlet temperature.

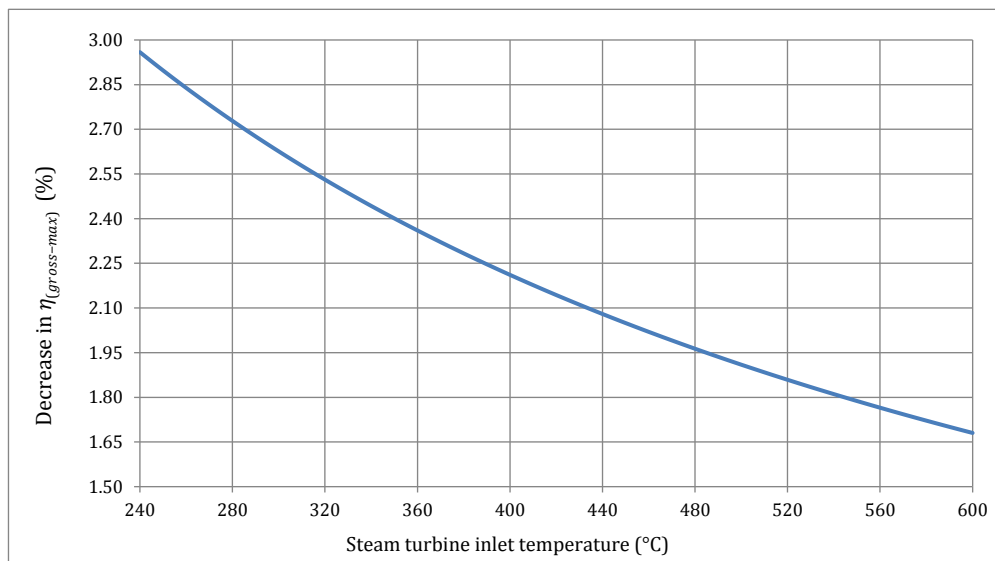


**Figure 9.3: Decrease in  $\eta_{gross-max}$  for a 20°C increase in turbine outlet temperature**

For a steam turbine inlet temperature of 240°C, the decrease in  $\eta_{gross-max}$  is about 3%, whereas for an inlet temperature of 600°C, the decrease is only about 1.7%. If we take 40°C as the nominal turbine outlet temperature with wet cooling and 60°C as the nominal outlet temperature for dry cooling, the relative decrease in the gross efficiency is given by  $(\eta_{gross-max}(Wet) - \eta_{gross-max}(Dry))/\eta_{gross-max}(Wet)$ .

This is shown as a function of turbine inlet temperature (Figure 9.4).

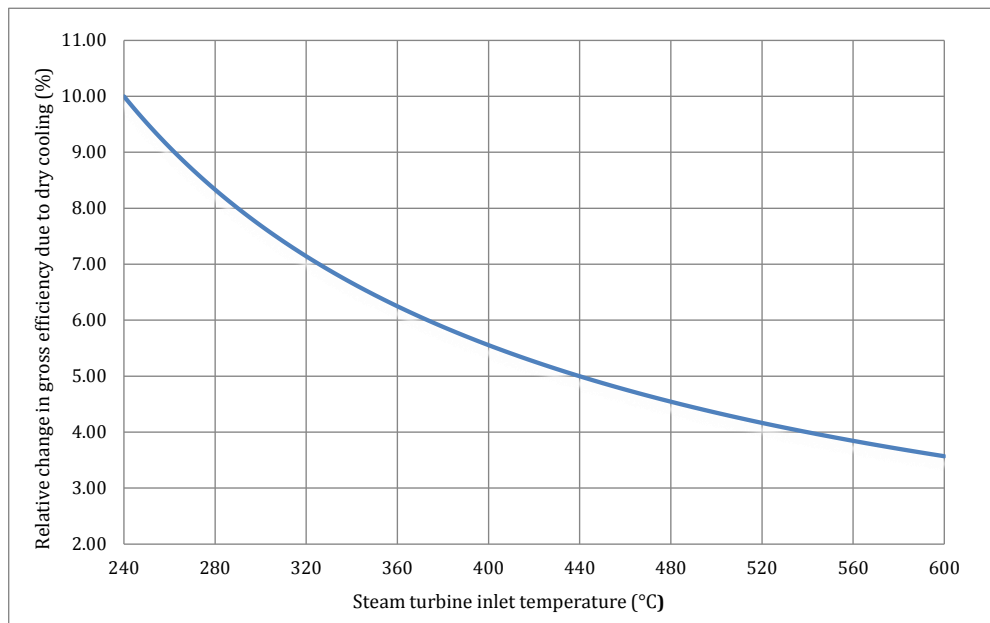


**Figure 9.4: Relative change in  $\eta_{gross-max}$  for a 20°C difference in turbine outlet temperature**

With higher turbine inlet temperatures gross efficiency increases and solar field per unit capacity becomes less and the relative decrease in gross efficiency due to air condensing is small (Table 9.2). Consequently the absolute increase in solar field area is small. On the other hand when turbine inlet temperature is low, the nominal gross efficiency for wet cooling is small and solar field is large. Also, the relative decrease in gross efficiency due to dry cooling is higher. Therefore, the absolute increase in solar field required is much higher. Thus, the impact of dry cooling is minimal for ST because of higher inlet temperatures.

### 9.3 Wet Cooling Condenser System

The schematic of wet cooling system normally employed in steam power cycles is shown in Figure 9.5. The saturated steam from the turbine outlet at temperature  $T_{turb,out}$  enters the condenser and gets condensed by the circulating water. This condensed water at the same temperature,  $T_{turb,out}$  gets fed to the feed water pump.

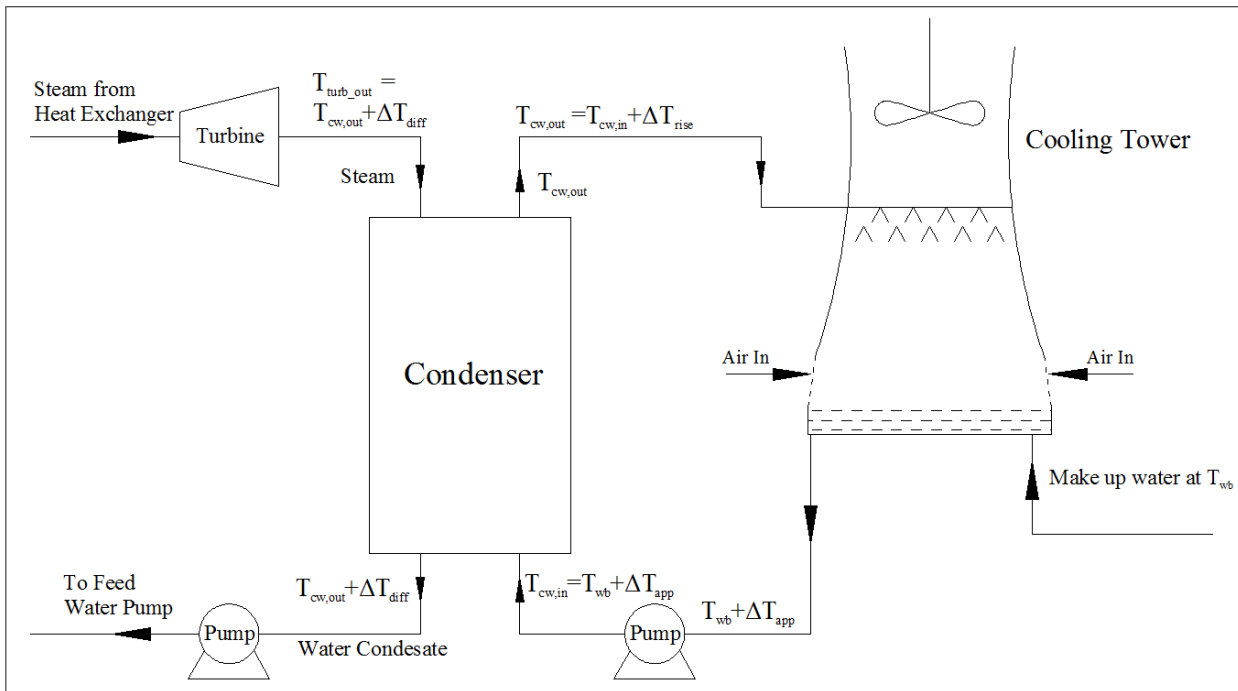


**Figure 9.5: Schematic of wet-cooling system**

Water from the cooling tower is circulated in the condenser to remove the latent heat of steam. The heated cooling water is sprayed in the cooling tower where a fan creates an opposite air draft to cool this before it gets collected in the well. In this process some water gets evaporated. To compensate for this evaporation and blow down/drift losses, makeup water is to be fed into the well.

The above description is to bring out the fact that the steam turbine outlet temperature is closely linked to the temperature of the makeup water as indicated below.

The makeup water will be at the wet bulb temperature ( $T_{wb}$ ) of the atmosphere. In the cooling tower, there must be a temperature difference between water spray and air for heat transfer to take place. Hence the temperature of water in the well will be higher than  $T_{wb}$  by  $\Delta T_{app}$ , which is of the order of 5°C.

Therefore, the temperature of the cooling water fed into the condenser is  $T_{cw,in} = T_{wb} + \Delta T_{app}$ . In the process of removing latent heat of steam to condense it, the temperature of the cooling water rises by  $\Delta T_{rise}$ . The water to the cooling tower will be at temperature  $T_{cw,out} = T_{cw,in} + \Delta T_{rise}$ .  $\Delta T_{rise}$  is generally of the order of 8°C.

For heat transfer to take place between the steam entering the condenser at  $T_{turb,out}$  and cooling water exiting the condenser at  $T_{cw,out}$ , there should be a temperature difference  $\Delta T_{diff}$ . This  $\Delta T_{diff}$  is generally of the order of 3°C.

$$\text{Thus } T_{turb,out} = T_{wb} + \Delta T_{app} + \Delta T_{rise} + \Delta T_{diff} = T_{wb} + 5 + 8 + 3 = T_{wb} + 16$$

Thus the turbine outlet temperature is linked to the wet bulb temperature of the atmosphere.

## 9.4 Air Cooled Condensing System

The schematic of the air cooled condensing system is shown in Figure 9.6. Here air is used directly to cool the saturated steam and condense it.

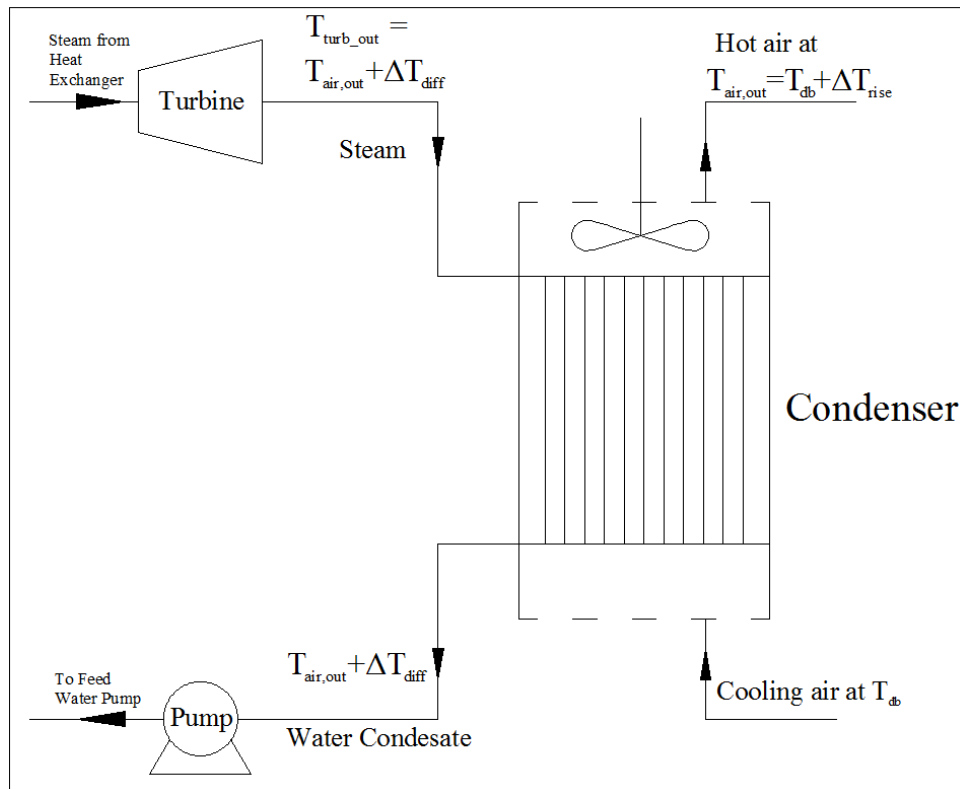


**Figure 9.6: Schematic of air cooled condensing system**

The temperature of the air entering is at the dry bulb temperature,  $T_{db}$  of the atmosphere. Also, since the heat transfer coefficient between steam and air is less compared to that of steam and water,  $\Delta T_{rise}$  for air is about 16°C and  $T_{air,out}$  is equal to  $T_{db} + 16$ . For the same reason,  $\Delta T_{diff}$  between  $T_{turb,out}$  and  $T_{air,out}$  has to be 5°C.

$$\text{Thus } T_{turb,out} = T_{db} + \Delta T_{rise} + \Delta T_{diff} = T_{db} + 16 + 5 = T_{db} + 21$$

The turbine outlet temperatures in the case of wet cooling and dry cooling are  $T_{wb} + 16$  and  $T_{db} + 21$  respectively. In arid regions, which are likely locations for CSP plants, the difference between dry bulb temperature and wet bulb temperature can be of the order of 20°C.

In such a case,  $T_{turb,out}$  for dry cooling option would be 25°C more than that for wet cooling system. As stated earlier, higher  $T_{turb,out}$  results in reduction of gross efficiency of the power block.

## 9.5 Auxiliary Loads in Wet Cooling

### 9.5.1 Power Required for Circulating Water Pump

Determination of  $T_{turb,out}$  for wet cooling is described in section 9.3. For given inlet and outlet temperatures of turbine, the gross efficiency is calculated using equation 9.2. Once this efficiency is obtained, heat rejection rate can be obtained for a given capacity of the plant using equation 9.3.

$$\dot{q}_{rej} = P_{g,d} \times \left( \frac{1}{\eta_{gross}} - 1 \right) \dots\dots\dots \text{Eqn.9.3}$$

where  $\dot{q}_{rej}$  is in J/s.

From the heat rejection rate and the given temperature rise of cooling water in condenser ( $\Delta T_{rise}$ ), the required mass flow rate of cooling water ( $\dot{m}_{cw}$ ) is calculated using the following expression.

$$\dot{m}_{cw} = \frac{\dot{q}_{rej}}{c_p \times \Delta T_{rise}}$$

where,  $\dot{m}_{cw}$  is in kg/s,  $c_p$  in J/kg K

A recirculation pump is required to overcome the pressure losses in the condenser ( $\Delta P_{cw}$ ). These pressure losses are assumed to be of the order of 0.37 bar (Truchi, 2010). The power required by the recirculation pump, ( $P_{pump-cw}$  in J/s) is calculated using following equation for given isentropic and mechanical efficiencies.

$$P_{pump-cw} = \frac{\Delta P_{cw} \times \dot{m}_{cw} \times 10^5}{\rho_{cw} \times \eta_{pump} \times \eta_{mech}}$$

where  $\rho_{cw}$  = density of cooling water in kg/m<sup>3</sup>

$\eta_{pump}$  = Isentropic efficiency of the pump

$\eta_{mech}$  = Mechanical efficiency of the pump

## 9.5.2 Power Required for Fan in Cooling Tower

The auxiliary load due to fan in cooling tower is calculated as follows:

The flow rate of air,  $\dot{m}_{air,ct}$  required to cool the exiting hot water from condenser is around 0.5 times the mass flow rate of the cooling water (Truchi, 2010).

The moist cooling air that enters the cooling tower is at an average temperature given by the following equation.

$$T_{fan,in} = \frac{T_{db} + T_{wb} + \Delta T_{app}}{2}$$

If the process of cooling of water with the use of fan is assumed to be isentropic, one can calculate the exit temperature of air from cooling fan ( $T_{fan,out,is}$ ) from the equation given below. This equation comes from the fact that  $PV^\gamma$  is constant and air is assumed to be an ideal gas.

$$T_{fan,out,is} = T_{fan,in} \times r_{p,fan}^{\gamma-1/\gamma}$$

where,  $r_{p,fan}$  is fan pressure ratio.

At these temperatures  $T_{fan,in}$  and  $T_{fan,out,is}$  the enthalpies of air ( $h_{air}$  in kJ/kg) are calculated from the following expression (Truchi, 2010).

$$h_{air}(kJ/kg) = 2.735 \times 10^5 + 1002.9 \times T_{air} + 0.0327 \times T_{air}^2$$

The actual enthalpy of exit air is normally higher than that computed from isentropic process. Thus, using an isentropic efficiency ( $\eta_{fan,is}$ ) of 0.8, one can calculate the exit air enthalpy ( $h_{fan,out}$ ) from following equation.

$$h_{fan,out} = h_{fan,out,is} + \left( \frac{h_{fan,out,is} - h_{fan,in}}{\eta_{fan,is}} \right)$$

The power required by the fan ( $P_{fan}$  in J/s) with mechanical efficiency of 0.72 can be calculated by

$$P_{fan} = \frac{(h_{fan,out} - h_{fan,in}) \times \dot{m}_{air,ct}}{\eta_{fan,mech}}$$

The overall auxiliary load,  $P_{aux}$  for the whole cooling process is obtained by summing up the pump and fan power requirements.

$$P_{aux} = P_{pump-cw} + P_{fan}$$

In wet cooling, the power needed for auxiliary loads in the plant is assumed to be about 10% of the gross power. This includes the power required for boiler feed water pump, HTF circulation pump etc. in addition to cooling power requirements here. Therefore we can calculate the power required for processes other than that taken by wet cooling and this is used in estimating the total auxiliary requirement for dry cooling also.

### 9.5.3 Make-up Water Requirements

Make-up water requirement for wet cooling system is computed as follows. The evaporation losses in the cooling tower normally depend on dry bulb temperature and humidity of the atmosphere along with the temperature of exit water from the condenser. To calculate the evaporation losses based on the above information, an empirical equation (Zubair & Bilal, 2006) is given by:

$$\dot{m}_{evp} = \left( \dot{m}_{cw} \times \frac{\Delta T_{ct}}{7 - (\Delta T_a^{1.1} / \Delta T_{max})} \right) / 100$$

where  $\Delta T_{ct}$  is the temperature difference between exit cooling water and water in cooling tower well ( $T_{wb} + 5$ ).

$\Delta T_a$  = difference between dry and wet bulb temperatures

$\Delta T_{max}$  = maximum possible temperature difference between exit water and water in the cooling tower well (for  $\Delta T_{max}$  to be maximum, we take  $\Delta T_{app} = 0$ )

The overall makeup water requirement is calculated using,

$$\dot{m}_{makeup} = \dot{m}_{evp} + \dot{m}_{cw} (f_{drift} + f_{blowdown})$$

where  $f_{drift}$  and  $f_{blowdown}$  are fractional losses due to drift and blow down in cooling tower ( $f_{drift} = 0.001$ ,  $f_{blowdown} = 0.003$  are assumed for present calculations).

## 9.6 Efficiency and Auxiliary Loads in Air Cooling

The methodology is similar to that used for wet cooling except that there is no cooling tower.

The gross efficiency is calculated using equation 9.2. The heat rejection rate is calculated using equation 9.3. Since air is used as cooling medium, the mass flow rate of air ( $\dot{m}_{air}$ ) is calculated from the following equation.

$$\dot{m}_{air} = \frac{\dot{q}_{rej}}{c_{p,air} \times \Delta T_{rise}}$$

The auxiliary power requirement in dry cooling is mainly due to the fan. Here it is assumed that air enters at dry bulb temperature and condenser fan pressure ratio (1.0028) is higher than the fan pressure ratio considered in wet cooling (1.0025). The same methodology (section 9.5) is used for estimating the power of cooling tower fan which constitutes the total auxiliary load.

## 9.7 Techno-Economic Analysis of Air Condensing

As stated earlier, the major effect of air condensing option is that the turbine outlet temperature is higher than that for wet cooling which reduces the overall efficiency and increases the solar field size. Further, the auxiliary requirements of the fan for air cooling is higher than the combined power requirements of cooling water pump and cooling tower fan of a water cooled system. The higher the difference between the dry bulb and the wet bulb temperatures, the higher is this impact. Since the techno-economic analysis of a 50 MW PT plant in Jodhpur has been carried out, it is felt that impact of air cooling option be considered for the same case. The hourly data for dry bulb temperature and humidity are available (IMD, 2009). Using that, wet bulb temperatures were

computed. From these data, wet bulb temperature of 20°C and dry bulb temperature of 35°C are taken as representative values.

### 9.7.1 Technical Impact of Air Cooling Option

The effect of air cooling option was computed for turbine inlet temperatures of 370°C and 560°C typical of PT and ST plants respectively. Once  $T_{turb\_in}$ ,  $T_{wb}$ ,  $T_{db}$  and capacity of the plant are known, then all the relevant technical parameters for the wet cooled option and air cooled option can be computed based on the methodology described in sections 9.5 and 9.6. A MATLAB program was written to carry out the computations. The results of the computations for a 50 MW plant with  $T_{turb\_in}$  temperatures of 370°C and 560°C are presented in Table 9.2.

**Table 9.2: Technical parameters of wet cooling & air cooling options**

	Wet cooling		Dry cooling	
$T_{turb\_out}$	36°C		56°C	
$T_{turb\_in}$	370°C	560°C	370°C	560°C
Gross efficiency (%)	36.35	44.02	34.39	42.5
Absolute decrease in efficiency w.r.t Wet Cooling (%)	-	-	1.96	1.42
Relative efficiency compared to efficiency of Wet Cooling (%)	-	-	94.6	96.5
Parasitic power for cooling (MW)	0.57	0.41	1.84	1.31
Water requirement (m <sup>3</sup> /MWh)	3.14	2.28	-	-

From the above table, one can see that for a PT plant which operates at a turbine inlet temperature of 370°C, the relative efficiency of plant with air-cooled option is 94.6% of that with wet cooling option. It means that the dry cooling option would require about 5.4% more solar field than a plant using wet cooling to achieve the same gross power output. Also auxiliary power used in the cooling system is 1.84 MW for dry cooling compared to 0.57 MW for wet cooling.

On the other hand, for a ST plant which can operate at a turbine inlet temperature of 560°C, the gross efficiency of the plant with air cooled option is 96.5% of the plant with wet cooling. It means that dry cooling option would require only about 3.5% more solar field as compared to 5.4% for a PT plant. It may also be noted that the auxiliary power required is only 1.31 MW for ST as compared to 1.84 MW for PT plant. Thus, air condensing option has less adverse impact in ST.

### 9.7.2 Economic Impact of Air Condensing Option

The technical inputs obtained for PT using air condensing option are used in the economic analysis as described section 3.3. The optimal SM and LCOE for both wet cooling and dry cooling with and without storage are calculated and shown in Table 9.3.

**Table 9.3: Economic impact of dry cooling option**

	Wet cooling		Dry cooling	
Turbine outlet temperature	36°C		56°C	
Turbine inlet temperature	370°C		370°C	
Storage (hours)	0	3	0	3
Gross efficiency (%)	36.35	36.35	34.39	34.39
Percentage of Auxiliary power	10	10	12.74	12.74
Optimal SM	1.6	2.1	1.6	2.1
Solar field area	439471	576805	464518	609679
LCOE (₹/kWh)	15.16	14.7	16.91	16.29
IRR (%)	16.97	17.66	14.7	15.45
Water requirement for cooling process (m <sup>3</sup> /MWh)	3.14	3.14	-	-

From Table 9.3 one can infer that LCOE increases by about 10% for air cooling compared to wet cooling. The main advantage of dry cooling is in setting up plants in arid zones where DNI is high and water is scarce.

# 10 Cost of Grid Connectivity

## 10.1 Introduction

Integration of variable power from wind and solar resources to grid poses considerable problems in terms of load balancing and grid stability. Problems are most severe in wind power generation, which varies as cube of wind speed. The variability in case of solar PV is less severe compared to wind as it is a bit more predictable than wind. The variability in case of solar power from concentrated solar thermal technology is least. Even when there is no storage, the thermal inertia of the system does not permit rapid fluctuations in the power generated by CSP plants. If sufficient thermal storage is employed, the CSP allows considerable flexibility in meeting both the base load and peak load.

The Gemasolar 20MW ST system in Spain, having 15 hours of thermal storage can supply power 24 hours a day and can be operated such that it can match the varying base and peak loads.

If CSP plants with sufficient storage capacity are utilised to meet the power demands in the vicinity of the plants, then the cost of grid connectivity will be minimum. On the other hand, if the power generated by the CSP plant is to be utilised at a distant location, power has to be fed to the grid. Then the cost of substation with transformer and all other necessary equipment to boost the output voltage and the cost of transmission of power to the nearest grid point are additional expenses that have to be accounted for in the cost of CSP plants. In this section rough estimates for the cost of substation and cost of transmission are given.

## 10.2 Cost of Substation

From literature survey it is found that the output voltage and capacity of the generator are linked, since the maximum current permitted in a conductor is limited from practical considerations. Table 10.1 gives the output voltages as a function of the capacity of the generators.

**Table 10.1: Voltage vs. capacity of generators**

Output Voltage (Volts)	Maximum Capacity (MW)
415	5
3300	40
6600	80
11000	140
13800	180
15000	200

Since the transmission voltages are 11 kV, 33 kV, 66 kV and 220 kV, suitable step-up transformers are needed in the substation located nearby the CSP plants.

The capacity of the transformers in substation is expressed in terms of MVA. Assuming a power factor of 0.8, substation capacity in MVA is 1.25 times the capacity of the generator in MW. From literature it is found that the total cost of substation including cost of land, transformer, circuit breakers, control panels etc. is about ₹ 20 lakhs/MVA.

## 10.3 Cost of Transmission

The cost depends on the transmission voltage and the distance between the substation and the nearest grid. The cost of different kV transmission lines per km length are given in Table 10.2.

**Table 10.2: Transmission costs vs. voltage**

<b>Voltage (kV)</b>	<b>Cost/km (₹ lakhs)</b>
33	12
66	16
110	20
220	40

# 11 Present Status of CSP Technologies in India

## 11.1 Introduction

Concentrated solar power technologies can be used either for thermal heating of a fluid medium or for electric power generation. In India, there have been several instances of application of solar thermal heating for cooking and other industrial process heating, where the demand for higher temperature does not exist. Several Scheffler dish systems are in operation in the country. However, there is limited success with electricity generation through CSP route. This is due to cost of solar PV declining rapidly in the last three years possibly due to excess supply of cheap PV modules from China. In addition the capital cost and the time to set up a PV plant are less than that of a CSP plant. This enabled many entrepreneurs to establish PV plants in preference to CSP. Notwithstanding the competition from PV, CSP could be a contender to PV because of its capability to attain higher efficiencies and storage.

The four technologies available for electricity generation through the CSP route are described in detail earlier in the report. The main point to be kept in mind is that the PT is the most matured technology, followed by the Solar Tower system. Linear Fresnel appears to be amenable for indigenisation and deserves consideration. It is heartening to note that under the JNNSM scheme, there are at least two promoters who have opted to put up plants based on Fresnel technology.

## 11.2 JNNSM and CERC Baseline

The JNNSM, launched in November 2009 set a target of 22,000 MW of solar power by 2022. It also envisages a large number of other solar applications such as solar lighting, heating and solar powered water pumps. The JNNSM opted for a “reverse bidding method” wherein discounts on benchmark tariffs set by CERC were invited from prospective project developers.

NTPC Vidyut Vyapar Nigam Ltd. (NVTN) was designated as the nodal agency for the execution of Phase I of the Mission. It entered into Power Purchase Agreements (PPA) with winning bidders. It purchased the expensive solar power from developers and bundled it with cheaper coal-based power from unallocated NTPC plants before selling the mixed power to the various state distribution utilities at a reduced average price.

The Central Electricity Regulatory Commission (CERC) announced benchmark feed-in tariffs for the financial year 2010–2011 and declared that PPA would have a validity of 25 years. It is assumed that at current cost levels, the tariff will allow investors to achieve an internal rate of return of about 16%–17% post tax. These tariffs were applicable for those projects that had their PPA signed on or before 31<sup>st</sup> March, 2011. As capital costs decreased, CERC revised the tariffs to ₹ 15.31 and 15.04 for PV and CSP respectively for projects where PPAs are signed after 31<sup>st</sup> March, 2011. Further, if accelerated depreciation at the rate of 80% is considered, the net LCOE would work out to ₹ 12.94 and ₹ 12.69 for solar PV and CSP respectively.

Provisions were also made to allow grid connected solar power projects that signed PPAs before February 2009 to migrate to JNNSM under certain conditions until February 28, 2010. This allowed them to avail benefits offered by the Mission’s incentive framework.

Under the first batch, a total of 30 solar PV projects, each with an individual capacity of 5 MWs (total capacity of 150 MWs) and solar thermal projects with a total capacity of 470 MWs were

allocated. Under the migration scheme, 84 MWs of existing projects got added. Out of this, 30 MWs pertain to CSP.

## 11.3 CSP Projects under JNNSM

### 11.3.1 Projects Bid

As mentioned earlier, as a result of the reverse bidding, seven companies were allotted the CSP projects totalling 470 MWs (Table 11.1).

Table 11.1: Projects in bid category

Project	Aurum Renewable Energy	Corporate Ispat Alloys	Diwakar Solar	Godawari Green Energy	KVK Energy Ventures	Megha Engineering	Rajasthan Sun Technique
<b>Promoter</b>	Aurum	Abhijeet	Lanco	Hira Group	Lanco	Megha Engineering Limited	Reliance
<b>Technology</b>	LFR	PT	PT	PT	PT	PT	CLFR
<b>Size (MW)</b>	20	50	100	50	100	50	100
<b>Bid (₹/ kWh)</b>	12.90	12.24	10.40	12.20	11.20	11.31	11.97
<b>Supplier(s)</b>	Sumitomo Shin Nippon	Siemens turbine & receivers	Siemens	Siemens, Schott Glass, Flabeg, Aalborg	Siemens	Ge, ShyFuel	Areva
<b>EPC Contractor</b>	Indure	Shriram EPC	Lanco Solar & Initec Energia	Lauren, Jyoti Structures	Lanco Infratech	MEIL Green Power Limited	Reliance Infrastructure
<b>Location</b>	Mitrالا, Porbandar, Gujarat	Nokh, Pokaran, Rajasthan	Askandra, Nachna, Rajasthan	Nokh, Pokarn, Rajasthan	Askandra, Nachna, Rajasthan	Anantapur, Andhra Pradesh	Dahanu, Pokaran, Rajasthan

The present status of these projects is given below:

**i. Aurum Renewable Energy**

AREVA is to set up a 20MW plant based on CLFR technology. It has acquired over 200 acres of land in Mitrala village of Porbandar district, Gujarat. The necessary infrastructure development is underway, according to the company's report. According to CSP Today, MNRE is not very sure about the progress of this project. It appears that Aurum wanted to change the technology and MNRE had asked them to submit a revised project proposal, but no action seems to have been taken by the company.

**ii. Corporate Ispat Alloys Ltd.**

CIAL has been approved for setting up a PT based plant at Nokh, Pokran, Rajasthan. Shriram EPC Limited has been chosen as the EPC contractor. CIAL also entered into a technology agreement with ENER-T International Ltd, Israel for providing the solar technology to this project. ENER-T is in charge of SEGS plants in California, USA. Shriram EPC will execute the work in partnership with ENER-T. UVAC receiver tubes and power blocks are supplied by Siemens for this 50 MW plant.

**iii. Diwakar Solar Projects Pvt. Ltd.**

For this 100 MW PT plant, SENER is supplying the troughs. Power block is supplied by Siemens.

**iv. Godawari Green Energy**

Lauren CCL is performing the engineering, procurement and construction management services for a 50 MW solar thermal power plant to be located near Nokh Village, Pokhran Tehsil, Jaisalmer District in Rajasthan. Siemens supplies the power block. Schott Solar has completed the shipment of more than 17,000 Schott PTR 70 receivers to Godawari Green Energy. The steam generator system for the project was delivered by Aalborg CSP and Sojitz.

**v. KVK Energy Ventures Ltd.**

This is a 100 MW PT plant and is to be set up at Jaisalmer district of Rajasthan by KVK. Lanco engineering is the EPC contractor for this plant. Sener Power & Process is supplying the PT collectors for this plant. Siemens supplies the power block.

**vi. Megha Engineering and Infrastructures Ltd.**

MEIL has obtained a 50 MW allocation for a PT based system. This plant is to be set up in Anantapur. SkyFuel has signed a memorandum of understanding with MEIL regarding the use of its parabolic trough collector in CSP projects. Siemens is supplying the Universal Vacuum Air Collectors (UVAC) for this project. GE has won the contract to supply power block for this project.

"SkyFuel's ReflecTech polymer film and lightweight trough will enable easy adoption into the nascent Indian solar market. Increasing the local supply content will further enhance its appeal to CSP plant developers in India," according to MEIL. SkyFuel's parabolic trough is priced 20% lower than competing products.

SkyTrough's design allows a high proportion of components to be provided by local fabricators, which allows Indian companies to expand manufacturing into the solar market. SkyFuel is working with partners in India to secure commitments for aluminium and steel fabrication.

### **vii. Rajasthan Sun Technique Energy Private Ltd.**

Reliance Power, through its subsidiary Rajasthan Sun Technique, is setting up the 100 MW plant at a total cost of ₹ 2,250 crore, which would be funded through 75% debt and 25% equity. This is one of the two plants based on CLFR system under the JNNSM. The project site is near Dhursar village in Pokaran Tehsil of Jaisalmer District in Rajasthan. Lauren CCL has been appointed as EPC contractors. 340 hectares of land have been leased for a period of 30 years. This will be AREVA Solar's largest stand-alone implementation of its CLFR technology.

Though all the above plants are expected to be commissioned by May 2013, a few have sought extension of the commissioning date citing delays in delivery of heat transfer fluid.

## **11.3.2 Migration Scheme**

The major problem with the migrated companies is the small sizes of CSP plants that are not financially viable.

### **i. ACME**

ACME in collaboration with eSolar is to set up a 10 MW ST plant at Bikaner in Rajasthan. The solar field design is in multiples of 2.5 MWs, with double axis software driven mirror tracking system and uses 1 m<sup>2</sup> flat heliostats. The plant uses tower mounted boilers as receivers. The first of this plant with a capacity of 2.5 MW has been commissioned recently. The time for commission the plant was 24 months from signing the PPA. The plant's output varied from 0.5 to 1.7 MW. The company realised that the reason for this was the wrong DNI data. Another reason was the low visibility due to sand and clouds. It is reported that ACME may be shifting the plant to another location where more favourable DNI exists.

### **ii. Dalmia Solar Power**

Dalmia Solar Power Ltd. will install the dish technology from Infinia Corp. for its project under the migration scheme. According to the company, their free-piston Stirling engine is coupled with a dish-style solar concentrator to produce 3.2 kW of grid-quality AC power. The Power Dish does not consume water or need flat ground to operate and can be deployed in numbers that fit within existing transmission and distribution system constraints. The company had secured financing backed by the EXIM (US) bank in 2011. This project was to be commissioned in December 2012 but the deadline has been extended to February 2013, which is also the official deadline for commissioning for migration projects.

According to MNRE, the developer is in danger of not only just losing the preferential tariffs available under JNNSM contracts but also the contract itself. Problems with raising finance have blighted their progress in Rajasthan that despite securing the contract nearly 12 months ago, building work has still not started on the ₹ 200 crores (US\$38 million) development scheme.

### **iii. Rajasthan Solar One**

This plant is based on parabolic trough technology with a 10MW capacity. A PPA for 25 years has been signed at a levelised tariff of ₹ 15.31 per unit with NVVN (a wholly owned subsidiary of NTPC). The estimated capital cost is ₹ 150 crores. Land of about 69 hectares has been acquired for the project (including land for 1 MW SPV project) at the Bhadla village in Jodhpur, Rajasthan. A topological survey of the land has been done and geotechnical investigations have been completed. All clearances for the project like the allocation of water from the Indira Gandhi Canal, the Pollution Control Board, Power evacuation etc. are in place. The DPR for the project is ready, and the turnkey EPC contractor has been chosen.

## 11.4 Projects outside JNNSM

Apart from the 7 projects allotted under the reverse bidding and the 3 that were brought in under the migration scheme, there are a few more CSP projects that are being built/ planned outside the JNNSM. These are as follows:

- i. NTPC's pilot project of 15MW, based on PT, is located in Rajasthan and it is being developed by NTPC itself.
- ii. A project in Andhra Pradesh of 50 MW capacity, again based on PT is being developed by SunBorne Energy in partnership with Khosla ventures and General Catalyst Partners.
- iii. A 25MW PT based system with thermal storage is being built at Kutch in Gujarat by Cargo Solar Power Project Gujarat Pvt. Ltd., a subsidiary of Cargo Power and Infrastructure. Lauren CCL is performing engineering, procurement and construction management services for this plant.
- iv. A National Solar Thermal Power Testing, Simulation and Research Facility have been established at Gwal Pahari, Haryana, where a 1 MW demonstration plant is being set up. This has different collector fields such as PT field with 8700 m<sup>2</sup> capable of delivering 3.3 MW<sub>th</sub>. It also has a Linear Fresnel Field of 7200 m<sup>2</sup> with a design capacity of 2.2 MW<sub>th</sub>. The project is being implemented by IIT Bombay and a consortium partners consisting of Tata Power, Tata Consulting Engineers, Larsen & Toubro, Clique, KIE Solatherm Abengoa are the EPC contractors.
- v. A modular ST plant has been awarded as an R&D project to SunBorne Energy to develop a cost effective solar power tower system with 1 MW<sub>th</sub> capacity. The collaborating institutions are IMDEA Energy, Spain and University of South Florida. The project is to address the current limitations of Indian industry for indigenous technological development and manufacturing of key components. This prototype system is to be located at SEC, Gurgaon, MNRE's Centre of Excellence for solar energy technologies. Heliostat and tower manufacturing are in progress.
- vi. Three units of dish Stirling engine of 3 kW capacity each, have been installed and commissioned in the SEC campus under a collaborative project of SEC and ONGC Research Centre. The engines have been synchronized with the campus PV grid. The objective of the project is to carryout long term performance evaluation under Indian conditions. The rated output of the facility is 9 kW (peak power) at solar insolation of 850 W/m<sup>2</sup> at 20°C ambient temperature.
- vii. Maharishi Solar Technology has launched a PT based low-cost solar heating system for the industries. The technology is a result of the strategic tie-up with US-based Abengoa Solar Inc. The company has set up a manufacturing facility to manufacture Parabolic Troughs in Noida, Uttar Pradesh. It has invested around ₹ 350 crore in this business and is setting up new facilities in Gujarat and Tamil Nadu (Business Standard, 2012).
- viii. Megawatt Solutions Pvt. Ltd. is collaborating with SEC of MNRE to develop renewable energy systems and technologies indigenously under a cost sharing basis. This demonstration project involves setting up 4 interconnected dish concentrators each of 90m<sup>2</sup> area to provide thermic fluids up to 400°C.
- ix. India One solar thermal plant being built at Abu Road in Rajasthan is based on Scheffler dish technology that has been adopted for cooking purposes. It has fixed point focus and uses hollow cast iron blocks both as receiver and storage unit for producing steam. The capacity of the plant is expected to be 1 MW and has 768 dishes each of which has 60 m<sup>2</sup> area. They

have built in enough storage such that the plant can operate throughout the day. The project is supported by MNRE.

- x. Karnataka has recently allotted two CSP projects of 10MW capacity each to Atria Power Corporation and SunBorne Energy Services India Pvt. Ltd.
- xi. A high efficiency Solar Thermal Air-conditioning system (100 kW cooling capacity) is being implemented by M/s Thermax Limited at Solar Energy Centre with an objective to integrate solar collectors, Vapour Absorption Machine (VAM) and appropriate thermal storage system to achieve consistent performance of the system with coefficient of performance (1 : 1.7).
- xii. Cold Storage with Solar – Biomass Hybrid System is a project in partnership with TERI, Thermax Limited, SEC and CSIRO, Australia with an objective to develop cold storage systems particularly in rural areas utilizing exhaust heat of biomass gasifier engine/ Scheffler dish.
- xiii. Clique Solar India has set up two 160 m<sup>2</sup> Arun Solar dishes on top of ITC Sheraton Hotel at a cost of ₹ 85 lakhs with MNRE subsidies to the tune of ₹ 24 lakhs. The system consists of Fresnel parabolic mirrors yielding an output between 0.5 and 0.6 million kcal on a normal sunny day, corresponding to 581 kWh<sub>th</sub>/day.

## 11.5 Progress of CSP in India

India has the opportunity to become a major contributor to the development of solar thermal power. As labour and manufacturing costs are lower in India in comparison with that of the western world, the projected costs are likely to be lower. However, to achieve a lower LCOE, we need to have a reasonable growth rate in establishing plants based on this technology, so that suitable manufacturing methodologies can be put in place to bring down the manufacturing costs. In addition, one can benefit from the learning curve.

According to Indian Meteorological Department (IMD), clear sunny weather is experienced for 250 to 300 days a year by most parts of India (Purohit & Michaelowa, 2008). IMD maintains a nationwide network of stations which measure solar radiation and also the daily duration of sunshine. The annual global radiation varies from 1600 to 2200 kWh/m<sup>2</sup> (Mani & Rangarajan, 1982). The highest annual global radiation ( $\geq 2400$  kWh/m<sup>2</sup>) is received in Rajasthan and northern Gujarat (Purohit & Garud, 2007). These two states are ideal locations for CSP plants in India. But, other states like Jammu and Kashmir, Maharashtra, Andhra Pradesh and Madhya Pradesh also have parts where the DNI is not unfavourable for establishing solar thermal plants.

While there is plenty of solar radiation, the major problem in setting up a solar plant is the reliability of solar radiation data. Estimation of solar field size critically depends on the Direct Normal Irradiation (DNI) at the chosen location. Any error in the DNI data would lead to unexpected outputs. Measured on-ground solar irradiation data are vital. In fact, one needs the average of over 20 years of data to arrive at the values corresponding to a Typical Meteorological Year (TMY). It is true that satellite information is available for locations of interest, but they need to be modified and validated with measured on-ground data. According to Price Waterhouse & Coopers, such crucial data are not available and developers have to opt for different sources of information (PWC, 2012). This uncertainty makes the bankers and financiers difficult to fund the projects. It should be pointed out that MNRE has initiated steps by assigning the work of establishing and collecting data in 50 different locations to the Centre for Wind Energy Technology (CWET).

The second problem is in relation to getting the land for the project. This process differs from state to state. Gujarat gave a free hand to developers to choose the land they thought was most

appropriate, Rajasthan wanted developers to set up their stations in waste lands. The lead time for getting the land clearance took more than 6 months and up to a year or more in some cases (PWC, 2012).

Water availability is another serious issue for developers. Both in Rajasthan and Gujarat, canals are the only sources of water and obtaining clearances for the annual requirement of water takes up to 6 months.

Availability of suitable human resources could be a constraint but, with major players entering the field, this may not be a problem either during the construction period or in operation and maintenance.

A recent report (ITP, 2011) spells out the barriers for the growth of solar power in India. The first and foremost is the LCOE of generated power. This is in addition to the high CAPEX required for CSP plants. This gets exacerbated with difficulties in financial closure, as financiers are not familiar with CSP technologies and related IRR issues. They also feel that power purchase agreement is not bankable. According to them, if India is to achieve its ambitious goals in CSP, then considerable effort is needed in skills and capability building.

If some of the constraints mentioned above are addressed promptly, there is no reason why solar thermal cannot be a better alternative to solar PV.

## 12 Indigenization Prospects of CSP

### 12.1 Introduction

The latest CERC tariff order fixes the normative capital cost of CSP at ₹ 13 Cr/MW. At this rate the LCOE works out to ₹ 12.46/kWh. However our earlier analysis suggests for utility scale PT systems the capital cost is in the range of 15 Cr/MW with a corresponding LCOE of ₹ 14.65 per kWh. This LCOE is very high compared to electricity generated from conventional sources such as coal, hydro and gas and is also more expensive than PV which is now less than ₹ 8 per kWh. In the long run for CSP to develop as a major renewable source, the LCOE should be brought down to about ₹ 5 to 6 per kWh. The capital cost also should come down to ₹ 6-8 Cr/MW. This may be possible with the following:

- Indigenization of various components

It should be possible to achieve cost reduction with indigenization. The power block for CSP is somewhat similar to that of conventional power plants in which the country has lot of expertise and experience. The engineering challenges of CSP can also be met, as the country has the expertise and manufacturing base to produce most of the components. It should be also mentioned that labour is cheap in India compared to that in western world. Therefore indigenization is an important component in the draft guidelines for phase two of JNNSM issued by MNRE in Dec 2012. The ministry intends to increase indigenization (domestic content) from existing 30% to 70% for both PV and CSP technologies.

- Economies of scale

Most of the cost data for components are based on a limited number of power plants proposed to be built in the near future. In the case of wind power the cost of manufacturing decreased significantly as more number of plants was installed. The same may apply to CSP also.

### 12.2 Current Global Cost Structure for CSP

PT is the most advanced CSP technology with a well-developed supply chain. There are several project developers today, mostly in Spain and US, who have successfully erected large scale CSP plants. The installed capacity of PT plants is more than 1168 MW while plants under construction would add another 1377 MW.

Though the installed capacity of ST plants is around 60 MW, plants under construction are expected to add over 2000 MW, indicating that ST technology has also attained reasonable maturity levels.

Fresnel systems though less complex have not been fully exploited. Present installed capacity is only 36 MW and 265 MW are likely to be added in the near future. In India, two plants totalling 120 MW are under construction.

Dish technology is still in the nascent stage. So this is not considered from the indigenization point of view.

In this section, an attempt is made to look into the cost estimates for CSP plants based on a detailed literature survey (Sargent & Lundy, 2003; ECOSTAR, 2003; ESMAP, 2010; Truchi, 2010; IRENA, 2012; ITP, 2012; Ernst & Young, 2011). The data available in most of the cases were for large scale utility plants, mostly based on PT and ST systems.

There is considerable variation in the cost structure possibly due to geographical location, DNI resource, efficiencies of various systems, labour costs etc. It was also found that there is very little difference in the overall costs between PT and ST plants. Based on the above reports, the mirror area was found to vary from 5500 m<sup>2</sup> to 8500 m<sup>2</sup> per equivalent MW capacity. Corresponding to this, a range of cost per MW as a function of thermal storage has been arrived at as shown in Figure 12.1. It may be mentioned here that under JNNSM the CAPEX was assumed at ₹ 15.3 Cr/MW. Probably this cost refers to basic plant without any storage.

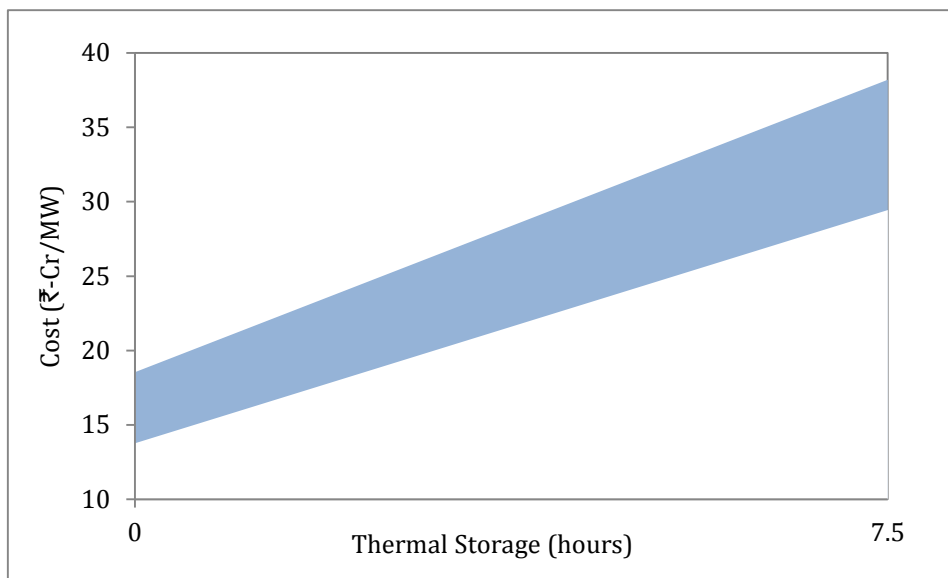


**Figure 12.1: Cost range for CSP plants (PT & ST)**

## 12.3 Indigenization Prospects

Components that are amenable for manufacturing in India are mirrors, support structure, storage system components, power block and balance of plant, which accounts for more than 60% of the plant cost. The major import would be the receivers which is approximately 10% of the plant cost. In the following sections the opportunities and challenges of local manufacturing of some of the components are discussed.

### Potential Manufacturers in India

#### i. Mirrors

In India, there are some big players in the glass industry even though they are limited to supply of glass for automobiles and buildings apart from meeting other domestic requirements. For solar applications, one of the major characteristics required is - low iron content in glass which increases the transmittance. Borosil® is producing low iron flat glass for PV applications in India.

Thermosol Glass, a Cargo Motors enterprise (<http://www.thermosolglass.com/>) based in Gujarat, have established a plant for monolithic parabolic mirrors and laminated parabolic mirrors with standard design configurations such as RP2, RP3 and RP4 used in the solar industry.

Indigenization of mirrors for ST and LFR systems is relatively simpler.

## **ii. Support Structure**

The manufacturing skills to build the requisite structure for solar technologies are adequate in India. There are a lot of industries which are into fabrication of steel structures for domestic as well as international customers. A few companies like Aaccess Cranes & Equipments, Shrijee Tower & Solar Structures etc. have started manufacturing and supplying support structures for CSP plants in India.

## **iii. Power Block**

Triveni turbines, in collaboration with GE, are considering manufacturing turbines for solar industry. Other industries such as Maxwatt, Turbotech etc. have provided turbines to CSP plants in India.

The balance of plant of the power block is nearly similar to that of a conventional power block. There is enough competence and experience in this field to deliver the required goods. McNally Bharat, Engineers India, etc. are a few companies in this area.

The switchgear, control gear and transformer industry is fully developed and can meet the needs of the solar industry.

## **iv. Receivers**

The receivers for the PT system consisting of evacuated glass encapsulated absorbers need to be imported at present. On the contrary the less complex receivers of ST and LFR systems are amenable for indigenization.

## **v. HTF Systems, Thermal Storage, Swivel Joints, Drives and Controls**

The above have a good potential for indigenization.

## **vi. EPC & Civil Works**

The presence of large number of EPC contractors like - Gammon, Jaypee, Lanco, L&T etc. in India are capable of handling challenges in construction and maintenance of the solar plant.

### **12.3.1 Possible Cost Reductions**

Based on the above and following our discussions with potential vendors we expect the cost reductions with indigenization for the following components.

Mirror – Cost reduction of about 50% is achievable through indigenization if the volume of manufacturing is large.

Support Structure – With improvements in design and reduction in weight of the support structure coupled with large scale production, the cost reduction in fabrication of support structure is expected to be around 30%.

Thermal Storage – The major cost share in the storage system is the cost of molten salt, accounting for about 50% of the cost of the system. Since it is an imported item, the cost reduction is expected in the rest of the components in the storage system. Thus an overall cost reduction of 20% is expected.

The other components like HTF system, hydraulic drives, swivel joints, electronics and controls can yield a reduction in cost of about 30%.

As an illustration we have considered a 50 MW plant with 6 hours of thermal storage. Table 12.1 shows the cost breakup based on our present estimates with indigenization.

**Table 12.1: Cost breakup of a 50 MW plant with 6 hours of storage**

	Cost (₹ crore)	
	Present Cost Estimates	After Indigenization
Solar Field	773	588
Thermal Storage	146	117
Cost of Power block	134	134
Land Costs	32	33
Indirect Capital Costs	220	176
Total	1305	1048

Lastly, a certainty is in reduction of costs in man-power. Hence, this is dealt with separately in the next chapter.

## 13 Manpower Requirements for CSP Plants

### 13.1 Introduction

For CSP plant, the manpower requirements can be categorized into two: (a) Indirect and (b) Direct. Indirect jobs relate to the construction period which is typically about two years whereas direct jobs pertain to O&M for the lifetime of the plant, typically about 25 – 30 years.

### 13.2 Manpower for PT & ST Plants

Table 13.1 and Table 13.2 present information on manpower utilization in PT and ST plants (NREL, 2012).

**Table 13.1: Data on manpower for PT plants**

Sl. No	Plant Name	Country	Capacity, MW	Storage hours	Solar Field Area, m <sup>2</sup>	Construction Man-years	O&M staff
1	Andasol-1	Spain	50	7.5	510120	600	40
2	Andasol-2	Spain	50	7.5	510120	600	40
3	Arcosol 50	Spain	50	7.5	510120	900	45
4	Aste 1A	Spain	50	8	510120	500	50
5	Aste 1B	Spain	50	8	510120	500	50
6	Astexol II	Spain	50	8	510120	500	50
7	Borges Termosolar	Spain	25	0	181000	-	30
8	Extresol-1	Spain	50	7.5	510120	600	40
9	Extresol-2	Spain	50	7.5	510120	600	40
10	Extresol-3	Spain	50	7.5	510120	600	40
11	Genesis Solar Energy Project	USA	2 x 125	0	-	1085	50
12	Helioenergy 1	Spain	50	0	300000	600	60
13	Helioenergy 2	Spain	50	0	300000	600	60
14	Helios I	Spain	50	0	300000	600	40
15	Helios II	Spain	50	0	300000	600	40
16	Ibersol Ciudad Real	Spain	50	0	287760	-	60
17	La Africana	Spain	50	7.5	550000	300	40
18	La Dehesa	Spain	50	7.5	552750	950	45
19	La Florida	Spain	50	7.5	552750	950	45
20	La Risca	Spain	50	0	-	350	31
21	Lebrija 1	Spain	50	0	412020	500	-
22	Majadas I	Spain	50	-	-	350	31
23	Manchasol-1	Spain	50	7.5	510120	600	40

**Table Continued**

24	Manchasol-2	Spain	50	7.5	510120	600	40
25	Moron	Spain	50	-	380000	600	45
26	Nevada Solar One	USA	75	0.5	357200	350	30
27	Olivenza 1	Spain	50	0	402000	600	45
28	Palma del Rio I	Spain	50	0	-	350	31
29	Palma del Rio II	Spain	50	0	-	350	31
30	Solaben 1	Spain	50	0	300000	700	85
31	Solaben 2	Spain	50	0	300000	700	85
32	Solaben 3	Spain	50	0	300000	700	85
33	Solaben 6	Spain	50	0	300000	700	85
34	Solacor 1	Spain	50	0	300000	450	40
35	Solacor 2	Spain	50	0	300000	450	40
36	Solana Generating Station	USA	280	6	-	1500	85
37	Termesol 50	Spain	50	7.5	510120	900	45
38	Thai Solar Energy 1	Thailand	5	0	45000	120	10

**Table 13.2: Data on manpower for ST plants**

Sl. No	Plant Name	Country	Capacity, MW	Storage hours	Solar Field Area, m <sup>2</sup>	Construction Man-years	O&M staff
1	Gemasolar Thermosolar Plant	Spain	19.9	15	3,04,750	800	45
2	Ivanpah Solar Electric Generating System	USA	392	0	26,00,000	1896	90
3	Rice Solar Energy Project	USA	150	-	10,71,361	450	45
4	Sierra Sun Tower	USA	5	0	27,670	130	12

From Table 13.1 and Table 13.2, it may be seen that O&M staff requirements are of the order of 50 irrespective of the capacity of the plant, but during the construction period, the man-year requirements vary widely and it is difficult to draw any inferences from the data.

Given the target of 10,000 MW from CSP, the potential man power requirement is high. Based on O&M staff of 50 for a 50 MW capacity plant, the requirement in direct jobs is likely to be about 10,000. However during the construction period taking an average value of 600 man years for a 50 MW plant it is estimated that this figure could be about 120,000 man years.

It may be worthwhile mentioning that the man power requirement for indigenous manufacturing of components would be very high.

## 14 Policy Options for CSP in India

During the 1<sup>st</sup> phase of JNNSM, the off take of CSP was rather low compared to PV. This raised questions about CSP being amenable for large-scale deployment in India. There were several reasons for the relatively slow deployment of solar thermal.

### 1. Price

When the Solar Mission was announced, the expectation was that solar PV would be costlier than solar thermal. In fact, CERC proposed a normative tariff of ₹ 17.91 per kWh for PV as against ₹ 15.31 per kWh for solar thermal. However in the two rounds of reverse bidding, solar PV prices rapidly declined to ₹ 7.49 per kWh, while solar thermal price declined only marginally. Solar PV was perceived to be a much simpler technology, with no moving parts and lower maintenance.

### 2. Bankability

Since the solar industry is nascent in India, it was difficult to get early financial closure of solar projects, particularly in case of solar thermal. The financial institutions were not convinced about the economic viability of the technologies and consequently were reluctant to fund these.

### 3. Land and water requirements

Solar thermal projects require large tracts of land, for instance a 50 MW plant needs about 400 acres of contiguous and level land with water availability. Many states had difficulty in identifying lands even for solar PV projects, which were much smaller in size.

### 4. Lack of indigenous manufacturers

Almost all the projects announced in Phase I involved collaboration with a foreign technology provider. There was almost no support for domestic vendors in the manufacturing supply chain.

Going forward, the question is whether solar thermal technology has a future in India's energy mix. We feel that solar thermal has the potential to be a crucial contributor in India's future energy scenario. There should be an active policy push to incentivize deployment of the technology. We propose the following policy options.

### 14.1 Storage and Hybridization

The first stage of the JNNSM has made it clear that CSP would find it hard to compete with solar PV if price was the only criterion. The capital cost of PV has already reached ₹ 9 crore per MW and the corresponding LCOE is about ₹ 9 per kWh. As against this, solar thermal power plants are expected to cost ₹ 13 crore per MW (probably with no storage). The cost of CSP might reduce with indigenization. However, even then it would be hard for CSP to compete with the present PV prices. Therefore, CSP should always be combined with thermal storage and hybridization for it to be competitive with PV. Our analysis suggests that while thermal storage for 3 – 6 hours will increase the capital cost due to requirement of a larger solar field, the LCOE remains constant or marginally decreases. The main benefit of storage is that solar power can be dispatched when required by the grid and it helps to manage the intermittency much better. Therefore, we propose that the government policy promotes CSP plants with a certain minimum storage component. This could

include the Regulatory Commissions mandating differential tariffs for CSP if they are able to supply peaking power. Similarly, there should be a hybridization component in all CSP projects. It may be difficult for biomass to be the hybridization fuel given the uncertainty in biomass supply and price, especially for large CSP projects. Also, managing intermittent cloud cover requires fast response, which is difficult with biomass. Therefore, natural gas hybridization will be a better option.

## 14.2 Land Zones

In the first phase of JNNSM, a few states acquired land to develop solar parks and made these available to solar developers. In other states, the developers had to find suitable lands to site the projects. This was difficult to do even for the small-scale solar PV projects. In case of solar thermal, the land requirements are higher and it would not be possible for a developer to acquire such tracts. Therefore, the state government should identify suitable tracts of lands in areas with good DNI and develop these as solar parks with the necessary infrastructure such as water supply and transmission for evacuation of power. The National Clean Energy Fund could be used for developing such infrastructure.

## 14.3 Small Capacity CSP

The global experience with CSP has been for plants of large capacities, 50 MW and beyond. This is because steam based Rankine cycle achieves high power block efficiency of around 38% for plants of large capacity. At lower capacities, the efficiency of steam cycle is less than 20%. Consequently, the size and cost of solar field per MW is very high for smaller scale CSP plants. Large scale CSP plants are possible in the USA and Europe, where land availability is not an issue. However, land and water are major constraints in a densely populated country such as India. While it is possible to build a few CSP plants, it might be hard to build a large number of such plants. Therefore, India perhaps has the opportunity to develop a different model for small – capacity CSP. This requires examining different prime mover options, such as Organic Rankine Cycle, which could work with the relatively low temperatures generated by a Fresnel solar field. This cycle doesn't require any water and can be developed at plant capacities of around 1 MW. The efficiency is around 10%; however Fresnel solar field has a low cost. These could operate in an off grid decentralized mode.

There is also potential in examining the Brayton cycle using either air or CO<sub>2</sub> as the working fluid. The Brayton cycles can potentially achieve efficiencies of 30% with an overall plant efficiency of around 15%. Using super critical CO<sub>2</sub> as the working fluid, one can increase the power block efficiency to nearly 40% and achieve an overall plant efficiency in excess of 20%. Further, this cycle doesn't require any water. These plants can be built at scales of lower than 1 MW and could be considered for decentralized village level applications. There is scope for research and development of these CSP technologies, which are ideally suitable for Indian conditions. India has the opportunity to emerge as the leader in these technologies.

## 14.4 Indigenization

There is a good potential for cost reduction in CSP with indigenization and economies of scale. The draft guidelines for Phase II of JNNSM also place emphasis on indigenous manufacturing of several CSP components. It is certainly possible for the Indian companies to manufacture the mirrors and concentrators, absorber tubes and thermal storage systems at a lower cost. In this report, our simple calculation suggests that indigenization could lead to at least 30% reduction in the capital cost. There is a possibility that large scale manufacture of specific components with established

supply chains could further reduce the cost of components, which are presently being imported. These include mirrors, receivers, thermal fluid, salts etc. It is beyond the scope of this report to examine the specific policy levers to incentivize indigenous manufacturing and we will examine these issues in a separate study.

## **14.5 Heating Applications**

Development of solar thermal technologies is not only important for power generation but also for industrial process heating. Industry consumes close to 30% of India's oil consumption. This is used for heating applications and steam generation. Solar thermal has an excellent opportunity to reduce furnace oil consumption in industries. The main attraction of process heating is the very high efficiency of solar energy collection. Most collectors have an efficiency of about 60%. As against this, electricity conversion has much lower efficiency of around 15%. Therefore, process heating is a more efficient utilization of the natural resource. However, the present policies do not adequately incentivize the adoption of solar thermal collectors. For instance, a grid connected electricity generation plant receives a generation-based tariff, which ensures reasonable returns to the investor; a process heating plant receives a capital subsidy, which is not adequate to cover the investors' risk. There is a need to look at the incentive structure for solar thermal applications that provide process heating.

## **14.6 Financing**

In Phase I of JNNSM, there was some difficulty in obtaining financial closure for solar projects. Financial institutions were not confident about the bankability of solar projects partly because of their unfamiliarity with the solar technologies and partly because of the doubts regarding utilities ability to purchase expensive solar power. PPA alone was not considered adequate. One option to gain the confidence of financial institutions is to place solar power among "priority lending" options. It is necessary to involve all stake holders to arrive at the most suitable policy options.

## References

- Alex, W. (2010). *Stirling SunCatcher with Heat Engine Technology*. Retrieved February 2012, from <http://www.buildgreen.com/live/index.cfm/2010/4/29/Alexs-Cool-Product-of-the-Week-Stirling-SunCatcher>
- AREVA. (2012, Nov). Retrieved from <http://www.areva.com/EN/news-9508/areva-integrates-energy-storage-in-its-solar-clfr-design-at-sandia-national-labs.html>;  
[http://www.areva.com/mediatheque/liblocal/docs/SWF/energies/ani-field-report/pdf/PW10/AREVA\\_Field-Report-10\\_SolarPositionPaperCLFR.pdf](http://www.areva.com/mediatheque/liblocal/docs/SWF/energies/ani-field-report/pdf/PW10/AREVA_Field-Report-10_SolarPositionPaperCLFR.pdf)
- Black & Veatch. (2008). *Solar Generation Technology Assessment*. Idaho Power Company.
- Buie, D., Dey, C., & Mills, D. (2002). Optical considerations in line focus Fresnel concentrators. *11th Proceedings of the SolarPACES International Symposium on Solar Thermal Concentrating Technologies*.
- Business Standard. (2012, February 24). <http://www.business-standard.com>. Retrieved November 2012, from <http://www.business-standard.com/india/news/maharishi-solar-offers-low-cost-solar-thermal-solutions/465616/>
- CERC. (2010). *Explanatory Memorandum for benchmark capital cost norms for Solar PV power projects and solar thermal power projects*. Central Electricity Regulatory Commission (CERC). Retrieved from [http://www.cercind.gov.in/2010/ORDER/Sept10/Explanatory\\_Memo\\_for\\_Project\\_cost\\_for\\_solar\\_PV\\_and\\_Solar\\_thermal\\_2011-12\\_255-2010.pdf](http://www.cercind.gov.in/2010/ORDER/Sept10/Explanatory_Memo_for_Project_cost_for_solar_PV_and_Solar_thermal_2011-12_255-2010.pdf)
- Csaba, S., Reiner, B., Robert, P.-P., & Hans, M. (2010). Assessment of Solar Power Tower Driven Ultrasupercritical Steam Cycles Applying Tubular Central Receivers with Varied Heat Transfer Media. *Journal of Solar Energy Engineering*.
- CSPToday. (2012). *CSP World Plant Locations*. CSP Today. Retrieved from <http://www.trec-uk.org.uk/images/CSPTodayWorldMap2011.pdf>
- DelPozo, Dunn, & Pye, J. (2011). Molten salt as heat transfer fluid for a 500 m<sup>2</sup> dish concentrator. *SolarPACES*. Spain.
- DLR. (2005). *10 MW solar thermal power plant for southern Spain*. European Commission. Retrieved August 2012, from [http://ec.europa.eu/energy/renewables/solar\\_electricity/doc/2006\\_ps10.pdf](http://ec.europa.eu/energy/renewables/solar_electricity/doc/2006_ps10.pdf)
- EASAC. (2011). *Concentrating Solar Power: Its potential contribution to a sustainable energy future*. European Academic Science Advisory Council.
- ECOSTAR. (2003). *European Concentrated Solar Thermal Road-Mapping*. ECOSTAR.

- Ernst & Young. (2011). *Middle East and North Africa Region Assessment of the Local Manufacturing Potential for Concentrated Solar Power Projects*. ESMAP.
- ESMAP. (2010). *Review of CSP Technologies and Cost Drivers Overview*. ESMAP & World Bank.
- Fichtner. (2010). *Assessment of Technology Options for Development of Concentrating Solar Power in South Africa for The World Bank*. ESMAP.
- FLABEG. (2012). Retrieved November 2012, from  
[http://www.flabeg.com/uploads/media/FLABEG\\_Solar\\_Ultimate\\_Trough\\_10.pdf](http://www.flabeg.com/uploads/media/FLABEG_Solar_Ultimate_Trough_10.pdf)
- Geritt, K., Hoffschmidt, B., Hennecke, K., Hartz, T., Schwarzbözl, P., Göttsche, J., & Beuter, M. (2009). *The Solar Power Tower Julich - A Solar Thermal Power Plant for Test and Demonstration of Air Receiver Technology*. Deutsches Zentrum für Luft- und Raumfahrt (DLR).
- Greg, B., Lovegrove, K., Scott, M., & Jose, Z. (2011). Direct steam generation using the SG4 500m<sup>2</sup> paraboloidal dish concentrator. *SolarPACES*. Spain.
- Gregory, K. J., Clifford, H., Thomas, M. R., & Jesse, G. A. (2011). *Power Tower Technology Roadmap and Cost Reduction Plan*. Sandia Laboratories.
- Hermann-Ulf, B.-K.-P. (2004). Two-tank Molten Salt Storage for Parabolic Trough Solar Power Plants. *Energy*, 29, 883-893.
- IMD. (2009). *Solar Radiant Energy over India*. Retrieved from  
<http://www.mnre.gov.in/centers/about-sec-2/solar-resources/>
- IRENA. (2012). *Renewable Energy Technologies: Cost Analysis Series*.
- ITP. (2011). *Concentrating Solar Power in India*. Dept. of Climate Change & Energy Efficiency.
- ITP. (2012). *Realising the potential of concentrating Solar Power in Australia*. IT Power.
- Jennifer, R. (2011, September). Solar Shakeout Continues: Stirling Energy Systems Files for Chapter 7 Bankruptcy. Retrieved from  
<http://www.renewableenergyworld.com/rea/news/article/2011/09/solar-shakeout-continues-stirling-energy-systems-files-for-chapter-7-bankruptcy>
- Kearney, A. T. (2010). *Solar Thermal Electricity 2025 - Clean electricity on demand:attractive STE cost stabilize energy production*. ESTELA.
- Lovegrove, K., Burgess, McCready, D., & John, P. (2009). ANU's new 500 m<sup>2</sup> paraboloidal dish solar concentrator - Technology & Sustainable Applications. *LSAA Conference*.
- Mani, A., & Rangarajan, S. (1982). *Solar Radiation over India*. New Delhi: Allied Publishers.
- Michael, W. J. (2012). *Results and comparison from the SAM Linear Fresnel Technology Performance Model*. NREL.
- Mills, & Morrison. (2000). Compact Linear Fresnel Reflector Solar Thermal Power Plants. *Solar Energy*, 68(3), 263-283.

- Montes, M., Abánades, A., Martínez-Val, J., & Valdés, M. (2009). Solar multiple optimization for a solar-only thermal power plant, using oil as heat transfer fluid in the parabolic trough collectors. *Solar Energy*, 83(12), 2165-2176.
- Mustafa, Abdelhady, & Elweteedy. (2012). Analytical Study of an Innovated Solar Power Tower (PS10) . *International Journal of Energy Engineering*, 2(6), 273-278.
- Novatec Solar. (2011, June). Retrieved from <http://www.novatecsolar.com/54-0-Fresnel-specialist-develops-next.html>;  
[http://www.novatecsolar.com/files/110915\\_press\\_release\\_supernova.pdf](http://www.novatecsolar.com/files/110915_press_release_supernova.pdf)
- NREL. (2012). *National Renewable Energy Laboratory*. Retrieved from [http://www.nrel.gov/csp/solarpaces/by\\_project.cfm](http://www.nrel.gov/csp/solarpaces/by_project.cfm)
- PSA. (2007). *Platforma Solar de Almeria (PSA)'s Annual Report*. Retrieved from <http://www.psa.es/webeng/techrep/2007/ATR2007-ing.pdf>
- Purohit, & Michaelowa. (2008). CDM potential of solar water heating systems in India. *Solar Energy*, 82(9), 799-811.
- Purohit, I., & Garud, S. (2007). Overview of technologies, Opportunities and Challenges. *Proceedings of All India Seminar on India's energy Independent Strategies and Strides*.
- PWC. (2012). Financial Engineering as a means to support Jawarharlal Nehru National Solar Mission.
- Ramakrishna, G., Thirumalai, N. C., & Ramaswamy, M. A. (2011). *Heat transfer calculations for an absorber tube of a solar thermal system using parabolic Trough*. Bangalore: CSTEP.
- Ramaswamy, M. A., Badri, S. R., Suresh, N. S., & Thirumalai, N. C. (2012). *Estimation of Hourly Direct Normal Irradiation (DNI) for 22 stations in India*. Bangalore: CSTEP.
- Ramaswamy, M. A., Badri, S. R., Suresh, N. S., Ramakrishna, G., & Thirumalai, N. C. (2010). *Solar energy impinging on unit aperture area of a Fresnel mirror located at different positions relative to the absorber*. Bangalore: CSTEP.
- Ramaswamy, M. A., Suresh, N. S., Badri, S. R., & Ramakrishna, G. (2010). *Solar Energy impinging on unit area of a parabolic trough, aligned N-S Axis and East-West tracking*. Bangalore: CSTEP.
- Robert-Pitz-Paal. (2012). *Parabolic Trough, Linear Fresnel, Power Tower - A Technology Comparison*. DLR.
- Sargent & Lundy. (2003). *Assessment of Parabolic. Trough and Power Tower Solar. Technology Cost and Performance Forecasts*. Department of Energy and National Renewable Energy Laboratories.
- SOLGATE. (2005). *Solar hybrid gas turbine electric power system*. European Commission.
- Tamme, R. (2006, June 27). *Developemnt of Storage System for SP Plants*. Retrieved from [http://ec.europa.eu/energy/res/events/doc/tamme\\_dlr\\_storage.pdf](http://ec.europa.eu/energy/res/events/doc/tamme_dlr_storage.pdf)

- Tania. (2011). *CSIRO's Solar Technical Blog*. Retrieved February 2011, from <http://csirosolarblog.com>
- Truchi, C. (2010). *Parabolic Trough Reference Plant for Cost Modelling with SAM*. NREL.
- William, B. S., & Michael, G. (2001). *Power from the Sun*. Retrieved from <http://www.powerfromthesun.net>
- Winter, C., Sizmann, R., & Vaut Hull, L. (Eds.). (1991). *Solar Power Plants: Fundamentals-Technology-Systems- Economics*. Berlin: Springer Berlin Heidelberg.
- Zubair, S., & Bilal, Q. (2006). Prediction of Evaporation Losses in Wet Cooling Towers. *Heat Transfer Engineering*, 27(9), 86-92.



Dr. Raja Ramanna Complex,  
Raj Bhavan Circle,  
High Grounds,  
Bangalore - 560 001  
Tel: +91 (80) 4249-0000  
Fax: +91 (80) 2237-2619  
[admin@cstep.in](mailto:admin@cstep.in)